Characterization of land plant-specific proteins required for mitochondrial translation initiation

Tran, Huy Cuong

2023

Characterization of land plant-specific proteins required for mitochondrial translation initiation

HUY CUONG TRAN
DEPARTMENT OF BIOLOGY | FACULTY OF SCIENCE | LUND UNIVERSITY

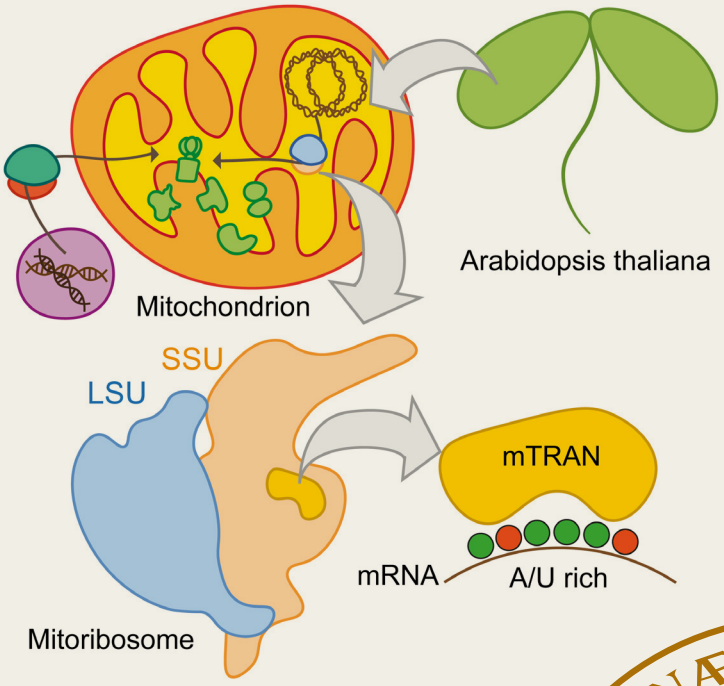

Characterization of land plant-specific proteins required for mitochondrial translation initiation

Characterization of land plant-specific proteins required for mitochondrial translation initiation

Huy Cuong Tran

DOCTORAL DISSERTATION

Doctoral dissertation for the degree of Doctor of Philosophy (PhD) at the Faculty of Science at Lund University to be publicly defended on the 5th of May at 13.00 in Biology Lecture Hall, Department of Biology, Sölvegatan 35, Lund, Sweden

Faculty opponent
Prof. Dr. Christian Schmitz-Linneweber

Humboldt-Universität zu Berlin, Berlin, Germany

Organization: LUND UNIVERSITY

Document name: DOCTORAL DISSERTATION **Date of issue:** 2023-05-05

Author: Huy Cuong Tran **Sponsoring organization:**

Title: Characterization of land plant-specific proteins required for mitochondrial translation initiation.

Abstract: Plant mitochondria produce the majority of adenosine triphosphate (ATP) – the cellular energy currency for metabolic reactions needed for plant growth, development, and maintenance. Despite a relatively thorough understanding of basic mitochondrial functions, many mitochondrial proteins and processes remain poorly understood. The aims of this thesis are to i) review and compare the mitochondrial unfolded protein response (UPR^{mt}) and related signalling across eukaryotic kingdoms, to ii) describe an efficient isolation method of Arabidopsis mitochondria using continuous Percoll density gradients, and to iii) characterize two *Arabidopsis thaliana* genes, *AT4G15640* and *AT3G21465*.

Paper I summarizes the current knowledge of UPR^{mt} across eukaryotic kingdoms, and describes a meta-analyis of UPR^{mt} regulators and target genes. UPR^{mt} is a mitochondria-to-nucleus "retrograde" response that regulates nuclear gene expression during mitochondrial dysfunction to maintain mitochondrial homeostasis. Although UPR^{mt} has been extensively studied in animals, relatively little is known about the plant UPR^{mt} and only few regulators have recently been identified. In yeast, very few unfolded protein responses that seem to be related to UPR^{mt} have been described. Here, the UPR^{mt} in animals, yeast and plants are compared. Our study indicates that each kingdom has evolved their own specific regulators, which however induce very similar groups of target genes. Our meta-analysis identifies homologs of known UPR^{mt} regulators and responsive genes across eukaryotic kingdoms.

Paper II describes a strategy for efficient purification of Arabidopsis mitochondria using continuous Percoll density gradients. By using this method, the purity of isolated mitochondria is greatly improved. Obtained mitochodria can be either used for assays requiring highly intact and functional mitochondria, e.g. import assay or respiration measurement, or be stored for later use, e.g. BN-PAGE or western blot.

Paper III describes the characterization of two *Arabidopsis thaliana* genes, *AT4G15640* and *AT3G21465*. Here, AT4G15640 and AT3G21465 are shown to be land plant-specific mitochondrial proteins that are critical for plant performance, but they are unlikely to be adenyl cyclases as previously annotated. Interestingly, knocking out both *AT4G15640* and *AT3G21465* results in low abundance and activity of mitochondrial oxidative phosphorylation complexes. Using co-immunoprecipitation, AT4G15640 and AT3G21465 are confirmed to be part of the mitoribosome small subunit (mtSSU). Therefore, AT4G15640 and AT3G21465 were named as mitochondrial TRANslation factor 1 (mTRAN1) and 2 (mTRAN2), respectively. *In organello* protein synthesis and polysome fractionation assays suggest that mTRANs are required for mitochondrial translation initiation. Moreover, the RNA electrophoretic mobility shift assays suggest that mTRAN1 binds to the A/U-rich regions in the 5'-untranslated regions of mitochondrial mRNAs to mediate mtSSU-mRNA binding to initiate translation. Finally, our mitoribosome profiling suggests that mTRAN proteins are universal mtSSU-embedded translation initiation factors. Together, these findings suggest that mitochondrial translation initiation occurs via a unique mechanism in plants, as compared to in bacteria, yeast and mammals.

Key words: Mitochondrial unfolded protein response, Arabidopsis mitochondrial isolation, mitoribosome, mitochondrial translation initiation, mitoribosome small subunit, mTRAN, mTRAN-mRNA interaction.

Classification system and/or index terms (if any) Supplementary bibliographical information

Language: English **ISSN and key title**:

ISBN: 978-91-8039-598-4 (electronic), 978-91-8039-599-1 (print)

Recipient's notes **Number of pages**: 67

Price Security classification

Signature Date 2023-03-13

Characterization of land plant-specific proteins required for mitochondrial translation initiation

Huy Cuong Tran

LUND
UNIVERSITY

Coverphoto by Vivian Schmitt and Huy Cuong Tran

Faculty of Science
Department of Biology

ISBN 978-91-8039-598-4 (electronic)
ISSN 978-91-8039-599-1 (print)

Printed in Sweden by Media-Tryck, Lund University
Lund 2023

Media-Tryck is a Nordic Swan Ecolabel certified provider of printed material. Read more about our environmental work at www.mediatryck.lu.se
MADE IN SWEDEN

To my family (Gửi tới gia đình)

Table of Contents

List of papers

Paper I

Huy Cuong Tran, Olivier Van Aken (2020). Mitochondrial unfolded protein-related responses across kingdoms: similar problems, different regulators. *Mitochondrion 53*: 166-177.

Paper II

Huy Cuong Tran, Olivier Van Aken (2022). Purification of leaf mitochondria from *Arabidopsis thaliana* using Percoll density gradients. *Methods in Molecular Biology* 2363: 1-12.

Paper III

Huy Cuong Tran, Vivian Schmitt, Sbatie Lama, Chuande Wang, Alexandra Launay-Avon, Katja Bernfur, Kristin Hofmann, Kasim Khan, Benoit Castandet, Fredrik Levander, Allan G. Rasmusson, Hakim Mireau, Etienne Delannoy, Olivier Van Aken. Mitochondrial translation in plants is initiated by a unique mTRAN-mRNA interaction mechanism. *In revision for Science*.

My contributions to the papers

Paper I

I participated in planning the project and performing the meta-analysis. I wrote the manuscript with input from my supervisor.

Paper II

I participated in planning the project and collecting data. I wrote the manuscript with input from my supervisor.

Paper III

I participated in conceiving and planning the project. I performed most of the experiments (with input from my supervisor), including phylogenetic analysis, confocal microscopy analysis, plant phenotyping, plant cAMP measurement, BN-PAGE following by Coomassie staining and activity measurement, oxygen consumption measurement, immunoblotting, co-immunoprecipitation, *in organello* protein synthesis, and polysome profiling. I also produced and collected the samples for RNA-seq and Ribo-seq. I co-supervised Vivian Schmitt doing her internship and master's thesis, in which she performed several immunoblot analysis, the bacterial cAMP synthase complementation assays, qRT-PCR on mitochondrial retrograde signalling genes, motif analysis of the 5'UTRs of mitochondrial mRNAs, recombinant protein expression and purification, and REMSAs. My supervisor and I wrote the manuscript with input from all co-authors.

List of additional papers not included in this thesis

Essam Darwish, Ritesh Ghosh, Abraham Ontiveros-Cisneros, **Huy Cuong Tran**, Marcus Petersson, Liesbeth De Milde, Martyna Broda, Alain Goossens, Alex Van Moerkercke, Kasim Khan and Olivier Van Aken (2022). Touch signaling and thigmomorphogenesis are regulated by complementary CAMTA3- and JA-dependent pathways. *Science Advances* 8 (20): eabm2091.

List of abbreviations

5'UTR	5' untranslated region
A	Adenine
AA	Antimycin A
ABI4	Abscisic acid-insensitive 4
Acetyl-CoA	Acetyl-Coenzyme A
AC	Adenyl cyclase
ADP	Adenosine diphosphate
ANAC017	Arabidopsis NAC domain containing 017
AOX	Alternative oxidase
ATP	Adenosine triphosphate
BLRP	Biotin ligase recognition peptide
BN-PAGE	Blue Native Polyacrylamide Gel-Electrophoresis
C	Cysteine
cAMP	3′,5′-cyclic adenosine monophosphate
CI-V	Complex I-V
C. elegans	*Caenorhabditis elegans*
cpUPR	Chloroplast unfolded protein response
Cryo-EM	Cryogenic electron microscopy
D-GAP	D-glyceraldehyde-3-phosphate
Dox	Doxycycline
DXP	1-deoxy-D-xylulose-5-phosphate
DXS	1-deoxy-D-xylulose-5-phosphate synthase
ER	Endoplasmic reticulum
$FADH_2$	Flavin adenine dinucleotide
G	Guanine
IF	Initiation factor
IMM	Inner mitochondrial membrane
IMS	Intermembrane space
IMTACT	Isolation of Mitochondria TAgged in specific Cell Types
Fe–S	Iron-sulfur
MAPK	Mitogen-activated protein kinase
MB	MitoBlock-6
MEP	Methylerythritol phosphate
MORF	Multiple Organellar RNA editing Factor
mRNA	Messenger RNA
mrpl1-1	Mitochondrial ribosomal protein L1
mtDNA	Mitochondrial DNA
mtETC	Mitochondrial electron transport chain
mtIF	Mitochondrial initiation factor

mtLSU	Mitoribosome large subunit
mTRAN1	Mitochondrial translation factor 1
mTRAN2	Mitochondrial translation factor 2
MTS	Mitochondrial targeting sequences
mtSSU	Mitoribosome small subunit
NADH	Nicotinamide adenine dinucleotide
NDB4	NAD(P)H dehydrogenase B4
nPG	n-propylgallate
OAA	Oxaloacetate
OM64	Outer membrane 64
OM66	Outer membrane protein of 66 kDa
OMM	Outer mitochondrial membrane
ORRM	Organellar RNA Recognition Motif
OXPHOS	Oxidative phosphorylation
PEP	Phosphoenolpyruvate
PNPase	Polynucleotide phosphorylase
PPR	Pentatricopeptide repeat
PVP	Polyvinylpyrrolidone
REMSA	RNA electrophoretic mobility shift assay
RIP-seq	RNA Immunoprecipitation Sequencing
RIP	RNA-editing factor interacting protein
ROS	Reactive oxygen species
RpoT	RNA polymerase of the T-phage type
rRNA	Ribosomal RNA
SD	Shine-Dalgarno
SHAM	Salicylhydroxamic acid
SUBA	Subcellular Localization Database for Arabidopsis Proteins
Succinyl-CoA	Succinyl-Coenzyme A
TCA	Tricarboxylic acid
TIM	Translocase of the inner membrane
TM	Transmembrane
TOM	Translocase of the outer membrane
TPR	Tetratricopeptide repeat
tRNA	Transfer RNA
U	Uridine
UGT74E2	Uridine diphosphate glycosyltransferase 74E2
UPOX1	Up regulated by oxidative stress AT2G21640 1
UPR^{mt}	Mitochondrial unfolded protein response
VDAC	Voltage-dependent anion channel

Popular scientific summary

Plants are of key importance as their photosynthesis produces a massive amount of oxygen in the atmosphere, which is mandatory for respiration of many other organisms as well as plants themselves. Similar to in other eukaryotes, plant cellular respiration is carried out by mitochondria – organelles producing cellular energy needed for plant growth, development and maintenance. Nowadays, most scientists agree with the evolutionary hypothesis suggesting that mitochondria originated from endosymbiotic bacteria approximately 1.5 billion years ago. Nevertheless, in a cell, mitochondrial operation is not independent, but closely interacts with the nucleus – the central regulator of eukaryotic cells that contains most genes encoding the genetic information of an organism. The nucleus can send signals and materials to mitochondria to regulate mitochondrial activity. Vice versa, mitochondria are also able to send signals to the nucleus and affect nuclear gene expression. Gene expression is the process by which information of a gene is passed onto a messenger RNA (mRNA) during transcription, which is then used as a template to synthesize a corresponding protein during translation. This ultimately may affect the phenotype – the final effect on an individual living organism.

Due to their bacterial origin, mitochondria have their own sets of genes and have partially retained their own machinery for gene expression, including essential components required for transcription and translation. Mitochondrial gene expression is important to maintain mitochondrial operation. Thus, one could expect that the cellular energy would be affected if mitochondrial gene expression is perturbed. To date, many aspects of mitochondrial translation in plants are still enigmatic. In this work, we use the plant "mouse-ear cress" (scientific name: *Arabidopsis thaliana*) to study the land plant-specific proteins of unknown functions that we named as mitochondrial TRANslation factors (mTRAN). For many years, mTRAN proteins have been poorly characterized. During the course of our study, two recent studies suggested that mTRAN proteins are mitochondria-targeted and are components of the plant mitochondrial ribosome (hereafter referred to as mitoribosome) – the protein-RNA complex that translates the genetic information encoded in a mRNA into a corresponding protein. To study the functions of mTRAN proteins, Arabidopsis mutants lacking functional mTRAN proteins were generated, and they displayed a severe growth phenotype, indicating that mTRAN proteins are essential for plant growth and development. Using a combination of molecular, biochemical and bioinformatic approaches, we showed that the importance of mTRAN proteins for plant performance is due to their critical role in efficient mitochondrial translation in plants. In particular, mTRAN proteins are required for the mitoribosome – RNA binding in the initiation step of translation. Of note, this unique mTRAN-RNA interaction mechanism to initiate plant mitochondrial translation is fundamentally different from bacterial translation and mitochondrial translation in other eukaryotes. In conclusion, our study not only gains a deeper

insight into mitochondrial translation in plants, but also contributes to the knowledge of mitochondrial translation in eukaryotes.

Introduction

An overview of cellular respiration in plants

Plants are autotrophs that uptake nutrients in inorganic form and produce organic molecules themselves. Plant photosynthesis is carried out by chloroplasts to synthesize carbohydrates (sucrose and/or starch) from carbon dioxide (CO_2) and water by using photon energy from sunlight. On the other hand, plant respiration consumes oxygen (O_2) as the electron acceptor and releases CO_2 as a by-product. Similar to in other eukaryotes, plants have mitochondria, where aerobic respiration partially occurs to generate adenosine triphosphate (ATP) – the cellular energy currency to fuel metabolism required for their growth, development, and maintenance. Plant respiration is composed of glycolysis, the tricarboxylic acid (TCA) cycle (also known as the Krebs cycle or the citric acid cycle) and the oxidative phosphorylation (OXPHOS) of adenosine diphosphate (ADP) to ATP by the mitochondrial electron transport chain (mtETC) and ATP synthase complex. Plant cellular respiration strongly resembles their animal counterparts, but it has several unique features. As plants are sessile, they are unable to move away from extreme environmental conditions. Therefore, plant metabolism in general and plant respiratory metabolism in particular have evolved to adapt with environmental stress (O'Leary and Plaxton, 2016). The overall regulation of plant respiration is complicated and can occur "locally" in different processes of the respiratory pathway. The widespread use of plant mutant lines, which have important enzymes of respiration knocked out, gives us a broader insight not only into the function of key respiratory components, but also into the flexibility of plant respiratory pathway. Plant respiration is of great importance for the global carbon cycle as the amount of CO_2 used by photosynthesis of terrestrial plants is returned to the atmosphere by plant respiration, representing approximately 50% of the total annual CO_2 released from terrestrial ecosystems (Gifford, 2003; O'Leary and Plaxton, 2016).

Mitochondrial origin

In 1967, Lynn Margulis proposed that eukaryotic organelles, including the chloroplast and the mitochondrion, originated from endosymbiotic bacteria in her

famous paper "On the origin of mitosing cells" (Sagan, 1967). Later, advanced phylogenomic analysis has shown that the mitochondrial endosymbiont is related to an α-proteobacterium either within, or as a sister group to, the Rickettsiales. The host organism was likely an archaeon of the Asgard clade (Spang et al., 2015; Wang and Wu, 2014, 2015; Zaremba-Niedzwiedzka et al., 2017). The mitochondrion-containing ancestor, also known as the "last eukaryote common ancestor", resembling the modern eukaryotes genetically and cellularly, evolved to all known eukaryotes nowadays. On one hand, the "mitochondria-early" evolutionary hypothesis proposes that the mitochondrial endosymbiotic event occurred very early in eukaryogenesis and/or even initiated the process (Martin et al., 2015). On the other hand, the "mitochondria-late" evolutionary hypothesis suggests that the mitochondrial endosymbiotic event took place when many other eukaryotic characteristics had already been established (Roger et al., 2017). Whether the former or the latter hypothesis is closer to what happened in the earliest stage of life, it is undeniable that the endosymbiotic origin of mitochondria is of key importance for the evolution of all modern eukaryotes.

A brief history of plant mitochondrial isolation

To study the structure and function of mitochondria, researchers attempted to isolate mitochondria from cells. The first attempt of mitochondrial isolation was carried out in guinea pig liver by Bensley and Hoerr in 1934 (Bensley and Hoerr, 1934) according to a recent review by Møller et al. (2021). Although mitochondria might be first described in plant cells in 1904 (Logan, 2012; Møller et al., 2021), the first plant mitochondria purification was done by Adele Millerd and her co-workers in 1951 (Millerd et al., 1951; Møller et al., 2021). At that stage, the crude mitochondria were isolated by differential centrifugations, thus they were however impure due to heavy contamination of thylakoid membranes from chloroplasts. Only in 1985, Day and his co-workers used differential centrifugations and Percoll-Polyvinylpyrrolidone (PVP) density gradients to successfully purify chlorophyll-free mitochondria from pea (*Pisum sativum*) leaves (Day et al., 1985). Also using the same approach, pure, intact and functional mitochondria of *Arabidopsis thaliana*, which became of great importance as the model dicot plant in the 1990s, were successfully purified from leaf tissues (Keech et al., 2005) and seedlings (Escobar et al., 2006). Nevertheless, this protocol of mitochondrial isolation requires a large amount of starting plant material and usually takes a few hours to accomplish. Recently, Boussardon et al. (2020) has developed a novel method of tissue-specific isolation of Arabidopsis mitochondria, named IMTACT (Isolation of Mitochondria TAgged in specific Cell Types). IMTACT, in which cell-specific biotinylated mitochondria are purified using streptavidin magnetic beads, yields pure and intact mitochondria in less than 30 min from sample preparation till final

extraction (Boussardon and Keech, 2022). This novel approach is much faster than traditional mitochondrial isolation methods using continuous or discontinuous gradients. To study plant mitochondrial compartments in depth, the protocols of isolating mitochondrial subfractions followed by biochemical approaches to study them have been developed and described in detail in the book "Plant Mitochondria: Methods and Protocols" edited by Whelan and Murcha (2015) and Van Aken and Rasmusson (2022).

Structure and basis composition of plant mitochondria

Plant mitochondria are often spherical or rod-shaped organelles that are 1-3 µm long and about 0.5 µm in diameter (Møller et al., 2021). With the availability of electron microscopes after World War II, the structure of an individual plant mitochondrion was revealed by electron micrographs (Palade, 1952). Similar to in other eukaryotes, plant mitochondria are double membranous organelles comprised of an outer mitochondrial membrane (OMM) separated from an inner mitochondrial membrane (IMM) by the intermembrane space (IMS), and the mitochondrial matrix, which is an aqueous electron-dense phase enclosed by the IMM and cristae formed by invaginations of the IMM (Figure 1). The OMM was shown to contain the voltage-dependent anion channel (VDAC), also referred as porin (Homble et al., 2012; Parsons et al., 1965; Zalman et al., 1980). Using electron tomography (available in the 1990s) to obtain 3D pictures of mitochondria, it turned out that the cristae look like narrow tubes running through the matrix (Frey and Mannella, 2000). A typical Arabidopsis mesophyll cell is comprised of many hundreds of mitochondria (Logan, 2006). Unlike mammalian and most yeast mitochondria, but resembling mitochondria in *Saccharomyces cerevisiae*, plant mitochondria move around mainly within the cytoplasm on the actin cytoskeleton (Logan, 2006; Olyslaegers and Verbelen, 1998; Van Gestel et al., 2002). Interestingly, mitochondrial fusion can occur, forming large, reticulated mitochondria. Mitochondrial fusion and fission can take place frequently to maintain the mitochondrial population in a cell homogenous (Logan, 2006; Møller et al., 2021). A recent review by Møller et al. (2021) has summarized the composition of mitochondrial compartments. In brief, the mitochondrial membranes are composed of lipids and proteins. The lipid in the mitochondrial membranes are usually phospholipids. The lipid composition of the OMM, including phosphatidylcholine, phosphatidylethanolamine, phosphatidylinositol and phosphatidylinositol, resembles that of the endoplasmic reticulum (ER) membrane. The IMM has a similar lipid composition as the OMM, but also contains a unique phospholipid, diphosphatidylglycerol (cardiolipin). The mitochondrial matrix does not contain phospholipids and has a very high concentration of proteins.

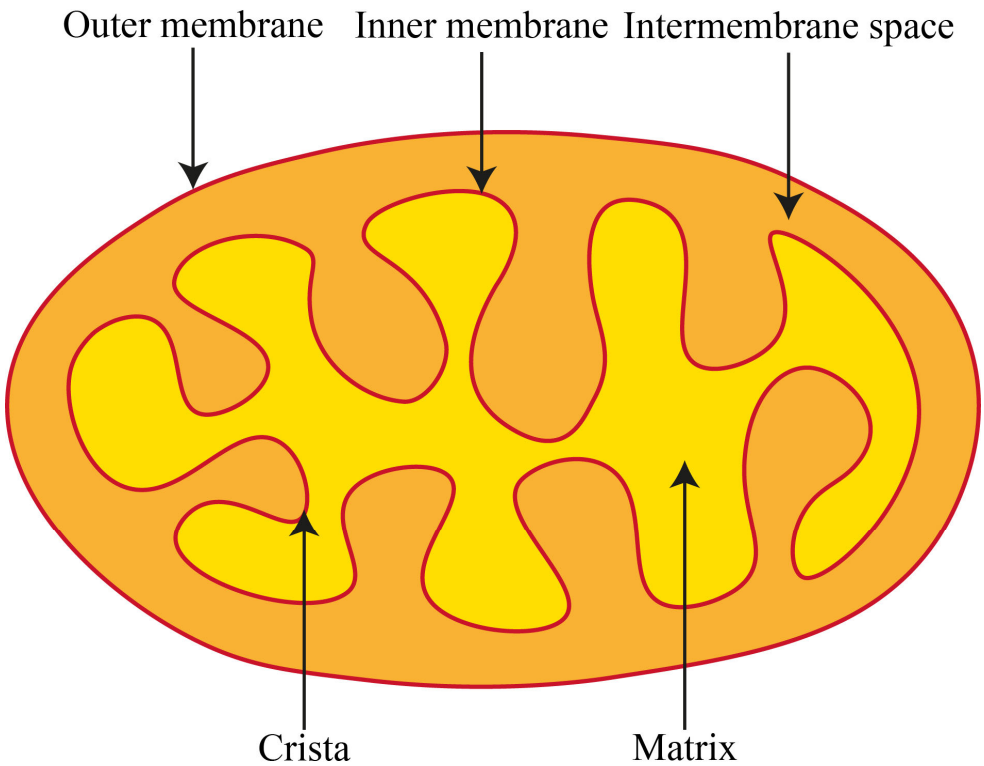

Figure 1. A simple diagram of plant mitochondrial structure.

Plant aerobic respiration partially occurs in mitochondria

As in other aerobic eukaryotes, the aerobic respiration in plants includes three processes occurring in different subcellular compartments: glycolysis, the TCA cycle and the OXPHOS system. Together, these processes produce ATP – the cellular energy currency. Mitochondria are thus considered as the cellular power houses. The following description of these three stages of plant aerobic respiration is written to a large extent based on chapter 12 “Respiration and Photorespiration” by Millar et al. (2015) in the textbook “Biochemistry and Molecular Biology of Plants” edited by Buchanan et al. (2015).

Glycolysis

Glycolysis takes place either in the cytosol or in the plastids, generating substrates that are subsequently used by the TCA cycle and the OXPHOS system, which occur within the mitochondria. Cytosolic glycolysis breaks down sucrose into glucose and fructose, which are converted into phosphoenolpyruvate (PEP). PEP can be turned either into pyruvate by pyruvate kinase and/or PEP phosphatase or into oxaloacetate (OAA) by PEP carboxylase. This glycolytic pathway generates reduced cofactor nicotinamide adenine dinucleotide (NADH) and ATP. Pyruvate is transferred directly into mitochondria whereas OAA is usually reduced to malate, which is then transported into mitochondria.

The tricarboxylic acid cycle

Once pyruvate and malate are imported into the mitochondrial matrix via carriers located in the IMM, pyruvate is oxidized and decarboxylated to generate CO_2, acetyl-Coenzyme A (acetyl-CoA) and NADH, while malate can be oxidized to either generate OAA and NADH by malate dehydrogenase or yield pyruvate, CO_2 and NADH by NAD^+-linked malic enzyme. Once the TCA cycle starts occurring within the mitochondrial matrix, acetyl-CoA and OAA combine to form citrate, which is isomerized to isocitrate that is oxidized and decarboxylated to form CO_2, 2-oxoglutarate, and NADH. 2-Oxoglutarate is further oxidized to produce CO_2, succinyl-Coenzyme A (succinyl-CoA) and NADH. Succinyl-CoA synthetase converts succinyl-CoA into succinate. Associating with this reaction, ADP is phosphorylated to ATP. Succinate is oxidized to fumarate by succinate dehydrogenase - the only IMM-localized enzyme involved in both the TCA cycle and mtETC. In the final step of the TCA cycle, fumarate is hydrated to form NADH and malate, which is oxidized to OAA that subsequently combines with another acetyl-CoA to continue the cycle (Figure 2).

The oxidative phosphorylation system

The OXPHOS system resides within the IMM and is based on the core of mtETC, which is composed of the four IMM-associated complexes: the NADH dehydrogenase (complex I), the succinate dehydrogenase (complex II), the cytochrome bc_1/cytochrome *c* reductase complex (complex III) and the cytochrome *c* oxidase (complex IV) (Figure 2). Complex I is the largest respiratory complex of the mtETC (Wirth et al., 2016). The high-resolution structure of plant complex I has recently been described by Maldonado et al. (2020) and Klusch et al. (2021). Plant complex I has an L-like shape and is comprised of the membrane arm embedded into the IMM, the peripheral arm extending into the mitochondrial matrix and another matrix-exposed domain linking to the membrane arm at the central position.

Complex I oxidizes NADH (formed by glycolysis and the TCA cycle) to regenerate NAD^+ at the peripheral arm site. Complex II, the smallest complex of four respiratory complexes (Millar et al., 2004), oxidizes succinate (generated as an intermediate in the TCA cycle) to fumarate with the concomitant oxidation of flavin adenine dinucleotide ($FADH_2$) to FAD^+ at the membrane-spanning domain site. Both complex I and complex II contain iron-sulfur (Fe–S) clusters involved in the transfer of electrons onto ubiquinone – a mobile electron transporter located within the mitochondrial IMM. The electron transport from NADH to ubiquinone causes conformational change in the membrane arm of complex I, resulting in pumping four protons from the mitochondrial matrix to the IMS. Unlike complex I, complex II cannot translocate protons across the IMM. By accepting two electrons, ubiquinone is reduced to ubiquinol, which is released from complex I and complex II and transfers electrons onto complex III – the central segment of the mtETC.

The atomic structure of plant complex III has recently been described by Maldonado et al. (2021). Plant complex III consists of 2 × 10 subunits, which can be functionally categorized as follows (Braun, 2020): subunits involved in the mtETC including the Rieske Fe-S protein, the heme-containing cytochrome c_1 and cytochrome *b* subunits (b_{566} and b_{560}); the large mitochondrial matrix-exposed domain of complex III containing the two subunits of mitochondrial processing peptidase (α-MPP and β-MPP), which cleaves the targeting peptides of nuclear-encoded mitochondrial proteins; and five small subunits QCR6-QCR10, which participate in electron transport. At complex III, electrons are transferred from ubiquinol to cytochrome *c* and protons are translocated from the matrix to the IMS by the Q cycle. During the Q cycle, ubiquinol binds to the center P of complex III, where it is oxidized and releases two electrons, one of which is transferred to cytochrome *c* via the Rieske Fe–S center and cytochrome c_1 and two protons are pumped into the IMS. The other electron is transferred by cytochrome *b*-type proteins within complex III to reduce ubiquinone (bound to the matrix side of complex III) to semiquinone at the center N. At this point, another ubiquinol attaches to the center P and passes through the same process, reduces semiquinone to ubiquinol, completes the Q cycle and pumps two more protons into the IMS. Once the Q cycle is completed, cytochrome *c*, a small heme-containing protein located on the outer surface of the IMM exposing it to the IMS, is reduced and released from complex III, carries one electron and transports it to complex IV - the terminal enzyme of the mtETC.

The molecular structure of plant complex IV has recently been described by Maldonado et al. (2021). At subunit II of complex IV, electrons from cytochrome *c* are transferred via Cu_A and cytochrome *a* then to the cytochrome a_3-Cu_B center of the subunit I, where one oxygen molecule (the final electron acceptor) is reduced by one electron to form two water molecules. This redox reaction is coupled to the translocation of two protons across the IMM. The K, D, H pathways (named after crucial amino acid residues in each pathway) were suggested to contribute to the pumping of protons by plant complex IV but it has recently been suggested that the

H pathway is not involved in this process (Maldonado et al., 2021). During one "cycle" of the mtETC, a total of 10 protons (4 from complex I, 4 from complex III and 2 from complex IV) are translocated from the mitochondrial matrix to the IMS, creating an electrochemical proton gradient, also known as the mitochondrial membrane potential. The protons in the IMS re-enter the mitochondrial matrix via the ATP synthase complex (also known as complex V) to dissipate the proton gradient. Complex V is composed of two major subcomplexes: F_o - the transmembrane subcomplex ("o" stands for oligomycin, which inhibits proton transfer through the subcomplex) and F_1 - the matrix-exposed subcomplex, are connected by a central stalk. The F_o subcomplex allows protons to pass through, causing conformational changes within the F_1 subcomplex, driving the phosphorylation of ADP to ATP. Generation of ATP – the final product of the OXPHOS system and more importantly, the cellular energy currency, is one of the prime functions of mitochondria.

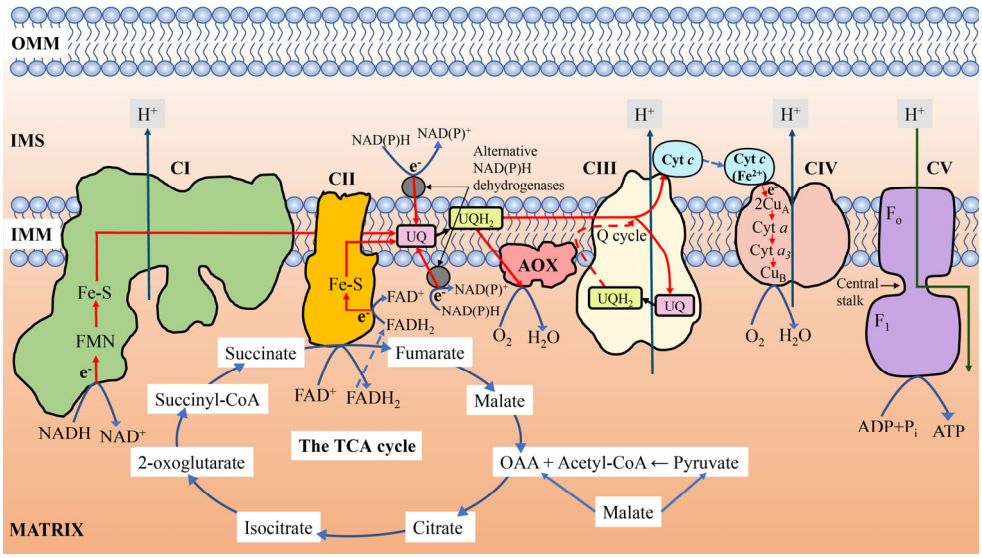

Figure 2. A diagram of the tricarboxylic acid (TCA) cycle and the oxidative phosphorylation (OXPHOS) system in plant mitochondria. Imported pyruvate is converted into acetyl-Coenzyme A (acetyl-CoA) whereas imported malate can be used to generate either pyruvate or oxaloacetate (OAA). As the TCA cycle starts in the mitochondrial matrix, acetyl-CoA and OAA combine to generate citrate, which is subsequently isomerized to isocitrate. Isocitrate is then converted into 2-oxoglutarate, which is in turn converted into succinyl-Coenzyme A (succinyl-CoA). Succinyl-CoA is turned into succinate, which is oxidized to fumarate by the inner mitochondrial membrane (IMM)-anchored succinate dehydrogenase (complex II (CII)). Concomitantly, flavin adenine dinucleotide ($FADH_2$) is oxidized to FAD^+. Fumarate is converted into and malate, which is oxidized to OAA that subsequently combines with another acetyl-CoA to continue the cycle. The OXPHOS system occurs within the IMM. Complex I (CI) oxidizes nicotinamide adenine dinucleotide (NADH) to

generate NAD^+ at the peripheral arm site and the electrons are transferred via flavin mononucleotide (FMN) and iron-sulfur (Fe-S) clusters onto ubiquinone (UQ). CII oxidizes $FADH_2$ to FAD^+ at the membrane-spanning domain site and the electrons are transported via Fe-S clusters to UQ. During the electron transport, CI pumps protons (H^+) from the mitochondrial matrix into the mitochondrial intermembrane space (IMS) whereas CII is a non-proton pumping complex. By receiving two electrons, UQ is reduced to ubiquinol (UQH_2), which transfers electrons to complex III (CIII). At CIII, electrons are transferred from UQH_2 to cytochrome *c* (cyt *c*) and protons are translocated from the matrix into the IMS by the Q cycle. Because one cyt *c* can accept only one electron from UQH_2 at a time, the second electron is transferred to UQ bound to CIII, which is reduced to form semi-UQ. During the second half of the Q cycle, another UQH_2 enters the first half of the Q cycle, donating one electron to another cyt *c* and the second electron is transported to semi-UQ, which is fully reduced to UQH_2 and this UQH_2 will travel to the IMM and re-enter the Q cycle. Reduced cyt *c* (cyt *c* (Fe^{2+})) transfers electrons from CIII to complex IV (CIV), where electrons are transferred via Cu_A and cytochrome *a* (cyt *a*) then to the cytochrome a_3 (cyt a_3)-Cu_B center to reduce oxygen (O_2) to water (H_2O). This redox reaction is coupled to the translocation of protons from the matrix to the IMS. During mitochondrial electron transport chain (mtETC), protons are pumped from the matrix to the IMS by CI, CIII and CIV, generating an electrochemical proton gradient. The protons in the IMS re-enter the mitochondrial matrix via the subcomplex F_o of the adenosine triphosphate (ATP) synthase (complex V (CV)). As a result, the subcomplex F_1 connected to the subcomplex F_o by the central stalk changes its conformation and drives the phosphorylation of adenosine diphosphate (ADP) to ATP. In addition to CI, plant mitochondria contain the alternative nicotinamide adenine dinucleotide (phosphate) (NAD(P)H) dehydrogenases located either on the outer surface of the IMM (exposed to the IMS) or on the inner surface of the IMM (exposed to the mitochondrial matrix). The alternative NAD(P)H dehydrogenases transport electrons from NAD(P)H to UQ, but do not pump protons across the IMM. Plants have an alternative respiratory pathway that bypasses cytochrome *c* oxidase and transfers electrons from UQH_2 to the nuclear-encoded alternative oxidase (AOX) localized in the IMM to reduce O_2 to H_2O. AOX does not pump protons, thus energy produced during the alternative respiratory pathway is lost as heat. OMM = outer mitochondrial membrane, e^- = electron. The figure is adapted from Millar et al. (2015) edited by Buchanan et al. (2015).

The respiratory complexes can associate into the respiratory supercomplexes in plants

Analyses by Blue Native Polyacrylamide Gel-Electrophoresis (BN-PAGE) have revealed that the plant respiratory complexes can associate into the respiratory supercomplexes (Figure 3) (Dudkina et al., 2006; Eubel et al., 2004; Eubel et al., 2003; Krause et al., 2004). Of note, all respiratory supercomplexes contain dimeric complex III (III_2). In supercomplexes, complex III_2 can interact either with the membrane arm of complex I or with one or two copies of monomeric complex IV or can even interact with both complex I and IV. Respiratory supercomplexes formed by complex I, III_2 and IV are referred as respirasomes because they can perform respiratory electron transport from NADH to reduce oxygen (Braun, 2020).

It is proposed that respirasomes can associate to form even larger structures, called respiratory megacomplexes, which are thought to be involved in defining the structure of the cristal membrane (Braun, 2020). Recently, the atomic structure of plant supercomplex III_2-IV has been revealed at high resolution by cryogenic electron microscopy (cryo-EM) (Maldonado et al., 2021).

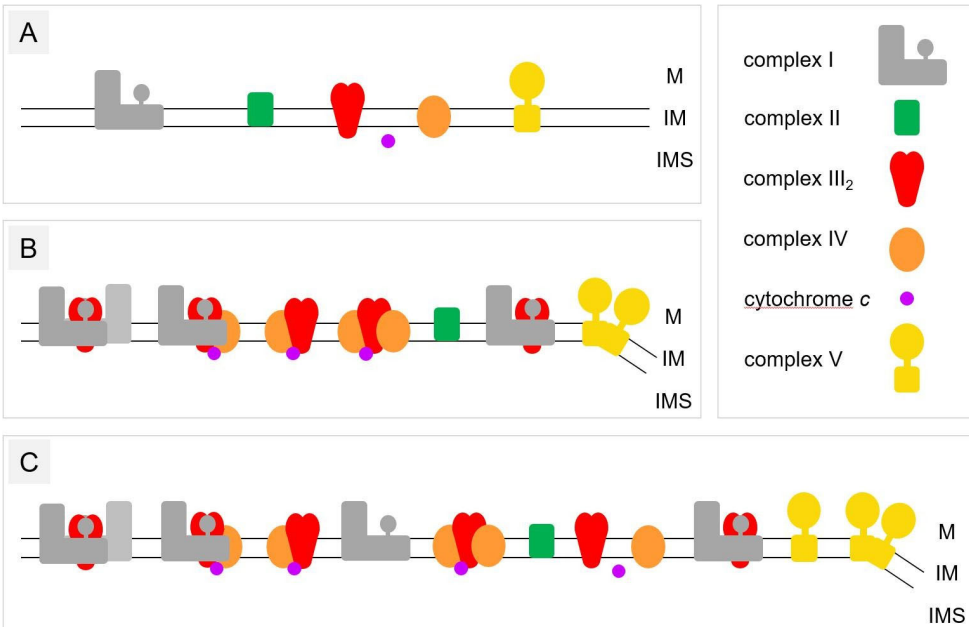

Figure 3. The respiratory complexes can associate into the respiratory supercomplexes in plants. Shapes and colors of the oxidative phosphorylation (OXPHOS) complexes and of cytochrome *c* are indicated in the legend at the top right. **A.** OXPHOS complexes in monomeric forms (except for complex III, which always occurs as a dimer). **B.** Respiratory supercomplexes in plant mitochondria. **C.** *In vivo*, monomeric OXPHOS complexes and supercomplexes are supposed to coexist within the inner mitochondrial membrane. M = matrix, IM = inner mitochondrial membrane, IMS = mitochondrial intermembrane space. The figure is taken from Braun (2020) with permission. Braun (2020) (DOI: 10.1016/j.mito.2020.04.007) is published under the terms of the Creative Commons Attribution-NonCommercial-No Derivatives License (CC BY NC ND).

Plants have an alternative electron transport pathway

The respiratory pathway described above (see "the oxidative phosphorylation system") is referred as the cytochrome *c* oxidase respiratory pathway, as it utilizes cytochrome *c* to carry electrons from complex III to complex IV. Plants have an alternative respiratory pathway that bypasses the cytochrome *c* oxidase and transfers electrons from ubiquinol to the nuclear-encoded alternative oxidase (AOX)

localized in the IMM to reduce oxygen to water. AOX is non-proton pumping, thus energy released during the alternative respiratory pathway is lost as heat. AOX is not only found in plants, but also found in many algae and fungi, animals and some protozoa (McDonald et al., 2009). The AOX pathway is resistant to classic inhibitors of complex III, such as antimycin A (AA; which inhibits the reduction of ubiquinone at the center N) and myxothiazol (which inhibits the oxidation of ubiquinol at the center P), and of complex IV, such as chemicals competing with oxygen for accepting electrons, including cyanide (CN^-), azide (N_3^-), carbon monoxide (CO) and nitric oxide (NO) (Millar et al., 2015). Nevertheless, AOX activity is inhibited by salicylhydroxamic acid (SHAM) and n-propylgallate (nPG) (Millar et al., 2015).

In addition to the NADH dehydrogenase/complex I, plant mitochondria contain the alternative (type II) nicotinamide adenine dinucleotide (phosphate) (NAD(P)H) dehydrogenases located either on the outer surface of the IMM (exposed to the IMS) or on the inner surface of the IMM (exposed to the mitochondrial matrix) (Rasmusson et al., 2004). As the name implies, the alternative NAD(P)H dehydrogenases transport electrons from NAD(P)H to ubiquinone, but do not pump protons across the IMM (Rasmusson et al., 2004). As a result, if plants are totally dependent on the alternative NAD(P)H dehydrogenases, the theoretical number of ATP generated by complex V will be reduced. The alternative NAD(P)H dehydrogenases are insensitive to rotenone, which inhibits electron transfer from the Fe-S center of complex I to ubiquinone. Due to the presence of the alternative NAD(P)H dehydrogenases, plants can survive without complex I (Braun, 2020), although mutants defective in complex I showed severe growth and development deficiencies (Fromm et al., 2016; Kuhn et al., 2015). Interestingly, the hemi-parasitic plant, mistletoe *Viscum album*, is the first reported multicellular eukaryote that completely lacks complex I due to the absence of mitochondrially-encoded *NAD* genes and other nuclear-encoded genes that encode subunits of complex I (Maclean et al., 2018; Senkler et al., 2018). Consequently, the abundance of complex IV and V are decreased whereas the abundance of alternative dehydrogenases and oxidases are increased in *Viscum album* as compared to in the model (non-parasitic) plant *Arabidopsis thaliana* (Maclean et al., 2018).

The genome of plant mitochondria

Similar to in other eukaryotes, the plant mitochondrion has its own genome (hereafter referred as to the mitochondrial DNA (mtDNA) or the mitogenome) that originated from the endosymbiotic ancestor, an α-proteobacterium (Sagan, 1967). Through evolution, the mitochondrial genome was decreased steadily through gene loss and/or transfer to the nuclear genome (Chevigny et al., 2020). Mitochondria

have partially retained their own genomes during evolution. On one hand, it is suggested that mitochondria need local regulation of gene expression to rapidly respond to the local redox state (Allen, 2015). On the other hand, it is proposed that mitochondrially-encoded membranous ETC proteins are highly hydrophobic, which causes a problem for importing the proteins into mitochondria (von Heijne, 1986). Indeed, Bjorkholm et al. (2015) proposed that hydrophobic membrane proteins could be targeted to the ER rather than to mitochondria. Nowadays, the plant mitogenomes can be diverse in size and structure depending on plant species, but the number of mitochondrially-encoded genes, including OXPHOS and mitochondrial ribosomal genes, transfer RNA (tRNA) and ribosomal RNA (rRNA), is relatively similar (Chevigny et al., 2020). In the model plant *Arabidopsis thaliana*, the mitogenome contains 57 genes, including OXPHOS proteins, ribosomal proteins, tRNAs and rRNAs (Table 1) (Unseld et al., 1997). To date, it is reported that the size of land plant mtDNA is the largest (Gualberto and Newton, 2017). The size of mammalian mtDNA is 15-17 kilobase pairs (kb), whereas the plant mitogenome is substantially larger: 13-96 kb in algae, usually 200-700 kb in angiosperms, but can be as enormous as 11 megabase pairs (mb) (in *Silene conica*) (Gualberto and Newton, 2017; Sloan et al., 2012). This is because the plant mitogenome mostly contains non-coding sequences that are not conserved across species rather than because the plant mtDNA encodes a few more genes and several genes possess introns (Gualberto and Newton, 2017). Although the plant mitogenome has non-coding sequences originating from chloroplastic, nuclear, or viral DNA by horizontal transfer, the origin of the vast majority of non-coding sequences are unknown (Bergthorsson et al., 2003; Chevigny et al., 2020; Gualberto and Newton, 2017). In addition to the high number of non-coding sequences, the plant mtDNA also contains a high abundance of repeated sequences, which can be categorized into large repeats (> 500 bp), intermediate-sized repeats (50-500 bp) and small repeats (< 50 bp) (Arrieta-Montiel et al., 2009; Davila et al., 2011; Gualberto et al., 2014). It is generally accepted to illustrate the plant mitogenome as a single circular chromosome. For example, the mitogenomes of *Marchantia polymorpha* and *Vicia faba* were observed as single circular DNA molecules (Negruk et al., 1986; Oda et al., 1992). However, using pulse field gel electrophoresis or electron microscopy failed to detect such a single circular chromosome (Backert et al., 1997; Oldenburg and Bendich, 1996). Rather, the plant mitogenome mainly contains a collection of circular subgenomes and linear and branched DNA molecules (Sloan, 2013). Due to the structural variability, the plant mitogenomes have distinct replication mechanisms. Replication of circular DNA molecules is likely to undergo rolling circle mechanisms whereas replication of linear DNA molecules is mediated by specific proteins that covalently interact with terminal inverted repeats (Gualberto and Newton, 2017; Handa, 2008). The plant mitogenome does not exist as naked DNA in the mitochondrial matrix but as part of nucleoids, which are regarded as the heritable units of mtDNA (Dai et al., 2005;

Gilkerson et al., 2013). In spite of the massive size of mitogenomes, the number of mitochondrially-encoded genes in plants is not much higher than that of animals and yeast (about 20 additional genes) (Chevigny et al., 2020). Interestingly, the plant mitogenomes are highly stable and conserved in most higher plant species as compared to in animals because of such lower mutation rates occurring in the plant mtDNA (Wolfe et al., 1987). This could be because plant mitochondria have efficient repair mechanisms, particularly homologous recombination, which is likely to be the main mtDNA repair mechanism in plants (Chevigny et al., 2020; Gualberto and Newton, 2017). Homologous recombination fixes the damaged copy by recruiting an undamaged DNA molecule, which can be brought by the continuous mitochondrial fusion and fission (Gualberto and Newton, 2017; Møller et al., 2021). Other DNA repair pathways existing in plant mitochondria, including direct repair, mismatch repair, nucleotide excision repair and base excision repair, are described in detail by Chevigny et al. (2020).

Table 1. The mitogenome of *Arabidopsis thaliana* contains 57 genes, encoding 25 proteins involved in the OXPHOS system (subunits of complex I, III, IV and V, and cytochrome *c* biogenesis), 7 ribosomal proteins, 22 transfer RNAs, and 3 ribosomal RNAs (5S, 18S, and 26S). The table is modified from Unseld et al. (1997). mtSSU = mitoribosome small subunit. mtLSU = mitoribosome large subunit.

Gene	Description
nad1	Subunit of complex I
nad2	
nad3	
nad4	
nad4L	
nad5	
nad6	
nad7	
nad9	
cob	Subunit of complex III
cox1	Subunit of complex IV
cox2	
cox3	
atp1	Subunit of complex V
atp4	
atp6-1	
atp6-2	
atp8	
atp9	
ccmB	Cytochrome *c* biogenesis
ccmF$_C$	
ccmFN$_1$	
ccmC	
ccmFN$_2$	

rpL2	mtLSU protein
rpL5	
rpL16	
rpS3	mtSSU protein
rpS4	
rpS7	
rpS12	
rrn18	mtSSU ribosomal RNA
rrn26	mtLSU ribosomal RNA
rrn5	
22 transfer RNAs	

The proteome of plant mitochondria

Proteomic studies have shown that the number of mitochondrial proteins is diverse across eukaryotic organisms, e.g. ~1800 proteins in mammals (Palmfeldt and Bross, 2017), ~1000 proteins in yeast (Schmidt et al., 2010) and 2000-3000 proteins in plants, of which 98-99% are nuclear-encoded, translated by cytosolic ribosomes and imported into mitochondria (Rao et al., 2017). Of note, plants possess 200-300 mitochondrial pentatricopeptide repeat (PPR) proteins (Møller et al., 2021), which are substantially more than in other eukaryotes: yeast and human have only 12 and 7 mitochondrial PPR proteins, respectively (Lightowlers and Chrzanowska-Lightowlers, 2013). Plants contain 20-40 mitochondrially-encoded proteins (Møller et al., 2021; Mower, 2020). About 70% of nuclear-encoded mitochondrial proteins have N-terminal mitochondrial targeting sequences (MTS). MTS are removed and degraded once nuclear-encoded mitochondrial proteins are imported into different sub-mitochondrial compartments via the translocase of the outer membrane (TOM) and the translocase of the inner membrane (TIM) channels (Chacinska et al., 2009; Kmiec et al., 2014; Prokisch et al., 2004; Schleiff and Becker, 2011). The remaining 30%, e.g. mitochondrial proteins associating with the IMM and subunits of OXPHOS, do not contain canonical MTS (Huang et al., 2009; Kmiec et al., 2014; Schleiff and Becker, 2011; Senkler et al., 2017a). Of note, mitochondrial fusion and fission could mix individual mitochondrial proteomes (Fuchs et al., 2020; Møller, 2016; Møller et al., 2021). In order to find out if a protein is potentially targeted to mitochondria, information on its subcellular localization can be found in the Subcellular Localization Database for Arabidopsis Proteins – SUBA5 (suba.live), which is the central resource for Arabidopsis protein subcellular location data (Hooper et al., 2017). SUBA5 suggested that 2562 proteins are targeted to mitochondria by either large scale proteomics or fluorescent localization (accessed 4th January 2023).

From genes to proteins in plant mitochondria

Mitochondrial transcription

As the mitochondrion originated from an α-proteobacterial ancestor, mitochondria have partially retained machinery for expression of their own genomes. Similar to nuclear-encoded genes, mitochondrially-encoded genes undergo transcription and translation, which however occur within mitochondria. In *Arabidopsis thaliana*, the 367 kb mtDNA encodes 25 OXPHOS proteins, 7 ribosomal proteins, 3 rRNAs (5S, 18S, and 26S) and 22 tRNAs (Table 1) (Unseld et al., 1997). Mitochondria have nuclear-encoded phage-type RNA polymerases, which are thought to have taken over from the original bacterial-type RNA polymerase (Cermakian et al., 1996; Gaspari et al., 2004; Gray and Lang, 1998; Greenleaf et al., 1986; Masters et al., 1987; Tiranti et al., 1997; Weihe, 2004; Weihe et al., 1997). Organellar phage-type RNA polymerases are highly similar to the bacterial T7 RNA polymerases (Liere and Börner, 2011). Plant phage-type RNA polymerases are encoded by RpoT gene family (RNA polymerase of the T-phage type) (Liere and Börner, 2011). The RpoT gene family of Arabidopsis contains mitochondria-targeted RpoTm, plastid-targeted RpoTp and dual-targeted RpoTmp (Hedtke et al., 1997, 2000; Hedtke et al., 2002; Hedtke et al., 1999; Kobayashi et al., 2002; Kobayashi et al., 2001). Kuhn et al. (2009) showed that RpoTm acts as the fundamental RNA polymerase in Arabidopsis mitochondria and is mandatory for the transcription of most, if not all, mitochondrially-encoded genes. Identified mitochondrial promoters in Arabidopsis contain the CRTA-type consensus motifs, loosely-unusual sequences for the tetra-nucleotide core-motif (e.g. ATTA and RGTA) and promoters without consensuses (Kuhn et al., 2005). Of note, the study by Kuhn et al. (2009) also showed that RpoTmp activity is gene specific and promoter independent, suggesting that there is an RpoTmp-dependent transcriptional mechanism allowing mitochondria to regulate the expression of specific mitochondrially-encoded genes.

Post-transcriptional processing of primary mitochondrially-transcribed RNA

Following transcription, mitochondrially-transcribed messenger RNA (mRNA), tRNA and rRNA are processed. According to Binder et al. (2011), processing of most 5' and 3' ends of mRNAs are accomplished via post-transcriptional modification, in which the mature 5' ends and 3' ends are achieved by endonucleolytic and/or exonucleolytic processing. Maturation of 5' and 3' ends of tRNAs recruits two nucleases RNAse P and RNAse Z, and tRNA processing is accomplished by the addition of 5'-CCA-3', by RNA editing (cysteine (C)-to-uridine (U)) and by normal base modification. Processing of the 5' ends of 18S and

5S rRNAs is likely to be done by endonucleolytic cleavage, however, very little is known about processing the 5' and 3' ends of rRNAs. The steady-state levels of functional mitochondrial RNAs are controlled by the rates of transcribing and degrading RNA. Plant mitochondrial RNAs can be polyadenylated for degradation and the Polynucleotide phosphorylase (PNPase) is a major player for RNA degradation (Holec et al., 2006).

Similar to primary nuclear-transcribed RNAs, mitochondrially-transcribed RNA precursors contain introns, which undergo splicing processes. Organellar introns in plants are categorized into group I and group II (Bonen, 2008; Bonen and Vogel, 2001; Lambowitz and Zimmerly, 2004; Michel et al., 1989; Zimmerly et al., 2001). In angiosperms (particularly vascular plants), most mitochondrial introns are group II introns, which are likely to be spliced by trans-acting cofactors (Brown et al., 2014). Identified proteins facilitating splicing of mitochondrial group II introns include a mitochondrially-encoded maturase MatR, nuclear-encoded maturases (nMATs), CRM-domain proteins (mCSF1 and mCSF2), a DEAD-box RNA-helicase (PMH2), PPR proteins (OTP43, BIR6 and ABO5), a PORR-domain protein (WTF9) and a RCC-domain protein RUG3 (Brown et al., 2014).

Another mitochondrial post-transcriptional modification is RNA editing – a process altering bases in transcript sequences relative to their corresponding genes (Knoop, 2011). About 80% of the plant mitochondrial transcripts have editing sites that are edited in high efficiencies (Bentolila et al., 2013). The most frequent RNA editing activity in plant organelles (both mitochondria and plastids) is C-to-U substitution in mRNAs (Chateigner-Boutin and Small, 2010; Small et al., 2020). Reverse U-to-C editing is however less frequent and has been observed in a few plant lineages, e.g. hornworts, lycophytes and ferns (Chateigner-Boutin and Small, 2010; Small et al., 2020). C-to-U editing also takes place in tRNAs and rRNAs (Binder et al., 1994; Fey et al., 2002; Grewe et al., 2011; Hecht et al., 2011; Marechal-Drouard et al., 1996; Marechal-Drouard et al., 1993; Schuster et al., 1991), in introns and in 5'- and 3'-untranslated regions of many mitochondrial mRNAs (Borner et al., 1995; Carrillo and Bonen, 1997; Farre et al., 2012; Lippok et al., 1994; Shi et al., 2017; Sutton et al., 1991; Wissinger et al., 1991; Zanlungo et al., 1995). RNA editing not only changes the amino acid sequence of a protein, but also influences the RNA structure, consequently affecting RNA splicing and stability and RNA-protein interaction (Bonen, 2008; Chateigner-Boutin and Small, 2010; Oldenkott et al., 2014; Small et al., 2020). Specific editing sites of plant organelles are recognized by site-specific binding of RNA-binding cofactors - PPR proteins containing repeats of a tandem domain of 35 amino acid motifs (a helix-turn-helix structure), the PPR domains (Small and Peeters, 2000).

Several studies on the structures of PPR protein–RNA complexes showed that PPR proteins bind to single-stranded RNAs in a sequence-specific manner (Coquille et al., 2014; Gully et al., 2015; Ke et al., 2013; Shen et al., 2016; Yin et al., 2013). Within one certain repeat, the amino acids at the 5th and 35th positions, which

correspond to residues 6 and 1' in Barkan et al. (2012) and residues 4 and ii in Yagi et al. (2013), specifically recognize RNA bases (Yan et al., 2019). These di-residues are termed as the PPR code. Several PPR codes have been identified: threonine and asparagine (TN), threonine and aspartic acid (TD), asparagine and serine (NS), and asparagine and aspartic acid (ND) at the 5th and 35th positions recognize the corresponding nucleotides adenine (A), guanine (G), cytosine (C) and uracil (U), respectively (Barkan and Small, 2014). Notably, the 5th position mainly determines the RNA base specificity. The presence of asparagine at this position prefers pyrimidine-binding whereas serine or threonine prefers purine-binding (Barkan and Small, 2014). The 35th position is the second main determinant. The presence of asparagine at this position prefers to bind to base A or C while aspartate results in preference of binding to base G or U (Barkan and Small, 2014). Recently, Yan et al. (2019) has further explored the correlation between PPR codes and RNA bases, which enriched the pool of PPR codes. Based on the results, Yan and co-workers developed the online PPRCODE web server (http://yinlab.hzau.edu.cn/pprcode/) to facilitate the prediction of PPR protein-RNA binding sites.

PPR proteins are categorized into two subclasses: the PPR-P subclass present in many eukaryotes, and the PPR-PLS subclass, which are land plant-specific and have long 35 or 36 amino acids and short 31 or 32 amino acids variants of the canonical 35 amino acid PPR motif (P) (Cheng et al., 2016; Lurin et al., 2004). The PPR-P subclass has been proposed to be involved in RNA transcription, splicing, editing, cleavage, stability and in mitochondrial translation (Barkan and Small, 2014; Haili et al., 2016; Rugen et al., 2019; Schmitz-Linneweber and Small, 2008; Uyttewaal et al., 2008; Waltz and Giege, 2020; Waltz et al., 2019; Waltz et al., 2020b). The PPR-PLS subclass is specific to C-to-U RNA editing (Barkan and Small, 2014; Small et al., 2020). The PPR-PLS proteins contain highly conserved domains E1, E2 and DYW (named after amino acid residues of the domain). E1 and E2 domains resemble PPR or tetratricopeptide repeat (TPR) motifs (Cheng et al., 2016) but their exact functions remain elusive. The DYW domain is likely to possess a cytidine deaminase activity that performs the nucleotide exchange process (Small et al., 2020). However, it remains unclear how many RNA-editing PPR proteins that do not contain the DYW domain can still perform editing (Small et al., 2020). In addition to the PPR-PLS subclass, non-PPR proteins, including Multiple Organellar RNA editing Factors (MORFs) (also known as RNA-editing factor Interacting Proteins (RIPs)), Other RNA Recognition Motif (ORRM) (e.g. ORRM4 and ORRM5) and NUWA-related proteins (a P-class PPR protein), are also found to be involved in plant mitochondrial RNA-editing (Andres-Colas et al., 2017; Bentolila et al., 2012; Guillaumot et al., 2017; Shi et al., 2017; Shi et al., 2016; Takenaka et al., 2012).

Mitochondrial translation

Similar to nuclear gene expression, the last step of mitochondrial gene expression is translation, a process in which the mRNA sequence is used as a template to synthesize a corresponding protein chain by the mitochondrial ribosome (hereafter referred as to the mitoribosome). Translation is composed of four phases: initiation, elongation, termination and ribosome recycling. Like the cytosolic ribosome, a mitoribosome is also composed of rRNAs and two main subunits: the small subunit, which binds to mRNA and reads the genetic information, and the large subunit, which has tRNA aminoacyl (A), peptidyl (P) and exit (E) sites to synthesize the protein chain. In contrast to plastid translation, very little is known about plant mitochondrial translation. However, recent studies on mitoribosome structures of eukaryotes, including plants, help us to predict some aspects of plant mitochondrial translation.

Using cryo-EM, the structure of bacterial ribosome and mitoribosome structures of mammals, yeast, trypanosomes and plants were described at very high resolution (Figure 4) (Amunts et al., 2015; Desai et al., 2017; Greber et al., 2015; Noeske et al., 2015; Ramrath et al., 2018; Waltz et al., 2020b; Watson et al., 2020). As compared to bacterial ribosomes, mitoribosomes from eukaryotic kingdoms are protein-rich and 1.2-1.5 time larger (Waltz et al., 2020a; Waltz and Giege, 2020). This is because the mitoribosome small subunit (mtSSU) is substantially larger, and even surpasses the size of the mitoribosome large subunit (mtLSU) in trypanosomes and plants (Ramrath et al., 2018; Rugen et al., 2019; Waltz et al., 2019). In addition to the size difference, the structure and composition of eukaryotic mitoribosomes are also very different from the bacterial counterparts (Waltz and Giege, 2020). The diversity of mitoribosomes across eukaryotes suggests that eukaryotic mitoribosomes have evolved to adapt to particular niches during evolution (Waltz et al., 2020a). The composition of plant mitoribosome was revealed by Waltz et al. (2019) and Rugen et al. (2019), identifying 19 plant-specific mitoribosome proteins, of which half are PPR proteins. The study by Waltz et al. (2020b) described the atomic structure of the plant mitoribosome. Briefly, the plant mitoribosome is extended in rRNAs and protein contents. Most of plant-specific PPR proteins bind to the plant-specific rRNA expansion segments, which leads to reshaping the overall structure of plant mitoribosome. The central protuberance of plant mitoribosomes, where the mtLSU inter-connects with the mtSSU, consists of a 5S rRNA (like the bacterial counterpart) and mitochondrial plant-specific proteins. This specific structure thus contributes to increasing and reshaping the overall volume of the plant ribosome central protuberance. Similar to mammalian and yeast mitoribosomes, the plant mitoribosome is likely to be attached to the IMM and to interact with the insertase OXA1 through linker(s) (possibly protein(s)) (Waltz et al., 2020a; Waltz et al., 2020b).

	Fungi	Mammals	Plants	Kinetoplastids	Ciliates
	Saccharomyces cerevisiae, Neurospora crassa	*Homo sapiens, Sus scrofa*	*Brassica oleracea*	*Trypanosoma* spp., *Leishmania tarantolae*	*Tetrahymena thermophila*
Sedimentation coefficient:	70–74S	55S	77–78S	50S	80S
Molecular weight:	~3–3.3 MDa	2.7 MDa	–	~4.5 MDa	~4.0 MDa
Number of rRNAs:	2 (15/16S, 21/23S)	3 (12S, 16S, mtRNA$^{Phe/Val}$)	3 (18S, 5S, 26S)	2 (9S, 12S)	2 (14S, 21S)
Number of mitoribosomal proteins:	~73–78	82	~86	~122	92

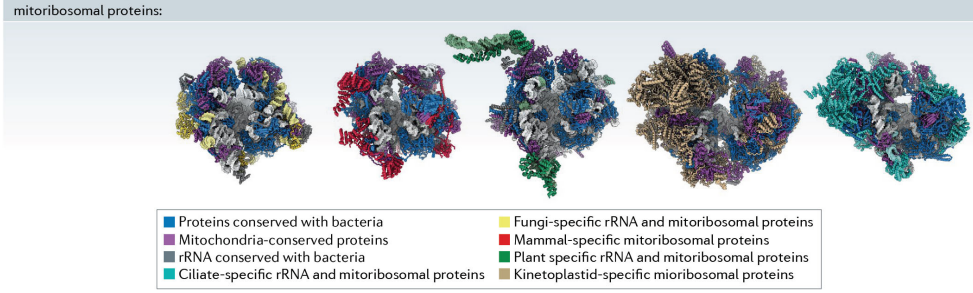

Figure 4. Advanced cryo-electron microscopy studies have recently revealed the structure of mitoribosomes and their diversification in fungi, mammals, plants and protozoans (kinetoplastids and ciliates). The figure is taken from Kummer and Ban (2021) (DOI: 10.1038/s41580-021-00332-2) with permission from Springer Nature.

In eukaryotes, including yeast, mammals and plants, mitochondrial mRNAs do not have Shine-Dalgarno (SD) sequences – the ribosomal binding site in bacterial mRNAs (Ayyub and Varshney, 2020; Derbikova et al., 2018; Hazle and Bonen, 2007). Of note, yeast mitochondrial mRNAs have very long 5' untranslated regions (5'UTRs) while mammalian mitochondrial mRNAs have very short 5'UTRs (maximum three-nucleotide length) or even do not have 5'UTRs (Ayyub and Varshney, 2020; Derbikova et al., 2018). Therefore, mitochondrial translation initiation in yeast and mammals strongly relies on translation initiation factors and/or activators (Ayyub and Varshney, 2020; Derbikova et al., 2018). A unique feature of mitochondrial translation initiation in mammals has recently been described by Kummer et al. (2018). Translation initiation in mammalian mitochondria is mediated by initiation factors, IF2 and IF3, and the mtSSU PPR protein mS39, which binds to an U-rich domain in the mRNA downstream of its start codon AUG (Kummer et al., 2018). Such U-rich regions are conserved and found downstream of codon 7 (after AUG) in 11 mRNAs (out of 13) of mammalian mitochondria (Amunts et al., 2015; Bieri et al., 2018; Kummer et al., 2018). In yeast, mitochondrial translation initiation seems to recruit universal translation initiation factors and specific translation activators to help the mtSSU interact with the 5'UTRs of mRNAs (Derbikova et al., 2018). Plant mitochondrial mRNAs also contain long 5'UTRs without SD sequences and plant mitochondrial rRNAs do not have anti-SD sequences either (Waltz et al., 2020b). To date, the mechanism of translation initiation in plant mitochondria is still enigmatic. The structure study of plant mitoribosome by Waltz et al. (2020b) suggested that mS83/rPPR10 is a PPR protein sitting in a cleft where the incoming mRNAs may be recruited. Waltz et al.

(2020b) also hypothesized that the PPR motifs of mS83/rPPR10 recognize AxAAA-related motifs in the 5'UTRs (located about 19 nucleotides upstream of the start codon) of 17 (out of 33) mitochondrial mRNAs, thus acting as a SD–anti-SD-like recognition system.

Mitochondrial retrograde signalling

Although mitochondria likely evolved from endosymbiotic α-protobacteria, mitochondria do not function independently, but their activities are integrated with other cellular organelles. To operate efficiently, a continuous flow of information between the nucleus and the mitochondrion is required, and it is described as anterograde and retrograde signalling (Ng et al., 2014). Anterograde signals from the nucleus are transmitted to the mitochondrion, as the nuclear regulation of the mitochondrial activity. Retrograde signals derived from the mitochondrion are sent to the nucleus and affect nuclear gene expression. In plants, mitochondrial retrograde signalling was first discovered by inhibition of mitochondrial function, resulting in the upregulation of *AOX1* transcript in tobacco (*Nicotiana tabacum*) (Vanlerberghe and McIntosh, 1996). Subsequently, the promoter region of *AOX1a* has been used as a "classical" bait for identification of mitochondrial retrograde signalling regulators in plants, including ABSCISIC ACID-INSENSITIVE 4 (ABI4) (Giraud et al., 2009), WRKY transcription factors (Van Aken et al., 2013; Vanderauwera et al., 2012), and MYB transcription factors (Ivanova et al., 2014; Zhang et al., 2017a; Zhang et al., 2017b). Nevertheless, the most well-studied and specific transcriptional regulators of mitochondrial retrograde signalling belong to the ARABIDOPSIS NAC DOMAIN CONTAINING (ANAC) protein family, including ANAC017 functioning as the main regulator and ANAC013 contributing as a downstream target in positive feedback loops (De Clercq et al., 2013; Ng et al., 2013; Van Aken et al., 2016). Of note, the study by Ng et al. (2013) showed that ANAC017 is a dual-targeted protein. ANAC017 is anchored in the ER membrane via a C-terminal transmembrane (TM) domain containing a consensus rhomboid protease cleavage site, which is suggested to be truncated proteolytically by rhomboid-related proteases during mitochondrial dysfunction. This allows ANAC017 to be released from the ER while its C-terminal TM domain stays in the ER, leading to the translocation of the N-terminal fragment of ANAC017 into the nucleus to activate gene expression (Ng et al., 2013). However, the exact mechanism of ANAC017 translocation remains enigmatic. In the nucleus, ANAC017 stimulates expression of mitochondrial retrograde signalling marker genes, including *AOX1a*, *UP REGULATED BY OXIDATIVE STRESS AT2G21640 1* (*UPOX1*), *URIDINE DIPHOSPHATE GLYCOSYLTRANSFERASE 74E2* (*UGT74E2*), *NAD(P)H DEHYDROGENASE B4* (*NDB4*), *At12CYS-2*, *H_2O_2 RESPONSE GENE 1* (*HRG1*)

and *OUTER MEMBRANE PROTEIN OF 66 KDA* (*OM66*) (Van Aken et al., 2016; Van Aken et al., 2007). Reactive oxygen species (ROS) generated by the mtETC and peptides from degraded proteins possibly trigger the ANAC017 pathway (Møller and Sweetlove, 2010; Ng et al., 2014; Vestergaard et al., 2012), but the molecular signals from a dysfunctional mitochondrion and how they initiate this signalling pathway remain elusive. Surprisingly, when mitochondrial function was sufficiently impaired, a consistent downregulation of chloroplast-encoded transcripts was observed (Adamowicz-Skrzypkowska et al., 2020; Zubo et al., 2014), suggesting that an as yet unknown (possibly retrograde) signalling pathway apparently can reduce chloroplast transcription.

Mitochondrial unfolded protein response

The mitochondrial unfolded protein response (UPR^{mt}) is described as the transcriptional response that regulates nuclear gene expression during mitochondrial malfunction to maintain mitochondrial homeostasis by inducing the mitochondrial protein quality control (chaperones and proteases). The UPR^{mt} can be triggered by mtDNA mutations (Lin et al., 2016), malfunctioning mitochondrial membrane potential (Rolland et al., 2019), imbalance between nuclear- and mitochondrially-encoded proteins (Houtkooper et al., 2013) or overloading concentration of unfolded/misfolded proteins in mitochondria (Zhao et al., 2002). Recent studies have gained insight into the plant UPR^{mt}. The study by Moullan et al. (2015) suggested that the plant UPR^{mt} is at least partially conserved to the animal UPR^{mt}. Wang and Auwerx (2017) showed that the UPR^{mt} in *Arabidopsis thaliana* is activated by a transient oxidative burst, resulting in the activation of mitogen-activated protein kinases (MAPKs) and hormonal signalling (ethylene, auxin and jasmonate) to recover mitochondrial proteostasis. Kacprzak et al. (2020) showed that ANAC017 – the main transcriptional regulator of mitochondrial retrograde signalling, induces many classes of genes that are classic targets of UPR^{mt} in response to AA treatment. Of note, ANAC017 induces "classical" mitochondrial retrograde signalling marker genes that have been also suggested as UPR^{mt} marker genes by Moullan et al. (2015) and Wang and Auwerx (2017). This thus suggests that "classical" mitochondrial retrograde signalling and UPR^{mt} in plants are most likely one and the same response (Kacprzak et al., 2020; Tran and Van Aken, 2020).

Adenyl cyclases in plants

Adenyl cyclases (ACs), also known as adenylyl cyclases or adenylate cyclases, are enzymes that convert ATP into 3′,5′-cyclic adenosine monophosphate (cAMP), which is a secondary messenger that can affect different physiological and biochemical processes in the cells. The important roles of cAMP as well as identification of ACs have been well-established in bacteria, animals and fungi. In plants, cAMP is involved in ion homeostasis, stomatal opening, pollen tube development, seed germination and cell cycle progression (Blanco et al., 2020). Nevertheless, comprehensive knowledge of plant cAMP and ACs is still missing. This could be due to two reasons. Firstly, it could be difficult to detect plant cAMP because the cAMP concentration is lower in plants than in animals. Reported cAMP concentration in plants is less than 40 pmol g^{-1} fresh weight in rye grass endosperm cell cultures, *Torenia* stem segments, and cultured cells of *Phaseolus vulgaris* and *Nicotiana tabacum*, 40-170 pmol g^{-1} fresh weight in *Daucus carota*, *Triticum aestivum*, and *Lemna paucicostata*, 200–250 pmol g^{-1} fresh weight in *Citrus*, *Lactuca*, *Hordeum*, and *Zea* (Sabetta et al., 2016). On the contrary, reported cAMP level in animals is usually greater than 250 pmol g^{-1} wet weight (Gehring, 2010). Secondly, it could be challenging to identify plant ACs because plant ACs seem not to have conserved catalytic domains (Gehring, 2010). However, Gehring (2010) proposed that plant ACs might have the conserved motif [RKS]X[DE]X(9,11)[KR]X(1,3)[ED] in their catalytic domains. To date, experimentally identified ACs in plants are PsiP in *Zea mays* (Moutinho et al., 2001), HpAC1 in *Hippeastrum x hybridum* (Swiezawska et al., 2014), AtKUP7, ATPPR-AC, AtClAP and LRRAC1 in *Arabidopsis thaliana* (Al-Younis et al., 2015; Bianchet et al., 2019; Chatukuta et al., 2018; Ruzvidzo et al., 2013), NbAC in *Nicotiana benthamiana* (Ito et al., 2014), and MpCAPE in *Marchantia polymorpha* (Kasahara et al., 2016). Of note, these plant ACs, except HpAC1 and MpCAPE, appeared to have the AC-motif proposed by Gehring (2010). Therefore, it seems to be difficult to identify plant ACs if just based on this motif search. It is also noticeable that *AT4G15640* and *AT3G21465* are annotated as ACs on The Arabidopsis Information Resource (TAIR), but there is no experimental confirmation.

The aims of this thesis

The mitochondrial unfolded protein response (UPR^{mt}) is described as the transcriptional response that regulates nuclear gene expression during mitochondrial malfunction to maintain mitochondrial homeostasis. The aim of paper I is to review and compare UPR^{mt}-related signalling across eukaryotic kingdoms, including animals, fungi and plants.

The study of plant mitochondria usually requires isolation of pure, intact and functional mitochondria from plant tissues. The aim of paper II is to present a strategy for efficient isolation of mitochondria from leaf tissues of *Arabidopsis thaliana* by using continuous Percoll density gradients.

Despite a relatively thorough understanding of basic mitochondrial functions, many mitochondrial proteins and processes remain poorly understood. The aim of paper III is to characterize the two *Arabidopsis thaliana* genes, *AT4G15640* and *AT3G21465*, which are predicted as mitochondria-targeted proteins and have been poorly annotated as adenyl cyclases on TAIR.

Summary of papers

Paper I summarizes the current knowledge of UPR^{mt} across eukaryotic kingdoms, including animals, fungi and plants. UPR^{mt} has been extensively studied in animals, whereas very few related-UPR^{mt} have been described in yeast. In plants, little is known about the UPR^{mt} and only few regulators have recently been identified. In this work, we compare the UPR^{mt} across kingdoms. Our study indicates that each kingdom has evolved their own specific regulators, which however induce very similar groups of target genes. Our meta-analysis identifies homologs of known UPR^{mt} regulators and their responsive genes across eukaryotic kingdoms, which could be of interest for future research.

Paper II describes two strategies for plant growth (in soil and in liquid half-strength Murashige and Skoog media) and an efficient method of mitochondrial isolation from leaf tissues of *Arabidopsis thaliana*. By using continuous Percoll density gradients, isolated mitochondria are relatively free from chloroplast contamination. Isolated Arabidopsis mitochondria obtained by this method can be either used for assays requiring intact mitochondria, e.g. import assays or respiration measurements, or be stored at -80°C for later use, e.g. BN-PAGE or western blot.

Paper III describes the characterization of two *Arabidopsis thaliana* genes, *AT4G15640* and *AT3G21465*. We show that AT4G15640 and AT3G21465 are unlikely to be ACs as previously annotated on TAIR. Instead, AT4G15640 and AT3G21465 are land plant-specific mitochondrial proteins that are essential for plant performance. Knocking out both *AT4G15640* and *AT3G21465* results in low abundance and activity of mitochondrial OXPHOS complexes, thus reducing capacity of oxygen consumption. Our immunoblotting and tandem mass spectrometry (MS/MS) analysis using isolation mitochondria show a severe perturbation of the mitochondrial proteome and reduction of many OXPHOS components due to loss of *AT4G15640* and *AT3G21465*. Using co-immunoprecipitation, we confirm that AT4G15640 and AT3G21465 are part of the mtSSU, in line with two proteomic studies of Arabidopsis mitoribosome during the course of our study. Therefore, we named AT4G15640 and AT3G21465 as mitochondrial TRANslation factor 1 (mTRAN1) and 2 (mTRAN2), respectively. Transcriptome profile of *mtran1 mtran2* mutant resembles most two mutants defective in a mitoribosomal protein and shows no clear effects on mitochondrial splicing and editing, thus indicating mitochondrial translation defects. *In organello* protein synthesis and polysome fractionation assays suggest that mTRAN proteins

are required for mitochondrial translation initiation. Our motif analysis suggests that the 5'UTRs of mitochondrial mRNAs contain two potential mitoribosome binding sites that are A/U-rich regions (CUUUxU and AAGAAx/AxAAAG). Moreover, the RNA electrophoretic mobility shift assays show that mTRAN1 binds to these A/U-rich domains in the 5'UTRs of mitochondrial mRNAs to initiate translation. Finally, our Ribo-seq analysis shows that not only a subset, but all mitochondrial mRNAs have lower ribosome loading levels in the *mtran* mutants compared to in the wild type, suggesting that mTRAN proteins are universal mtSSU-embedded translation initiation factors.

Discussion

In paper I, the current knowledge of UPR^{mt}-related signalling across eukaryotic kingdoms, including animals, fungi and plants, was summarized and compared. The comparison indicates that each kingdom has evolved their own specific regulators, which however induce very similar groups of target genes, such as mitochondrial (co-)chaperones and proteases. Homologs of known UPR^{mt} regulators and responsive genes are identified across eukaryotic kingdoms, which might be interesting for future research. The authors hypothesized that such different UPR^{mt} pathways occurring across kingdoms could be due to major evolutionary events, such as rise of multicellularity or colonization of land. Indeed, the ANAC017 group – one of the main UPR^{mt} regulators in land plants, is suggested to be evolved from ancestral NACs (found in at least some green algae) during the period of land colonization by plants (Khan and Van Aken, 2022). In plants, "classical" mitochondrial retrograde signalling and UPR^{mt} appear to be the same response during mitochondrial dysfunction. In Arabidopsis, UPR^{mt} is activated in response to mitochondrial malfunction by treatment of Doxycycline (Dox) - a mitochondrial ribosome inhibitor, MitoBlock-6 (MB) - an inhibitor of protein import into mitochondria and AA, which inhibits electron transfer at the center N of complex III leading to an increase in ROS. However, the molecular signals from a dysfunctional mitochondrion and how they initiate this signalling pathway remain enigmatic.

In paper II, we described an efficient method of mitochondrial isolation from leaf tissues of *Arabidopsis thaliana* by using continuous Percoll-PVP density gradients. The most advantage of this protocol is that freshly isolated mitochondria are intact and pure (relatively free form chloroplast contamination), which is of great importance for following assays requiring functional mitochondria, e.g. *in organello* protein synthesis (Kwasniak-Owczarek et al., 2022), import assays (Zhang et al., 2012) and oxygen consumption measurement (Keech et al., 2005). However, this method usually requires a large amount of starting plant material and takes a few hours to complete. Another method of plant mitochondrial isolation, IMTACT (Boussardon et al., 2020), in which transgenic Arabidopsis carrying mitochondrial OUTER MEMBRANE 64 (OM64) - biotin ligase recognition peptide (BLRP) placed under tissue-specific promoters, enables cell-specific biotinylated mitochondria to be purified with streptavidin magnetic beads in less than 30 min (Boussardon and Keech, 2022). As compared to IMTACT, our described

mitochondrial isolation protocol is slower (timewise) and requires much more plant material. Nevertheless, IMTACT requires generation of transgenic plants, which would take time to produce a desired plant line. For instance, if we want to apply IMTACT on the *mtran* double mutants for mitochondrial isolation, we must cross the *mtran* double mutant line with the OM64-BLRP line, which would take at least several months to get a homozygous *mtran* double mutant line expressing OM64-BLRP. Depending on the purposes plus time management, we recommend you to wisely choose which method of Arabidopsis mitochondrial isolation will be suitable for your project.

In paper III, the two *Arabidopsis thaliana* genes, *AT4G15640* and *AT3G21465*, were characterized. It turned out that these genes are unlikely to be ACs as annotated on TAIR. The study shows that AT4G15640 and AT3G21465 are land-plant specific mitochondrial proteins that are critical for plant growth. Strikingly, AT4G15640 and AT3G21465 are shown to be part of the mtSSU and are of great importance for efficient mitochondrial translation initiation. Therefore, AT4G15640 and AT3G21465 are suggested to be annotated as mitochondrial TRANslation factor 1 (mTRAN1) and mitochondrial TRANslation factor 2 (mTRAN2), respectively. Of note, comparison of transcriptomic data (the *mtran1 mtran2* mutant versus *rps10* mutants, which have reduced expression of mtSSU ribosomal protein *RPS10*) showed that UPR^{mt} was activated, leading to induction of target genes in ANAC017 pathway in both mutants. Wang and Auwerx (2017) showed that in the Arabidopsis *mitochondrial ribosomal protein L1* (*mrpl1-1*) mutant, UPR^{mt} was activated, which in turn induced ethylene responses as a systemic signal. Together, these suggest that UPR^{mt} is activated by impairment of mitochondrial translation. Such a UPR^{mt} activation was not only observed in plants, but also in animals, for instance, knockout of mitochondrial ribosomal protein triggered mitonuclear protein imbalance, which activated the UPR^{mt} in *Caenorhabditis elegans* (*C. elegans*) (Houtkooper et al., 2013). Therefore, imbalance between nuclear- and mitochondrially-encoded proteins probably induces the plant UPR^{mt} during malfunctioning mitochondrial translation. Upon UPR^{mt} activation, ANAC017 and ethylene signalling pathways are independently induced. This suggests that there are possibly specific signal molecules inducing different signalling responses. However, the specific signals from mitochondria defective in translation and how they induce the UPR^{mt} in plants remain elusive.

Knockout of *mTRAN1* and *mTRAN2* showed a reduction in OXPHOS complex abundance and activity, which resulted in a strong decrease in capacity of the cytochrome *c* oxidase respiratory pathway. Such a defect caused *mtran1 mtran2* mutants to rely on the alternative respiration. Rolland et al. (2019) proposed that the UPR^{mt} in *C. elegans* was activated when most mitochondrial processes required for the maintenance of mitochondrial homeostasis, e.g mtETC, were compromised. A general signal that possibly triggers UPR^{mt} is a decrease in mitochondrial membrane potential, which results in a decrease in mitochondrial protein import, likely leading

to accumulation of non-imported mitochondrial proteins (Tran and Van Aken, 2020). As loss of *mTRAN1* and *mTRAN2* impaired mtETC, one could expect that mitochondrial membrane potential was possibly reduced though it was not confirmed experimentally, causing activation of UPR^{mt}. In addition, *mtran1 mtran2* mutants showed a defect in complex I and III, which could lead to an increase in the rate of superoxide production (Cadenas et al., 1977; Møller, 2001; Murphy, 2009). Although ROS measurement was not carried out in the study, superoxide – a signal that could trigger the plant UPR^{mt} (Tran and Van Aken, 2020), could be expected to be increased and activate UPR^{mt} due to loss of *mTRAN1* and *mTRAN2*.

Surprisingly, the RNA-seq data of *mtran1 mtran2* mutant showed a downregulation of 117 chloroplast-encoded transcripts, which was also observed in two previous studies (Adamowicz-Skrzypkowska et al., 2020; Zubo et al., 2014). Of note, the chloroplast transcriptome of *mtran1 mtran2* mutant showed that all chloroplast-encoded tRNAs were significantly downregulated, indicating that chloroplast gene expression was likely to be decreased, which could lead to a decrease in photosynthesis and an increase in ROS production in chloroplast (Arsova et al., 2010; Kindgren et al., 2012; Myouga et al., 2008). ROS can damage proteins inside the chloroplasts, causing activation of chloroplast unfolded protein response (cpUPR) (Kessler and Longoni, 2019). Indeed, *ClpB3* – a cpUPR marker gene (Llamas et al., 2017), was upregulated in the *mtran1 mtran2* mutant. ClpB3 is a nuclear-encoded chloroplastic Clp protease that helps refolding unfolded/misfolded/aggregated 1-deoxy-D-xylulose-5-phosphate synthase (DXS) – an enzyme that converts pyruvate and D-glyceraldehyde-3-phosphate (D-GAP) into 1-deoxy-D-xylulose-5-phosphate (DXP) in the first step of the methylerythritol phosphate (MEP) pathway occurring within the chloroplasts (Pulido et al., 2016). DXS aggregation was formed after chloroplast translation was specifically inhibited by lincomycin even though DXS transcript levels remained unchanged and only its protein levels increased (Llamas et al., 2017). The *mtran1 mtran2* mutant had all chloroplast-encoded tRNAs downregulated, suggesting that chloroplast translation was likely to be perturbed. Therefore, one could expect that DXS aggregation would occur, leading to the upregulation of *ClpB3*. Taken together, we suggest that loss of *mTRAN* genes not only induces UPR^{mt} but also activates cpUPR.

All in all, compromised mitochondrial translation in plants could result in (i) mitonuclear protein imbalance, (ii) a decrease in mitochondrial membrane potential leading to accumulation of non-import protein in mitochondria, and (iii) impaired mtETC causing an increase in ROS production in mitochondria. These consequences could activate UPR^{mt} and another as yet known (probably retrograde) signalling pathway that apparently can reduce chloroplast transcription, possibly leading to a decrease in chloroplast gene expression, which causes activation of cpUPR. Another hypothesis is that there is possibly a crosstalk between mitochondria and chloroplasts (but not via the nucleus), in which mitochondrial

gene expression could somehow affect transcription and/or even gene expression in chloroplasts.

To date, the full mechanism of mitochondrial translation in plants remains elusive. The atomic structure of cauliflower mitoribosomes revealed by Waltz et al. (2020b) helps predicting how plant mitoribosome initiates translation. Waltz and his co-workers suggested that mTRAN1 (named as mS83/rPPR10 by the authors) is a PPR protein, which functions as a RNA-binding protein. However, the PPR codes of mTRAN proteins could not be predicted by the PPRCODE web server (Yan et al., 2019). mTRAN1 resides in a cleft of the mtSSU, where its PPR domains might recognize and bind to AxAAA-related motifs of mRNAs to initiate translation because plant mitochondrial mRNAs do not contain SD sequences nor do plant mitochondrial rRNAs have anti-SD sequences. These AxAAA-related motifs were found in the 5'UTRs of 17 out of 33 mitochondrially-encoded mRNAs (Waltz et al., 2020b). In contrast, our polysome profiling showed that mTRAN1 and mTRAN2 are required for mitoribosome binding/translation initiation of not only mitochondrial mRNAs containing such an AxAAA 5'UTR motif (*NAD9*, *COX2* and *ATP9*) but also mitochondrial mRNAs that do not appear to contain this binding site (*NAD7*, *COB*, *ATP1* and *ATP8*). Moreover, the Ribo-seq analysis of mitochondrial genes further supports that mTRAN proteins are universal mtSSU-embedded translation initiation factors, which could recognize the motif CUUUxU/AxAAAG/AAGAAx in the 5'UTRs of mitochondrial mRNAs to initiate translation based on our motif analysis and RNA electrophoretic mobility shift assays (REMSAs). To verify the interaction between mTRAN1 and mitochondrial mRNAs *in vivo*, we will perform RNA Immunoprecipitation Sequencing (RIP-seq) using Arabidopsis cell culture transformed with mTRAN1-GFP and/or isolated mitochondria from a stably transformed Arabidopsis line expressing mTRAN1-GFP. Transcripts interacting with mTRAN1-GFP complexes will be purified using GFP-affinity purification and subsequently sequenced to find out if mTRAN1 interacts with the vast majority of mitochondrial mRNAs *in planta*, further supporting our finding that mTRAN1 is a universal translation initiation factor of mtSSU. In addition, RIP-seq could also allow us to identify the mitoribosomal binding sites to validate our REMSA results.

As mitochondria originated from the ancient endosymbiotic bacteria, mitochondrial translation could be expected to resemble bacterial translation, at least partially. However, comparison of bacterial ribosomes versus mitoribosomes of mammals, yeast and plants showed the diversity of mitoribosome structure, indicating that eukaryotic mitoribosomes have evolved to adapt to particular niches during evolution (Waltz et al., 2020a). This suggests that mitochondrial translation in general and mitochondrial translation initiation in particular could also be diverse across eukaryotic kingdoms. In bacteria, the ribosomal small subunit binds to the SD motif of mRNA using an anti-SD sequence of 16S rRNA (Shine and Dalgarno, 1974). In addition, bacterial translation initiation requires initiation factor (IF) 1, 2

and 3. Unlike bacteria, eukaryotes, including yeast, mammals and plants, do not have SD sequences in the 5'UTRs of mitochondrially-encoded mRNAs. In mammals (at least in humans), most of mitochondrial mRNAs do not have 5'UTRs (Montoya et al., 1981). Kummer et al. (2018) suggested that the PPR protein mS39, which is located in the mtSSU, binds to the U-rich motif downstream the start codon of mRNAs to initiate translation. Notably, the PPRCODE prediction tool–Yin Lab (Yan et al., 2019) predicts that mS39 has four PPR motifs that bind to RNA bases (G)(C>U)(C>U>A)(-) with low scores. Thus, it is possible that both mS39 and mTRAN proteins are PPR-like proteins that do not obey the "classical" PPR code rule. Mammals lack mitochondrial IF1 (mtIF1) and require mtIF2 and mtIF3 for translation initiation (Ayyub and Varshney, 2020). In yeast, the mtSSU contains a platform formed by mS35, mS46 and extensions of uS3m and uS5m, which is suggested to be the mtSSU-mRNA interaction site during translation initiation (Itoh et al., 2020). Mitochondrial translation initiation in yeast seems to recruit universal mtIFs and specific translation activators that are likely to recognize specific 5'UTRs of mitochondrial mRNAs (Derbikova et al., 2018). Therefore, the mtSSU-mRNA interaction site proposed by Itoh et al. (2020) is expected to act as a platform for mtIFs and translation activators to bind to the 5'UTRs of mitochondrial mRNAs to initiate translation. In fact, several translation activators were co-purified with the yeast mitoribosome (Desai et al., 2017). In plants, mTRAN1 is likely to be a PPR-like protein acting as a mRNA-binding factor of the mtSSU. Of note, both yeast and plant mitochondrial mRNAs have long 5'UTRs (Derbikova et al., 2018; Waltz et al., 2020a). Therefore, one could speculate that yeast and plant mitochondrial translation initiation/mtSSU-mRNA binding could somehow use a comparable mechanism. Our findings suggest that mTRAN proteins act as universal recognition factors for mitochondrial mRNAs, however, there is a high possibility that mtIFs and/or mitochondrial translation activators required for recognition of different specific motifs of mRNAs exist in plants. To date, very little is known about mtIFs in plants, e.g. only MTL1 and RFL8 have recently been identified as specific proteins mandatory for translation of *NAD7* and $ccmFN_2$, respectively (Haili et al., 2016; Nguyen et al., 2021). We attempted to perform a BLAST search in *Arabidopsis thaliana* to identify proteins that are similar to bacterial translation IFs (unpublished data). The putative subcellular localization of identified proteins was searched in SUBA5 (Hooper et al., 2017). Bacterial translation IF1 has a similar protein, AT4G11175, which is targeted to chloroplasts and enables mRNA-binding (Bach-Pages et al., 2020; Millen et al., 2001; Trotta et al., 2019). Bacterial translation IF2 has 64 similar proteins with low scores of similarities, of which, 11 are targeted to mitochondria. Bacterial translation IF3 resembles 11 proteins, of which, AT1G34360 annotated as a translation IF3 family protein, is targeted to mitochondria (Senkler et al., 2017b). It is worth to mention that AT1G34360 did not give a high score of similarity by BLAST, but it is probably because the length of bacterial IF3 protein sequence (180 amino acids) is shorter as compared to that of AT1G34360 (520 amino acids). Atkinson et al. (2012) attempted to find functional

orthologues of mtIF3 in yeast by a sensitive PSI-Blast across eukaryotes, as BlastP searches alone could not detect mtIF3 homologues from distantly related eukaryotes. They found that Aim23p in yeast was a "missing" orthologue similar to mtIF3 in other eukaryotes and successfully showed that it functioned as the mtIF3 in yeast. Surprisingly, their phylogenetic analysis also revealed AL6G45350 as an orthologue of mtIF2 in *Arabidopsis lyrata*, which is a homologue to AT4G11160 in *Arabidopsis thaliana*. AT4G11160 was also found in our BLAST search but with a low score of similarity. According to SUBA5, it is predicted to be localized in cytosol, chloroplasts and mitochondria and no experimental studies have confirmed its subcellular localization. Atkinson et al. (2012) also identified SMO171G0119 as an orthologue of mtIF3 in *Selaginella moellendorffii* (an early vascular plant), which is a homologue to AT1G34360 in *Arabidopsis thaliana*.

Taken together, our findings suggest that AT4G11160 and AT1G34360 in *Arabidopsis thaliana* could function similarly to mtIF2 and mtIF3 in other eukaryotes, although AT4G11160 is only predicted to be targeted to mitochondria. If it is true, eukaryotic mitochondria seem to have lost mtIF1 and retain mtIF2 and mtIF3 for translation initiation during evolution. Mammalian mtIF2 has an extension domain (37 amino acids long) that functionally compensates for the absence of mtIF1 (Gaur et al., 2008; Yassin et al., 2011). This domain prevents tRNA from binding to the ribosomal A site, thus facilitating the fMet-tRNA to bind to the ribosomal P site during translation initiation (Kummer et al., 2018; Yassin et al., 2011). However, the conservation of this extension domain is limited to vertebrates (Atkinson et al., 2012). The role of mammalian mtIF3 is not clear. It is suggested that the mtSSU associates with mtIF2 and mtIF3 to form a translation initiation complex, ensuring that mRNA is stably bound to mtSSU prior to tRNA recruitment and before mtSSU and mtLSU assemble into a monosome (Kummer and Ban, 2021). In yeast, mtIF3 seems not to be a core component for translation of all mRNAs, but mitochondrial translation lacking mtIF3 is strongly imbalanced (Derbikova et al., 2018; Kuzmenko et al., 2016). In fact, yeast mitochondria are likely to recruit specific translation activator complexes to bind to the 5'UTRs of mRNAs to initiate translation (Derbikova et al., 2018). Therefore, it is difficult to predict whether plant mtIF2 and mtIF3 (if any) function in a comparable way as in other eukaryotes. In this study, we propose that mTRANs are PPR-like proteins that do not follow the "classical" PPR code rule and bind to the A/U-rich domains in the 5'UTRs of mRNAs to initiate translation. Perhaps due to their substantial length, the plant mitochondrial mRNA's 5'UTRs might form either the 2D or 3D structures to bring the binding sites physically closer to the start codon. Universal mtIFs and/or specific mtIFs/translation activators possibly help the mtSSU find the correct binding site and/or stably bind to mRNAs during the initiation step.

Conclusion

In conclusion, the thesis work suggests that compromised mitochondrial translation results in the UPR^{mt} activation in plants. In addition, we show that mTRAN proteins act as universal recognition factors of mtSSU for mitochondrial mRNAs to initiate translation. This indicates that translation initiation by mitochondrial ribosomes occurs in a fundamentally different way in plants as compared to in bacteria, yeast and mammals. mtSSU-mRNA binding in plants may also require mitochondrial translation IFs, which could be at least partially similar to in other eukaryotes. Therefore, further studies, such as characterizing Arabidopsis mutant(s) lacking functional mtIF2 and/or mtIF3 (see discussion), are required to demonstrate this hypothesis and to gain a broader insight into the mechanism of mitochondrial translation in plants.

Acknowledgements

I would like to thank my main supervisor, Olivier Van Aken, for his guidance, support, and encouragement throughout my PhD study. I appreciate the fact that Olivier's office door is always open so I can bother him whenever I need his support. Thank you, Olivier, for everything you have done for me during my journey at Lund University (LU).

I also want to thank my co-supervisor, Allan Rasmusson, for his support and advice. I have to admit that I have "borrowed" quite many chemicals and equipment from Allan's lab, but he is always chill whenever I do it.

I would like to thank my examiner (the department representative), Klas Flärdh, and my scientific mentor, Courtney Stairs, for supporting me throughout my PhD study.

Regarding the mTRAN project, I would like to thank all the co-authors for their amazing work: Vivian Schmitt, Sbatie Lama, Chuande Wang, Alexandra Launay-Avon, Katja Bernfur, Kristin Hofmann, Kasim Khan, Benoit Castandet, Fredrik Levander, Allan Rasmusson, Hakim Mireau and Etienne Delannoy. I am grateful for the financial support from the Swedish Research Council (Vetenskapsrådet 2017-03854; 2021-04358), Crafoord Foundation (20170862; 20190868), Carl Trygger Foundation (CTS 17 487), Kungl. Fysiografiska Sällskapet i Lund, Jörgen Lindström's Foundation, Axel Hallströms donation and the Department of Biology at LU.

My sincere thanks go to all members (former and current) of Van Aken's lab: Abraham Ontiveros Cisneros, Vivian Schmitt, Kasim Khan, Oliver Moss, Jule Salfeld, Helene Röhricht, Essam Darwish, Sylwia Kacprzak, Ritesh Ghosh, Ameneh Khani, Berivan Mansuroglu and Alex Van Moerkercke. Thank you for always helping me and creating such a nice working environment that I have enjoyed a lot. I want to especially thank Abraham for being my best friend both at work and outside the lab. Thanks for all your support, advice and the BS talks we have had together. Without you, I would have never made the most important decision here (only you understand, for sure). My special thanks also go to Vivian Schmitt – the very first student that I have ever supported. Thanks for all memorable funny moment and your hardworking experiment, especially mitoprep (though I know you did not like it) and REMSAs. Thank you, Kasim Khan, for supporting me and having fun with me in the lab.

My special thanks go to Ewa Krupinska (LP3) for always supporting and giving me advice regarding the difficulty of mTRAN protein expression and purification.

I would like to thank the PhD students (former and current) at the Biology Building, LU. Thank you, Juan Manuel Orozco-Rodríguez, for helping with my protein expression, and I really enjoyed doing teaching with you. Thank you, Humberto Itriago, Katie Laschanzky, Karla Iveth Aguilera Campos, Judith Matavacas, Dima Massri and Teresa Garibo Domingo, for having fun with me during the time I spent at LU. I also want to thank other PhD students: Veronica Ekdahl, David Stuart, Beer Sen, Vinardas Kelpas, Oscar Miguel Rollano Penaloza, Swati Aggarwal and Mengshu Hao.

I also want to thank the PIs, post-docs, administrative staffs, research engineerings and service technicians at the Biology Building, LU: Wolfgang Knecht, Mats Hansson, Lars Hederstedt, Sara Bengtsson, Lena Magnusson, Elisabeth Gauger Nilsson, Eva Svensson, Parminder Singh Mavi, Saritha Panthapulakkal Narayanan, Lars Fredriksson, Heather Sullivan, Nils Sundqvist, Sakthivel Kailasam, Shakhira Zakhrabekova, Chatarina Mattson, Torbjörn Säll, Carin Jarl-Sunesson, Rawana Alkhalili, Bradley Dotson, Deepak Anand, Claes von Wachenfeldt, Marita Cohn, Fredric Carlsson, Julia Lienard, Maria Gourdon, Céleste Sele and Anna Rasmussen.

Last but not least, I would like to say thanks to my family and friends, which will be written in my mother tongue, Vietnamese.

Trước hết, con muốn gửi lời cảm ơn đến gia đình: bố, mẹ, và chị. Con cảm ơn bố mẹ vì đã luôn luôn lo lắng, ủng hộ và yêu thương con vô điều kiện trong suốt quá trình học tập và làm việc nghiên cứu khoa học của con. Con đã đi xa nhà gần tám năm và bố mẹ cũng đã già đi nhiều nhưng vẫn luôn theo dõi và ủng hộ con. Con xin cảm ơn vì bố mẹ đã làm những điều tuyệt vời nhất cho con. Cảm ơn bà chị Thỏ vì đã luôn theo sát, kèm cặp, đốc thúc và cho tiền thằng em học hành chăm chỉ (và cả đi chơi) trong suốt những năm qua. Có chị gái luôn là số một! Con cũng gửi lời cảm ơn đến các ông, bà, bác, chú, cô, dì, cậu, mợ đã luôn hỏi thăm và động viên con.

Cảm ơn những người bạn ở Lund trong suốt quãng thời gian qua. Cảm ơn anh Thông và chị Âu vì những chuyến đi hiking, những bữa ăn vui vẻ, và đã luôn giúp đỡ em và Linh. Cảm ơn Hà và Đạt vì những bữa ăn và chuyến đi chơi vui vẻ. Đặc biệt, cảm ơn hai đứa vì đã giúp anh gặp được Linh. Cảm ơn Tâm vì đã chơi điện tử với tao mặc dù bây giờ tao đã bỏ rơi không chơi game với mày nữa. Cảm ơn Huy vì đã đến thăm và đi chơi với tao.

Gửi đến Võ Hoàng Yến Linh (tức Linh béo hay em béo, nhưng bây giờ gầy rồi): Cảm ơn em vì đã đến Lund để anh gặp được em và mình đã quen nhau. Cảm ơn em đã luôn chịu đựng và luôn ủng hộ anh trong suốt quãng thời gian qua. Em là động lực lớn để anh cố gắng trong suốt chặng đường của mình ở Lund. Anh mong rằng chúng mình sẽ không chỉ dừng lại ở đây mà sẽ còn đi xa hơn nữa cùng với nhau

trong mối quan hệ này và trong tương lai. Cho dù tương lai có thế nào, em vẫn luôn là kỉ niệm đáng nhớ và đáng trân trọng nhất mà anh đã có được ở Lund!

References

Adamowicz-Skrzypkowska, A., Kwasniak-Owczarek, M., Van Aken, O., Kazmierczak, U., and Janska, H. (2020). Joint inhibition of mitochondrial complex IV and alternative oxidase by genetic or chemical means represses chloroplast transcription in Arabidopsis. Philosophical Transactions of the Royal Society of London Series B, Biological Sciences *375*, 20190409.

Al-Younis, I., Wong, A., and Gehring, C. (2015). The *Arabidopsis thaliana* K^+-uptake permease 7 (AtKUP7) contains a functional cytosolic adenylate cyclase catalytic centre. FEBS letters *589*, 3848-3852.

Allen, J.F. (2015). Why chloroplasts and mitochondria retain their own genomes and genetic systems: Colocation for redox regulation of gene expression. Proceedings of the National Academy of Sciences *112*, 10231-10238.

Amunts, A., Brown, A., Toots, J., Scheres, S.H.W., and Ramakrishnan, V. (2015). The structure of the human mitochondrial ribosome. Science *348*, 95-98.

Andres-Colas, N., Zhu, Q., Takenaka, M., De Rybel, B., Weijers, D., and Van Der Straeten, D. (2017). Multiple PPR protein interactions are involved in the RNA editing system in Arabidopsis mitochondria and plastids. Proceedings of the National Academy of Sciences of the United States of America *114*, 8883-8888.

Arrieta-Montiel, M.P., Shedge, V., Davila, J., Christensen, A.C., and Mackenzie, S.A. (2009). Diversity of the Arabidopsis mitochondrial genome occurs via nuclear-controlled recombination activity. Genetics *183*, 1261-1268.

Arsova, B., Hoja, U., Wimmelbacher, M., Greiner, E., Ustun, S., Melzer, M., Petersen, K., Lein, W., and Bornke, F. (2010). Plastidial thioredoxin z interacts with two fructokinase-like proteins in a thiol-dependent manner: evidence for an essential role in chloroplast development in *Arabidopsis* and *Nicotiana benthamiana*. The Plant Cell *22*, 1498-1515.

Atkinson, G.C., Kuzmenko, A., Kamenski, P., Vysokikh, M.Y., Lakunina, V., Tankov, S., Smirnova, E., Soosaar, A., Tenson, T., and Hauryliuk, V. (2012). Evolutionary and genetic analyses of mitochondrial translation initiation factors identify the missing mitochondrial IF3 in *S. cerevisiae*. Nucleic Acids Research *40*, 6122-6134.

Ayyub, S.A., and Varshney, U. (2020). Translation initiation in mammalian mitochondria - a prokaryotic perspective. RNA Biology *17*, 165-175.

Bach-Pages, M., Homma, F., Kourelis, J., Kaschani, F., Mohammed, S., Kaiser, M., van der Hoorn, R.A.L., Castello, A., and Preston, G.M. (2020). Discovering the RNA-binding proteome of plant leaves with an improved RNA interactome capture method. Biomolecules *10*, 661.

Backert, S., Lynn Nielsen, B., and Börner, T. (1997). The mystery of the rings: structure and replication of mitochondrial genomes from higher plants. Trends in Plant Science *2*, 477-483.

Barkan, A., Rojas, M., Fujii, S., Yap, A., Chong, Y.S., Bond, C.S., and Small, I. (2012). A combinatorial amino acid code for RNA recognition by pentatricopeptide repeat proteins. PLoS Genetics *8*, e1002910.

Barkan, A., and Small, I. (2014). Pentatricopeptide repeat proteins in plants. Annual Review of Plant Biology *65*, 415-442.

Bensley, R.R., and Hoerr, N.L. (1934). Studies on cell structure by the freezing-drying method VI. The preparation and properties of mitochondria. The Anatomical Record *60*, 449-455.

Bentolila, S., Heller, W.P., Sun, T., Babina, A.M., Friso, G., van Wijk, K.J., and Hanson, M.R. (2012). RIP1, a member of an Arabidopsis protein family, interacts with the protein RARE1 and broadly affects RNA editing. Proceedings of the National Academy of Sciences of the United States of America *109*, E1453-1461.

Bentolila, S., Oh, J., Hanson, M.R., and Bukowski, R. (2013). Comprehensive high-resolution analysis of the role of an Arabidopsis gene family in RNA editing. PLoS Genetics *9*, e1003584.

Bergthorsson, U., Adams, K.L., Thomason, B., and Palmer, J.D. (2003). Widespread horizontal transfer of mitochondrial genes in flowering plants. Nature *424*, 197-201.

Bianchet, C., Wong, A., Quaglia, M., Alqurashi, M., Gehring, C., Ntoukakis, V., and Pasqualini, S. (2019). An *Arabidopsis thaliana* leucine-rich repeat protein harbors an adenylyl cyclase catalytic center and affects responses to pathogens. Journal of Plant Physiology *232*, 12-22.

Bieri, P., Greber, B.J., and Ban, N. (2018). High-resolution structures of mitochondrial ribosomes and their functional implications. Current Opinion in Structural Biology *49*, 44-53.

Binder, S., Hölzle, A., and Jonietz, C. (2011). RNA processing and RNA stability in plant mitochondria. In Plant Mitochondria, F. Kempken, ed. (Springer, New York, NY), pp. 107-130.

Binder, S., Marchfelder, A., and Brennicke, A. (1994). RNA editing of $tRNA^{Phe}$ and $tRNA^{Cys}$ in mitochondria of *Oenothera berteriana* is initiated in precursor molecules. Molecular and General Genetics *244*, 67-74.

Bjorkholm, P., Harish, A., Hagstrom, E., Ernst, A.M., and Andersson, S.G. (2015). Mitochondrial genomes are retained by selective constraints on protein targeting. Proceedings of the National Academy of Sciences of the United States of America *112*, 10154-10161.

Blanco, E., Fortunato, S., Viggiano, L., and de Pinto, M.C. (2020). Cyclic AMP: A polyhedral signalling molecule in plants. International Journal of Molecular Sciences *21*, 4862.

Bonen, L. (2008). Cis- and trans-splicing of group II introns in plant mitochondria. Mitochondrion *8*, 26-34.

Bonen, L., and Vogel, J. (2001). The ins and outs of group II introns. Trends in Genetics *17*, 322-331.

Borner, G.V., Morl, M., Wissinger, B., Brennicke, A., and Schmelzer, C. (1995). RNA editing of a group II intron in *Oenothera* as a prerequisite for splicing. Molecular and General Genetics *246*, 739-744.

Boussardon, C., and Keech, O. (2022). Cell type-specific isolation of mitochondria in Arabidopsis. Methods in Molecular Biology *2363*, 13-23.

Boussardon, C., Przybyla-Toscano, J., Carrie, C., and Keech, O. (2020). Tissue-specific isolation of Arabidopsis/plant mitochondria - IMTACT (isolation of mitochondria tagged in specific cell types). The Plant Journal *103*, 459-473.

Braun, H.P. (2020). The oxidative phosphorylation system of the mitochondria in plants. Mitochondrion *53*, 66-75.

Brown, G.G., Colas des Francs-Small, C., and Ostersetzer-Biran, O. (2014). Group II intron splicing factors in plant mitochondria. Frontiers in Plant Science *5*, 35.

Buchanan, B.B., Gruissem, W., and Jones, R.L. (2015). Biochemistry and molecular biology of plants, 2nd edition. John Wiley and Sons.

Cadenas, E., Boveris, A., Ragan, C.I., and Stoppani, A.O. (1977). Production of superoxide radicals and hydrogen peroxide by NADH-ubiquinone reductase and ubiquinol-cytochrome c reductase from beef-heart mitochondria. Archives of Biochemistry and Biophysics *180*, 248-257.

Carrillo, C., and Bonen, L. (1997). RNA editing status of *nad7* intron domains in wheat mitochondria. Nucleic Acids Research *25*, 403-409.

Cermakian, N., Ikeda, T.M., Cedergren, R., and Gray, M.W. (1996). Sequences homologous to yeast mitochondrial and bacteriophage T3 and T7 RNA polymerases are widespread throughout the eukaryotic lineage. Nucleic Acids Research *24*, 648-654.

Chacinska, A., Koehler, C.M., Milenkovic, D., Lithgow, T., and Pfanner, N. (2009). Importing mitochondrial proteins: machineries and mechanisms. Cell *138*, 628-644.

Chateigner-Boutin, A.L., and Small, I. (2010). Plant RNA editing. RNA Biology *7*, 213-219.

Chatukuta, P., Dikobe, T.B., Kawadza, D.T., Sehlabane, K.S., Takundwa, M.M., Wong, A., Gehring, C., and Ruzvidzo, O. (2018). An Arabidopsis clathrin assembly protein with a predicted role in plant defense can function as an adenylate cyclase. Biomolecules *8*, 15.

Cheng, S., Gutmann, B., Zhong, X., Ye, Y., Fisher, M.F., Bai, F., Castleden, I., Song, Y., Song, B., Huang, J., *et al.* (2016). Redefining the structural motifs that determine RNA binding and RNA editing by pentatricopeptide repeat proteins in land plants. The Plant Journal *85*, 532-547.

Chevigny, N., Schatz-Daas, D., Lotfi, F., and Gualberto, J.M. (2020). DNA repair and the stability of the plant mitochondrial genome. International Journal of Molecular Sciences *21*, 328.

Coquille, S., Filipovska, A., Chia, T., Rajappa, L., Lingford, J.P., Razif, M.F., Thore, S., and Rackham, O. (2014). An artificial PPR scaffold for programmable RNA recognition. Nature Communications *5*, 5729.

Dai, H., Lo, Y.S., Litvinchuk, A., Wang, Y.T., Jane, W.N., Hsiao, L.J., and Chiang, K.S. (2005). Structural and functional characterizations of mung bean mitochondrial nucleoids. Nucleic Acids Research *33*, 4725-4739.

Davila, J.I., Arrieta-Montiel, M.P., Wamboldt, Y., Cao, J., Hagmann, J., Shedge, V., Xu, Y.Z., Weigel, D., and Mackenzie, S.A. (2011). Double-strand break repair processes drive evolution of the mitochondrial genome in Arabidopsis. BMC Biology *9*, 64.

Day, D., Neuburger, M., and Douce, R. (1985). Biochemical characterization of chlorophyll-free mitochondria from pea leaves. Functional Plant Biology *12*, 219-228.

De Clercq, I., Vermeirssen, V., Van Aken, O., Vandepoele, K., Murcha, M.W., Law, S.R., Inze, A., Ng, S., Ivanova, A., Rombaut, D., *et al.* (2013). The membrane-bound NAC transcription factor ANAC013 functions in mitochondrial retrograde regulation of the oxidative stress response in Arabidopsis. The Plant Cell *25*, 3472-3490.

Derbikova, K.S., Levitsky, S.A., Chicherin, I.V., Vinogradova, E.N., and Kamenski, P.A. (2018). Activation of yeast mitochondrial translation: Who is in charge? Biochemistry (Moscow) *83*, 87-97.

Desai, N., Brown, A., Amunts, A., and Ramakrishnan, V. (2017). The structure of the yeast mitochondrial ribosome. Science *355*, 528-531.

Dudkina, N.V., Heinemeyer, J., Sunderhaus, S., Boekema, E.J., and Braun, H.P. (2006). Respiratory chain supercomplexes in the plant mitochondrial membrane. Trends in Plant Science *11*, 232-240.

Escobar, M.A., Geisler, D.A., and Rasmusson, A.G. (2006). Reorganization of the alternative pathways of the Arabidopsis respiratory chain by nitrogen supply: opposing effects of ammonium and nitrate. The Plant Journal *45*, 775-788.

Eubel, H., Heinemeyer, J., and Braun, H.P. (2004). Identification and characterization of respirasomes in potato mitochondria. Plant Physiology *134*, 1450-1459.

Eubel, H., Jansch, L., and Braun, H.P. (2003). New insights into the respiratory chain of plant mitochondria. Supercomplexes and a unique composition of complex II. Plant Physiology *133*, 274-286.

Farre, J.C., Aknin, C., Araya, A., and Castandet, B. (2012). RNA editing in mitochondrial trans-introns is required for splicing. PloS One *7*, e52644.

Fey, J., Weil, J.H., Tomita, K., Cosset, A., Dietrich, A., Small, I., and Marechal-Drouard, L. (2002). Role of editing in plant mitochondrial transfer RNAs. Gene *286*, 21-24.

Frey, T.G., and Mannella, C.A. (2000). The internal structure of mitochondria. Trends in Biochemical Sciences *25*, 319-324.

Fromm, S., Senkler, J., Eubel, H., Peterhansel, C., and Braun, H.P. (2016). Life without complex I: proteome analyses of an Arabidopsis mutant lacking the mitochondrial NADH dehydrogenase complex. Journal of Experimental Botany *67*, 3079-3093.

Fuchs, P., Rugen, N., Carrie, C., Elsasser, M., Finkemeier, I., Giese, J., Hildebrandt, T.M., Kuhn, K., Maurino, V.G., Ruberti, C., *et al.* (2020). Single organelle function and organization as estimated from Arabidopsis mitochondrial proteomics. The Plant Journal *101*, 420-441.

Gaspari, M., Falkenberg, M., Larsson, N.G., and Gustafsson, C.M. (2004). The mitochondrial RNA polymerase contributes critically to promoter specificity in mammalian cells. The EMBO Journal *23*, 4606-4614.

Gaur, R., Grasso, D., Datta, P.P., Krishna, P.D., Das, G., Spencer, A., Agrawal, R.K., Spremulli, L., and Varshney, U. (2008). A single mammalian mitochondrial translation initiation factor functionally replaces two bacterial factors. Molecular Cell *29*, 180-190.

Gehring, C. (2010). Adenyl cyclases and cAMP in plant signaling - past and present. Cell Communication and Signalling *8*, 15.

Gifford, R.M. (2003). Plant respiration in productivity models: conceptualisation, representation and issues for global terrestrial carbon-cycle research. Functional Plant Biology *30*, 171-186.

Gilkerson, R., Bravo, L., Garcia, I., Gaytan, N., Herrera, A., Maldonado, A., and Quintanilla, B. (2013). The mitochondrial nucleoid: integrating mitochondrial DNA into cellular homeostasis. Cold Spring Harbor Perspectives in Biology *5*, a011080.

Giraud, E., Van Aken, O., Ho, L.H., and Whelan, J. (2009). The transcription factor ABI4 is a regulator of mitochondrial retrograde expression of ALTERNATIVE OXIDASE 1A. Plant Physiology *150*, 1286-1296.

Gray, M.W., and Lang, B.F. (1998). Transcription in chloroplasts and mitochondria: a tale of two polymerases. Trends in Microbiology *6*, 1-3.

Greber, B.J., Bieri, P., Leibundgut, M., Leitner, A., Aebersold, R., Boehringer, D., and Ban, N. (2015). The complete structure of the 55S mammalian mitochondrial ribosome. Science *348*, 303-308.

Greenleaf, A.L., Kelly, J.L., and Lehman, I.R. (1986). Yeast RPO41 gene product is required for transcription and maintenance of the mitochondrial genome. Proceedings of the National Academy of Sciences of the United States of America *83*, 3391-3394.

Grewe, F., Herres, S., Viehover, P., Polsakiewicz, M., Weisshaar, B., and Knoop, V. (2011). A unique transcriptome: 1782 positions of RNA editing alter 1406 codon identities in mitochondrial mRNAs of the lycophyte *Isoetes engelmannii*. Nucleic Acids Research *39*, 2890-2902.

Gualberto, J.M., Mileshina, D., Wallet, C., Niazi, A.K., Weber-Lotfi, F., and Dietrich, A. (2014). The plant mitochondrial genome: dynamics and maintenance. Biochimie *100*, 107-120.

Gualberto, J.M., and Newton, K.J. (2017). Plant mitochondrial genomes: dynamics and mechanisms of mutation. Annual Review of Plant Biology *68*, 225-252.

Guillaumot, D., Lopez-Obando, M., Baudry, K., Avon, A., Rigaill, G., Falcon de Longevialle, A., Broche, B., Takenaka, M., Berthome, R., De Jaeger, G., *et al.* (2017). Two interacting PPR proteins are major Arabidopsis editing factors in plastid and mitochondria. Proceedings of the National Academy of Sciences of the United States of America *114*, 8877-8882.

Gully, B.S., Shah, K.R., Lee, M., Shearston, K., Smith, N.M., Sadowska, A., Blythe, A.J., Bernath-Levin, K., Stanley, W.A., Small, I.D., *et al.* (2015). The design and structural characterization of a synthetic pentatricopeptide repeat protein. Acta Crystallographica Section D-biological Crystallography *71*, 196-208.

Haili, N., Planchard, N., Arnal, N., Quadrado, M., Vrielynck, N., Dahan, J., des Francs-Small, C.C., and Mireau, H. (2016). The MTL1 pentatricopeptide repeat protein is required for both translation and splicing of the mitochondrial *NADH DEHYDROGENASE SUBUNIT7* mRNA in Arabidopsis. Plant Physiology *170*, 354-366.

Handa, H. (2008). Linear plasmids in plant mitochondria: peaceful coexistences or malicious invasions? Mitochondrion *8*, 15-25.

Hazle, T., and Bonen, L. (2007). Comparative analysis of sequences preceding protein-coding mitochondrial genes in flowering plants. Molecular Biology and Evolution *24*, 1101-1112.

Hecht, J., Grewe, F., and Knoop, V. (2011). Extreme RNA editing in coding islands and abundant microsatellites in repeat sequences of *Selaginella moellendorffii* mitochondria: the root of frequent plant mtDNA recombination in early tracheophytes. Genome Biology and Evolution *3*, 344-358.

Hedtke, B., Borner, T., and Weihe, A. (1997). Mitochondrial and chloroplast phage-type RNA polymerases in Arabidopsis. Science *277*, 809-811.

Hedtke, B., Borner, T., and Weihe, A. (2000). One RNA polymerase serving two genomes. EMBO Reports *1*, 435-440.

Hedtke, B., Legen, J., Weihe, A., Herrmann, R.G., and Borner, T. (2002). Six active phage-type RNA polymerase genes in *Nicotiana tabacum*. The Plant Journal *30*, 625-637.

Hedtke, B., Meixner, M., Gillandt, S., Richter, E., Börner, T., and Weihe, A. (1999). Green fluorescent protein as a marker to investigate targeting of organellar RNA polymerases of higher plants *in vivo*. The Plant Journal *17*, 557-561.

Holec, S., Lange, H., Kuhn, K., Alioua, M., Borner, T., and Gagliardi, D. (2006). Relaxed transcription in Arabidopsis mitochondria is counterbalanced by RNA stability control mediated by polyadenylation and polynucleotide phosphorylase. Molecular Cell Biology *26*, 2869-2876.

Homble, F., Krammer, E.M., and Prevost, M. (2012). Plant VDAC: facts and speculations. Biochimica et Biophysica Acta *1818*, 1486-1501.

Hooper, C.M., Castleden, I.R., Tanz, S.K., Aryamanesh, N., and Millar, A.H. (2017). SUBA4: the interactive data analysis centre for Arabidopsis subcellular protein locations. Nucleic Acids Research *45*, D1064-D1074.

Houtkooper, R.H., Mouchiroud, L., Ryu, D., Moullan, N., Katsyuba, E., Knott, G., Williams, R.W., and Auwerx, J. (2013). Mitonuclear protein imbalance as a conserved longevity mechanism. Nature *497*, 451-457.

Huang, S., Taylor, N.L., Whelan, J., and Millar, A.H. (2009). Refining the definition of plant mitochondrial presequences through analysis of sorting signals, N-terminal modifications, and cleavage motifs. Plant Physiology *150*, 1272-1285.

Ito, M., Takahashi, H., Sawasaki, T., Ohnishi, K., Hikichi, Y., and Kiba, A. (2014). Novel type of adenylyl cyclase participates in tabtoxinine-beta-lactam-induced cell death and occurrence of wildfire disease in *Nicotiana benthamiana*. Plant Signaling & Behavior *9*, e27420.

Itoh, Y., Naschberger, A., Mortezaei, N., Herrmann, J.M., and Amunts, A. (2020). Analysis of translating mitoribosome reveals functional characteristics of translation in mitochondria of fungi. Nature Communications *11*, 5187.

Ivanova, A., Law, S.R., Narsai, R., Duncan, O., Lee, J.H., Zhang, B., Van Aken, O., Radomiljac, J.D., van der Merwe, M., Yi, K., *et al.* (2014). A functional antagonistic relationship between auxin and mitochondrial retrograde signaling regulates *Alternative Oxidase 1a* expression in Arabidopsis. Plant Physiology *165*, 1233-1254.

Kacprzak, S.M., Dahlqvist, A., and Van Aken, O. (2020). The transcription factor ANAC017 is a key regulator of mitochondrial proteotoxic stress responses in plants. Philosophical transactions of the Royal Society of London Series B, Biological Sciences *375*, 20190411.

Kasahara, M., Suetsugu, N., Urano, Y., Yamamoto, C., Ohmori, M., Takada, Y., Okuda, S., Nishiyama, T., Sakayama, H., Kohchi, T., *et al.* (2016). An adenylyl cyclase with a phosphodiesterase domain in basal plants with a motile sperm system. Scientific Reports *6*, 39232.

Ke, J., Chen, R.Z., Ban, T., Zhou, X.E., Gu, X., Tan, M.H., Chen, C., Kang, Y., Brunzelle, J.S., Zhu, J.K., *et al.* (2013). Structural basis for RNA recognition by a dimeric PPR-protein complex. Nature Structural & Molecular Biology *20*, 1377-1382.

Keech, O., Dizengremel, P., and Gardeström, P. (2005). Preparation of leaf mitochondria from *Arabidopsis thaliana*. Physiologia Plantarum *124*, 403-409.

Kessler, F., and Longoni, P. (2019). How chloroplasts protect themselves from unfolded proteins. Elife *8*, e51430.

Khan, K., and Van Aken, O. (2022). The colonization of land was a likely driving force for the evolution of mitochondrial retrograde signalling in plants. Journal of Experimental Botany *73*, 7182-7197.

Kindgren, P., Kremnev, D., Blanco, N.E., de Dios Barajas Lopez, J., Fernandez, A.P., Tellgren-Roth, C., Kleine, T., Small, I., and Strand, A. (2012). The plastid redox insensitive 2 mutant of Arabidopsis is impaired in PEP activity and high light-dependent plastid redox signalling to the nucleus. The Plant Journal *70*, 279-291.

Klusch, N., Senkler, J., Yildiz, O., Kuhlbrandt, W., and Braun, H.P. (2021). A ferredoxin bridge connects the two arms of plant mitochondrial complex I. The Plant Cell *33*, 2072-2091.

Kmiec, B., Teixeira, P.F., and Glaser, E. (2014). Shredding the signal: targeting peptide degradation in mitochondria and chloroplasts. Trends in Plant Science *19*, 771-778.

Knoop, V. (2011). When you can't trust the DNA: RNA editing changes transcript sequences. Cellular and Molecular Life Sciences *68*, 567-586.

Kobayashi, Y., Dokiya, Y., Kumazawa, Y., and Sugita, M. (2002). Non-AUG translation initiation of mRNA encoding plastid-targeted phage-type RNA polymerase in *Nicotiana sylvestris*. Biochemical and Biophysical Research Communications *299*, 57-61.

Kobayashi, Y., Dokiya, Y., and Sugita, M. (2001). Dual targeting of phage-type RNA polymerase to both mitochondria and plastids is due to alternative translation initiation in single transcripts. Biochemical and Biophysical Research Communications *289*, 1106-1113.

Krause, F., Reifschneider, N.H., Vocke, D., Seelert, H., Rexroth, S., and Dencher, N.A. (2004). "Respirasome"-like supercomplexes in green leaf mitochondria of spinach. The Journal of Biological Chemistry *279*, 48369-48375.

Kuhn, K., Obata, T., Feher, K., Bock, R., Fernie, A.R., and Meyer, E.H. (2015). Complete mitochondrial complex I deficiency induces an up-regulation of respiratory fluxes that is abolished by traces of functional complex I. Plant Physiology *168*, 1537-1549.

Kuhn, K., Richter, U., Meyer, E.H., Delannoy, E., de Longevialle, A.F., O'Toole, N., Borner, T., Millar, A.H., Small, I.D., and Whelan, J. (2009). Phage-type RNA polymerase RPOTmp performs gene-specific transcription in mitochondria of *Arabidopsis thaliana*. The Plant Cell *21*, 2762-2779.

Kuhn, K., Weihe, A., and Borner, T. (2005). Multiple promoters are a common feature of mitochondrial genes in Arabidopsis. Nucleic Acids Research *33*, 337-346.

Kummer, E., and Ban, N. (2021). Mechanisms and regulation of protein synthesis in mitochondria. Nature Reviews Molecular Cell Biology *22*, 307-325.

Kummer, E., Leibundgut, M., Rackham, O., Lee, R.G., Boehringer, D., Filipovska, A., and Ban, N. (2018). Unique features of mammalian mitochondrial translation initiation revealed by cryo-EM. Nature *560*, 263-267.

Kuzmenko, A., Derbikova, K., Salvatori, R., Tankov, S., Atkinson, G.C., Tenson, T., Ott, M., Kamenski, P., and Hauryliuk, V. (2016). Aim-less translation: loss of *Saccharomyces cerevisiae* mitochondrial translation initiation factor mIF3/Aim23 leads to unbalanced protein synthesis. Scientific Reports *6*, 18749.

Kwasniak-Owczarek, M., Tomal, A., and Janska, H. (2022). Assessment of protein synthesis in mitochondria isolated from rosette leaves and liquid culture seedlings of Arabidopsis. Methods in Molecular Biology *2363*, 183-197.

Lambowitz, A.M., and Zimmerly, S. (2004). Mobile group II introns. Annual Reviews of Genetics *38*, 1-35.

Liere, K., and Börner, T. (2011). Transcription in plant mitochondria. In Plant Mitochondria, F. Kempken, ed. (Springer, New York, NY), pp. 85-105.

Lightowlers, R.N., and Chrzanowska-Lightowlers, Z.M. (2013). Human pentatricopeptide proteins: only a few and what do they do? RNA Biology *10*, 1433-1438.

Lin, Y.F., Schulz, A.M., Pellegrino, M.W., Lu, Y., Shaham, S., and Haynes, C.M. (2016). Maintenance and propagation of a deleterious mitochondrial genome by the mitochondrial unfolded protein response. Nature *533*, 416-419.

Lippok, B., Brennicke, A., and Wissinger, B. (1994). Differential RNA editing in closely related introns in *Oenothera* mitochondria. Molecular and General Genetics *243*, 39-46.

Llamas, E., Pulido, P., and Rodriguez-Concepcion, M. (2017). Interference with plastome gene expression and Clp protease activity in Arabidopsis triggers a chloroplast unfolded protein response to restore protein homeostasis. PLoS Genetics *13*, e1007022.

Logan, D.C. (2006). Plant mitochondrial dynamics. Biochimica et Biophysica Acta *1763*, 430-441.

Logan, D.C. (2012). Mitochondrial dynamics: when form meets function. Available at: http://6e.plantphys.net/essay12.03.html [Accessed 4th January 2023].

Lurin, C., Andres, C., Aubourg, S., Bellaoui, M., Bitton, F., Bruyere, C., Caboche, M., Debast, C., Gualberto, J., Hoffmann, B., *et al.* (2004). Genome-wide analysis of Arabidopsis pentatricopeptide repeat proteins reveals their essential role in organelle biogenesis. The Plant Cell *16*, 2089-2103.

Maclean, A.E., Hertle, A.P., Ligas, J., Bock, R., Balk, J., and Meyer, E.H. (2018). Absence of complex I is associated with diminished respiratory chain function in European mistletoe. Current Biology *28*, 1614-1619 e1613.

Maldonado, M., Guo, F., and Letts, J.A. (2021). Atomic structures of respiratory complex III_2, complex IV, and supercomplex III_2-IV from vascular plants. Elife *10*, e62047.

Maldonado, M., Padavannil, A., Zhou, L., Guo, F., and Letts, J.A. (2020). Atomic structure of a mitochondrial complex I intermediate from vascular plants. Elife *9*, e56664.

Marechal-Drouard, L., Kumar, R., Remacle, C., and Small, I. (1996). RNA editing of larch mitochondrial $tRNA^{His}$ precursors is a prerequisite for processing. Nucleic Acids Research *24*, 3229-3234.

Marechal-Drouard, L., Ramamonjisoa, D., Cosset, A., Weil, J.H., and Dietrich, A. (1993). Editing corrects mispairing in the acceptor stem of bean and potato mitochondrial phenylalanine transfer RNAs. Nucleic Acids Research *21*, 4909-4914.

Martin, W.F., Garg, S., and Zimorski, V. (2015). Endosymbiotic theories for eukaryote origin. Philosophical transactions of the Royal Society of London Series B, Biological Sciences *370*, 20140330.

Masters, B.S., Stohl, L.L., and Clayton, D.A. (1987). Yeast mitochondrial RNA polymerase is homologous to those encoded by bacteriophages T3 and T7. Cell *51*, 89-99.

McDonald, A.E., Vanlerberghe, G.C., and Staples, J.F. (2009). Alternative oxidase in animals: unique characteristics and taxonomic distribution. Journal of Experimental Botany *212*, 2627-2634.

Michel, F., Umesono, K., and Ozeki, H. (1989). Comparative and functional anatomy of group II catalytic introns - a review. Gene *82*, 5-30.

Millar, A.H., Eubel, H., Jansch, L., Kruft, V., Heazlewood, J.L., and Braun, H.P. (2004). Mitochondrial cytochrome *c* oxidase and succinate dehydrogenase complexes contain plant specific subunits. Plant Molecular Biology *56*, 77-90.

Millar, A.H., Siedow, J.N., and Day, D. (2015). Respiration and photorespiration. In Biochemistry and Molecular Biology of Plants, 2nd edition, B.B. Buchanan et al., eds. (John Wiley and Sons), pp. 610-655.

Millen, R.S., Olmstead, R.G., Adams, K.L., Palmer, J.D., Lao, N.T., Heggie, L., Kavanagh, T.A., Hibberd, J.M., Gray, J.C., Morden, C.W., *et al.* (2001). Many parallel losses of infA from chloroplast DNA during angiosperm evolution with multiple independent transfers to the nucleus. The Plant Cell *13*, 645-658.

Millerd, A., Bonner, J., Axelrod, B., and Bandurski, R. (1951). Oxidative and phosphorylative activity of plant mitochondria. Proceedings of the National Academy of Sciences of the United States of America *37*, 855-862.

Møller, I.M. (2001). Plant mitochondria and oxidative stress: electron transport, NADPH turnover, and metabolism of reactive oxygen species. Annual Review of Plant Physiology and Plant Molecular Biology *52*, 561-591.

Møller, I.M. (2016). What is hot in plant mitochondria? Physiologia Plantarum *157*, 256-263.

Møller, I.M., Rasmusson, A.G., and Van Aken, O. (2021). Plant mitochondria - past, present and future. The Plant Journal *108*, 912-959.

Møller, I.M., and Sweetlove, L.J. (2010). ROS signalling – specificity is required. Trends in Plant Science *15*, 370-374.

Montoya, J., Ojala, D., and Attardi, G. (1981). Distinctive features of the 5'-terminal sequences of the human mitochondrial mRNAs. Nature *290*, 465-470.

Moullan, N., Mouchiroud, L., Wang, X., Ryu, D., Williams, E.G., Mottis, A., Jovaisaite, V., Frochaux, M.V., Quiros, P.M., Deplancke, B., *et al.* (2015). Tetracyclines disturb mitochondrial function across eukaryotic models: a call for caution in biomedical research. Cell Reports *10*, 1681-1691.

Moutinho, A., Hussey, P.J., Trewavas, A.J., and Malho, R. (2001). cAMP acts as a second messenger in pollen tube growth and reorientation. Proceedings of the National Academy of Sciences of the United States of America *98*, 10481-10486.

Mower, J.P. (2020). Variation in protein gene and intron content among land plant mitogenomes. Mitochondrion *53*, 203-213.

Murphy, M.P. (2009). How mitochondria produce reactive oxygen species. The Biochemical Journal *417*, 1-13.

Myouga, F., Hosoda, C., Umezawa, T., Iizumi, H., Kuromori, T., Motohashi, R., Shono, Y., Nagata, N., Ikeuchi, M., and Shinozaki, K. (2008). A heterocomplex of iron superoxide dismutases defends chloroplast nucleoids against oxidative stress and is essential for chloroplast development in Arabidopsis. The Plant Cell *20*, 3148-3162.

Negruk, V.I., Eisner, G.I., Redichkina, T.D., Dumanskaya, N.N., Cherny, D.I., Alexandrov, A.A., Shemyakin, M.F., and Butenko, R.G. (1986). Diversity of *Vicia faba* circular mtDNA in whole plants and suspension cultures. Theoretical and Applied Genetics *72*, 541-547.

Ng, S., De Clercq, I., Van Aken, O., Law, S.R., Ivanova, A., Willems, P., Giraud, E., Van Breusegem, F., and Whelan, J. (2014). Anterograde and retrograde regulation of nuclear genes encoding mitochondrial proteins during growth, development, and stress. Molecular Plant *7*, 1075-1093.

Ng, S., Ivanova, A., Duncan, O., Law, S.R., Van Aken, O., De Clercq, I., Wang, Y., Carrie, C., Xu, L., Kmiec, B., *et al.* (2013). A membrane-bound NAC transcription factor, ANAC017, mediates mitochondrial retrograde signaling in Arabidopsis. The Plant Cell *25*, 3450-3471.

Nguyen, T.T., Planchard, N., Dahan, J., Arnal, N., Balzergue, S., Benamar, A., Bertin, P., Brunaud, V., Dargel-Graffin, C., Macherel, D., *et al.* (2021). A case of gene fragmentation in plant mitochondria fixed by the selection of a compensatory restorer of fertility-like PPR gene. Molecular Biology and Evolution *38*, 3445-3458.

Noeske, J., Wasserman, M.R., Terry, D.S., Altman, R.B., Blanchard, S.C., and Cate, J.H. (2015). High-resolution structure of the *Escherichia coli* ribosome. Nature Structural & Molecular Biology *22*, 336-341.

O'Leary, B.M., and Plaxton, W.C. (2016). Plant Respiration. In eLS, pp. 1-11.

Oda, K., Yamato, K., Ohta, E., Nakamura, Y., Takemura, M., Nozato, N., Akashi, K., Kanegae, T., Ogura, Y., Kohchi, T., *et al.* (1992). Gene organization deduced from the complete sequence of liverwort *Marchantia polymorpha* mitochondrial DNA: A primitive form of plant mitochondrial genome. Journal of Molecular Biology *223*, 1-7.

Oldenburg, D.J., and Bendich, A.J. (1996). Size and structure of replicating mitochondrial DNA in cultured tobacco cells. The Plant Cell *8*, 447-461.

Oldenkott, B., Yamaguchi, K., Tsuji-Tsukinoki, S., Knie, N., and Knoop, V. (2014). Chloroplast RNA editing going extreme: more than 3400 events of C-to-U editing in the chloroplast transcriptome of the lycophyte *Selaginella uncinata*. RNA *20*, 1499-1506.

Olyslaegers, G., and Verbelen, J.-P. (1998). Improved staining of F-actin and co-localization of mitochondria in plant cells. Journal of Microscopy *192*, 73-77.

Palade, G.E. (1952). The fine structure of mitochondria. The Anatomical Record *114*, 427-451.

Palmfeldt, J., and Bross, P. (2017). Proteomics of human mitochondria. Mitochondrion *33*, 2-14.

Parsons, D.F., Bonner Jr, W.D., and Verboon, J.G. (1965). Electron microscopy of isolated plant mitochondria and plastids using both the thin-section and negative-staining techniques. Canadian Journal of Botany *43*, 647-655.

Prokisch, H., Scharfe, C., Camp, D.G., 2nd, Xiao, W., David, L., Andreoli, C., Monroe, M.E., Moore, R.J., Gritsenko, M.A., Kozany, C., *et al.* (2004). Integrative analysis of the mitochondrial proteome in yeast. PLoS Biology *2*, e160.

Pulido, P., Llamas, E., Llorente, B., Ventura, S., Wright, L.P., and Rodriguez-Concepcion, M. (2016). Specific Hsp100 chaperones determine the fate of the first enzyme of the plastidial isoprenoid pathway for either refolding or degradation by the stromal Clp protease in Arabidopsis. PLoS Genetics *12*, e1005824.

Ramrath, D.J.F., Niemann, M., Leibundgut, M., Bieri, P., Prange, C., Horn, E.K., Leitner, A., Boehringer, D., Schneider, A., and Ban, N. (2018). Evolutionary shift toward protein-based architecture in trypanosomal mitochondrial ribosomes. Science *362*, 6413.

Rao, R.S., Salvato, F., Thal, B., Eubel, H., Thelen, J.J., and Møller, I.M. (2017). The proteome of higher plant mitochondria. Mitochondrion *33*, 22-37.

Rasmusson, A.G., Soole, K.L., and Elthon, T.E. (2004). Alternative NAD(P)H dehydrogenases of plant mitochondria. Annual Review of Plant Biology *55*, 23-39.

Roger, A.J., Munoz-Gomez, S.A., and Kamikawa, R. (2017). The origin and diversification of mitochondria. Current Biology *27*, R1177-R1192.

Rolland, S.G., Schneid, S., Schwarz, M., Rackles, E., Fischer, C., Haeussler, S., Regmi, S.G., Yeroslaviz, A., Habermann, B., Mokranjac, D., *et al.* (2019). Compromised mitochondrial protein import acts as a signal for UPR^{mt}. Cell Reports *28*, 1659-1669 e1655.

Rugen, N., Straube, H., Franken, L.E., Braun, H.P., and Eubel, H. (2019). Complexome profiling reveals association of PPR proteins with ribosomes in the mitochondria of plants. Molecular & Cellular Proteomics *18*, 1345-1362.

Ruzvidzo, O., Dikobe, B.T., Kawadza, D.T., Mabadahanye, G.H., Chatukuta, P., and Kwezi, L. (2013). Recombinant expression and functional testing of candidate adenylate cyclase domains. Methods in Molecular Biology *1016*, 13-25.

Sabetta, W., Vannini, C., Sgobba, A., Marsoni, M., Paradiso, A., Ortolani, F., Bracale, M., Viggiano, L., Blanco, E., and de Pinto, M.C. (2016). Cyclic AMP deficiency negatively affects cell growth and enhances stress-related responses in tobacco Bright Yellow-2 cells. Plant Molecular Biology *90*, 467-483.

Sagan, L. (1967). On the origin of mitosing cells. Journal of Theoretical Biology *14*, 255-274.

Schleiff, E., and Becker, T. (2011). Common ground for protein translocation: access control for mitochondria and chloroplasts. Nature Reviews Molecular Cell Biology *12*, 48-59.

Schmidt, O., Pfanner, N., and Meisinger, C. (2010). Mitochondrial protein import: from proteomics to functional mechanisms. Nature Reviews Molecular Cell Biology *11*, 655-667.

Schmitz-Linneweber, C., and Small, I. (2008). Pentatricopeptide repeat proteins: a socket set for organelle gene expression. Trends in Plant Science *13*, 663-670.

Schuster, W., Ternes, R., Knoop, V., Hiesel, R., Wissinger, B., and Brennicke, A. (1991). Distribution of RNA editing sites in *Oenothera* mitochondrial mRNAs and rRNAs. Current Genetics *20*, 397-404.

Senkler, J., Rugen, N., Eubel, H., Hegermann, J., and Braun, H.P. (2018). Absence of complex I implicates rearrangement of the respiratory chain in European mistletoe. Current Biology *28*, 1606-1613 e1604.

Senkler, J., Senkler, M., and Braun, H.P. (2017a). Structure and function of complex I in animals and plants - a comparative view. Physiologia Plantarum *161*, 6-15.

Senkler, J., Senkler, M., Eubel, H., Hildebrandt, T., Lengwenus, C., Schertl, P., Schwarzlander, M., Wagner, S., Wittig, I., and Braun, H.P. (2017b). The mitochondrial complexome of *Arabidopsis thaliana*. The Plant Journal *89*, 1079-1092.

Shen, C., Zhang, D., Guan, Z., Liu, Y., Yang, Z., Yang, Y., Wang, X., Wang, Q., Zhang, Q., Fan, S., *et al.* (2016). Structural basis for specific single-stranded RNA recognition by designer pentatricopeptide repeat proteins. Nature Communications *7*, 11285.

Shi, X., Castandet, B., Germain, A., Hanson, M.R., and Bentolila, S. (2017). ORRM5, an RNA recognition motif-containing protein, has a unique effect on mitochondrial RNA editing. Journal of Experimental Botany *68*, 2833-2847.

Shi, X., Germain, A., Hanson, M.R., and Bentolila, S. (2016). RNA Recognition Motif-Containing Protein ORRM4 broadly affects mitochondrial RNA editing and impacts plant development and flowering. Plant Physiology *170*, 294-309.

Shine, J., and Dalgarno, L. (1974). The 3'-terminal sequence of *Escherichia coli* 16S ribosomal RNA: complementarity to nonsense triplets and ribosome binding sites. Proceedings of the National Academy of Sciences of the United States of America *71*, 1342-1346.

Sloan, D.B. (2013). One ring to rule them all? Genome sequencing provides new insights into the "master circle" model of plant mitochondrial DNA structure. The New Phytologist *200*, 978-985.

Sloan, D.B., Alverson, A.J., Chuckalovcak, J.P., Wu, M., McCauley, D.E., Palmer, J.D., and Taylor, D.R. (2012). Rapid evolution of enormous, multichromosomal genomes in flowering plant mitochondria with exceptionally high mutation rates. PLoS Biology *10*, e1001241.

Small, I.D., and Peeters, N. (2000). The PPR motif - a TPR-related motif prevalent in plant organellar proteins. Trends in Biochemical Sciences *25*, 46-47.

Small, I.D., Schallenberg-Rudinger, M., Takenaka, M., Mireau, H., and Ostersetzer-Biran, O. (2020). Plant organellar RNA editing: what 30 years of research has revealed. The Plant Journal *101*, 1040-1056.

Spang, A., Saw, J.H., Jorgensen, S.L., Zaremba-Niedzwiedzka, K., Martijn, J., Lind, A.E., van Eijk, R., Schleper, C., Guy, L., and Ettema, T.J.G. (2015). Complex archaea that bridge the gap between prokaryotes and eukaryotes. Nature *521*, 173-179.

Sutton, C.A., Conklin, P.L., Pruitt, K.D., and Hanson, M.R. (1991). Editing of pre-mRNAs can occur before cis- and trans-splicing in Petunia mitochondria. Molecular Cell Biology *11*, 4274-4277.

Swiezawska, B., Jaworski, K., Pawelek, A., Grzegorzewska, W., Szewczuk, P., and Szmidt-Jaworska, A. (2014). Molecular cloning and characterization of a novel adenylyl cyclase gene, HpAC1, involved in stress signaling in *Hippeastrum x hybridum*. Plant Physiology and Biochemistry/Societe Francaise de Physiologie Vegetale *80*, 41-52.

Takenaka, M., Zehrmann, A., Verbitskiy, D., Kugelmann, M., Hartel, B., and Brennicke, A. (2012). Multiple Organellar RNA Editing Factor (MORF) family proteins are required for RNA editing in mitochondria and plastids of plants. Proceedings of the National Academy of Sciences of the United States of America *109*, 5104-5109.

Tiranti, V., Savoia, A., Forti, F., D'Apolito, M.F., Centra, M., Rocchi, M., and Zeviani, M. (1997). Identification of the gene encoding the human mitochondrial RNA polymerase (h-mtRPOL) by cyberscreening of the Expressed Sequence Tags database. Human Molecular Genetics *6*, 615-625.

Tran, H.C., and Van Aken, O. (2020). Mitochondrial unfolded protein-related responses across kingdoms: similar problems, different regulators. Mitochondrion *53*, 166-177.

Trotta, A., Bajwa, A.A., Mancini, I., Paakkarinen, V., Pribil, M., and Aro, E.M. (2019). The role of phosphorylation dynamics of CURVATURE THYLAKOID 1B in plant thylakoid membranes. Plant Physiology *181*, 1615-1631.

Unseld, M., Marienfeld, J.R., Brandt, P., and Brennicke, A. (1997). The mitochondrial genome of *Arabidopsis thaliana* contains 57 genes in 366,924 nucleotides. Nature Genetics *15*, 57-61.

Uyttewaal, M., Mireau, H., Rurek, M., Hammani, K., Arnal, N., Quadrado, M., and Giege, P. (2008). PPR336 is associated with polysomes in plant mitochondria. Journal of Molecular Biology *375*, 626-636.

Van Aken, O., Ford, E., Lister, R., Huang, S., and Millar, A.H. (2016). Retrograde signalling caused by heritable mitochondrial dysfunction is partially mediated by ANAC017 and improves plant performance. The Plant Journal *88*, 542-558.

Van Aken, O., Pecenkova, T., van de Cotte, B., De Rycke, R., Eeckhout, D., Fromm, H., De Jaeger, G., Witters, E., Beemster, G.T., Inze, D., *et al.* (2007). Mitochondrial type-I prohibitins of *Arabidopsis thaliana* are required for supporting proficient meristem development. The Plant Journal *52*, 850-864.

Van Aken, O., and Rasmusson, A.G. (2022). Plant Mitochondria: Methods and Protocols. In New York: Humana Press.

Van Aken, O., Zhang, B., Law, S., Narsai, R., and Whelan, J. (2013). AtWRKY40 and AtWRKY63 modulate the expression of stress-responsive nuclear genes encoding mitochondrial and chloroplast proteins. Plant Physiology *162*, 254-271.

Van Gestel, K., Kohler, R.H., and Verbelen, J.P. (2002). Plant mitochondria move on F-actin, but their positioning in the cortical cytoplasm depends on both F-actin and microtubules. Journal of Experimental Botany *53*, 659-667.

Vanderauwera, S., Vandenbroucke, K., Inze, A., van de Cotte, B., Muhlenbock, P., De Rycke, R., Naouar, N., Van Gaever, T., Van Montagu, M.C., and Van Breusegem, F. (2012). AtWRKY15 perturbation abolishes the mitochondrial stress response that steers osmotic stress tolerance in Arabidopsis. Proceedings of the National Academy of Sciences of the United States of America *109*, 20113-20118.

Vanlerberghe, G.C., and McIntosh, L. (1996). Signals regulating the expression of the nuclear gene encoding Alternative Oxidase of plant mitochondria. Plant Physiology *111*, 589-595.

Vestergaard, C.L., Flyvbjerg, H., and Møller, I.M. (2012). Intracellular signaling by diffusion: can waves of hydrogen peroxide transmit intracellular information in plant cells? Frontiers in Plant Science *3*, 295.

von Heijne, G. (1986). Why mitochondria need a genome. FEBS letters *198*, 1-4.

Waltz, F., Corre, N., Hashem, Y., and Giege, P. (2020a). Specificities of the plant mitochondrial translation apparatus. Mitochondrion *53*, 30-37.

Waltz, F., and Giege, P. (2020). Striking diversity of mitochondria-specific translation processes across eukaryotes. Trends in Biochemical Sciences *45*, 149-162.

Waltz, F., Nguyen, T.T., Arrive, M., Bochler, A., Chicher, J., Hammann, P., Kuhn, L., Quadrado, M., Mireau, H., Hashem, Y., *et al.* (2019). Small is big in Arabidopsis mitochondrial ribosome. Nature Plants *5*, 106-117.

Waltz, F., Soufari, H., Bochler, A., Giege, P., and Hashem, Y. (2020b). Cryo-EM structure of the RNA-rich plant mitochondrial ribosome. Nature Plants *6*, 377-383.

Wang, X., and Auwerx, J. (2017). Systems phytohormone responses to mitochondrial proteotoxic stress. Molecular Cell *68*, 540-551 e545.

Wang, Z., and Wu, M. (2014). Phylogenomic reconstruction indicates mitochondrial ancestor was an energy parasite. PloS One *9*, e110685.

Wang, Z., and Wu, M. (2015). An integrated phylogenomic approach toward pinpointing the origin of mitochondria. Scientific Reports *5*, 7949.

Watson, Z.L., Ward, F.R., Meheust, R., Ad, O., Schepartz, A., Banfield, J.F., and Cate, J.H. (2020). Structure of the bacterial ribosome at 2 Å resolution. Elife *9*, e60482.

Weihe, A. (2004). The transcription of plant organelle genomes. In Molecular Biology and Biotechnology of Plant Organelles, H. Daniell, and C. Chase, eds. (Springer, Dordrecht), pp. 213-237.

Weihe, A., Hedtke, B., and Borner, T. (1997). Cloning and characterization of a cDNA encoding a bacteriophage-type RNA polymerase from the higher plant *Chenopodium album*. Nucleic Acids Research *25*, 2319-2325.

Whelan, J., and Murcha, M.W. (2015). Methods in Molecular Biology: Plant mitochondria. In New York: Springer.

Wirth, C., Brandt, U., Hunte, C., and Zickermann, V. (2016). Structure and function of mitochondrial complex I. Biochimica et Biophysica Acta *1857*, 902-914.

Wissinger, B., Schuster, W., and Brennicke, A. (1991). Trans splicing in *Oenothera* mitochondria: *nad1* mRNAs are edited in exon and trans-splicing group II intron sequences. Cell *65*, 473-482.

Wolfe, K.H., Li, W.H., and Sharp, P.M. (1987). Rates of nucleotide substitution vary greatly among plant mitochondrial, chloroplast, and nuclear DNAs. Proceedings of the National Academy of Sciences *84*, 9054-9058.

Yagi, Y., Hayashi, S., Kobayashi, K., Hirayama, T., and Nakamura, T. (2013). Elucidation of the RNA recognition code for pentatricopeptide repeat proteins involved in organelle RNA editing in plants. PloS One *8*, e57286.

Yan, J., Yao, Y., Hong, S., Yang, Y., Shen, C., Zhang, Q., Zhang, D., Zou, T., and Yin, P. (2019). Delineation of pentatricopeptide repeat codes for target RNA prediction. Nucleic Acids Research *47*, 3728-3738.

Yassin, A.S., Haque, M.E., Datta, P.P., Elmore, K., Banavali, N.K., Spremulli, L.L., and Agrawal, R.K. (2011). Insertion domain within mammalian mitochondrial translation initiation factor 2 serves the role of eubacterial initiation factor 1. Proceedings of the National Academy of Sciences of the United States of America *108*, 3918-3923.

Yin, P., Li, Q., Yan, C., Liu, Y., Liu, J., Yu, F., Wang, Z., Long, J., He, J., Wang, H.W., *et al.* (2013). Structural basis for the modular recognition of single-stranded RNA by PPR proteins. Nature *504*, 168-171.

Zalman, L.S., Nikaido, H., and Kagawa, Y. (1980). Mitochondrial outer membrane contains a protein producing nonspecific diffusion channels. The Journal of Biological Chemistry *255*, 1771-1774.

Zanlungo, S., Quinones, V., Moenne, A., Holuigue, L., and Jordana, X. (1995). Splicing and editing of *rps10* transcripts in potato mitochondria. Current Genetics *27*, 565-571.

Zaremba-Niedzwiedzka, K., Caceres, E.F., Saw, J.H., Backstrom, D., Juzokaite, L., Vancaester, E., Seitz, K.W., Anantharaman, K., Starnawski, P., Kjeldsen, K.U., *et al.* (2017). Asgard archaea illuminate the origin of eukaryotic cellular complexity. Nature *541*, 353-358.

Zhang, B., Carrie, C., Ivanova, A., Narsai, R., Murcha, M.W., Duncan, O., Wang, Y., Law, S.R., Albrecht, V., Pogson, B., *et al.* (2012). LETM proteins play a role in the accumulation of mitochondrially encoded proteins in *Arabidopsis thaliana* and AtLETM2 displays parent of origin effects. The Journal of Biological Chemistry *287*, 41757-41773.

Zhang, X., Ivanova, A., Vandepoele, K., Radomiljac, J., Van de Velde, J., Berkowitz, O., Willems, P., Xu, Y., Ng, S., Van Aken, O., *et al.* (2017a). The transcription factor MYB29 is a regulator of *ALTERNATIVE OXIDASE 1A*. Plant Physiology *173*, 1824-1843.

Zhang, Y., Beard, K.F.M., Swart, C., Bergmann, S., Krahnert, I., Nikoloski, Z., Graf, A., Ratcliffe, R.G., Sweetlove, L.J., Fernie, A.R., *et al.* (2017b). Protein-protein interactions and metabolite channelling in the plant tricarboxylic acid cycle. Nature Communications *8*, 15212.

Zhao, Q., Wang, J., Levichkin, I.V., Stasinopoulos, S., Ryan, M.T., and Hoogenraad, N.J. (2002). A mitochondrial specific stress response in mammalian cells. The EMBO Journal *21*, 4411-4419.

Zimmerly, S., Hausner, G., and Wu, X. (2001). Phylogenetic relationships among group II intron ORFs. Nucleic Acids Research *29*, 1238-1250.

Zubo, Y.O., Potapova, T.V., Tarasenko, V.I., Borner, T., and Konstantinov, Y.M. (2014). The rate of transcription in Arabidopsis chloroplasts depends on activity of alternative electron transfer pathway in mitochondria. Doklady Biochemistry and Biophysics *455*, 76-79.

Paper I-III

Paper I

Mitochondrion 53 (2020) 166–177

Contents lists available at ScienceDirect

Mitochondrion

journal homepage: www.elsevier.com/locate/mito

Mitochondrial unfolded protein-related responses across kingdoms: similar problems, different regulators

Huy Cuong Tran, Olivier Van Aken*

Department of Biology, Lund University, Lund, Sweden

ARTICLE INFO

Keywords:
Mitochondria
Unfolded protein response
Retrograde signalling
UPR^{mt}
UPR^{am}
mitoCPR

ABSTRACT

Mitochondria are key components of eukaryotic cells, so their proper functioning is monitored via different mitochondrial signalling responses. One of these mitochondria-to-nuclear 'retrograde' responses to maintain mitochondrial homeostasis is the mitochondrial unfolded protein response (UPR^{mt}), which can be activated by a variety of defects including blocking mitochondrial translation, respiration, protein import or transmembrane potential. Although UPR^{mt} was first reported in cultured mammalian cells, this signalling pathway has also been extensively studied in the nematode *Caenorhabditis elegans*. In yeast, there are no published studies focusing on UPR^{mt} in a strict sense, but other unfolded protein responses (UPR) that appear related to UPR^{mt} have been described, such as the UPR activated by protein mistargeting (UPR^{am}) and mitochondrial compromised protein import response (mitoCPR). In plants, very little is known about UPR^{mt} and only recently some of the regulators have been identified. In this paper, we summarise and compare the current knowledge of the UPR^{mt} and related responses across eukaryotic kingdoms: animals, fungi and plants. Our comparison suggests that each kingdom has evolved its own specific set of regulators, however, the functional categories represented among UPR^{mt}–related target genes appear to be largely overlapping. This indicates that the strategies for preserving proper mitochondrial functions are partially conserved, targeting mitochondrial chaperones, proteases, import components, dynamics and stress response, but likely also non-mitochondrial functions including growth regulators/hormone balance and amino acid metabolism. We also identify homologs of known UPR^{mt} regulators and responsive genes across kingdoms, which may be interesting targets for future research.

1. Introduction

The mitochondrion is a key organelle involved in eukaryotic respiration. Although the mitochondrion is suggested to have originated through an endosymbiotic event, the mitochondrion does not function on its own and its activity is integrated with other cellular organelles. The quality and activity of mitochondria are strictly regulated to secure the production of metabolic products and to avoid generating toxic compounds, for instance, reactive oxygen species (ROS) produced by malfunctioning respiration (Moller, 2001; Murphy, 2009; Baker et al.,

Abbreviations: AA, antimycin A; ABC, ATP-binding cassette; ALAAT2, alanine aminotransferase 2; ANAC017, *Arabidopsis* NAC domain containing protein 17; AOX1a, alternative oxidative 1a; ASP2, aspartate aminotransferase 2; ATF-4, activating transcription factor 4; ATF-5, activating transcription factor 5; ATFS-1, Activating Transcription Factor associated with Stress-1; ATPase, adenosine triphosphatase; bHLH, basic helix-loop-helix; bZIP, basic leucine zipper; *C. elegans*, *Caenorhabditis elegans*; CAP, chloramphenicol; CHOP, C/EBP homologous protein; Dox, doxycycline; DVE-1, Defective proVEntriculus 1; EIF2A, eukaryotic initiation factor 2 alpha; EndoG, endonuclease G; ER, endoplasmic reticulum; GPCR, G protein-coupled receptor; IMM, inner mitochondrial membrane; IMS, intermembrane space; IPGAM2, 2,3-biphosphoglycerate-independent phosphoglycerate mutase; ISR, integrated stress response; MAGIC, mitochondria as guardian in cytosol; MAPK, mitogen-activated protein kinase; MB, MitoBlock-6; MGE1, mitochondrial grpe 1; mitoCPR, mitochondrial compromised protein import response; mPOS, mitochondrial precursor over-accumulation stress; MRPs, mitochondrial ribosomal proteins; MRR, mitochondrial retrograde regulation; mtDNA, mitochondrial DNA; mtPQC, mitochondrial protein quality control; MTS, mitochondrial targeting sequence; NLS, nuclear localization sequence; NRF1, nuclear respiratory factor 1; OMM, outer mitochondrial membrane; OPA3, optic atrophy 3; OXPHOS, oxidative phosphorylation; ROS, reactive oxygen species; *S. cerevisiae*, *Saccharomyces cerevisiae*; SOD2, superoxide dismutase 2; SOT12, sulphotransferase 12; TCA, tricarboxylic acid; TF, transcription factor; TIM, translocase of the inner membrane; TOM, translocase of the outer membrane; TOR, target of rapamycin; UBL-5, Ubiquitin-like protein 5; UPR, unfolded protein response; UPR^{am}, unfolded protein responses activated by protein mistargeting; UPR^{ER}, endoplasmic reticulum unfolded protein responses; UPR^{IMS}, UPR in the mitochondrial IMS; UPR^{mt}, mitochondrial unfolded protein response; WT, wild type

* Corresponding author at Molecular Cell Biology, Department of Biology, Lund University, Sölvegatan 35, Lund 223 62, Sweden.
E-mail address: olivier.van_aken@biol.lu.se (O. Van Aken).

https://doi.org/10.1016/j.mito.2020.05.009
Received 12 February 2020; Received in revised form 19 May 2020; Accepted 22 May 2020
Available online 02 June 2020

2011). Human mitochondrial dysfunction is caused by either normal mitochondrial aging or by environmental changes such as fever and medication, or by age-related diseases, such as coronary artery disease, Alzheimer's disease and Parkinson's disease (Ballinger, 2005; Krzywanski et al., 2011; Pellegrino et al., 2013; Selfridge et al., 2013; Duarte et al., 2014; Wolff et al., 2014; Vuda and Kamath, 2016; Abramov et al., 2017). In plants, little is known about which natural conditions cause mitochondrial signalling. Comparative transcriptomics suggested that natural low-oxygen stress, e.g. flooding, may be a natural scenario where mitochondrial signalling is important (Wagner et al., 2018). Many mitochondrial retrograde regulation (MRR) target genes are also induced by a wide variety of biotic and abiotic stress in plants, but it is less clear whether they are regulated by MRR or by other stress-response pathways that converge on overlapping genes (Van Aken et al., 2009; Schwarzlander et al., 2012; Van Aken and Whelan, 2012). Thus, it is important to decipher the underlying mechanisms of mitochondrial signalling to provide new directions for future research, with potential applications in health care and agriculture.

The mitochondrion is a double membrane organelle that is composed of the outer membrane (OMM), the intermembrane space (IMS), the inner membrane (IMM), the cristae and cristae lumen (originated from invagination of the IMM), and the compartment enclosed by the IMM, called the mitochondrial matrix. Aerobic respiration includes three stages: glycolysis (in the cytosol and partly in the plastids), the tricarboxylic acid (TCA) cycle and oxidative phosphorylation (OXPHOS), which occur in the mitochondria. Together, these processes produce adenosine triphosphate (ATP) - the cellular energy currency. Thus, mitochondria are considered as the powerhouses of eukaryotic cells. To allow efficient operation, a continuous flow of information between the nucleus and the mitochondrion is required. Signals originating from the nucleus are transmitted to the mitochondrion, as the nuclear 'anterograde' regulation of mitochondrial activities. This is often of importance during early development and in response to external factors. In return, retrograde signals derived from the mitochondrion are sent to the nucleus and affect nuclear gene expression.

The number of mitochondrial proteins can vary across eukaryotes, e.g. ~1800 proteins in mammals (Palmfeldt and Bross, 2017), > 2000 proteins in plants (Rao et al., 2017) and ~1000 proteins in yeasts (Schmidt et al., 2010). Although mitochondria possess their own protein translation machinery inside the matrix, the vast majority of the mitochondrial proteins is nuclear-encoded, translated by cytosolic ribosomes and imported into mitochondria using a specialized import machinery (Schmidt et al., 2010; Rao et al., 2017). In humans, only 13 crucial OXPHOS proteins, required for the assembly of the respiratory complexes I, III and IV as well as the ATP synthase/complex V, are encoded in the mitochondrial genome (Anderson et al., 1981). In plants, the mitochondrial genome contains 20–40 protein-coding genes (Kubo and Newton, 2008). Approximately 70% of nuclear-encoded mitochondrial proteins have mitochondrial targeting sequences (MTS) in the N-terminus that are chopped off and degraded after import via the translocase of the outer membrane (TOM) and the translocase of the inner membrane (TIM) channels to different sub-mitochondrial compartments (Prokisch et al., 2004; Chacinska et al., 2009; Schleiff and Becker, 2011; Kmiec et al., 2014). The remaining 30%, e.g. mitochondrial proteins residing within the IMM and subunits of the respiratory chain, have non-removable internal signals (Huang et al., 2009; Schleiff and Becker, 2011; Kmiec et al., 2014; Senkler et al., 2017). Mitochondrial protein quality control (mtPQC), including chaperones and proteases, ensures that both imported, and mitochondrially-synthesized proteins are folded correctly, and their quality is approved to maintain mitochondrial proteostasis.

Proper mitochondrial function is maintained via different mitochondrial stress responses. Mitochondrial stress responses include changes in mitochondrial dynamics, selective autophagy of mitochondria (mitophagy), retrograde signalling and the mitochondrial unfolded protein response (UPR^{mt}) (Broda et al., 2018; Hernando-Rodriguez and Artal-Sanz, 2018). Mitochondrial dynamics refers to mitochondrial fission and fusion to preserve mitochondrial shape, distribution and size. In response to stresses, mitochondrial dynamics maintain mitochondrial stability, abundance, distribution and quality, and support compensatory changes by participating in reshaping, rebuilding and recycling impaired mitochondria (Logan, 2010; Eisner et al., 2018). Severely impaired mitochondria may be identified and selectively degraded by mitophagy.

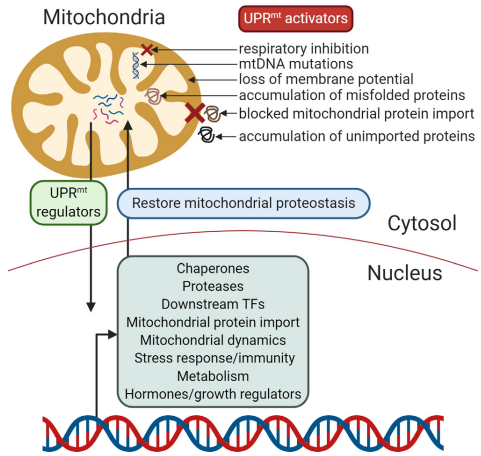

Fig. 1. Overview of the mitochondrial unfolded protein responses (UPR^{mt}) across kingdoms. UPR^{mt} can be activated by various stresses: respiratory inhibition, mutations in mitochondrial DNA (mtDNA), loss of mitochondrial membrane potential, accumulation of misfolded proteins within mitochondria, mitochondrial protein import block and accumulation of mitochondrial unimported proteins. UPR^{mt} activation restores mitochondrial proteostasis by triggering the translocation of UPR^{mt} regulators into the nucleus, resulting in the transcriptional responses of mitochondrial chaperones and proteases, downstream transcription factors (TFs), mitochondrial import components, mitochondrial dynamics, proteins involved in stress response/immunity and metabolism, and hormones/growth regulators. Unfolded proteins accumulating within mitochondria are degraded into peptides by mitochondrial proteases and these peptides can be exported out of the mitochondria to the cytosol. This phenomenon leads to an excessive level of peptides in the cytosol, which can be a signal that activates UPR^{mt}. The figure was created with Biorender.com.

Abnormal mitochondrial proteostasis can robustly activate the UPR^{mt}. UPR^{mt} is defined as the transcriptional response that regulates nuclear gene expression during mitochondrial dysfunction to recover mitochondria and the mitochondrial network, to support cell survival and adaptation. UPR^{mt} can be activated by mutations in the mitochondrial DNA (mtDNA) (Lin et al., 2016), malfunction of the mitochondrial membrane potential (Rolland et al., 2019), imbalance between nuclear- and mitochondria-encoded proteins (Houtkooper et al., 2013), or excessive levels of unfolded or misfolded proteins within mitochondria (Zhao et al., 2002) (Fig. 1). UPR^{mt} is activated to preserve mitochondrial proteostasis by inducing the mitochondrial protein quality control machinery, including chaperones and proteases to control protein folding, assembly and degradation.

In addition to mitophagy and UPR^{mt}, two other mitochondrial stress response pathways have been proposed: translation attenuation (Rainbolt et al., 2013) and the unfolded protein response (UPR) activated by protein mistargeting (UPR^{am}) (Wrobel et al., 2015). Translation attenuation decreases the import of proteins into mitochondria to prevent perturbing mitochondrial proteostasis and disturbing mitochondrial activities. During mitochondrial dysfunction, the influx of

proteins into mitochondria is reduced. As the consequence of translation attenuation, non-imported mitochondrial proteins accumulate in the cytosol, leading to UPR^{am}. Subsequently, activation of UPR^{am} leads to removal of the toxic mislocalized proteins by elevating proteasome activity and decreasing the rate of translation (Al Rawi et al., 2011; Sato and Sato, 2011; Wrobel et al., 2015).

UPR^{mt} was first reported in mammalian cultured cells, where mtDNA was damaged by exposure to ethidium bromide, leading to the transcription of mitochondrial chaperones and proteases (Zhao et al., 2002). Subsequent studies have been mainly carried out on *Caenorhabditis elegans* (*C. elegans*) and mammalian model systems, revealing various components involved in UPR^{mt} activation, including mitochondrial function sensors, regulators of communication between mitochondria and nucleus, regulators of chromatin and transcription factors (Melber and Haynes, 2018). As mitochondrial proteotoxic stress-inducing conditions are likely to occur in all mitochondria-containing eukaryotes, it is likely that UPR^{mt}-like responses are conserved across kingdoms. In this paper, we review and compare current knowledge on UPR^{mt}-related signalling across eukaryotic kingdoms including animals, fungi and plants.

2. The UPR^{mt} in *C. elegans*

In *C. elegans*, the basic leucine zipper (bZIP) transcription factor 'Activating Transcription Factor associated with Stress-1′ (ATFS-1), is a key regulator of UPR^{mt} (Haynes et al., 2010; Melber and Haynes, 2018) (Table 1) (Fig. 2). ATFS-1 contains both a nuclear localization sequence (NLS) and a MTS, allowing its translocation between mitochondria and nucleus to mediate mitochondria-to-nuclear communication (Haynes et al., 2010; Nargund et al., 2012). As a result of mitochondrial dysfunction (see section '*What are the molecular signals triggering UPR^{mt}?*'), unfolded or misfolded proteins inside the mitochondrial matrix are chopped into peptides by the mitochondrial protease ClpP (Haynes et al., 2007). Subsequently, these peptides are transported to the cellular cytoplasm via the mitochondrial ATP-binding cassette (ABC) transporter, HAF-1 (Haynes et al., 2007; Haynes et al., 2010). This phenomenon leads to an excessive level of peptides in the cytosol. Furthermore, the capacity of mitochondrial protein import decreases (Wright et al., 2001; Narendra et al., 2010; Nargund et al., 2012; Wrobel et al., 2015), resulting in reduced mitochondrial import of ATFS-1. Consequently, ATFS-1 accumulates in the cytosol, causing it to translocate from the cytosol to the nucleus and together with Defective proVEntriculus 1 (DVE-1) and Ubiquitin-like protein 5 (UBL-5) (Benedetti et al., 2006; Haynes et al., 2007), it activates the transcription of mitochondrial chaperones *HSP-6* and *HSP-60*, proteases *CLPP1*, *LONP-1*, *SPG-7* and *YMEL-1*, the fission factor *DRP-1* and mitochondrial transporters *TIM-23* and *TIM-17* (Nargund et al., 2012; Nargund et al., 2015). ATFS-1 was found to be negatively regulated by the bZIP protein ZIP-3 to repress UPR^{mt} during *Pseudomonas aeruginosa* infection (Deng et al., 2019). Interestingly, the reduced mitochondrial import of certain trigger proteins such as PINK1 also acts as a signal to induce mitophagy (Narendra et al., 2010).

Of note, nuclear accumulation of ATFS-1 induces the transcription of over 500 genes, indicating UPR^{mt} is a wide cellular response that not only affects genes encoding mitochondrial proteins (Nargund et al., 2012; Nargund et al., 2015; Lin et al., 2016). Under homeostatic conditions, ATFS-1 is transported to mitochondria effectively, its MTS is cleaved off, and the mature protein is degraded by the LON protease. This suggests that the efficiency of mitochondrial protein import negatively regulates UPR^{mt} (Nargund et al., 2012). In addition, although the majority of ATFS-1 is imported into the nucleus under mitochondrial dysfunction conditions, ATFS-1 is also found within mitochondria and limits mtDNA-encoded OXPHOS transcription via direct binding to mtDNA (Nargund et al., 2015). This suggests that ATFS-1 is a regulator of metabolism and supports recovery of dysfunctional mitochondria (Hernando-Rodriguez and Artal-Sanz, 2018).

If triggering UPR^{mt} relies on impaired mitochondrial protein import, the question can be raised how the UPR^{mt} can rescue the mitochondrial defect by importing newly transcribed and translated chaperones and other mitochondrial proteins into mitochondria that have a severe mitochondrial import defect to begin with. One solution could be that ATFS-1 has a weak MTS (Fukasawa et al., 2015; Rolland et al., 2019), resulting in poor import into partially dysfunctional mitochondria. However, mitochondrial chaperones, e.g. *HSP-60*, and proteases, e.g. *SPG-7*, induced by ATFS-1 have a more effective MTS and may still be imported into dysfunctional mitochondria (Rolland et al., 2019). The MTS of ATFS-1 acts as a sensor for decreased mitochondrial membrane potential, which is a signal that triggers UPR^{mt} (Rolland et al., 2019). ATFS-1 induces the transcription of mitochondrial import complex components, such as *TIM-17* and *TIM-23*, to facilitate the import of mitochondrial chaperones and proteases to restore mitochondrial proteostasis and support mitochondrial recovery. Apart from changes in gene expression, dysfunctional mitochondria cause changes in nuclear chromatin structure, which induces UPR^{mt} activation. The histone methyltransferase MET-2, the nuclear co-factor LIN-65 and two conserved demethylases (the jumonji family proteins JMJD-1.2 and JMJD-

Table 1
Conservation of UPR^{mt} regulators across kingdoms. Gene names in bold are experimentally-confirmed regulators as indicated by respective references. Gene names in normal case (not bold) indicate where a homologous gene exists in the genome of the respective organism, but a role in UPR^{mt} has not been shown experimentally. Dash ('-') indicates that no homologous gene was found in the genome. Gene names between brackets indicate very distant homology (BLAST E-value smaller than 10).

Animals *C. elegans*	 *H. sapiens*	Yeasts *S. cerevisiae*	Plants *A. thaliana*	Function	Reference
ATFS-1	**ATF-4, ATF-5**	Cst6/ACA2/ YIL036W	–	bZIP transcription factor	Haynes et al., 2010; Fiorese et al., 2016
ZIP-3	**ATF-4, ATF-5**	–	–	bZIP transcription factor	Deng et al., 2019
- (bZIP)	**CHOP**	–	–	bZIP transcription factor	Teske et al., 2013
–	–	**Pdr3**	–	Zinc-finger transcription factor	Weidberg and Amon, 2018
–	–	–	**ANAC017**	NAC domain containing transcription factor	Kacprzak et al., 2020
DVE-1	SATB2	Pho2	WOX13	Homeodomain-containing transcription factor	Haynes et al., 2007
UBL-5	UBL-5	Hub1	UBL-5	Small ubiquitin-like protein	Haynes et al., 2007
NHR-14	**ERα**	–	–	Estrogen receptor alpha	Papa and Germain, 2011
FSHR-1	FSHR	- (FMP27/YLR454w)	- (LRR-like R genes)	Follicle-stimulating hormone receptor	Kim and Sieburth, 2020
SPHK-1	SPHK-1	LCB5/YLR260W	SPHKs	Sphingosine kinase	Kim and Sieburth, 2018
GCN2	**EIF2A family (GCN2 etc.)**	GCN2	GCN2	Eukaryotic initiation factor 2 alpha kinases	Teske et al., 2013
SIR-2.1	**SIRT1/3**	HST2/YPL015C	SIRT	Sirtuins: lysine deacetylases and ADP-ribosyltransferases	Mouchiroud et al., 2013; Papa and Germain, 2014
–	–	–	**AP2/ERF**	Ethylene hormone signalling components	Wang and Auwerx, 2017

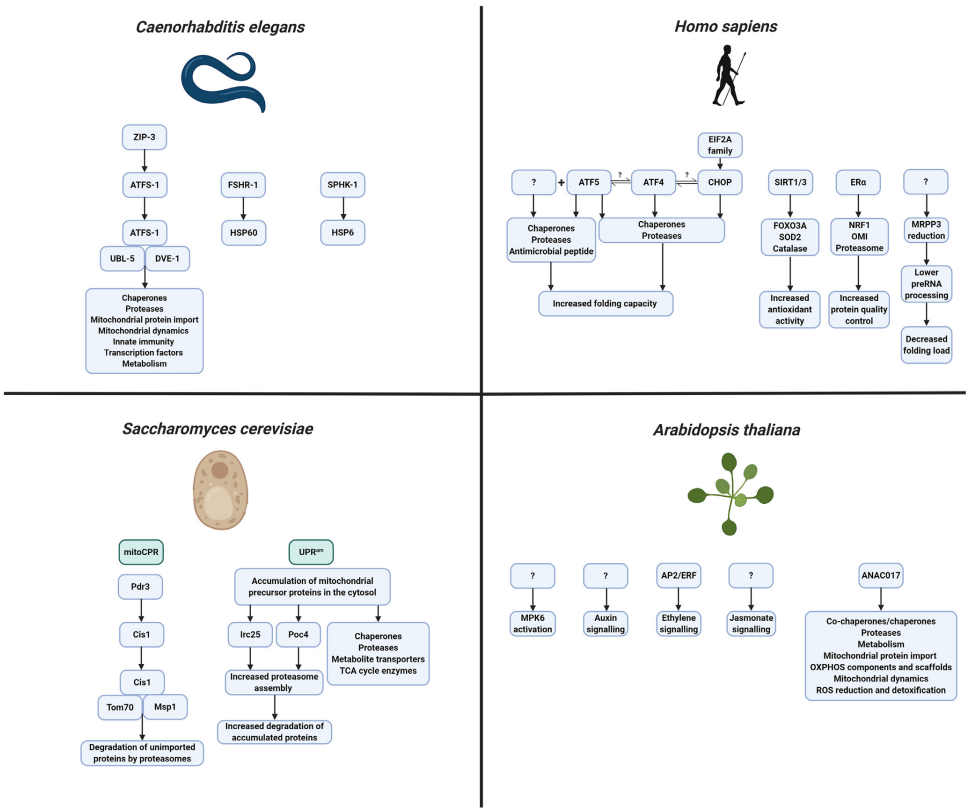

Fig. 2. Overview of the main players of the mitochondrial unfolded protein responses (UPR^{mt}) across kingdoms. Different eukaryotic organisms have developed their own signalling pathways to respond to mitochondrial proteotoxic stress, however the target genes of these pathways are often similar. The main regulators and downstream target genes are represented (more detailed information can be found in Tables 1 and 2, and the main text). The figure was created with Biorender.com.

3.1), have been reported to be necessary for UPR^{mt} induction (Merkwirth et al., 2016).

Recently, it was proposed that the conserved follicle-stimulating hormone G protein-coupled receptor (GPCR) FSHR-1 is a novel regulator of the UPR^{mt} that induces transcriptional response of *HSP6* and *HSP60* in *C. elegans* (Kim and Sieburth, 2020). A previous study suggested that sphingosine kinase SPHK-1 positively regulates UPR^{mt} activation in *C. elegans* (Kim and Sieburth, 2018). SPHK-1 induces HSP6 and associates with mitochondria from cytoplasmic pools, which might be an early signal to trigger UPR^{mt} (Liu et al., 2014; Kim and Sieburth, 2018). Notably, it was shown that FSHR-1 and SPHK-1 are involved in a common genetic pathway that activates UPR^{mt} (Kim and Sieburth, 2020). Kim and Sieburth (2020) also showed that FSHR-1 positively regulates mitochondrial association of SPHK-1 under non-stressed conditions and is mandatory for SPHK-1 induction under stress conditions in the intestine. Moreover, FSHR-1 activates the UPR^{mt} in the nervous system to enhance survival, whereas SPHK-1 is likely to function in the intestine.

3. The UPR^{mt} in mammals

Although UPR^{mt} was first reported in mammalian cells (Zhao et al., 2002), the UPR^{mt} in mammals is less understood than in *C. elegans*, and several pathways have been proposed (Fig. 2). In mammalian systems, a functional ortholog of *C. elegans* ATFS-1, is transcription factor 5 (ATF-5), a bZIP transcription factor regulated by the efficiency of mitochondrial protein import (Fiorese et al., 2016). Under normal conditions, ATF5 localizes to mitochondria. During mitochondrial stress, ATF5 may induce nuclear gene expression of mitochondrial chaperones *HSP60* (*HSPD1*), *HSP10* (*HSPE1*), *mtHSP70* (*HSPA9*), mitochondrial protease *LONP1*, and *HD-5* (Fiorese et al., 2016). Notably, ATF5 is able to rescue UPR^{mt} activation in nematodes lacking ATFS-1 (Fiorese et al., 2016). Besides ATF5, two other bZIP transcription factors, activating transcription factor 4 (ATF4) and C/EBP homologous protein (CHOP) also associate with mammalian UPR^{mt} (Quiros et al., 2017). CHOP is involved in the integrated stress response (ISR) and is induced by any of the four kinases: the eukaryotic initiation factor 2 alpha (EIF2A) kinases GCN2, HRI, PERK or PKR (Teske et al., 2013). Phosphorylation of EIF2A results in activation of ATF4, which in turn induces *CHOP* gene expression in ISR (Pakos-Zebrucka et al., 2016). The ATF-5

transcription factor is induced by ATF4 and CHOP, however, not via the UPR^{mt} but via the endoplasmic reticulum (ER) UPR (UPR^{ER}) (Teske et al., 2013; Fusakio et al., 2016). The relationship among ATF5, ATF4 and CHOP in the UPR^{mt} remains unclear. The changes in localization and levels of CHOP, ATF4 and ATF5, and together with other unknown transcription factors, leads to the induction of chaperonins, chaperones and proteases to elevate the folding capacity within dysfunctional mitochondria.

Another cellular mechanism of reducing the misfolded or unfolded protein load is to decrease the level of proteins imported into the organelle or to decrease translation. In response to stresses, mitochondria can reduce their translation, and this type of stress response is termed the UPR^{mt} translation response (Munch and Harper, 2016). Upon UPR^{mt} activation, a decrease in transcript and protein levels of MRPP3 (part of the RNase P complex) lowered the rate of mitochondrial pre-RNA processing, which in turn decreased mitochondrial translation (Munch and Harper, 2016; Munch 2018). The UPR^{mt} translation axis occurs locally in dysfunctional mitochondria and serves as the first response to mitochondrial damage that seems to be caused by internal mitochondrial stimuli. If only a few mitochondria are dysfunctional, this response is activated to restore proteostasis without causing cell-wide effects. If many mitochondria are dysfunctional, the other UPR^{mt} responses are triggered involving global transcriptional responses. The underlying mechanism of the UPR^{mt} translation axis is elusive.

Antioxidant activity can be enhanced by recruiting sirtuins to counter a proteotoxic oxidative environment caused by dysfunctional mitochondria (Munch, 2018). Sirtuins are lysine deacetylases and ADP-ribosyltransferases that can interfere with many mitochondrial activities (Houtkooper et al., 2012; Dang, 2014). Among seven sirtuins (SIRT1-7) that have been reported in mammalian cells, SIRT1 and SIRT3 have been suggested to be part of the UPR^{mt} (Mouchiroud et al., 2013; Papa and Germain, 2014). SIRT1/SIRT3 deacetylate the transcription factor FOXO3A, causing FOXO3A to translocate to the nucleus (Brunet et al., 2004; Tao et al., 2010). Nuclear-imported FOXO3A induces the expression of antioxidant enzymes such as the mitochondrial superoxide dismutase 2 (SOD2) and catalase (Salminen et al., 2013; Tao et al., 2014). Notably, other mitochondrial stresses not associated with protein misfolding cause ROS production, leading to activation of SIRT3, indicating that SIRT3 cannot act as a specific regulator for the UPR^{mt}. Inhibition of SIRT3 activity showed no impact on CHOP activity, suggesting that SIRT3-FOXO3A activity is independent and is likely to be complementary to the UPR^{mt} triggered by CHOP and ATF4/5 to secure mitochondrial health.

Misfolded/unfolded endonuclease G (EndoG), an IMS endonuclease, triggers a UPR in the mitochondrial IMS (UPR^{IMS}) that is likely to be independent of the UPR^{mt} mediated within the mitochondrial matrix, and does not activate CHOP or HSP60. The UPR^{IMS} response caused by misfolded/unfolded proteins in the IMS occurs by activation of estrogen receptor alpha (ERα) and is mediated by ROS-dependent phosphorylation of ERα by protein kinase B (PKB or AKT) (Papa and Germain, 2011). Activated ERα results in an increase in nuclear respiratory factor 1 (NRF1)-regulated transcriptional response, which enhances mitochondrial respiration (Scarpulla, 2006). UPR^{IMS} target genes include the IMS protease OMI (also known as 'High-temperature Requirement 2′ (HTRA2)) (Clausen et al., 2011; Papa and Germain, 2011) and the elevation of proteasome activity (Papa and Germain, 2011). All the effects caused by activating ERα promote the protein quality control to prevent misfolded/unfolded IMS proteins from accumulating in the IMS. The activation of the UPR^{IMS}-ERα pathways seems to occur in parallel with other UPR^{mt} pathways.

4. The UPR^{mt} in yeast

General mitochondrial retrograde signalling was first described in the yeast *Saccharomyces cerevisiae* (*S. cerevisiae*) and has since been studied extensively (Liao et al., 1991; Jazwinski and Kriete, 2012; Trendeleva and Zvyagilskaya, 2018). Interestingly, there have been no publications strictly related to the UPR^{mt} in yeasts. However, other UPR that might be related to UPR^{mt} are described in some studies (Fig. 2).

A pathway of mitochondria-mediated cell death in yeast was identified and named mitochondrial precursor over-accumulation stress (mPOS) (Wang and Chen, 2015). Mitochondrial damage affects the organellar protein import, resulting in the accumulation of misfolded and unimported mitochondrial proteins in the cytosol, causing mPOS that then induces cell death. Fourty suppressor genes of mPOS (in the cytosol) were identified: Thirty-two of them could be divided into five functional groups: target of rapamycin (TOR) signalling, mRNA silencing/turnover, ribosomal function/protein translation, tRNA methylation, and cytosolic protein chaperoning/degradation. Two ribosome-associated proteins, Gis2 and Nog2, were found to be upregulated in response to mPOS to promote cell survival and protect cells against mPOS.

Wrobel et al (2015) identified the UPR^{am} in yeast, which is defined as the inhibition of protein synthesis and the activation of proteasomes in the cytosol (the protein complexes that degrade cellular proteins by proteolysis) caused by mistargeting of proteins. Notably, the authors suggested that UPR^{am} is different from UPR^{mt} because UPR^{mt} in higher eukaryotes leads to the nuclear expression of chaperones and proteases, whereas UPR^{am} activates proteasomes. Accumulation of mitochondrial precursor proteins in the cytosol results in activation of UPR^{am}, leading to an increased protein level of the proteasome assembly factors Irc25 and Poc4, which enhances the degradation of accumulated proteins. The RNA-seq data in *mia40* (a mitochondrial IMS import component) provided by this study clearly suggest induction of many genes encoding mitochondrial proteins, including metabolite transporters and TCA cycle enzymes. In addition, several genes encoding chaperones and proteases are differentially expressed in the *mia40* mutant, suggesting at least some overlap between UPR^{mt} and UPR^{am}.

Ruan et al (2017) proposed a mitochondria-mediated proteostasis mechanism in yeast, termed MAGIC (mitochondria as guardian in cytosol). They showed that cytosolic proteins aggregating under heat stress are imported into mitochondria via interaction with organellar import receptors TOM70 and TOM40 for degradation by mitochondrial protease PIM1 (LON1). Protein aggregates imported into mitochondria do not require cytosolic HSP70, but require the disaggregase Hsp104, suggesting that aggregate proteins are dissociated in order to pass the import channels. MAGIC seems to be important for the turnover of proteins aggregating under stress. Of note, Ruan et al (2017) also showed that cytosolic proteins prone to aggregation are also imported into mitochondria in human RPE-1 cells.

Another interesting study described a mitochondrial import surveillance mechanism in budding yeast, termed the mitoCPR for mitochondrial compromised protein import response (Weidberg and Amon, 2018). MitoCPR is activated to protect mitochondrial function during protein import stress. When mitochondrial proteins accumulate on the organelle's surface and bind to the translocases due to mitochondrial protein import deficiency, the transcription factor Pdr3 induces the peripheral outer membrane protein Cis1. In turn, Cis1 interacts with the mitochondrial import receptor Tom70 and recruits the AAA–adenosine triphosphatase (ATPase) Msp1 to the outer-membrane translocase to mediate the degradation of unimported proteins by proteasomes on the mitochondrial surface. The signal (or signals) that activates the mitoCPR in budding yeast has not been identified.

Although no pathways in yeast have been strictly classified as UPR^{mt}, it is clear that very similar mechanisms exist, which activate nuclear gene expression to resolve or compensate for mitochondrial defects.

5. Is there a UPR^{mt} in plants?

The plant UPR^{mt} has been even less studied than UPR^{mt} in *C. elegans* and mammals, but was found to be at least partially conserved in

Table 2
Conservation of UPR^{mt} target genes across kingdoms. Gene names in bold are experimentally-confirmed target genes (animals as summarised by Melber and Haynes, 2018, Munch, 2018, Quiros et al., 2017; yeast based on Wrobel et al., 2015; plants taken from Kacprzak et al. (2020), Wang and Auwerx (2017). Gene names in normal case (not bold) indicate where a homologous gene exists in the genome of the respective organism, but a role in UPR^{mt} has not been shown experimentally. Dash ('–') indicates no homologous genes were found in the genome. Gene names between brackets indicate very distant homology (BLAST E-value smaller than 10).

	Animals		Yeasts	Plants	
	C. elegans	*H. sapiens*	*S. cerevisiae*	*A. thaliana*	Function
Mitochondrial (co-)chaperones and proteases	**dnj-10**	DNAJA3	Mdj1	DNAJ Protein	Mitochondrial DnaJ, protein chaperone
	hsp-6	**mtHSP70**	ssc1	**mtHSC70-1**	Mitochondrial Hsp70, protein chaperone
	hsp-60	**HSP60**	hsp60	HSP60	Mitochondrial chaperone
	Uncharacterized protein Y22D7AL.10.1	**HSP10**	hsp10	CPN10	Mitochondrial chaperone
	GrpE protein homolog, mitochondrial	GrpE-like protein cochaperone	Mge1	**MGE1**	Mitochondrial GrpE 1, co-chaperone
	ppgn-1	SPG7	afg3	FTSH protease 10	Paraplegin AAA protease (mitochondrial)
	ymel-1	YME1L1	Yme1	FTSH protease 4	Mitochondrial AAA protease
	clpp-1	CLPP	–	CLPP2	CLP protease
	lonp-1	**LONP1**	pim1	LON1	Protease
	–	**OMI**	nma11	Trypsin family protein	IMS protease
	–	–	–	**sHSP23.5**	Mitochondrial heat shock protein
Mitochondrial protein import	**tom-20**	TOM20	tom20	TOM20-1	Translocase of the outer membrane subunit
	tim-23	TIM23	tim23	TIM23-1	Translocase of the inner membrane subunit
	tim-17	TIM17	tim17	**TIM17-1**	Translocase of the inner membrane subunit
Mitochondrial dynamics	**drp-1**	DNM1L	Dnm1	Dynamin-related protein	Dynamin-related protein, mitochondrial fission
	mff-2	–	–	–	Mitochondrial fission factor
	Uncharacterized protein CELE_H43I07.1	(OPA3)	(OPA3)	**OPA3**	Optic Atrophy 3, unknown function
Innate immunity	**abf-2**	–	–	Defensin-like (DEFL) protein	Antimicrobial peptide
	–	**HD-5**	–	–	Antimicrobial peptide
	lys-2	–	–	–	Secreted lysosome
	–	**IL20RB**	–	–	Interleukin 20 Receptor subunit B
Transcription factors	**atfs-1**	**ATF-4, ATF-5, ATF-3**	Cst6/ACA2/YIL036W	–	bZIP transcription factor, UPR^{mt} regulator
	skn-1	NRF2	–	–	bZIP transcription factor, Nrf2 ortholog
	bZIP transcription factor family	bZIP transcription factor family	**CIN5**	bZIP transcription factor family	bZIP transcription factor
	bZIP transcription factor family	**CHOP**	–	–	Transcription factor, UPR^{mt} regulator
	–	–	–	**ANAC013**	NAC transcription factor
	–	–	–	**ERFs (see below)**	AP2-like ethylene-responsive transcription factors
	Fork-head protein	**FOXO3A**	hcm1	**–**	Forkhead box protein O3
	bZIP domain-containing protein	**NRF1**	–	–	Nuclear respiratory factor 1
Metabolism	**glna-1**	glutaminase	aim33	(Ankyrin-repeat proteins)	Glutaminase
	clk-1	COQ7	COQ7	–	Coenzyme Q biosynthesis
	ldh-2	LDHA, LDHB	gtr1	D-LDH	Lactate dehydrogenase
	Alanine aminotransferase	Alanine aminotransferase 1/2	alt2	**ALAAT2**	Alanine aminotransferase 2 , metabolic component
	Aspartate aminotransferase	**PSAT2**	aat1/2	**ASP2**	Aspartate aminotransferase 2, involved in metabolism
	BCAT	BCAT	**BAT1**	BCAT	Mitochondrial BCAA aminotransferase
	Aconitase	Aconitase	**ACO2/CIT3**	Aconitase	Aconitase
	PEP carboxykinase	**PCK2**	**–**	–	Phosphoenolpyruvate carboxykinase 2, mitochondrial
	Asparagine synthetase	**ASNS**	Asparagine synthetase	Asparagine synthetase	Asparagine synthetase (glutamine-hydrolyzing)
	–	**ASS1**	Argininosuccinate synthase	Argininosuccinate synthase	Argininosuccinate synthase 1
	IPGAM	–	–	**IPGAM2**	2,3-biphosphoglycerate-independent phosphoglycerate mutase
	Amino acid carriers	**SLC1A4, SLC1A5,SLC6A6,SLCyA11**	Amino acid carriers	Amino acid carriers	Amino acid carriers
	Mitochondrial substrate carriers	Mitochondrial substrate carriers	**CTP1/SFC1/OAC1/CRC1**	**PiC/DIC**	Mitochondrial substrate carriers
Nucleases	–	**MRPP3**	–	PRORP	Mitochondrial ribonuclease P
	EndoG	EndoG	**NUC1**	–	Mitochondrial ribonuclease

(*continued on next page*)

Table 2 (*continued*)

	Animals		Yeasts	Plants	
Hormone/growth factors	–	–	–	**ERF5/6**	Ethylene response factor
	–	–	–	**ERF13**	Ethylene response factor
	–	–	–	**ERF054/104**	Ethylene response factor
	–	–	–	**ERF2/091**	Ethylene response factor
	–	–	–	**SHN3**	Ethylene response factor
	–	–	–	**LEP**	Ethylene response factor
	–	–	–	**ERF113**	Ethylene response factor
	–	–	–	**ERF1/2/5**	Ethylene response factor
	–	–	–	**BBM**	AP2-like ethylene-responsive transcription factor
	–	–	–	**PLT2**	AP2-like ethylene-responsive transcription factor
	–	–	–	**RAP2.11**	Ethylene-responsive transcription factor
	–	–	–	**EDF2/4**	Ethylene response dna binding factor
	–	–	–	**EIN2**	Ethylene-insensitive protein 2
	S-adenosylmethionine synthase	S-adenosylmethionine synthase	sam1	**SAM1**	S-adenosylmethionine synthetase-1
	–	–	–	**EIL1**	Ethylene insensitive 3-like 1
	ACS-like protein	ACS-like protein	alt1	**ACS6/8**	1-aminocyclopropane-1-carboxylic acid (acc) synthase
	–	**VEGFA**	–	**–**	Vascular endothelial growth factor A
	CET-1	**GDF15**	–	**–**	Growth differentiation factor 15
Abiotic and biotic stress response	mpk1	MPK1/7/14	hog1	**MPK6**	Mitogen-activated protein kinase
Hypersensitive response (plant defense)	–	–	–	**BCS1/OM66**	AAA ATPase
OXPHOS protein components and scaffolds	–	–	–	**AOX1a**	Alternative oxidative 1a, OXPHOS component
	–	–	Nde1/2	**NDB2**	OXPHOS protein component
	–	–	Nde1/2	**NDB4**	OXPHOS protein component
	Stomatin-like	Stomatin-like	–	**Stomatin-like 1/2**	OXPHOS protein scaffolds
ROS reduction and detoxification	Catalase	**Catalase**	Catalase	Catalase	Catalase
	sod-2	**SOD2**	SOD-2	SODA (At3g10920)	Mitochondrial superoxide dismutase
	MATE protein	MATE protein	MATE protein	**MATE protein (At2g04050)**	Multidrug and toxin efflux carriers
	Glutathione S-Transferase	Glutathione S-Transferase	Glutathione S-Transferase	**TAU25**	Glutathione S-transferase, ROS reduction and detoxification
	Sulfotransferase	Sulfotransferase 1C3	–	**SOT12**	Sulphotransferase 12, ROS reduction and detoxification

Arabidopsis thaliana (Moullan et al., 2015) (Fig. 2, Table 2). The UPR^{mt} in *Arabidopsis thaliana* was shown to be activated by a transient oxidative burst, leading to the activation of mitogen-activated protein kinases (MAPKs) and hormonal signalling (ethylene, auxin and jasmonate) to restore mitochondrial proteostasis (Wang and Auwerx, 2017). Members of the AP2/ERF (APETALA2/ethylene responsive factor), MYB, NAC (NAM, ATAF1, 2, CUC2), bHLH (basic helix-loop-helix) and WRKY transcription factor families were suggested to serve as sensors/effectors of the plant UPR^{mt} (Wang and Auwerx, 2017). Wang and Auwerx (2017) showed that in the *Arabidopsis* mitochondrial ribosomal protein L1 *mrpl1-1* mutant, AP2/ERF transcription factors are highly induced: drought stress responsive genes *ERF5/6*, *DREB2H*, and *EDF2/4* (Zhang et al., 2008; Dubois et al., 2013; Fu et al., 2014); wounding responsive gene *ERF13* (Sogabe et al., 2011); high light stress responsive gene *ERF054/104* (Bechtold et al., 2008; Vogel et al., 2014); low-potassium responsive gene *RAP2.11* (Kim et al., 2012); pathogen defensive genes *ERF2/091* and *SHN3* (Onate-Sanchez and Singh, 2002; Aharoni et al., 2004; McGrath et al., 2005); genes involved in development: *LEP*, *BBM*, *PLT2*, and *ERF113* (van der Graaff et al., 2000; Asahina et al., 2011; Horstman et al., 2014); and genes involved in ethylene signalling (*EIN2* and *ERF1/2/5*) and biosynthesis (*SAM1* and *ACS6/8*) (Chang, 2016). In addition, they showed that treatment with doxycycline (Dox), a mitochondrial ribosome inhibitor, increased the transcript levels of *ERF1/2/5* and *EIL1*, which is a transcription factor and a positive regulator of the ethylene signalling pathway (Alonso et al., 2003). These results suggest that the UPR^{mt} in plants activates ethylene responses as a systemic signal. Dox, chloramphenicol (CAP) (another inhibitor of bacterial and organellar ribosomes), MitoBlock-6 (MB) (an inhibitor of protein translocation into mitochondria) and rotenone (an inhibitor of the mitochondrial electron transport chain) treatment increased MPK6 phosphorylation in wild type (WT) seedlings, suggesting that activation of MAPKs signalling is involved in the plant UPR^{mt} (Wang and Auwerx, 2017). Auxin and jasmonate action was induced in root tips of WT seedlings treated with Dox, CAP and MB, but not when treated with rotenone and antimycin A (AA) (a mitochondrial complex III inhibitor), indicating that auxin and jasmonate signalling are activated by the UPR^{mt} in plants (Wang and Auwerx, 2017). Mitochondrial ribosomal proteins (MRPs) were also suggested to be important for mtPQC and the UPR^{mt}, and to be target genes of mitochondria-to-nuclear communication. Mitochondrial translation was shown to affect lifespan in plants: long-term treatment with Dox decreased mitochondrial translation efficiency, and consequently slowed plant growth and development.

The suggested UPR^{mt}-controlled transcriptional induction of nuclear-encoded mitochondrial ribosome subunits must, however, be viewed with caution. The proposed transcriptional inductions by treatment of *Arabidopsis* plants with Dox or by knocking out mitochondrial ribosomal protein MRPL1 were generally very weak, mostly in the order of 1.2–1.8 fold (Wang and Auwerx, 2017). Furthermore, the RNA-seq analysis of Dox treatment and *mrpl1* mutants in the same study could not confirm a consistent upregulation of nuclear transcripts encoding mitochondrial ribosomal proteins observed by qRT-PCR (Kacprzak et al., 2020; Wang and Auwerx, 2017). Finally, despite very strong effects on mitochondrial translation and plant development in plants with reduced expression of mitochondrial ribosomal protein *RPS10*, such an increase of nuclear transcripts encoding mitochondrial ribosomal proteins was also not observed in *rps10* mutants (Adamowicz-Skrzypkowska et al., 2020).

Recently, Kacprzak et al. (2020) showed that plants treated with Dox and AA induced expression of many common genes. The transcription factor *Arabidopsis* NAC domain containing protein 17 (ANAC017), which was previously proposed as a regulator of MRR pathways (Ng et al., 2013; Ng et al., 2014; Van Aken et al., 2016a,b), was shown to be the major regulator of the UPR^{mt} in plants. Kacprzak et al. (2020) suggested that in response to AA treatment, ANAC017 targets many types of genes that are classic targets of UPR^{mt} (Table 2): heat shock proteins (*mtHSC70-1* and *sHSP23.5* (a plant-specific protein)), co-chaperones/chaperones (a GrpE family protein the *Mitochondrial Grpe 1* (*MGE1*), and AAA ATPase *AtOM66* (*BCS1*)) and mitochondrial import component *TIM17-1*. *TIM17-1* is an isoform of *TIM17* that is expressed in dry seed (Wang et al., 2014). Interestingly, *TIM17-1* is the only isoform of *TIM17* that was induced by UPR^{mt} in plants. Previous studies showed that *TIM17-1* was induced by mitochondrial perturbation, e.g. in prohibitin *atphb3* mutants (an IMM scaffold protein) and by AA treatment; however, the other isoforms *TIM17-2* and *TIM17-3* were not induced (Ng et al., 2013; Van Aken et al., 2016a,b). This could be explained by the difference in the structure of the C-terminus of these *TIM17* isoforms, which was previously shown to be important for protein import into mitochondria via the general import pathway (Murcha et al., 2005). ANAC017 targets OXPHOS protein components and scaffolds: *Alternative Oxidative 1a (AOX1a), NDB2*, *NDB4* and *Stomatin-Like 1/2* proteins; proteins that regulate metabolism like *Alanine Aminotransferase 2 (ALAAT2), Aspartate Aminotransferase 2 (ASP2)*, *2,3-Biphosphoglycerate-Independent Phosphoglycerate Mutase (IPGAM2)*; proteins involved in mitochondrial dynamics *Optic Atrophy 3 (OPA3)*; and proteins involved in ROS reduction and detoxification: *AOX1a*, Multidrug And Toxin Efflux carriers (*At2g04050*), *glutathione S-transferase TAU 25* and *Sulphotransferase 12* (*SOT12*). Treatment with CAP, MB and FCCP (a protonophore that collapses the mitochondrial membrane potential) showed ANAC017-dependent induction of *AOX1a*, *UPOX1*, *UGT74E2* and *OM66* (Kacprzak et al., 2020). ANAC017 also enhanced plant growth and development during mitochondrial dysfunction caused by treatment with AA, Dox, CAP or MB (Kacprzak et al., 2020). Despite significant effort, we were unable to detect consistent marker genes that were differentially expressed only in *mrpl1*, *rps10* and Dox-treated Col-0 plants, but not for instance, in AA-treated plants. The genes that were in common, were ANAC017-dependent marker genes associated with classical MRR in plants (Kacprzak et al., 2020; Adamowicz-Skrzypkowska et al., 2020). It thus appears that 'classical' mitochondrial retrograde signalling and UPR^{mt} in plants are most likely one and the same response. It has also been suggested that proteolytic degradation products of mitochondrial proteins could be exported into the cytosol, where these peptides could act as signalling molecules for retrograde signalling (or UPR^{mt}) (Møller and Sweetlove, 2011), as was observed in *C. elegans* (Haynes et al., 2007; Haynes et al., 2010).

It was proposed that in response to inhibition of electron transport by AA, signals from mitochondria result in the cleavage of ANAC017 by a rhomboid protease, leading to the translocation of ANAC017 from the ER membrane to the nucleus (Ng et al., 2013). However, the mechanism underlying ANAC017 migration is still mysterious. It is possible that hydrogen peroxide (H_2O_2) produced during mitochondrial stresses, e.g. treatments that impair OXPHOS complexes, mitochondrial translation, protein import, or proton gradient (Ng et al., 2013; Quiros et al., 2017; Wang and Auwerx, 2017), could result in ANAC017 cleavage. ER stress in plants is caused by the accumulation of misfolded/unfolded proteins in the ER, leading to UPR^{ER} (Howell, 2013). One hypothesis could be that ANAC017 is both an ER stress sensor/transducer and a regulator of UPR^{mt}. However, activation of the plant UPR^{mt} in response to AA treatment did not induce the classic UPR^{ER} marker genes (Kim et al., 2018) *IRE1A*, *IRE1B*, *TMS1*, *NAC089* and even suppressed several UPR^{ER} marker genes, including *PDI6*, *PDI9*, *BIP1*, *CRT1* or *SDF2* (Ng et al., 2013). Therefore, it seems that the plant UPR^{mt} does not involve activation of UPR^{ER} and ANAC017 is likely to act as a specific regulator of the UPR^{mt}/MRR in plants. Further work will be required to identify the cause of ANAC017 migration during mitochondrial stresses. Activation of UPR^{mt} by Dox leads to the induction of ethylene responsive genes, but this was unaffected in *anac017* mutants, indicating that ethylene production and signalling are potentially ANAC017-independent (Kacprzak et al., 2020). In conclusion, there are possibly four signalling pathways that are activated during UPR^{mt} in plants: induction of gene expression regulated by ANAC017, ethylene

signalling that promotes the growth reduction and (ANAC017-independent) ethylene responsive gene expression, auxin signalling to keep check on the growth versus stress response balance (Ivanova et al., 2014; Kacprzak et al., 2020; Wang and Auwerx, 2017), and jasmonate signalling (Wang and Auwerx, 2017).

6. A comparison of UPR^{mt} regulators across eukaryotic kingdoms

To obtain a more systematic overview of how UPR^{mt} is regulated in various organisms, we summarized the current knowledge on UPR^{mt} signalling across eukaryote kingdoms (Fig. 2). Table 1 provides an overview of currently identified upstream regulators of UPR^{mt}, and how they are conserved across eukaryotes. As UPR^{mt} and MRR are transcriptional responses, identification of master transcription factors (TFs) is of key importance. bZIP type TFs have key roles in animal UPR^{mt}, with ATFS-1 in *C. elegans* and the related ATF-4/ATF-5 in mammalian systems (Table 1). Indeed, ATF-5 could complement *atfs-1* loss-of-function mutation in *C. elegans*, demonstrating that they are homologs (Fiorese et al., 2016). Interestingly, also the yeast *S. cerevisiae* appears to contain a transcription factor with homology to ATF-5/ATFS1, Cst6, which is involved in low CO_2 and potentially hypoxia response. The Cst6p knock-out mutant shows decreased respiratory growth on non-fermentable carbon sources (Steinmetz et al., 2002), indicating it may indeed have a role in regulation of mitochondrial function. A specific role of Cst6p in yeast UPR^{mt} has to date not been reported. In contrast, no clear homolog of ATFS-1 can be found in *Arabidopsis thaliana*, indicating that the role for bZIP transcription factors in UPR^{mt}-like signalling is confined to animals and potentially yeast. In yeast, a Zinc-finger transcription factor Pdr3 was identified with a role in mitoCPR (Weidberg and Amon, 2018). Pdr3 appears to be restricted to yeast genomes and no homolog could be found in plants or animals.

The data in table 1 suggests that UPR^{mt}-related signalling in plants is regulated quite differently at the transcriptional level. An initial study in plants highlighted a potentially highly complex transcriptional network and suggested the involvement of a wide range of TFs of the ERF, WRKY, MYB, NAC and bHLH families (Wang and Auwerx, 2017). However, no clear individual upstream TFs were identified in this study. A recent study in *Arabidopsis* identified the NAC transcription factor ANAC017 as a core regulator of UPR^{mt} and proteotoxic stress (Kacprzak et al., 2020). Many of the reported gene families, including NAC, WRKY and ERF TFs, are plant specific, indicating that plants have independently evolved their own UPR^{mt} and mitochondrial retrograde signalling pathways. The NAC family pre-dates the land plants, as distant homologs can be found in streptophyte green algae (Maugarny-Cales et al., 2016). The ANAC017 regulatory network seems to have evolved together with embryophytes, and thus appears to be associated with colonization of land (Lama et al., 2019). Recent results showed that ANAC017 is important for tolerance to flooding, which reduces oxygen availability for mitochondrial respiration (Bui et al., 2020; Meng et al., 2020). This further confirms the hypothesis that the ANAC017 pathway evolved as part of the new adaptations required for growth on land.

Some regulators identified in UPR^{mt} such as FSHR, ERα and ZIP-3 appear to be conserved in animals, while others belong to highly conserved protein families across all eukaryotes including eIF2A kinases, sphingosine kinases and sirtuins. Sirtuins are also associated with mitochondrial function in plants, but a direct role in UPR^{mt} or related signalling is unclear (Konig et al., 2014). More research will be needed to show whether these regulators have conserved functions in UPR^{mt} regulation across kingdoms.

7. UPR^{mt} target genes across eukaryotic kingdoms

The above analysis suggests that key upstream regulators of UPR^{mt}-related responses are not fully conserved across eukaryotes (Table 1) and specific regulators have evolved that may be specific to one or more kingdoms. The outcome of UPR^{mt}-related signalling is nevertheless the alteration of gene expression of specific target genes. Therefore, we also analysed what types of proteins are encoded by the UPR^{mt}-regulated genes (Table 2).

In common, UPR^{mt} in animals and plants induces the classic targets: nuclear expression of chaperones, proteases, mitochondrial import components and proteins involved in primary metabolism. Of note, UPR^{mt} activation leads to the induction of proteins involved in (innate) immunity in both animals and plants, but the target genes are different: *ABF-2* and *LYS-2* in *C. elegans*, *HD-5* and *ILR20B* in humans, and *MPK6* in *Arabidopsis thaliana*. This indicates that each kingdom has developed their own responsive genes in stress response/immunity. Interestingly, *ATFS-1* in *C. elegans* and *ATF4/5* in humans play roles as both transcriptional regulators and target genes in UPR^{mt}, while *ATF3* appears to be a target gene as well (Quiros et al., 2017). Plant UPR^{mt} contains a very specific group of target genes, ethylene responsive factors (Table 2, section "Hormones/growth factors"). In addition, Kacprzak et al. (2020) reported that UPR^{mt} targets OXPHOS protein components and scaffolds in plants, of which AOX1a is an OXPHOS component and a specific marker of plant retrograde signalling. Alternative mitochondrial NAD(P)H dehydrogenases appear to be conserved retrograde target genes in plants and yeasts (Table 2). UPR^{mt} also induces proteins that are involved in ROS reduction and detoxification, but previous studies so far only showed such responses in humans and plants. Cellular metabolism also appears to be a common target, with amino acid metabolism and transport genes common to all kingdoms. In agreement, changes in amino acid levels seem to be common in response to UPR^{mt} in plants and humans (Meyer et al., 2009; Van Aken et al., 2016a,b; Quiros et al., 2017).

8. What are the molecular signals triggering UPR^{mt}?

Each kingdom has developed its own specific regulators (Table 1) that induce and target different genes in the nucleus (Table 2). UPR^{mt} was activated by the accumulation of unfolded proteins in *C. elegans* (Yoneda et al., 2004). This proposal was then consistently supported by the work of Haynes et al (2007) and (2010), and Houtkooper et al (2013). In mammalian cells, UPR^{mt} was activated by introducing a mutation (deletion of amino acids 30–114) in the mitochondrial matrix protein ornithine transcarbamylase (OTC) to prevent protein import into mitochondria and leading to the induction of nuclear genes encoding molecular chaperones *Cpn60* and *Cpn10*, *mtDnaJ*, and the protease, *ClpP* (Zhao et al., 2002). There are additional reports suggesting that unfolded proteins, which are unable to be imported into mitochondria, lead to the activation of UPR^{mt} to maintain mitochondrial functions (Haynes et al., 2007; Haynes et al., 2010; Nargund et al., 2012). A genome-wide RNAi screen in *C. elegans* showed that UPR^{mt} was induced when most mitochondrial processes (electron transport, TCA cycle, lipid catabolism, cardiolipin and phosphatidyl ethanolamine biosynthesis) required for the maintenance of mitochondrial homeostasis were compromised (Rolland et al., 2019). Notably, mitochondrial defects in Ca^{2+} homeostasis and mitophagy failed to induce UPR^{mt} (Rolland et al., 2019). Rolland and his co-workers also proposed that a decrease in mitochondrial membrane potential is a general signal that triggers UPR^{mt}. This is consistent with previous studies that showed drugs, which reduced the size of the mitochondrial membrane potential, e.g. rotenone or AA (Johnson et al., 1981), induced UPR^{mt} (Kacprzak et al., 2020; Liu et al., 2014; Runkel et al., 2013). In *Arabidopsis*, Dox, MB and AA treatment induced gene expression of many common genes and induced UPR^{mt}. As mitochondrial membrane potential is required for import of most mitochondrial proteins, a less negative membrane potential would result in reduced mitochondrial import, again likely resulting in non-imported mitochondrial proteins accumulating, which could trigger UPR^{mt}. A recent report also suggested that accumulation of non-imported chloroplast proteins could be

a signal for plastid-to-nucleus signalling (Wu et al., 2019), involving cytosolic UPR mediating plastid-derived communication. AA blocks the mitochondrial electron transport chain at the N site of complex III and increases the rate of superoxide production (Cadenas et al., 1977; Moller, 2001; Murphy, 2009), suggesting that superoxide might also be a signal that triggers UPR^{mt} in plants. Further work will be needed to determine the precise factors that mediate UPR^{mt} and mitochondria-to-nuclear signalling in general.

9. Conclusions

Here, we have reviewed and compared the current knowledge of the UPR^{mt} across eukaryotic kingdoms. Although each kingdom has developed their own specific regulators, UPR^{mt} activation leads to the nuclear induction of common genes that restore mitochondrial function, so the strategies to resolve the mitochondrial dysfunctions are more or less conserved. Furthermore, UPR^{mt} and related pathways also induce genes encoding non-mitochondrial metabolic and regulatory proteins that might enhance survival and restore (inter-) cellular balance, for instance, by affecting hormone/growth factor signalling. Specific regulatory components and responsive genes of the UPR^{mt} in animals and plants have been identified, but the precise signals that trigger UPR^{mt} are still elusive. One reason for the apparently independent evolution of different mitochondria-to-nuclear signalling pathways across kingdoms could be that specific needs for such control arose with major evolutionary events, such as the colonisation of land or development of multicellularity.

Acknowledgements

OVA and HCT were supported by the Swedish Research Council (Vetenskapsrådet 2017-03854), Crafoord Foundation (20170862; 20190868), Carl Trygger Foundation (CTS 17 487).

References

Abramov, A.Y., Berezhnov, A.V., Fedotova, E.I., Zinchenko, V.P., Dolgacheva, L.P., 2017. Interaction of misfolded proteins and mitochondria in neurodegenerative disorders. Biochem. Soc. Trans. 45, 1025–1033.
Adamowicz-Skrzypkowska, A., Kwasniak-Owczarek, M., Van Aken, O., Kazmierczak, U., Janska, H., 2020. Joint restriction of two terminal mitochondrial oxidases, complex IV and AOX, represses chloroplast transcription in Arabidopsis. Philos. Trans. R. Soc. Lond. B. Biol. Sci. 375 (1801), 20190409.
Aharoni, A., Dixit, S., Jetter, R., Thoenes, E., van Arkel, G., Pereira, A., 2004. The SHINE clade of AP2 domain transcription factors activates wax biosynthesis, alters cuticle properties, and confers drought tolerance when overexpressed in Arabidopsis. Plant Cell 16, 2463–2480.
Al Rawi, S., Louvet-Vallee, S., Djeddi, A., Sachse, M., Culetto, E., Hajjar, C., Boyd, L., Legouis, R., Galy, V., 2011. Postfertilization autophagy of sperm organelles prevents paternal mitochondrial DNA transmission. Science 334, 1144–1147.
Alonso, J.M., Stepanova, A.N., Solano, R., Wisman, E., Ferrari, S., Ausubel, F.M., Ecker, J.R., 2003. Five components of the ethylene-response pathway identified in a screen for weak ethylene-insensitive mutants in Arabidopsis. Proc. Natl. Acad. Sci. U.S.A. 100, 2992–2997.
Anderson, S., Bankier, A.T., Barrell, B.G., de Bruijn, M.H., Coulson, A.R., Drouin, J., Eperon, I.C., Nierlich, D.P., Roe, B.A., Sanger, F., Schreier, P.H., Smith, A.J., Staden, R., Young, I.G., 1981. Sequence and organization of the human mitochondrial genome. Nature 290, 457–465.
Asahina, M., Azuma, K., Pitaksaringkarn, W., Yamazaki, T., Mitsuda, N., Ohme-Takagi, M., Yamaguchi, S., Kamiya, Y., Okada, K., Nishimura, T., Koshiba, T., Yokota, T., Kamada, H., Satoh, S., 2011. Spatially selective hormonal control of RAP2.6L and ANAC071 transcription factors involved in tissue reunion in Arabidopsis. Proc. Natl. Acad. Sci. U.S.A. 108, 16128–16132.
Baker, M.J., Tatsuta, T., Langer, T., 2011. Quality control of mitochondrial proteostasis. Cold Spring Harb. Perspect. Biol. 3.
Ballinger, S.W., 2005. Mitochondrial dysfunction in cardiovascular disease. Free Radic. Biol. Med. 38, 1278–1295.
Bechtold, U., Richard, O., Zamboni, A., Gapper, C., Geisler, M., Pogson, B., Karpinski, S., Mullineaux, P.M., 2008. Impact of chloroplastic- and extracellular-sourced ROS on high light-responsive gene expression in Arabidopsis. J. Exp. Bot. 59, 121–133.
Benedetti, C., Haynes, C.M., Yang, Y., Harding, H.P., Ron, D., 2006. Ubiquitin-like protein 5 positively regulates chaperone gene expression in the mitochondrial unfolded protein response. Genetics 174, 229–239.
Broda, M., Millar, A.H., Van Aken, O., 2018. Mitophagy: a mechanism for plant growth and survival. Trends Plant Sci. 23, 434–450.
Brunet, A., Sweeney, L.B., Sturgill, J.F., Chua, K.F., Greer, P.L., Lin, Y., Tran, H., Ross, S.E., Mostoslavsky, R., Cohen, H.Y., Hu, L.S., Cheng, H.L., Jedrychowski, M.P., Gygi, S.P., Sinclair, D.A., Alt, F.W., Greenberg, M.E., 2004. Stress-dependent regulation of FOXO transcription factors by the SIRT1 deacetylase. Science 303, 2011–2015.
Bui, L.T., Shukla, V., Giorgi, F.M., Trivellini, A., Perata, P., Licausi, F., Giuntoli, B., 2020. Differential submergence tolerance between juvenile and adult Arabidopsis plants involves the ANAC017 transcription factor. bioRxiv.
Cadenas, E., Boveris, A., Ragan, C.I., Stoppani, A.O., 1977. Production of superoxide radicals and hydrogen peroxide by NADH-ubiquinone reductase and ubiquinol-cytochrome c reductase from beef-heart mitochondria. Arch. Biochem. Biophys. 180, 248–257.
Chacinska, A., Koehler, C.M., Milenkovic, D., Lithgow, T., Pfanner, N., 2009. Importing mitochondrial proteins: machineries and mechanisms. Cell 138, 628–644.
Chang, C., 2016. Q&A: how do plants respond to ethylene and what is its importance? BMC Biol. 14, 7.
Clausen, T., Kaiser, M., Huber, R., Ehrmann, M., 2011. HTRA proteases: regulated proteolysis in protein quality control. Nat. Rev. Mol. Cell Biol. 12, 152–162.
Dang, W., 2014. The controversial world of sirtuins. Drug Discov. Today Technol. 12, e9–e17.
Deng, P., Uma Naresh, N., Du, Y., Lamech, L.T., Yu, J., Zhu, L.J., Pukkila-Worley, R., Haynes, C.M., 2019. Mitochondrial UPR repression during Pseudomonas aeruginosa infection requires the bZIP protein ZIP-3. Proc. Natl. Acad. Sci. U.S.A. 116, 6146–6151.
Duarte, J.M., Schuck, P.F., Wenk, G.L., Ferreira, G.C., 2014. Metabolic disturbances in diseases with neurological involvement. Aging Dis. 5, 238–255.
Dubois, M., Skirycz, A., Claeys, H., Maleux, K., Dhondt, S., De Bodt, S., Vanden Bossche, R., De Milde, L., Yoshizumi, T., Matsui, M., Inze, D., 2013. Ethylene Response Factor6 acts as a central regulator of leaf growth under water-limiting conditions in Arabidopsis. Plant Physiol. 162, 319–332.
Eisner, V., Picard, M., Hajnoczky, G., 2018. Mitochondrial dynamics in adaptive and maladaptive cellular stress responses. Nat. Cell Biol. 20, 755–765.
Fiorese, C.J., Schulz, A.M., Lin, Y.F., Rosin, N., Pellegrino, M.W., Haynes, C.M., 2016. The transcription factor ATF5 mediates a mammalian mitochondrial UPR. Curr. Biol. 26, 2037–2043.
Fu, M., Kang, H.K., Son, S.H., Kim, S.K., Nam, K.H., 2014. A subset of Arabidopsis RAV transcription factors modulates drought and salt stress responses independent of ABA. Plant Cell Physiol. 55, 1892–1904.
Fukasawa, Y., Tsuji, J., Fu, S.C., Tomii, K., Horton, P., Imai, K., 2015. MitoFates: improved prediction of mitochondrial targeting sequences and their cleavage sites. Mol. Cell. Proteomics 14, 1113–1126.
Fusakio, M.E., Willy, J.A., Wang, Y., Mirek, E.T., Al Baghdadi, R.J., Adams, C.M., Anthony, T.G., Wek, R.C., 2016. Transcription factor ATF4 directs basal and stress-induced gene expression in the unfolded protein response and cholesterol metabolism in the liver. Mol. Biol. Cell 27, 1536–1551.
Haynes, C.M., Petrova, K., Benedetti, C., Yang, Y., Ron, D., 2007. ClpP mediates activation of a mitochondrial unfolded protein response in C. elegans. Dev. Cell 13, 467–480.
Haynes, C.M., Yang, Y., Blais, S.P., Neubert, T.A., Ron, D., 2010. The matrix peptide exporter HAF-1 signals a mitochondrial UPR by activating the transcription factor ZC376.7 in C. elegans. Mol. Cell 37, 529–540.
Hernando-Rodriguez, B., Artal-Sanz, M., 2018. Mitochondrial Quality Control Mechanisms and the PHB (Prohibitin) Complex. Cells 7.
Horstman, A., Willemsen, V., Boutilier, K., Heidstra, R., 2014. AINTEGUMENTA-LIKE proteins: hubs in a plethora of networks. Trends Plant Sci. 19, 146–157.
Houtkooper, R.H., Mouchiroud, L., Ryu, D., Moullan, N., Katsyuba, E., Knott, G., Williams, R.W., Auwerx, J., 2013. Mitonuclear protein imbalance as a conserved longevity mechanism. Nature 497, 451–457.
Houtkooper, R.H., Pirinen, E., Auwerx, J., 2012. Sirtuins as regulators of metabolism and healthspan. Nat. Rev. Mol. Cell Biol. 13, 225–238.
Howell, S.H., 2013. Endoplasmic reticulum stress responses in plants. Annu. Rev. Plant Biol. 64, 477–499.
Huang, S., Taylor, N.L., Whelan, J., Millar, A.H., 2009. Refining the definition of plant mitochondrial presequences through analysis of sorting signals, N-terminal modifications, and cleavage motifs. Plant Physiol. 150, 1272–1285.
Ivanova, A., Law, S.R., Narsai, R., Duncan, O., Lee, J.H., Zhang, B., Van Aken, O., Radomiljac, J.D., van der Merwe, M., Yi, K., Whelan, J., 2014. A functional antagonistic relationship between auxin and mitochondrial retrograde signaling regulates alternative oxidase1a expression in arabidopsis. Plant Physiol. 165, 1233–1254.
Jazwinski, S.M., Kriete, A., 2012. The yeast retrograde response as a model of intracellular signaling of mitochondrial dysfunction. Front. Physiol. 3, 139.
Johnson, L.V., Walsh, M.L., Bockus, B.J., Chen, L.B., 1981. Monitoring of relative mitochondrial membrane potential in living cells by fluorescence microscopy. J. Cell Biol. 88, 526–535.
Kim, J.S., Yamaguchi-Shinozaki, K., Shinozaki, K., 2018. ER-Anchored transcription factors bZIP17 and bZIP28 regulate root elongation. Plant Physiol. 176, 2221–2230.
Kacprzak, S., Dahlqvist, A., Van Aken, O., 2020. The transcription factor ANAC017 is a key regulator of mitochondrial proteotoxic stress responses in plants. Philos. Trans. R Soc. Lond. B Biol. Sci. 375 (1801), 20190411.
Kim, M.J., Ruzicka, D., Shin, R., Schachtman, D.P., 2012. The Arabidopsis AP2/ERF transcription factor RAP2.11 modulates plant response to low-potassium conditions. Mol Plant 5, 1042–1057.
Kim, S., Sieburth, D., 2018. Sphingosine kinase activates the mitochondrial unfolded protein response and is targeted to mitochondria by stress. Cell Rep. 24 (2932–2945), e2934.
Kim, S., Sieburth, D., 2020. FSHR-1/GPCR regulates the mitochondrial unfolded protein response in caenorhabditis elegans. Genetics 214, 409–418.
Kmiec, B., Teixeira, P.F., Glaser, E., 2014. Shredding the signal: targeting peptide

degradation in mitochondria and chloroplasts. Trends Plant Sci. 19, 771–778.
Konig, A.C., Hartl, M., Pham, P.A., Laxa, M., Boersema, P.J., Orwat, A., Kalitventseva, I., Plochinger, M., Braun, H.P., Leister, D., Mann, M., Wachter, A., Fernie, A.R., Finkemeier, I., 2014. The Arabidopsis class II sirtuin is a lysine deacetylase and interacts with mitochondrial energy metabolism. Plant Physiol. 164, 1401–1414.
Krzywanski, D.M., Moellering, D.R., Fetterman, J.L., Dunham-Snary, K.J., Sammy, M.J., Ballinger, S.W., 2011. The mitochondrial paradigm for cardiovascular disease susceptibility and cellular function: a complementary concept to Mendelian genetics. Lab. Invest. 91, 1122–1135.
Kubo, T., Newton, K.J., 2008. Angiosperm mitochondrial genomes and mutations. Mitochondrion 8, 5–14.
Lama, S., Broda, M., Abbas, Z., Vaneechoutte, D., Belt, K., Sall, T., Vandepoele, K., Van Aken, O., 2019. Neofunctionalization of mitochondrial proteins and incorporation into signaling networks in plants. Mol. Biol. Evol. 36, 974–989.
Liao, X.S., Small, W.C., Srere, P.A., Butow, R.A., 1991. Intramitochondrial functions regulate nonmitochondrial citrate synthase (CIT2) expression in Saccharomyces cerevisiae. Mol. Cell. Biol. 11, 38–46.
Lin, Y.F., Schulz, A.M., Pellegrino, M.W., Lu, Y., Shaham, S., Haynes, C.M., 2016. Maintenance and propagation of a deleterious mitochondrial genome by the mitochondrial unfolded protein response. Nature 533, 416–419.
Liu, Y., Samuel, B.S., Breen, P.C., Ruvkun, G., 2014. Caenorhabditis elegans pathways that surveil and defend mitochondria. Nature 508, 406–410.
Logan, D.C., 2010. Mitochondrial fusion, division and positioning in plants. Biochem. Soc. Trans. 38, 789–795.
Maugarny-Cales, A., Goncalves, B., Jouannic, S., Melkonian, M., Ka-Shu Wong, G., Laufs, P., 2016. Apparition of the NAC transcription factors predates the emergence of land plants. Mol Plant 9, 1345–1348.
McGrath, K.C., Dombrecht, B., Manners, J.M., Schenk, P.M., Edgar, C.I., Maclean, D.J., Scheible, W.R., Udvardi, M.K., Kazan, K., 2005. Repressor- and activator-type ethylene response factors functioning in jasmonate signaling and disease resistance identified via a genome-wide screen of Arabidopsis transcription factor gene expression. Plant Physiol. 139, 949–959.
Melber, A., Haynes, C.M., 2018. UPR(mt) regulation and output: a stress response mediated by mitochondrial-nuclear communication. Cell Res. 28, 281–295.
Meng, X., Li, L., Narsai, R., De Clercq, I., Whelan, J., Berkowitz, O., 2020. Mitochondrial signalling is critical for acclimation and adaptation to flooding in Arabidopsis thaliana. Plant J In Press.
Merkwirth, C., Jovaisaite, V., Durieux, J., Matilainen, O., Jordan, S.D., Quiros, P.M., Steffen, K.K., Williams, E.G., Mouchiroud, L., Tronnes, S.U., Murillo, V., Wolff, S.C., Shaw, R.J., Auwerx, J., Dillin, A., 2016. Two conserved histone demethylases regulate mitochondrial stress-induced longevity. Cell 165, 1209–1223.
Meyer, E.H., Tomaz, T., Carroll, A.J., Estavillo, G., Delannoy, E., Tanz, S.K., Small, I.D., Pogson, B.J., Millar, A.H., 2009. Remodeled respiration in ndufs4 with low phosphorylation efficiency suppresses Arabidopsis germination and growth and alters control of metabolism at night. Plant Physiol. 151, 603–619.
Moller, I.M., 2001. Plant mitochondria and oxidative stress: electron transport, NADPH Turnover, and Metabolism of Reactive Oxygen Species. Annu Rev Plant Physiol Plant Mol Biol 52, 561–591.
Møller, I.M., Sweetlove, L.J., 2011. ROS signalling – specificity is required. Trends Plant Sci. 15, 370–374.
Mouchiroud, L., Houtkooper, R.H., Moullan, N., Katsyuba, E., Ryu, D., Canto, C., Mottis, A., Jo, Y.S., Viswanathan, M., Schoonjans, K., Guarente, L., Auwerx, J., 2013. The NAD(+)/sirtuin pathway modulates longevity through activation of mitochondrial UPR and FOXO signaling. Cell 154, 430–441.
Moullan, N., Mouchiroud, L., Wang, X., Ryu, D., Williams, E.G., Mottis, A., Jovaisaite, V., Frochaux, M.V., Quiros, P.M., Deplancke, B., Houtkooper, R.H., Auwerx, J., 2015. Tetracyclines disturb mitochondrial function across eukaryotic models: a call for caution in biomedical research. Cell Rep 10, 1681–1691.
Munch, C., 2018. The different axes of the mammalian mitochondrial unfolded protein response. BMC Biol. 16, 81.
Munch, C., Harper, J.W., 2016. Mitochondrial unfolded protein response controls matrix pre-RNA processing and translation. Nature 534, 710–713.
Murcha, M.W., Elhafez, D., Millar, A.H., Whelan, J., 2005. The C-terminal region of TIM17 links the outer and inner mitochondrial membranes in Arabidopsis and is essential for protein import. J. Biol. Chem. 280, 16476–16483.
Murphy, M.P., 2009. How mitochondria produce reactive oxygen species. Biochem. J. 417, 1–13.
Narendra, D.P., Jin, S.M., Tanaka, A., Suen, D.F., Gautier, C.A., Shen, J., Cookson, M.R., Youle, R.J., 2010. PINK1 is selectively stabilized on impaired mitochondria to activate Parkin. PLoS Biol. 8, e1000298.
Nargund, A.M., Fiorese, C.J., Pellegrino, M.W., Deng, P., Haynes, C.M., 2015. Mitochondrial and nuclear accumulation of the transcription factor ATFS-1 promotes OXPHOS recovery during the UPR(mt). Mol. Cell 58, 123–133.
Nargund, A.M., Pellegrino, M.W., Fiorese, C.J., Baker, B.M., Haynes, C.M., 2012. Mitochondrial import efficiency of ATFS-1 regulates mitochondrial UPR activation. Science 337, 587–590.
Ng, S., De Clercq, I., Van Aken, O., Law, S.R., Ivanova, A., Willems, P., Giraud, E., Van Breusegem, F., Whelan, J., 2014. Anterograde and retrograde regulation of nuclear genes encoding mitochondrial proteins during growth, development, and stress. Mol Plant 7, 1075–1093.
Ng, S., Ivanova, A., Duncan, O., Law, S.R., Van Aken, O., De Clercq, I., Wang, Y., Carrie, C., Xu, L., Kmiec, B., Walker, H., Van Breusegem, F., Whelan, J., Giraud, E., 2013. A membrane-bound NAC transcription factor, ANAC017, mediates mitochondrial retrograde signaling in Arabidopsis. Plant Cell 25, 3450–3471.
Onate-Sanchez, L., Singh, K.B., 2002. Identification of Arabidopsis ethylene-responsive element binding factors with distinct induction kinetics after pathogen infection. Plant Physiol. 128, 1313–1322.
Pakos-Zebrucka, K., Koryga, I., Mnich, K., Ljujic, M., Samali, A., Gorman, A.M., 2016. The integrated stress response. EMBO Rep. 17, 1374–1395.
Palmfeldt, J., Bross, P., 2017. Proteomics of human mitochondria. Mitochondrion 33, 2–14.
Papa, L., Germain, D., 2011. Estrogen receptor mediates a distinct mitochondrial unfolded protein response. J. Cell Sci. 124, 1396–1402.
Papa, L., Germain, D., 2014. SirT3 regulates the mitochondrial unfolded protein response. Mol. Cell. Biol. 34, 699–710.
Pellegrino, M.W., Nargund, A.M., Haynes, C.M., 2013. Signaling the mitochondrial unfolded protein response. Biochim. Biophys. Acta, Mol. Cell. Biol. Lipids 1833, 410–416.
Prokisch, H., Scharfe, C., Camp 2nd, D.G., Xiao, W., David, L., Andreoli, C., Monroe, M.E., Moore, R.J., Gritsenko, M.A., Kozany, C., Hixson, K.K., Mottaz, H.M., Zischka, H., Ueffing, M., Herman, Z.S., Davis, R.W., Meitinger, T., Oefner, P.J., Smith, R.D., Steinmetz, L.M., 2004. Integrative analysis of the mitochondrial proteome in yeast. PLoS Biol. 2, e160.
Quiros, P.M., Prado, M.A., Zamboni, N., D'Amico, D., Williams, R.W., Finley, D., Gygi, S.P., Auwerx, J., 2017. Multi-omics analysis identifies ATF4 as a key regulator of the mitochondrial stress response in mammals. J. Cell Biol. 216, 2027–2045.
Rainbolt, T.K., Atanassova, N., Genereux, J.C., Wiseman, R.L., 2013. Stress-regulated translational attenuation adapts mitochondrial protein import through Tim17A degradation. Cell Metab. 18, 908–919.
Rao, R.S., Salvato, F., Thal, B., Eubel, H., Thelen, J.J., Moller, I.M., 2017. The proteome of higher plant mitochondria. Mitochondrion 33, 22–37.
Rolland, S.G., Schneid, S., Schwarz, M., Rackles, E., Fischer, C., Haeussler, S., Regmi, S.G., Yeroslaviz, A., Habermann, B., Mokranjac, D., Lambie, E., Conradt, B., 2019. Compromised mitochondrial protein import acts as a signal for UPR(mt). Cell Rep 28 (1659–1669), e1655.
Ruan, L., Zhou, C., Jin, E., Kucharavy, A., Zhang, Y., Wen, Z., Florens, L., Li, R., 2017. Cytosolic proteostasis through importing of misfolded proteins into mitochondria. Nature 543, 443–446.
Runkel, E.D., Liu, S., Baumeister, R., Schulze, E., 2013. Surveillance-activated defenses block the ROS-induced mitochondrial unfolded protein response. PLoS Genet. 9, e1003346.
Salminen, A., Kaarniranta, K., Kauppinen, A., 2013. Crosstalk between oxidative stress and SIRT1: impact on the aging process. Int. J. Mol. Sci. 14, 3834–3859.
Sato, M., Sato, K., 2011. Degradation of paternal mitochondria by fertilization-triggered autophagy in C. elegans embryos. Science 334, 1141–1144.
Scarpulla, R.C., 2006. Nuclear control of respiratory gene expression in mammalian cells. J. Cell. Biochem. 97, 673–683.
Schleiff, E., Becker, T., 2011. Common ground for protein translocation: access control for mitochondria and chloroplasts. Nat. Rev. Mol. Cell Biol. 12, 48–59.
Schmidt, O., Pfanner, N., Meisinger, C., 2010. Mitochondrial protein import: from proteomics to functional mechanisms. Nat. Rev. Mol. Cell Biol. 11, 655–667.
Schwarzlander, M., Konig, A.C., Sweetlove, L.J., Finkemeier, I., 2012. The impact of impaired mitochondrial function on retrograde signalling: a meta-analysis of transcriptomic responses. J. Exp. Bot. 63, 1735–1750.
Selfridge JE, E L, Lu J, Swerdlow RH (2013) Role of mitochondrial homeostasis and dynamics in Alzheimer's disease. Neurobiol Dis., 51: 3–12.
Senkler, J., Senkler, M., Braun, H.P., 2017. Structure and function of complex I in animals and plants – a comparative view. Physiol. Plant. 161, 6–15.
Sogabe, Y., Nakamura, H., Nakagawa, T., Hasegawa, S., Asano, T., Ohta, H., Yamaguchi, K., Mueller, M.J., Kodama, H., Nishiuchi, T., 2011. Visualization of wounding-induced root-to-shoot communication in Arabidopsis. Plant Signal Behav. 6, 1037–1039.
Steinmetz, L.M., Scharfe, C., Deutschbauer, A.M., Mokranjac, D., Herman, Z.S., Jones, T., Chu, A.M., Giaever, G., Prokisch, H., Oefner, P.J., Davis, R.W., 2002. Systematic screen for human disease genes in yeast. Nat. Genet. 31, 400–404.
Tao, R., Coleman, M.C., Pennington, J.D., Ozden, O., Park, S.H., Jiang, H., Kim, H.S., Flynn, C.R., Hill, S., Hayes McDonald, W., Olivier, A.K., Spitz, D.R., Gius, D., 2010. Sirt3-mediated deacetylation of evolutionarily conserved lysine 122 regulates MnSOD activity in response to stress. Mol. Cell 40, 893–904.
Tao, R., Vassilopoulos, A., Parisiadou, L., Yan, Y., Gius, D., 2014. Regulation of MnSOD enzymatic activity by Sirt3 connects the mitochondrial acetylome signaling networks to aging and carcinogenesis. Antioxid. Redox Signal. 20, 1646–1654.
Teske, B.F., Fusakio, M.E., Zhou, D., Shan, J., McClintick, J.N., Kilberg, M.S., Wek, R.C., 2013. CHOP induces activating transcription factor 5 (ATF5) to trigger apoptosis in response to perturbations in protein homeostasis. Mol. Biol. Cell 24, 2477–2490.
Trendeleva, T.A., Zvyagilskaya, R.A., 2018. Retrograde signaling as a mechanism of yeast adaptation to unfavorable factors. Biochemistry (Mosc) 83, 98–106.
Van Aken, O., De Clercq, I., Ivanova, A., Law, S.R., Van Breusegem, F., Millar, A.H., Whelan, J., 2016a. Mitochondrial and chloroplast stress responses are modulated in distinct touch and chemical inhibition phases. Plant Physiol. 171, 2150–2165.
Van Aken, O., Ford, E., Lister, R., Huang, S., Millar, A.H., 2016b. Retrograde signalling caused by heritable mitochondrial dysfunction is partially mediated by ANAC017 and improves plant performance. Plant J. 88, 542–558.
Van Aken, O., Whelan, J., 2012. Comparison of transcriptional changes to chloroplast and mitochondrial perturbations reveals common and specific responses in Arabidopsis. Front. Plant Sci. 3, 281.
Van Aken, O., Zhang, B., Carrie, C., Uggalla, V., Paynter, E., Giraud, E., Whelan, J., 2009. Defining the mitochondrial stress response in Arabidopsis thaliana. Mol Plant 2, 1310–1324.
van der Graaff, E., Dulk-Ras, A.D., Hooykaas, P.J., Keller, B., 2000. Activation tagging of the LEAFY PETIOLE gene affects leaf petiole development in Arabidopsis thaliana. Development 127, 4971–4980.

Vogel, M.O., Moore, M., Konig, K., Pecher, P., Alsharafa, K., Lee, J., Dietz, K.J., 2014. Fast retrograde signaling in response to high light involves metabolite export, MITOGEN-ACTIVATED PROTEIN KINASE6, and AP2/ERF transcription factors in Arabidopsis. Plant Cell 26, 1151–1165.
Vuda, M., Kamath, A., 2016. Drug induced mitochondrial dysfunction: Mechanisms and adverse clinical consequences. Mitochondrion 31, 63–74.
Wagner, S., Van Aken, O., Elsasser, M., Schwarzlander, M., 2018. Mitochondrial energy signaling and its role in the low-oxygen stress response of plants. Plant Physiol. 176, 1156–1170.
Wang, X., Auwerx, J., 2017. Systems phytohormone responses to mitochondrial proteotoxic stress. Mol. Cell 68 (540–551), e545.
Wang, X., Chen, X.J., 2015. A cytosolic network suppressing mitochondria-mediated proteostatic stress and cell death. Nature 524, 481–484.
Wang, Y., Law, S.R., Ivanova, A., van Aken, O., Kubiszewski-Jakubiak, S., Uggalla, V., van der Merwe, M., Duncan, O., Narsai, R., Whelan, J., Murcha, M.W., 2014. The mitochondrial protein import component, Translocase of the inner membrane17-1, plays a role in defining the timing of germination in Arabidopsis. Plant Physiol. 166, 1420–1435.
Weidberg, H., Amon, A., 2018. MitoCPR-A surveillance pathway that protects mitochondria in response to protein import stress. Science 360.
Wolff, S., Weissman, J.S., Dillin, A., 2014. Differential scales of protein quality control. Cell 157, 52–64.
Wright, G., Terada, K., Yano, M., Sergeev, I., Mori, M., 2001. Oxidative stress inhibits the mitochondrial import of preproteins and leads to their degradation. Exp. Cell Res. 263, 107–117.
Wrobel, L., Topf, U., Bragoszewski, P., Wiese, S., Sztolsztener, M.E., Oeljeklaus, S., Varabyova, A., Lirski, M., Chroscicki, P., Mroczek, S., Januszewicz, E., Dziembowski, A., Koblowska, M., Warscheid, B., Chacinska, A., 2015. Mistargeted mitochondrial proteins activate a proteostatic response in the cytosol. Nature 524, 485–488.
Wu, G.Z., Meyer, E.H., Richter, A.S., Schuster, M., Ling, Q.H., Schottler, M.A., Walther, D., Zoschke, R., Grimm, B., Jarvis, R.P., Bock, R., 2019. Control of retrograde signalling by protein import and cytosolic folding stress. Nat. Plants 5, 525–538.
Yoneda, T., Benedetti, C., Urano, F., Clark, S.G., Harding, H.P., Ron, D., 2004. Compartment-specific perturbation of protein handling activates genes encoding mitochondrial chaperones. J. Cell Sci. 117, 4055–4066.
Zhang, X., Wollenweber, B., Jiang, D., Liu, F., Zhao, J., 2008. Water deficits and heat shock effects on photosynthesis of a transgenic Arabidopsis thaliana constitutively expressing ABP9, a bZIP transcription factor. J. Exp. Bot. 59, 839–848.
Zhao, Q., Wang, J., Levichkin, I.V., Stasinopoulos, S., Ryan, M.T., Hoogenraad, N.J., 2002. A mitochondrial specific stress response in mammalian cells. EMBO J. 21, 4411–4419.

Paper II

Chapter 1

Purification of Leaf Mitochondria from *Arabidopsis thaliana* Using Percoll Density Gradients

Huy Cuong Tran and Olivier Van Aken

Abstract

The study of plant mitochondria often requires isolation of mitochondria from plant tissues in intact and functional form. Here, we describe an effective procedure of mitochondrial isolation from leaf tissues and whole seedlings of the model dicot species *Arabidopsis thaliana* by using differential centrifugation and continuous Percoll density gradients.

Key words Mitochondria, Mitochondrial isolation, Density gradients, Arabidopsis

1 Introduction

Mitochondria are the powerhouses of eukaryotic cells. One way to study plant mitochondria is to isolate pure, intact and functional mitochondria from plant tissues. In this chapter, we present two strategies for plant growth (in soil and in liquid half-strength Murashige and Skoog (MS) media) and mitochondrial isolation from leaf tissues of *Arabidopsis thaliana*. This protocol was adapted from [1–3]. A major problem of mitochondrial isolation is contamination with chloroplast-derived material, especially thylakoids. By using continuous Percoll density gradients, the purity of the extracted mitochondria is greatly improved. Freshly isolated plant mitochondria obtained by this protocol can be used for assays that require intact mitochondria, for example, *in organello* translation assay [4], import assays [5] and respiration measurements [3]. Extracted mitochondria can also be stored at −80 °C and later used for assays that do not require freshly isolated mitochondria, for example blue native polyacrylamide gel (BN-PAGE) followed by colloidal Coomassie staining [5] or in-gel activity assay, and immunoblotting assays [5].

In this chapter, we provide two options to grow starting material for isolating mitochondria, either in soil or in vitro. Soil growth

Olivier Van Aken and Allan G. Rasmusson (eds.), *Plant Mitochondria: Methods and Protocols*, Methods in Molecular Biology, vol. 2363, https://doi.org/10.1007/978-1-0716-1653-6_1,

provides the most natural environment for plants to develop and mitochondria isolated from soil-grown plants can thus be considered most physiologically relevant. Growing plants in soil has nevertheless a number of downsides. For instance, to get enough biomass, a large number of pots and trays are needed, which take up a significant proportion of growth space. Also, many mitochondrial mutants have reduced growth phenotypes [6–8], which makes access to healthy leaf material even more difficult. Prolonged Arabidopsis growth in standard long day conditions (e.g., 16 h light and 8 h dark) results in flowering after 4–5 weeks, which will reduce the gain in usable fresh leaf material (unless mitochondria are desired from flowers and/or stems). To circumvent flowering, researchers can grow their plants under short day conditions (e.g., 8 h light and 16 h dark) for up to several months, resulting in very large vegetative rosettes that provide more input material for mitochondrial preparation, but at a significant cost in time.

In contrast to soil-grown plants, in vitro growth of seedlings (whether on MS media plates or in shaking liquid cultures) is less similar to natural conditions, potentially with waterlogging and hypoxia as a result if the plants are submerged, but has a number of significant advantages. Severe mitochondrial mutants grow extremely poorly in soil [6–8], but perform relatively better in in vitro conditions supplied with nutrients, vitamins and an external carbohydrate. In vitro growth also has the advantages that mitochondria can be isolated in relatively sterile conditions, free from bacterial and/or fungal growth, which is of great importance, for instance, in *in organello* translation assays where bacterial translation can cause a strong background [4]. In addition, in vitro growth of seedlings is useful to grow larger quantities of young tissues (which tend to have a higher mitochondrial content per fresh weight than expanded leaves) in a relatively short period of time (e.g., 2 weeks or less for Col-0), potentially producing large quantities of mitochondria in a short period of time, and using limited growth chamber space. This, however, comes at a significant cost in terms of how many seeds are required per preparation, and thus requires ample bulking of good quality seeds for the assays. Bulking plants to collect a high quantity of seeds can be time-consuming, especially for slow-growing mutants that often have reduced seed yields per plant. A further practical disadvantage of sterile growth is obviously the higher risk for microbial contamination during growth, which could result in complete loss of a sample. Therefore, great care must be taken in seed sterilization and good sterile laboratory practices. Depending on which of these factors are the most important or limiting, researchers can decide to go with soil or in vitro growth.

2 Materials

2.1 Arabidopsis Growth in Soil

1. 6 × 6 × 6 cm pots with draining holes, placed in trays (*see* **Note 1**).
2. Soil mix with vermiculite and perlite at a 4:1:1 ratio.

2.2 Arabidopsis Growth in Shaking Liquid Culture Flasks

1. 500 mL glass wide-mouthed Erlenmeyer conical flasks.
2. Orbital shaker.
3. Liquid half-strength Murashige and Skoog (MS) media: 2.15 g/L MS basal salts powder, 0.5 g/L MES-KOH, pH 5.7, 1% (w/v) sucrose, 1 mL/L Gamborg B5 vitamins 1000×, set pH to 5.7 with KOH. Autoclave and cool-down to room temperature before adding sterilized seeds.
4. Aluminum foil.
5. Commercial chlorine bleach (we use Klorin with 27 g sodium hypochlorite per kg).
6. 70% ethanol.
7. Sterile MilliQ (MQ) water.
8. 1.5 mL Eppendorf tubes.

2.3 Purification of Mitochondria Using Continuous Percoll Density Gradients

1. Mortars and pestles.
2. Funnels.
3. Beckman Coulter Avanti ® J-HC centrifuge with Beckman rotor JA25.50 or similar.
4. 50-mL polycarbonate centrifuge tubes compatible with rotor JA25.50 (Beckman).
5. A gradient mixer.
6. Standard peristaltic pump (e.g., Econo Gradient Pump, Bio-Rad or MINIPULS 3, Gilson).
7. Silicone tubing (e.g., Bio-Rad).
8. A small magnetic stir bar.
9. A magnetic stirrer.
10. Miracloth.
11. Soft paintbrushes.
12. Teflon Dounce homogenizers.
13. Transfer pipettes.
14. 50 mL falcon tubes (Sarstedt).
15. 500 mL glass Erlenmeyer conical flasks.
16. Grinding medium: 0.3 M sucrose, 25 mM tetrasodium pyrophosphate, 2 mM EDTA (disodium salt), 10 mM KH_2PO_4-HCl, pH 7.5, 1% (w/v) polyvinylpyrrolidone-40 (PVP-40), 1%

(w/v) bovine serum albumin (BSA). All chemicals are dissolved well in MQ water before adding BSA. The buffer is stored overnight at 4 °C to allow proper cooling. For 300 mL grinding buffer, 1.06 g of sodium ascorbate and 0.74 g of L-cysteine are added just prior to use on the morning of the mitochondrial isolation. ~30–40 g leaf material can be ground with 150 ml grinding medium.

17. 2× Wash buffer with BSA: 0.6 M sucrose, 20 mM TES, 0.2% (w/v) BSA, pH 7.5 (NaOH). The buffer is stored overnight at 4 °C.
18. 2× Wash buffer without BSA: 0.6 M sucrose, 20 mM TES, pH 7.5 (NaOH). The buffer is stored overnight at 4 °C (*see* **Note 2**).
19. Heavy and light gradient solutions:

Heavy gradient solution (4.4% w/v PVP)	2 gradient tubes (35 mL)	4 gradient tubes (70 mL)
2× wash buffer with BSA	17.5 mL	35 mL
Percoll	9.8 mL	19.6 mL
20% (w/v) PVP-40	7.7 mL	15.4 mL

Light gradient solution (0% w/v PVP)	2 gradient tubes (35 mL)	4 gradient tubes (70 mL)
2× wash buffer with BSA	17.5 mL	35 mL
Percoll	9.8 mL	19.6 mL
MQ water	7.7 mL	15.4 mL

3 Methods

3.1 Arabidopsis Growth in Soil

1. Sow approximately 5–10 Arabidopsis seeds onto a pot containing soil mixed with vermiculite and perlite at a 4:1:1 ratio.
2. Place pots in a larger tray (53 × 32 × 6 cm). At least two full trays (56 pots in total) are required for one mitochondrial isolation (~2–3 mg mitochondrial protein).
3. For stratification, place the trays at 4 °C in the dark for 2–3 days prior to transferring plants to the growth chamber.
4. About 7–10 days after stratification, remove excess seedlings so only one plant grows in each pot to optimize plant growth.
5. Grow plants for a further 3 weeks (*see* **Note 3**).

3.2 Arabidopsis Grown in Liquid Half-Strength MS Medium (Fig. 1)

1. Liquid sterilization of Arabidopsis seeds (about 200–400 seeds/1.5 mL Eppendorf tube): Incubate with 1 mL 70% ethanol for 5 min; remove ethanol and incubate with 1 mL 5× diluted bleach for 15 min, exchange with fresh 5× diluted bleach after every 5 min; remove the 5× diluted bleach and wash with 1 mL sterile MQ water at least 5 times (this step must be carried out under the sterile laminar flow hood to prevent contamination); maintain the seeds in 1 mL sterile MQ water in the tube.
2. Pour 200 mL liquid half-strength MS medium into a 500 mL glass Erlenmeyer conical flask. Cover the top of the flask with aluminum foil.
3. Autoclave MS medium (120 °C, 20 psi, 20 min) and allow the medium to completely cool down to room temperature.
4. In the laminar flow hood, use a P1000 pipette with a sterile tip to transfer sterile 200–400 seeds (maintained in sterile MQ

Fig. 1 Arabidopsis Col-0 grown in liquid half-strength MS medium for 14 days

water) into a flask containing 200 mL autoclaved liquid half-strength MS medium. 200–400 seeds/flask can yield 10–15 g of seedling tissues, which can yield ~1.5 mg mitochondria per flask. Reseal the flask well with the autoclaved aluminum foil.

5. Place the flasks onto a shaker in standard long day plant growth conditions (16 h light/8 h dark, approximately 120 μmol photons m^{-2} s^{-1}) and shake them gently at 100 rpm.
6. Grow seedlings for 14 days (*see* **Notes 3–5**).

3.3 Preparation of Continuous Percoll Density Gradients

1. Prepare heavy and light gradients in 50 mL conical tubes (*see* **item 19**, Subheading 2.2).
2. Wash the chambers of the gradient mixer and the silicone tubing with MQ water and make sure that the flow is not blocked.
3. Place two 50-mL centrifuge tubes on ice and tape the tubing outlet to the inside of the tubes so the gradient solution runs down on the wall of the tubes (Fig. 2).
4. Place the gradient mixer on a magnetic stirrer and close the valve of the gradient mixer (lever in "horizontal" position).
5. Pour the heavy gradient into the first chamber (the chamber with tubing outlet) and place a magnetic stir bar in the chamber.
6. Pour the light gradient into the second chamber (the chamber without tubing outlet).

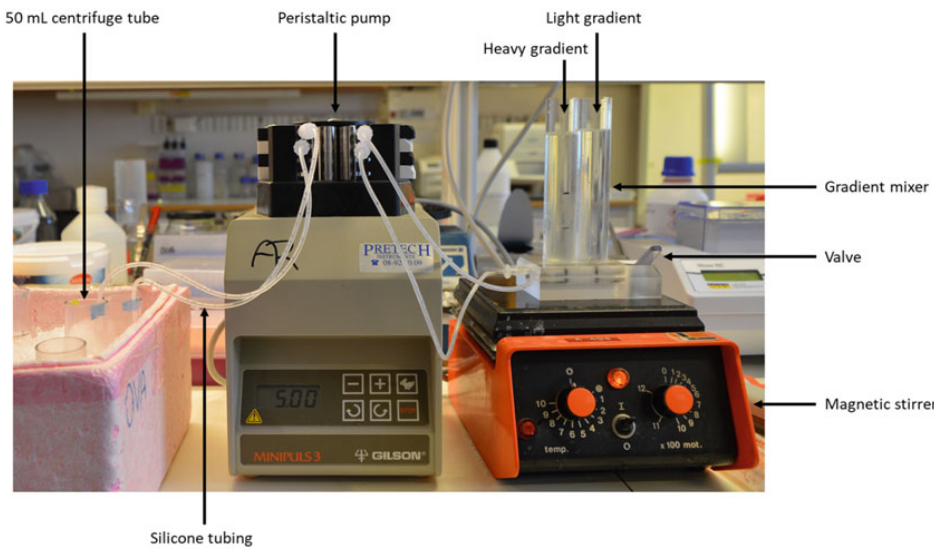

Fig. 2 Preparation of the continuous Percoll gradients

7. Start the stirrer and start the pump to allow the heavy gradient to run until half is dispensed.
8. Open the valve of the gradient mixer to allow the gradients to mix (lever in up position). Set the pump with an appropriate speed of approximately 1 mL per minute (setting 5 on a Gilson MINIPULS 3), until all liquid has passed through the tubing. Multiple gradient tubes can be made at the same time if the pump can pump multiple lines at equal flow rates.
9. Wash the tubing and gradient mixer well with MQ water after use.

3.4 Purification of Arabidopsis Mitochondria

1. For soil-grown plants: collect leaf tissues from plants grown in soil by cutting the rosettes away from the roots and gently rinse them with MQ water to get rid of excess soil. For liquid-culture plants: collect tissues (mainly leaf tissues) from plants grown in liquid culture by filtering seedlings from excess media using a sieve and gently rinsing with MQ water.
2. Pour the grinding medium into a large precooled mortar and grind plant material with a precooled pestle on ice/in the cold room (4 °C) (*see* **Note 6**). Leave a few deciliters of grinding buffer for regrinding a second time (*see* **step 4**).
3. Filter homogenate through a miracloth that is set up in a funnel (Fig. 3).
4. Scrape and regrind any solid material left on the miracloth using the last bit of grinding medium. Pass this last bit of material again through the miracloth and funnel with the first fraction.
5. Transfer the filtered homogenate to 4–6 precooled 50-mL centrifuge tubes.

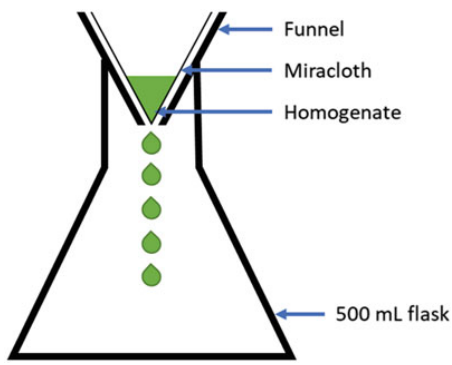

Fig. 3 Collecting plant homogenate from leaf tissues

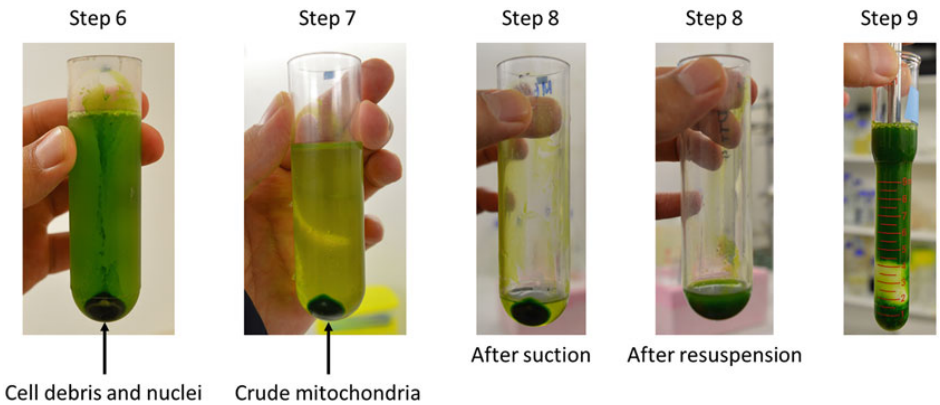

Fig. 4 Collecting crude mitochondria by centrifugation

6. Centrifuge for 5 min at 2500 × *g* at 4 °C to pellet cellular debris and nuclei, and transfer the supernatant into new cold 50-mL centrifuge tubes (Fig. 4).
7. Centrifuge 20 min at 17,500 × *g* at 4 °C to pellet crude mitochondria.
8. Remove the supernatant by suction in the cold room and gently resuspend the pellets in residual supernatant with a soft paintbrush.
9. Use a prechilled glass–Teflon homogenizer to ensure that there are no clumps due to poor resuspension (this step can be omitted and should be done in the cold room).
10. Combine the resuspension from 4 tubes into one 50-mL centrifugation tube per genotype/treatment and fill the tube with 1x Wash buffer with BSA (*see* **Note 7**).
11. Repeat **steps 6–9**.
12. Use a transfer pipette to carefully transfer the crude mitochondria onto the surface of the 0–4.4% (w/v) PVP-Percoll gradient.
13. Balance the tubes with 1× Wash buffer with BSA and centrifuge for 40 min at 40,000 ×*g* at 4 °C with the brake off (*see* **Note 8**).
14. Mitochondria should be present as a light-yellow layer at the bottom of the tube after centrifugation. Remove upper layers above by suction in the cold room, without disturbing the mitochondria at the bottom (Fig. 5).
15. Fill the tube with 1× Wash buffer with/without BSA and centrifuge for 15 min at 31,000 × *g* at 4 °C with slow brakes (*see* **Note 2**).

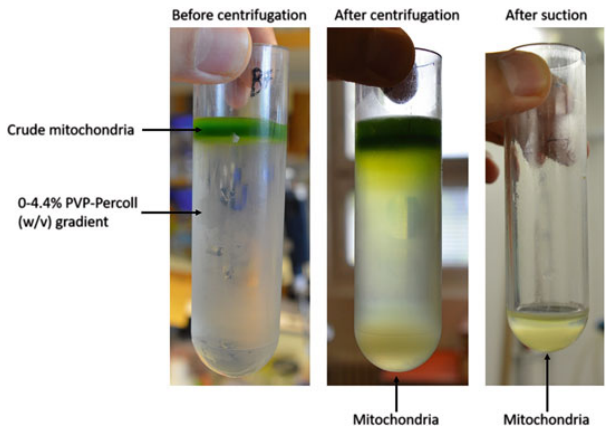

Fig. 5 Collecting mitochondria by using continuous Percoll gradient

Fig. 6 Wash and collect the final mitochondrial fraction (**steps 15–18**)

16. Mitochondria should be at the bottom of the tube and the pellet is very loose (Fig. 6). Remove the supernatant by suction.
17. Repeat **steps 15** and **16**.
18. Transfer mitochondria into a prechilled 1.5 mL microcentrifuge tube.
19. The concentration of mitochondria can be determined by Bradford assays (Bio-Rad).
20. Isolated mitochondria can be aliquoted to desired quantity, so consider what are logical aliquot sizes that are required for your future experiments (e.g., respiration assays, western blotting,

BN-PAGE, import assays). Based on the protein concentration and future application, transfer the appropriate volume of resuspended mitochondria to 1.5–2 mL Eppendorf tubes and centrifuge at 16,100 × *g* for 5 min at 4 °C. Remove the supernatant and for example resuspend mitochondria in 1× Wash buffer for further experimentation requiring intact mitochondria or store at −80 °C for later use.

4 Notes

1. Other common pot types that allow sufficient draining and provide sufficient space for individual plants to grow can also be used.
2. If isolated mitochondria will be used for BN-PAGE or immunoblotting assays, use 1× Wash buffer without BSA in the two final washes (**steps 15–17**).
3. Four weeks of total growth is usually sufficient for Col-0 wild-type plants. If mutants with significant growth delays are being used, this time needs to be extended by for example 1–2 weeks, or sometimes more. It is advisable to start growing the mutants the required extra time before starting growth of Col-0 wild type or normal-growing mutants, so all mitochondrial preps can be done on the same day. This generally gives more consistent results and equal loading in downstream application, and saves on time, rather than doing mitochondrial isolations on separate days when the slow mutants have reached an equivalent size to a 4-week-old wild-type plant. This approach is also advisable for in vitro grown seedlings and needs to be established empirically for each individual mutant line.
4. Regularly check the flasks for potential contamination. If contamination is observed, the flask should be removed from the experiment. It is generally wise to prepare a few extra flasks (e.g., 1–2) to ensure sufficient uncontaminated flasks remain at the end. We recommend sterilizing Arabidopsis seeds by using liquid sterilization method to minimize the chance of microbial contamination (*see* Subheading 3.1, **step 2**). Dry sterilization by chlorine gas overnight can also be performed but avoid having too many seeds in a single tube, as the gas will not penetrate fully.
5. An alternative fast way to grow the seedlings in vitro with normal air exposure, is to sow sterilized seeds on large square plates (e.g., 10 cm × 10 cm) with solid half-strength MS medium (as described for liquid culture) with 0.8% plant agar. Seeds should be evenly spread in a lawn over the media plates (seal the plates with porous tape afterward). Approximately

100 μL of dry seeds can be spread evenly over four 10 cm × 10 cm plates and grown for 2 weeks (or longer for slow growing mutants). Seedlings can be plucked from the agar plates for collection. Make sure the majority of agar media is removed from the roots for example by gently washing with clean water. *Dry the collected and washed seedlings* with tissue paper to remove excess water before proceeding to grinding.

6. We recommend doing all steps of mitochondrial isolation in the cold room (4 °C) to prevent degradation. It is also possible to keep the precooled mortar and pestle in a large cooler box filled with ice and grind the samples on the bench in the lab (room temperature). Extra care must of course be taken that everything stays very well cooled. Always store the centrifugation tubes on ice to preserve sample integrity.
7. 2× Wash buffer should be diluted into 1× Wash buffer with ice-cold MQ water.
8. It is important to switch off maximum brakes (use slow brakes) on the centrifuge when the gradient is loaded. Strong braking will cause turbulence and disrupt the gradient or resuspend the loose mitochondrial pellets in the wash-steps after the gradients. In some cases, the centrifuge may experience errors that override the brake settings into maximum breaks (e.g., vacuum/pump seal failure), destroying the gradient and resulting in a homogeneous green suspension. If the samples are important enough to salvage, one can rerun **step 13** (40,000 × *g* spin) with these tubes, and the gradient will largely reform by itself, allowing recovery of the mitochondria from the bottom with still relatively good purity.

Acknowledgments

OVA and HCT were supported by the Swedish Research Council (Vetenskapsrådet 2017-03854), Crafoord Foundation (20170862;20190868), Carl Tryggers Foundation (CTS 17: 487).

References

1. Murcha MW, Whelan J (2015) Isolation of intact mitochondria from the model plant species Arabidopsis thaliana and Oryza sativa. Methods Mol Biol 1305:1–12. https://doi.org/10.1007/978-1-4939-2639-8_1
2. Day D, Neuburger M, Douce R (1985) Biochemical characterization of chlorophyll-free mitochondria from pea leaves. Aust J Plant Physiol 12(3):219–228. https://doi.org/10.1071/PP9850219
3. Keech O, Dizengremel P, Gardeström P (2005) Preparation of leaf mitochondria from Arabidopsis thaliana. Physiol Plant 124(4):403–409. https://doi.org/10.1111/j.1399-3054.2005.00521.x
4. Kwasniak-Owczarek M, Tomal A, Janska H (2021) Assessment of protein synthesis in mitochondria isolated from rosette leaves and liquid culture seedlings of Arabidopsis. In: Van Aken O, Rasmusson AG (eds) Plant

mitochondria: methods and protocols. Methods in molecular biology, vol 2363. Springer, New York

5. Zhang B, Carrie C, Ivanova A, Narsai R, Murcha MW, Duncan O, Wang Y, Law SR, Albrecht V, Pogson B, Giraud E, Van Aken O, Whelan J (2012) LETM proteins play a role in the accumulation of mitochondrially encoded proteins in Arabidopsis thaliana and AtLETM2 displays parent of origin effects. J Biol Chem 287 (50):41757–41773. https://doi.org/10.1074/jbc.M112.383836
6. Kuhn K, Yin G, Duncan O, Law SR, Kubiszewski-Jakubiak S, Kaur P, Meyer E, Wang Y, Small CC, Giraud E, Narsai R, Whelan J (2015) Decreasing electron flux through the cytochrome and/or alternative respiratory pathways triggers common and distinct cellular responses dependent on growth conditions. Plant Physiol 167(1):228–250. https://doi.org/10.1104/pp.114.249946
7. Meyer EH, Tomaz T, Carroll AJ, Estavillo G, Delannoy E, Tanz SK, Small ID, Pogson BJ, Millar AH (2009) Remodeled respiration in ndufs4 with low phosphorylation efficiency suppresses Arabidopsis germination and growth and alters control of metabolism at night. Plant Physiol 151(2):603–619. https://doi.org/10.1104/pp.109.141770
8. Van Aken O, Ford E, Lister R, Huang S, Millar AH (2016) Retrograde signalling caused by heritable mitochondrial dysfunction is partially mediated by ANAC017 and improves plant performance. Plant J 88(4):542–558. https://doi.org/10.1111/tpj.13276

Paper III

Mitochondrial translation in plants is initiated by a unique mTRAN-mRNA interaction mechanism

Huy Cuong Tran[1], Vivian Schmitt[1], Sbatie Lama[1,2], Chuande Wang[3], Alexandra Launay-Avon[4,5], Katja Bernfur[6], Kristin Hofmann[7], Kasim Khan[1], Benoit Castandet[4,5], Fredrik Levander[7,8], Allan G. Rasmusson[1], Hakim Mireau[3], Etienne Delannoy[4,5], Olivier Van Aken[1*]

[1] Department of Biology, Lund University, Lund, Sweden

[2] Current address: Department of Plant Breeding, Swedish University of Agricultural Sciences, Alnarp, Sweden

[3] Institut Jean-Pierre Bourgin, INRAE, AgroParisTech, CNRS, Université Paris-Saclay, RD10, 78026 Versailles Cedex, France

[4] Université Paris-Saclay, CNRS, INRAE, Université d'Évry, Institute of Plant Sciences Paris-Saclay (IPS2), 91405, Orsay, France

[5] Université Paris Cité, CNRS, INRAE, Institute of Plant Sciences Paris-Saclay (IPS2), 91405, Orsay, France

[6] Department of Chemistry, Lund University, Lund, Sweden

[7] Department of Immunotechnology, Lund University, Lund, Sweden

[8] National Bioinformatics Infrastructure Sweden, Science for Life Laboratory, Lund University, Lund, Sweden

*Corresponding author Olivier Van Aken
Molecular Cell Biology Unit
Department of Biology
Lund University
Sölvegatan 35
Lund 223 62 – Lund, Sweden
Tel: +46 76 210 14 03
E-mail: olivier.van_aken@biol.lu.se

ABSTRACT

Plant mitochondria collectively represent the largest group of respiring organelles on our planet. They contain their own set of ribosomes to produce an essential set of proteins, yet the mechanism of mitochondrial translation initiation is currently elusive. Despite their bacterial origin, plant mitochondrial mRNAs do not contain Shine-Dalgarno-like ribosome-binding sites, so it is unknown how plant mito-ribosomes recognise and bind mRNA. We show that "mitochondrial translation factors" mTRAN1 and mTRAN2 are land plant-specific proteins, essential for biogenesis of the mitochondrial respiration chain. Our studies suggest that mTRANs are non-canonical pentatricopeptide repeat-like (PPR) proteins and are part of the mitoribosomal 'small' subunit. As PPR proteins are RNA-binding proteins, we searched the 5' untranslated regions (UTRs) of Arabidopsis mitochondrial mRNAs and identified conserved A/U-rich motifs. Furthermore, we show that mTRAN1 directly binds this motif, indicating it is a homing factor for the mito-ribosome to identify mRNAs and start translation. Using a combination of *in organello* translation assays, polysome profiling and ribosome footprinting, we demonstrate that mTRANs are indeed the elusive universal translation initiation factors, required for translation of all mitochondrial mRNAs in plant mitochondria. Plant mitochondrial translation initiation thus appears to use protein-mRNA interaction, and is fundamentally different compared to in bacteria or mammalian mitochondria.

INTRODUCTION

Plant mitochondria produce a large amount of adenosine triphosphate (ATP) to power the metabolic reactions needed for their growth, development, and maintenance. As mitochondria originated from an endosymbiotic event, they have partially retained their own genome and translational machinery, although most of the mitochondrial proteins are nuclear-encoded (Rao et al., 2017; Schmidt et al., 2010). In plants, the number of unique mitochondrial proteins is estimated to be from around 1000 to >2000 (Fuchs et al., 2020; Rao et al., 2017), but the mitochondrial genome only encodes 20–40 protein-coding genes (Moller et al., 2021; Mower, 2020). Despite a bacterial origin, mitochondrial translation, whose core components include tRNA, rRNA and mitoribosomal proteins, is substantially different from its bacterial counterpart (Greber and Ban, 2016; Mai et al., 2017; Planchard et al., 2018). In yeast, mitochondrial translation initiation is regulated by the coordinated action of general translational factors associated with the mitoribosome and mRNA-specific factors that bind specific regions of transcript 5'-untranslated regions (5'UTRs) to properly position translation initiation sites (Derbikova et al., 2018; Green-Willms et al., 1998). Mammalian mitochondrial mRNAs have no or extremely short 5'UTRs and translation can start directly on non-AUG start codons (Kummer et al., 2018; Montoya et al., 1981).

In flowering plants, a bacterial-type Shine–Dalgarno sequence needed for translation initiation and mitoribosome binding cannot be found within the 5'UTRs (Hazle and Bonen, 2007). Therefore, how mitoribosomes interact with 5'UTRs of plant mitochondrial mRNAs and how plant mitoribosomal small subunits (mtSSU) identify correct translation start codons is poorly understood. Strikingly, plant mitoribosomes are larger than bacterial ribosomes, mammalian and yeast mitoribosomes, as the mtSSU is substantially larger, even larger than the plant mitoribosomal large subunit (mtLSU) (Rugen et al., 2019; Waltz et al., 2019). The plant mitoribosome structure and core components have recently been studied (Rugen et al., 2019; Waltz et al., 2019; Waltz et al., 2020), which showed that plant-specific pentatricopeptide repeat (rPPR) proteins have become *bona fide* ribosomal constituents. PPR proteins contain repeats of 35 amino-acid tandem motifs, each of which forming two anti-parallel α-helices that interact with each other to generate a helix-turn-helix motif (Manna, 2015; Small and Peeters, 2000). The series of helix-turn-helix motifs generated by PPR domains forms a superhelix with a central groove, allowing the PPR protein to interact with the RNA strand (Schmitz-Linneweber and Small, 2008; Small and Peeters, 2000).

In this work, we characterized Arabidopsis genes *AT4G15640* and *AT3G21465*, which are annotated as adenylyl cyclases (ACs) on The Arabidopsis Information Resource (TAIR), but were also suggested to be part of the mitochondrial ribosome (Rugen et al., 2019; Waltz et al., 2019). ACs are enzymes that catalyze the conversion of ATP to 3'-5'-cyclic adenosine monophosphate (cAMP) – a second messenger that can affect different physiological and biochemical processes. ACs have been extensively studied in animals, but little is known about ACs in plants (Al-Younis et al., 2015; Moutinho et al., 2001). Here, we show that AT4G15640 and AT3G21465 are mitochondrial land plant-specific proteins that are crucial for plant growth and development. Interestingly, we found that AT4G15640 and AT3G21465 do not appear to be ACs. However, loss of *AT4G15640* and *AT3G21465* strongly reduces abundance and activity of mitochondrial respiratory complexes and decreases the abundance of mitochondrially-encoded OXPHOS proteins. Co-immunoprecipitation followed by tandem mass spectrometry shows that AT4G15640 and AT3G21465 are part of the mtSSU. In agreement, polysome profiling showed that AT4G15640 and AT3G21465 are required for translation initiation by the plant mitoribosomes. Therefore, we propose a new annotation for AT4G15640 and AT3G21465: MITOCHONDRIAL TRANSLATION FACTOR 1 (mTRAN1) and MITOCHONDRIAL TRANSLATION FACTOR 2 (mTRAN2), respectively. Our further analysis shows that both the mTRAN1 and mTRAN2 seem to be non-canonical PPR proteins, which are known as RNA-binding proteins. Moreover, RNA electrophoretic mobility shift assays (REMSAs) reveal that mTRAN1 - the main isoform present in Arabidopsis - could directly bind to conserved sequences in the 5'UTRs of mitochondrial mRNAs, suggesting these are the mitoribosomal binding sites required for translation initiation. Finally, analysis of mitochondrial ribosome footprints indicates that mTRAN1 and mTRAN2 are universal mtSSU translation initiation factors.

RESULTS

mTRAN1 and mTRAN2 are plant-specific proteins

A BLAST search of mTRAN1 (AT4G15640) and mTRAN2 (AT3G21465) showed that they are plant-specific proteins, present only in the genomes of *Embryophyta* (land plants). Protein sequence alignment showed that mTRANs are highly similar to one another (84% identical), suggesting that they could be paralogs in *Arabidopsis thaliana*. To construct a phylogenetic tree, we selected representative vascular and non-vascular land plant species (Fig. 1A and S1).

Interestingly, some angiosperms, including three members of *Brassicaceae* family, and *Glycine max* contain two mTRAN proteins, indicating that the duplication event of mTRAN proteins occurred relatively late in evolution, with the divergence of *Fabaceae* dating back around 70 million years ago (Centeno-Gonzalez et al., 2021). This also suggests that one of the mTRAN proteins may be redundant to the other mTRAN protein. Notably, *Physcomitrium patens*, a non-vascular moss, also has two mTRAN proteins, suggesting independent duplication events may have occurred throughout the lineages. The remaining land plant species examined here contain only one mTRAN protein.

mTRAN1 and mTRAN2 are targeted to mitochondria

Based on available databases, mTRAN1 is suggested to be mitochondrially targeted (Hooper et al., 2017). Indeed, mTRAN1 is potentially localized in mitochondria as it was found in mitochondrial complexome profiling by Senkler et al. (2017). Therefore, we performed a detailed analysis of the subcellular localization of both mTRAN1 and mTRAN2. mTRAN1-GFP and mTRAN2-GFP translational fusions were stably expressed in Arabidopsis Col-0 plants. Confocal microscopy analysis in root tissue revealed that mTRAN1-GFP and mTRAN2-GFP co-localized with the MitoTracker Red labelled-mitochondria (Fig. 1B). To further confirm that mTRANs are targeted to mitochondria, we performed immunoblot analysis on purified cytosolic, mitochondrial and chloroplastic fractions isolated from Arabidopsis seedlings expressing mTRAN1/2-GFP (Fig. 1C). The mitochondrial and chloroplastic fractions were confirmed using antibodies against chloroplast-targeted PGR5-LIKE PHOTOSYNTHETIC PHENOTYPE 1 (PGRL1) and mitochondrially-targeted TRANSLOCASE OF THE OUTER MITOCHONDRIAL MEMBRANE 40 (TOM40), respectively. The purified mitochondrial and chloroplastic fractions were relatively free of contamination, since no signals could be detected using antibodies against PGRL1 and TOM40 for mitochondrial and chloroplastic fractions, respectively. Using an antibody against GFP, mTRAN1-GFP and mTRAN2-GFP could be detected only in the mitochondrial fractions. Together, our findings indicate that mTRAN1 and mTRAN2 are mitochondria-localized proteins.

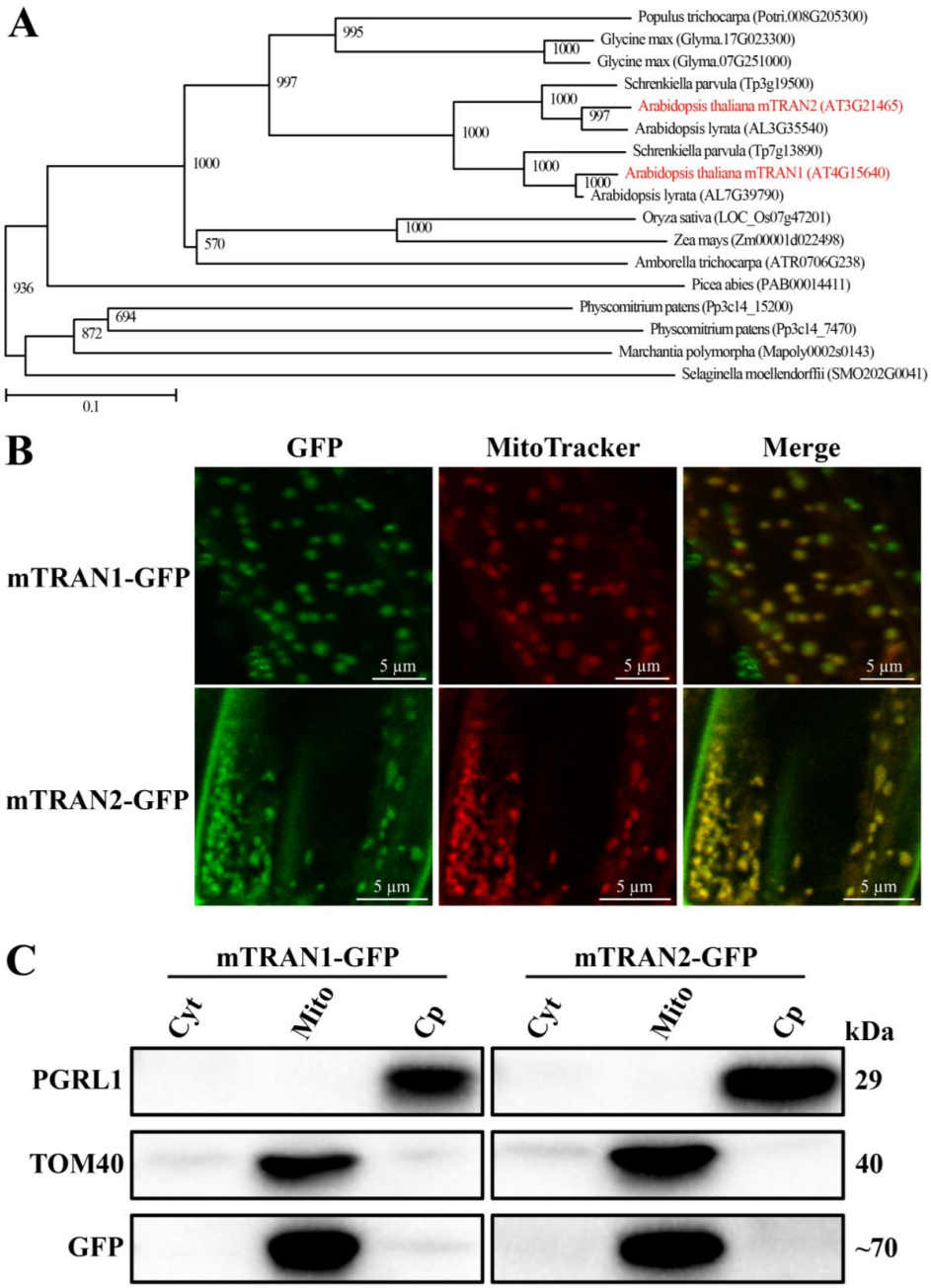

Figure 1. mTRAN1 and mTRAN2 are land plant-specific proteins targeted to mitochondria. A. Phylogenetic tree of mTRAN1 (AT4G15640) and mTRAN2 (AT3G21465) from *Arabidopsis thaliana* with mTRAN proteins from other *Embryophyta* (land plants). Scale bar indicates 10% sequence divergence, node numbers indicate bootstrap values. **B.** Full-length coding sequences of mTRAN1 and mTRAN2 were fused with GFP at the C-termini to assess

GFP targeting in stably transformed Arabidopsis plants. Imaging was done by confocal microscopy on root cells. Mitochondria were labelled with MitoTracker Red. Scale bars: 5 µm. **C.** Immunoblot analysis of cytosolic, mitochondrial and chloroplastic fractions isolated from homozygous Arabidopsis seedlings carrying *mTRAN1-GFP* and *mTRAN2-GFP*. Blots were probed with antibodies against chloroplast-targeted PGRL1, mitochondrially-targeted TOM40 and GFP. The molecular weight (kDa) is shown on the right side of each blot. Cyt = Cytosol, Mito = Mitochondria, Cp = Chloroplast.

The *mtran* mutants have a growth reduction phenotype

mTRAN1 and *mTRAN2* genes show relatively similar expression patterns during plant development (Fig. S2). Of note, mTRAN proteins are expressed very early in seeds during germination (one day after imbibition) (Fig. S2), suggesting that they might be critical for plant growth and development. To characterize Arabidopsis mTRAN proteins, three independent knockout lines were obtained for each gene (Fig. 2A). We were able to obtain double homozygous knockout plants *mtran1-1* x *mtran2-1* (*mtran1-1/2-1*) and *mtran1-2* x *mtran2-2* (*mtran1-2/2-2*), in which loss of both *mTRAN1* and *mTRAN2* transcripts was verified by qRT-PCR (Fig. S3C). Only plants that were homozygous for either *mtran1-3* or *mtran2-3* and hemizygous for the other mutations could be obtained, indicating that *mtran1-3/2-3* was lethal (Fig. S3A and S3B). The *mtran1* single mutants seemed to be smaller than Col-0 (the wild type), while the *mtran2* mutants appeared closer to Col-0 (Fig. 2B). *mtran1-1/2-1* was also smaller than Col-0, while *mtran1-2/2-2* showed severe growth retardation compared to Col-0 at the same age (Fig. 2B). Plate-based germination and development analysis (Boyes et al., 2001) showed that both the *mtran* single and double mutants were significantly slower to germinate (stage 0.5) and develop true leaves (stage 1.02/1.04) (Fig. 2C). Primary roots of the *mtran* single and double mutants were significantly shorter than those of the wild type (Fig. 2D). Again, particularly the double mutants showed a severely reduced growth of the primary root compared to the wild type. Measurement of rosette leaf area and determination of flowering time showed that the *mtran* single and double mutants were significantly smaller in sizes and slower to flower compared to the wild type, respectively (Figure 2E and S3D). Notably, *mtran1-2/2-2* had a stronger phenotype against the wild type compared to *mtran1-1/2-1* (Fig. 2B-E). The milder phenotype of *mtran1-1/2-1* is likely because of the presence of the T-DNA in the 10th intron of *mTRAN1*, likely resulting in a partially active protein, whereas the T-DNA is inserted in the 5th and 7th exon of *mTRAN1*, probably leading to the severe growth and lethality of *mtran1-2/2-2* and *mtran1-3/2-3*, respectively. Overall, the phenotypic analysis

indicates that loss of *mTRAN1* and *mTRAN2* caused a growth retardation phenotype, in some cases leading to lethality (*mtran1-3/2-3*).

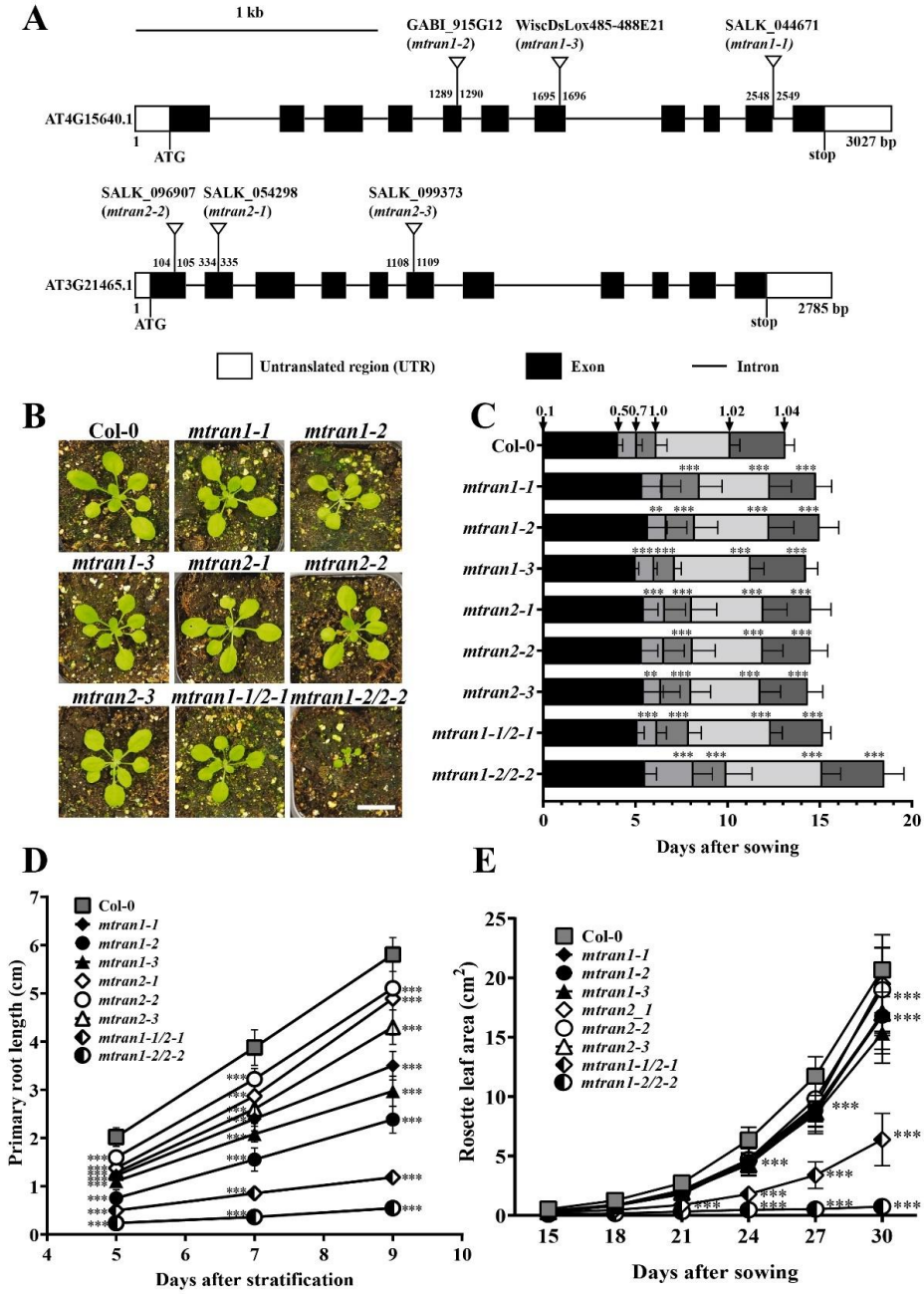

Figure 2. Phenotypic analysis of the *mtran* single and double mutants. A. *mTRAN1* and *mTRAN2* T-DNA insertion positions. White boxes = untranslated regions (UTRs), black boxes = exons, black lines = introns. **B.** A representative picture of 25-day-old soil-grown plants.

Scale bar: 2 cm. **C.** Plate-based phenotypic analysis (n>60). Arrows indicate growth stages as described previously (Boyes et al., 2001): 0.1: Seed imbibition; 0.5: Radicle emergence; 0.7: Hypocotyl and cotyledon emergence; 1.0: Cotyledons fully open; 1.02: two rosette leaves > 1 mm; 1.04: four rosette leaves > 1mm. The boxes indicate the time between the growth stages. Data are based on at least 60 plants/genotype. **D.** Primary root length of vertically-grown plants (n=15). **E.** Rosette leaf area of soil-grown plants (n=9). Statistical significance was based on Student's *t* test (*=P<0.05, **=P<0.01, ***=P<0.001).

mTRAN1 and mTRAN2 are unlikely to be adenylyl cyclases

mTRAN1 and mTRAN2 are both annotated as adenylyl cyclases (ACs) in TAIR, but we could not find any experimental evidence for their AC activity, nor could we find a defined source for this annotation. To investigate whether mTRAN1 and mTRAN2 have AC activity, we performed a bacterial cAMP synthase complementation assay. The bacterial cAMP synthase complementation assay was based on the method of the Bacterial Adenylate Cyclase Two-Hybrid (BACTH) System (Karimova et al., 1998) (see Supplementary Info). The BACTH system can be used for reporting AC activity as the *BTH101* (*cya) E. coli* strain lacks endogenous AC activity. As positive control, the plasmids pKT25-*zip* and pUT18C-*zip* were co-transformed into *BTH101* (*E. coli cya*) (Fig. S4A), which formed colored colonies on MacConkey/maltose and LB/X-gal media, and could grow on the M63 medium (Fig. S4A). As negative control, the empty vector pUT18 was transformed into *E. coli cya*. Full-length coding sequences of *mTRAN1* and *mTRAN2* were cloned into the pUT18 vector and transformed into *E. coli cya*. On all tested media, colonies formed by pUT18-*mTRAN1* and pUT18-*mTRAN2* had the same phenotype as the negative control (Fig. S4A). This indicates that *mTRAN1* and *mTRAN2* could not rescue the *E. coli cya* mutation and thus the proteins do not appear to have AC activity in the bacterial system. To test whether mTRAN1 and mTRAN2 have AC activity *in planta*, we measured cAMP content in both double mutant lines. There was no significant difference in cAMP concentration between the wild type and the *mtran* double knockout mutants (Fig. S4B), despite their clear growth retardation phenotype (Fig. 2B-E), strongly supporting that mTRAN1 and mTRAN2 are not likely to be ACs.

OXPHOS complexes show reduced activity, causing a decrease in mitochondrial respiration in the *mtran* double mutants

To find out the cause for the slow growth phenotype of the *mtran* double knockout mutants, mitochondria isolated from *mtran1-1/2-1* and *mtran1-2/2-2* were analyzed by BN-PAGE. The *mtran* double knockout mutants showed a decrease in abundance of the supercomplex I/III,

complex I, complex III and complex V compared to the wild type (Fig. 3A). Furthermore, the activity of complex I, III, IV and V was reduced in the *mtran* double knockout mutants (Fig. 3B). This indicates that OXPHOS complexes were reduced in abundance and activity due to the loss of function of *mTRAN1* and *mTRAN2*, which could consequently affect mitochondrial respiration. Therefore, freshly isolated mitochondria from *mtran1-1/2-1* and *mtran1-2/2-2* were used for measurement of oxygen consumption rates (Fig. 3C). The state III respiration rates (succinate+ADP+NADH) of the *mtran* double knockout mutants were significantly lower compared to the wild type. The *mtran* double knockout mutants had a significantly higher capacity of the alternative oxidase (AOX) pathway (KCN+DTT+pyruvate) compared to the wild type. In addition, the ratio of AOX capacity to state III was also significantly higher in the *mtran* double knockout mutants, suggesting they rely heavily on alternative respiration, while wild type plants under normal growth conditions mostly rely on the cytochrome *c* oxidase pathway. In conclusion, the loss of function of *mTRAN1* and *mTRAN2* compromised OXPHOS complex abundance and activity, which resulted in a strong decrease in capacity of the cytochrome *c* oxidase respiratory pathway and induction of the AOX pathway.

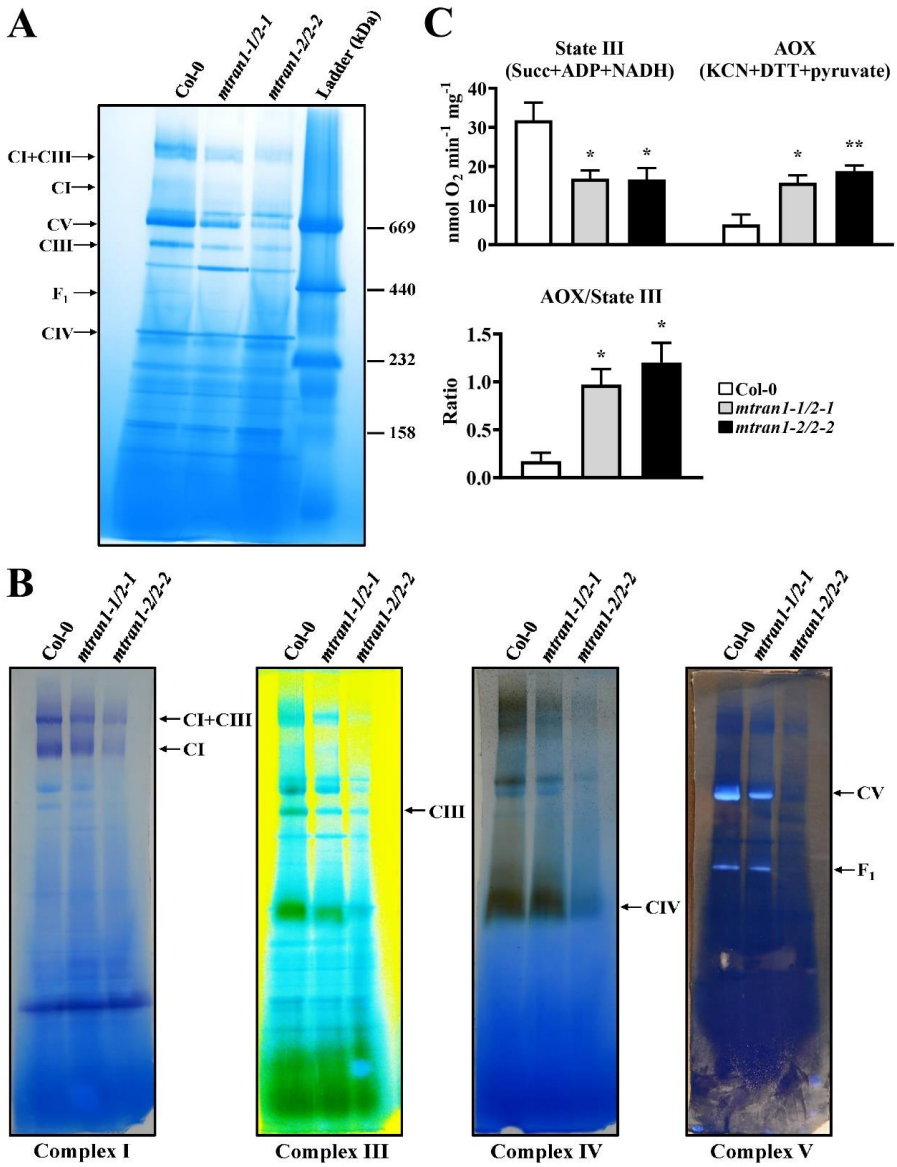

Figure 3. Analysis of mitochondrial complexes in the *mtran* double mutants. A. Analysis of abundance of mitochondrial complexes by Coomassie-Colloidal stained-BN-PAGE. Arrows indicate respiratory complexes and supercomplexes. The molecular weight (kDa) is shown on the right side of the gel. **B.** Activity measurement of the respiratory complexes I, III, IV and V in BN-PAGE. Arrows indicate respiratory complexes and supercomplexes. CI+CIII = supercomplex I+III, CIII=complex III, CIV=complex IV, CV=complex V, F_1= F_1-subcomplex of complex V. **C.** Oxygen consumption rates of isolated mitochondria using a Clark-type oxygen electrode. The ratio of maximal AOX respiration/state III respiration = maximized KCN resistant respiration (KCN+DTT+pyruvate)/state III respiration (succinate+ADP+NADH). Statistical significance was based on Student's *t* test (n=3) (*=P<0.05, **=P<0.01).

Loss of *mTRAN1* and *mTRAN2* causes changes in abundance of mitochondrial proteins

Isolated mitochondria were used for immunoblot analysis using antibodies against subunits of respiratory complexes (Fig. 4). In the *mtran* double knockout mutants, proteins from complex I, III, IV and V were less abundant, which is in agreement with a decrease in the abundance and activity of these complexes (Fig. 3A and 3B). Interestingly, mitochondrially-encoded mitoribosomal subunits RIBOSOMAL PROTEIN S4 (RPS4) and RIBOSOMAL PROTEIN L16 (RPL16), and nuclear-encoded mitochondrial translation factor LEUCINE ZIPPER-EF-HAND-CONTAINING TRANSMEMBRANE PROTEIN 1 (LETM1) were more abundant in the *mtran* double knockout mutants. Nuclear-encoded mitoribosomal subunit RIBOSOMAL PROTEIN S10 (RPS10) did not show clear differences in abundance in the mutants.

Proteins encoded by mitochondrial retrograde signalling marker genes, including ALTERNATIVE OXIDASE (AOX), UP REGULATED BY OXIDATIVE STRESS AT2G21640 (UPOX) and TRANSLOCASE OF THE INNER MEMBRANE 17 (TIM17) (Van Aken et al., 2016; Van Aken et al., 2007), were more abundant in both double mutants. This indicates that the loss of function of *mTRAN1* and *mTRAN2* induced mitochondrial retrograde/ unfolded protein response (UPR^{mt}) signalling (Fig. 4). Upregulation of AOX protein is in agreement with the observed reliance of the *mtran* double knockout mutants on alternative respiration (Fig. 3C). There were no changes in abundance of mitochondrial outer membrane (OMM) proteins TOM40 and VOLTAGE DEPENDENT ANION CHANNEL (VDAC) between the *mtran* double knockout mutants and the wild type.

To gain a broader insight into the global changes in abundance of mitochondrial proteins, we used isolated mitochondria for tandem mass spectrometry (MS/MS) analysis (Table S1). We could only detect mTRAN1 but not mTRAN2 in the wild-type mitochondria, suggesting mTRAN1 is much more abundant than mTRAN2, which is in agreement with a recent mitochondrial proteome meta-analysis (Fuchs et al., 2020). Interestingly, mTRAN1 could still be found in *mtran1-1/2-1* plants and was not significantly different in abundance as compared to the wild type. This confirms our hypothesis that mTRAN1 is (partially) active due to the T-DNA insertion in the 10th intron of *mTRAN1*, leading to the milder phenotype of *mtran1-1/2-1*. However, mTRAN1 was not detected in *mtran1-2/2-2* as the T-DNA was inserted in the 5th exon of *mTRAN1*, resulting in the likely knockout of the gene and the more severe phenotype of *mtran1-2/2-2* plants. This explains why we found 684 and only 24 proteins to be significantly different in abundance in *mtran1-2/2-2* and *mtran1-1/2*-1 ($P_{adj} < 0.2$), as compared

to Col-0, respectively. Using a less stringent unadjusted $P < 0.05$, nevertheless 247 proteins were found differentially abundant in the *mtran1-1/2-1* mitochondria, representing subunits of complex I, III, IV and V, in agreement with immunoblot blot results (Fig. 4). Of the 684 proteins affected in *mtran1-2/2-2*, mitochondrially-encoded OXPHOS proteins, including NADH DEHYDROGENASE 1, 7 and 9 (NAD1, NAD7 and NAD9), APOCYTOCHROME B (COB), CYTOCHROME OXIDASE 2 (COX2), and ATP SYNTHASE SUBUNIT 1, 4 and 8 (ATP1, ATP4 and ATP8), were less abundant. However, subunits of complex II, all of which are nuclear-encoded, were not affected in the mutants. Mitochondrially-encoded RIBOSOMAL PROTEIN L5 (RPL5) and RPL16, AOX1A, AOX1D and LETM1 were more abundant. This is consistent with the results of our immunoblot analysis. 407 of the 684 proteins significantly different in abundance between *mtran1-2/2-2* and Col-0 are predicted/known to be mitochondrially-targeted. Of these proteins, heat shock proteins (HSP23.5, HSP70 and HSP89), ADP/ATP carrier proteins, ALTERNATIVE NAD(P)H DEHYDROGENASES NDA1/NDB2, proteases (CLP, PREP and FTSH10), many mitochondrially-targeted ribosomal proteins and PPR proteins, ovule abortion (OVA) proteins, and amino acid-tRNA ligases were more abundant. Interestingly, MULTIPLE ORGANELLAR RNA EDITING FACTOR (MORF) 3, 6 and 8 were significantly higher in abundance between *mtran1-2/2-2* and Col-0, suggesting that loss of *mTRAN1* and *mTRAN2* might affect mitochondrial RNA editing. In conclusion, loss of both mTRAN proteins results in a severe perturbation of the mitochondrial proteome and reduction of many OXPHOS components.

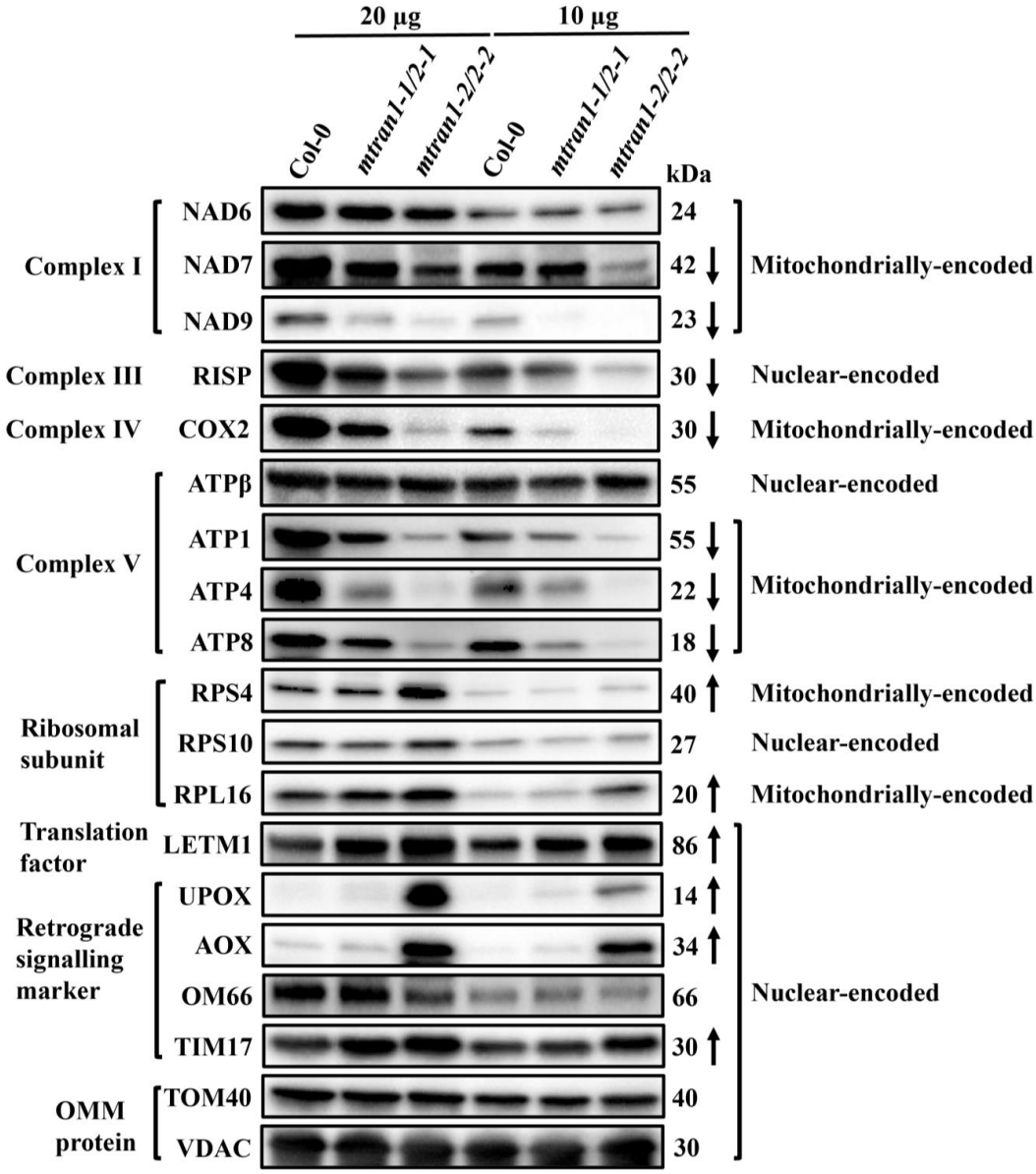

Figure 4. Immunoblot analysis of mitochondrial proteins in the *mtran* double mutants. 20 µg and 10 µg of mitochondrial proteins were loaded onto SDS-PAGE. The antibodies and the molecular weight (kDa) are shown on the left and right sides of each blot, respectively. The arrows next to the molecular weight of proteins indicate whether proteins are more abundant (up arrowheads) and less abundant (down arrowheads). Organellar origin of the protein (nuclear-encoded or mitchondrially-encoded) is shown on the right side of the blots. OMM = outer membrane.

mTRAN1 and mTRAN2 are part of the mitoribosome small subunit

Since loss of *mTRAN1* and *mTRAN2* caused low activity and abundance of mitochondrial respiratory complexes, we wanted to identify the proteins that interact with mTRAN1 and mTRAN2 *in planta*. Therefore, homozygous transgenic plants expressing either mTRAN1-GFP or mTRAN2-GFP were used for co-immunoprecipitation (co-IP) followed by MS/MS analysis. A mitochondria-targeted GFP line (mito-GFP) (Logan and Leaver, 2000) was used as the negative control. The phenotypes of complementation lines *mtran1-2/2-2 35S:mTRAN1-GFP* and *mtran1-2/2-2 35S:mTRAN2-GFP* were similar to the wild type (Fig. S5), indicating that mTRAN1-GFP and mTRAN2-GFP fusion proteins can perform their native function and interact with potential binding proteins. A summary list of proteins that were co-immunoprecipitated with mTRAN1-GFP and mTRAN2-GFP is presented in Table S2A. mTRAN1 and mTRAN2 were identified as the baits in our mTRAN1-GFP and mTRAN2-GFP co-IP, respectively, which further supports that the co-IP was successful. Strikingly, we found that mTRAN1 and mTRAN2 interacted with 27 proteins found as components of the mitoribosome small subunit (mtSSU), as proposed by Rugen et al. (2019) and Waltz et al. (2019) during the course of our study. In contrast, no mitoribosome core subunits were pulled down using the mito-GFP control, indicating the specificity of the interactions. This shows that mTRAN1 and mTRAN2 are part of the mtSSU. All ribosomal proteins interacting with mTRAN proteins belonged to the mtSSU, except mitochondrial ribosomal protein L11, which is part of the mtLSU. mtLSU L11 was however only identified in the first replicate. Most rPPR proteins found in Waltz et al. (2019) and Rugen et al. (2019) interacted with mTRAN proteins, though rPPR3a (AT1G55890) was only co-immunoprecipitated with mTRAN1. Fuchs et al. (2020) also found that an individual mitochondrion contains on average around 520 copies of mtSSU proteins, which is very close to the estimated 534 copies that we found for mTRAN1, strongly supporting that mTRANs are integral parts of the plant mitoribosome. We also found proteins interacting with mTRAN proteins that were only detected in our analysis (Table S2A, gray color). Interestingly, we found three additional mitochondrially-targeted ribosomal proteins, a PPR protein (AT3G61520), RNA-EDITING FACTOR INTERACTING PROTEIN 1 (RIP1/MORF8), and four heat shock proteins that were co-immunoprecipitated with mTRAN proteins. It is also interesting that mTRAN1 and mTRAN2 interacted with mitochondrially-encoded NAD7 and NAD9, which were found to be less abundant in the *mtran* double mutants (Fig. 5, Table S1). All in all, our co-IP results show that mTRAN1 and mTRAN2 are most

likely part of the mtSSU, suggesting that mTRAN1 and mTRAN2 might be important for mitochondrial translation.

Transcriptome analysis of the *mtran1-2/2-2* mutant indicates mitochondrial translation defects

To gain insight into the genome-wide effect on transcript levels, RNA-seq analysis was carried out on Col-0 and *mtran1-2/2-2*, which has the stronger phenotype against Col-0 (Fig. 2B-E). Nuclear transcripts were considered to be significantly differentially expressed between *mtran1-2/2-2* and Col-0 if $P_{adj} < 0.05$ (after False Discovery Rate (FDR) correction) with a fold change (FC) greater than 2 or smaller than 0.5. 2143 nuclear-encoded differentially expressed genes (DEGs) were found in *mtran1-2/2-2* versus Col-0, of which 1117 were upregulated and 1026 were downregulated (Table S3). A gene ontology analysis showed that stress responsive genes were found to be upregulated, while oxygen level, hypoxia and hormone (auxin) responsive genes were downregulated (Table S4). Mitochondrial retrograde signalling marker genes like *AOX1a* were significantly upregulated (Table S3), indicating that loss of *mTRAN1* and *mTRAN2* activates mitochondrial unfolded protein response (UPR^{mt}) signalling likely via ANAC017 (Kacprzak et al., 2020). We could confirm upregulation of UPR^{mt} marker genes in *mtran1-2/2-2* and *mtran1-1/2-1* by qRT-PCR (Fig. S6).

To further analyze the transcriptomic effects caused by loss of *mTRAN1* and *mTRAN2*, the RNA-seq dataset of *mtran1-2/2-2* was compared with the transcript profiles of 22 additional Arabidopsis mitochondrial mutants and chemical treatments affecting mitochondrial function, representing 17 different types of mitochondrial perturbations (Figure 5A; Table S5A). The similarities among all datasets were evaluated by comparison of common pairwise DEGs calculated via the Sørensen-Dice similarity coefficient (DSC) (Table S5B). The complete matrix of DSC values for *mtran1-2/2-2* and 22 additional datasets was hierarchically clustered and represented as a heat map (Fig. 5A). *mtran1-2/2-2* clustered most closely to the *rps10* P2 and P3 mutants, in which the transcript level of mtSSU *RIBOSOMAL PROTEIN S10* (*RPS10*) is reduced (Adamowicz-Skrzypkowska et al., 2020). This further supports that mTRAN proteins are involved in mitochondrial translation. *mtran1-2/2-2* also clustered relatively closely to the antimycin A (AA) (inhibitor of complex III), oligomycin (inhibitor of complex V) and rotenone (inhibitor of complex I) datasets, in line with the observed loss of activity of these complexes in *mtran* double mutants (Fig. 3). We created a Venn diagram to visualize the similarities of nuclear transcript profiles among *mtran1-2/2-2*, *rps10* mutants and *atphb3*,

which did not cluster closely to *mtran1-2/2-2* (Fig. 5B). *atphb3* is a mutant defective in *PROHIBITIN 3* (a mitochondrial inner-membrane scaffolding protein) (Van Aken et al., 2016). *mtran1-2/2-2* shared 326 and 651 DEGs with *rps10* P2 and P3, respectively, whereas 106 common DEGs were found between *mtran1-2/2-2* and *atphb3*. 288 DEGS were commonly found between *mtran1-2/2-2* and both *rps10* mutants. 31 DEGs were common among all genotypes, including many mitochondrial retrograde/UPR^{mt} signalling markers like *AOX1a* (Fig. 5C).

As we prepared the RNA-seq libraries using an rRNA-depletion strategy, we could also analyze *mtran1-2/2-2* mitochondrial and chloroplast transcript profiles (Table S6A and S6B). Surprisingly, all 57 mitochondrially-encoded genes were significantly upregulated (FC > 1.4, $P_{adj} < 0.05$), ranging in fold change from 4.39x for *trnY* to 1.4x for *RRN26* (Table S6A). It thus seems that mitochondrial transcription is globally increased to compensate for reduced translation, considering mTRANs are part of the mitoribosome. Interestingly, all 6 genes that were more than 4x induced encoded tRNA's, further suggesting a compensation for lack of translation. The mitochondrial transcriptome was further compared to two other mitochondrial mutants, including mitochondrial/chloroplast RNA polymerase *rpotmp* and *atphb3* mutants (Kuhn et al., 2015; Van Aken et al., 2016). While in *rpotmp* and *atphb3* mutants a mix of up- and down-regulated genes could be observed, in *mtran1-2/2-2* all genes were upregulated (Fig. 5D, Table S6C). Moreover, the strength of inductions was generally higher in *mtran1-2/2-2* mutants compared to the other mutants. In contrast, all 117 annotated chloroplast-encoded genes were slightly but significantly downregulated ($P_{adj} < 0.05$) (Table S6B).

As the co-IP analysis also picked up mitochondrial editing factor MORF8/RIP1 and PPR proteins, we analyzed the mitochondrial transcriptome for alterations in splicing and editing (Table S7). The rate of C-to-U editing was significantly different between *mtran1-2/2-2* and Col-0 for 262 cytosines of mitochondrial transcripts (FDR < 0.05) (Table S7A). The majority (208) of these editing sites were relatively less edited in the mutant than in the wild type (Table S7A). However, considering that the mitochondrial transcripts were generally more abundant in *mtran1-2/2-2*, for 244 of the differentially edited sites there was still more edited transcript in absolute terms in *mtran1-2/2-2* compared to in Col-0. We therefore suggest that, although the editing rate is globally lower in the mutant, there are still more than enough correctly edited mitochondrial transcripts in *mtran1-2/2-2* mitochondria. This reduced editing rate therefore likely reflects an overall limitation in editing capacity of plant mitochondria, combined with a higher abundance of mitochondrial transcripts in the mutants. Mitochondrial transcript splicing

was also analyzed and for six splice sites, a significant difference was observed in the mutants versus Col-0 (FDR < 0.05) (Table S7B). Also here, for all transcripts there was still a higher absolute number of spliced transcripts in the mutant than in Col-0, indicating that the overall lower abundance of many mitochondrially-encoded proteins (Fig. 4) is unlikely to be explained by a lack of correctly spliced/edited mitochondrial transcripts. The observed similarities in nuclear transcriptome between *mtran1-2/2-2* and *rps10* mutants, as well as the excessive expression of mitochondrial transcripts, thus point to a defect in mitochondrial translation.

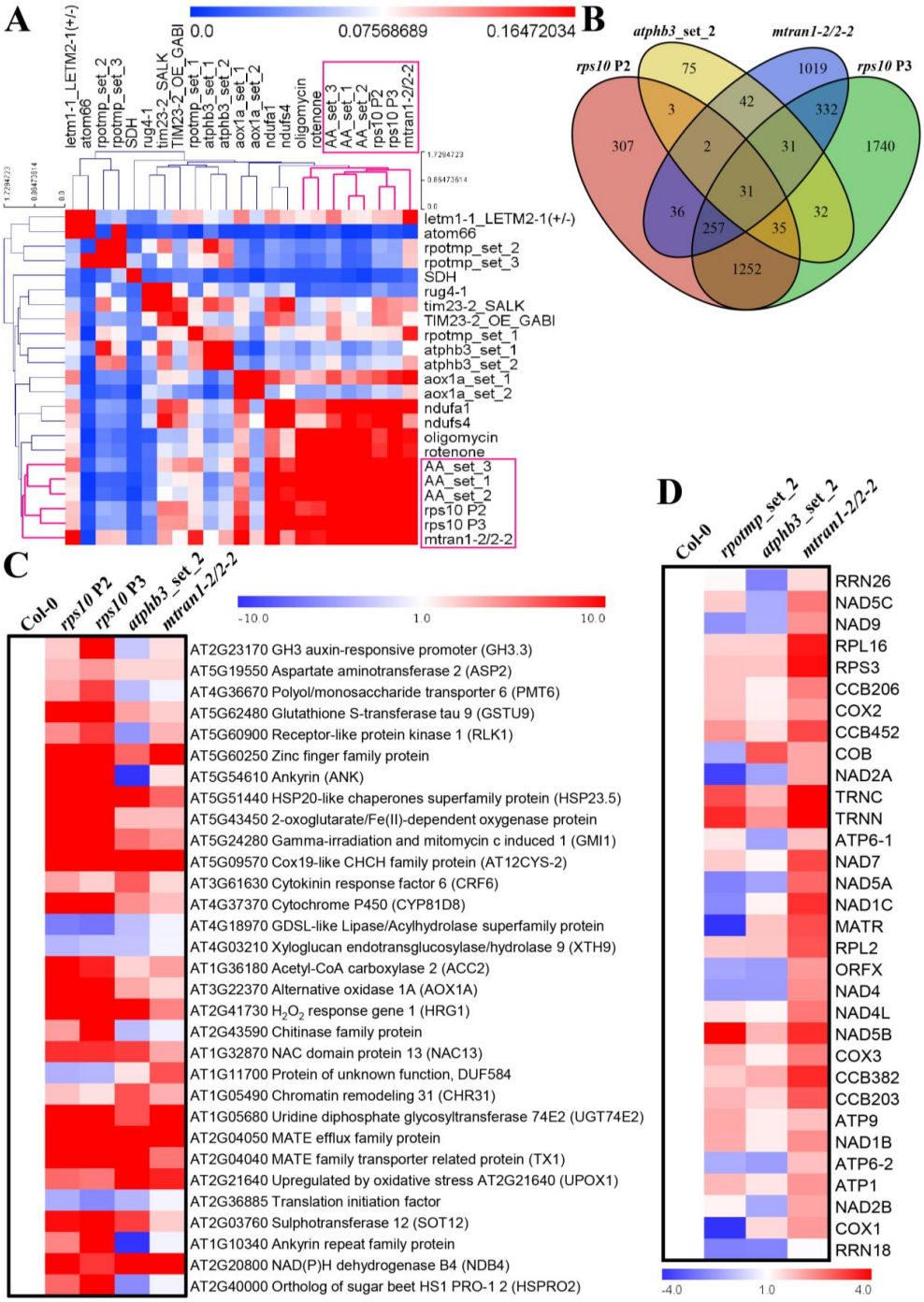

Figure 5. Nuclear and organellar transcriptome comparison of the *mtran1-2/2-2* mutant with other Arabidopsis mutants defective in fundamental mitochondrial functions. A. A heat map represents common pairwise differentially expressed genes (DEGs) among the

transcriptomic datasets analysed by the Sørensen-Dice similarity coefficient (DSC). The complete matrix of DSC values for *mtran1-2/2-2* and 22 additional datasets was hierarchically clustered using Euclidean Distance. The subbranch including *mtran1-2/2-2* is highlighted for clarity. Color bar indicates linear fold change. **B.** A Venn diagram represents common DEGs among *mtran1-2/2-2*, *rps10* P2 and P3 and *atphb3*. **C.** Heat map of 31 common DEGs among *mtran1-2/2-2*, *rps10* P2 and P3 and *atphb3*. Color bar indicates linear fold change. **D.** Heat map of mitochondrially-encoded transcripts differentially expressed among *mtran1-2/2-2*, *rpotmp* and *atphb3*. Color bar indicates linear fold change.

mTRAN1 and mTRAN2 are required for translation initiation in mitochondria

To validate whether mitochondrial translation was indeed affected in the *mtran* double knockout mutants, *in organello* protein synthesis assays were performed using freshly isolated mitochondria from Arabidopsis seedlings. Synthesized radiolabelled mitochondrial translation products were evaluated after 10, 30 and 60 min of translation (Fig. 6A and S7). In the control reactions (60 min), sodium acetate, a unique substrate for bacterial translation, was used as a substrate instead of malic acid and pyruvate to evaluate bacterial contamination during mitochondrial purification. Several distinct protein bands, including ATP1, COB, COX2 and ATP SYNTHASE SUBUNIT 9 (ATP9), could be identified based on their molecular mass (Kwasniak-Owczarek et al., 2022). ATP1, COB, COX2 and ATP9 had a slower rate of translation in the *mtran* double knockout mutants than in the wild type. This was consistent with our immunoblot and MS/MS analysis (Fig. 4, Table S1), in which we observed a reduction in the abundance of ATP1 and COX2 in the *mtran* double knockout mutants. These findings thus confirm our hypothesis that mTRAN1 and mTRAN2 are required for efficient translation in mitochondria.

The efficiency of translation is dependent on both the efficiency of translation initiation and elongation. If translation initiation is impacted, one would expect too few ribosomes to be attached to a given mRNA. If translation elongation is defective, one would expect a larger number of ribosomes to be attached to the mRNA, due to difficulties to complete the full translation. To allow us to distinguish between these two possibilities and further understand how the efficiency of mitochondrial translation was affected by knockout of *mTRAN1* and *mTRAN2*, we assessed ribosome-loading along mitochondrially-encoded transcripts in mutant and wild-type seedlings (Fig. 6B). Polysomes are composed of mRNAs bound to two or more ribosomes, whereas monosomes consist of mRNAs bound to a single ribosome and/or “vacant couples”, which are a stable association of the small and large ribosomal subunits without binding to mRNAs (Noll et al., 1973). In this analysis, polysomes were separated from

monosomes and free mRNAs by sucrose gradient ultracentrifugation. After centrifugation, 10 fractions were collected along the gradient (fraction 1-10 corresponding to the lightest and the heaviest fraction) and subjected to total RNA extraction, followed by qRT-PCR to determine the percentage of each mitochondrial mRNA present in the fractions. We analyzed polysome-bound mRNAs representing subunits of complex I, III, IV and V. We also performed this analysis on mitochondrially-encoded mitoribosomal *RPS4* transcript as the encoded protein showed increased abundance in the *mtran* double mutants versus Col-0 (Fig. 4). Overall, all analyzed mitochondrially-encoded mRNAs of both *mtran1-1/2-1* and *mtran1-2/2-2* distributed mainly in fractions 2 and 3, whereas mRNAs in the wild type were mostly found in fractions 3 and 4 (Fig. 6B). These shifts towards the lighter fractions indicate that the number of ribosomes associated with the analyzed mRNAs was lower in the *mtran* double mutants, suggesting that the lower efficiency of mitochondrial translation is likely due to inefficient translation initiation/mitoribosomal binding to mRNAs. To determine the distribution of the mitoribosomes, we analyzed rRNA *MITOCHONDRIAL 18S RIBOSOMAL RNA* (*RRN18*) of the mtSSU. The rRNA *RRN18* of the wildtype mainly presented in fraction 3 and 4, colocalizing that of the protein-encoding mRNAs (Fig. 6B). This indicates that most wild type mRNAs are bound by mitoribosomes and are actively translated. In the *mtran1-2/2-2* mutant, the mitoribosomes were still present mainly in fraction 3 and 4, as observed in the wild type. Interestingly, in *mtran1-1/2-1*, the mitoribosomes were mainly found in fractions 8-9, and to a lesser extent in fractions 3 and 5. In all cases, the mRNA levels in fraction 2 were much higher in the mutants than in the wild type. As fraction 2 contains almost no mitoribosomes according to our analysis, our results show that a large proportion of mitochondrial mRNAs are likely devoid of ribosomes in the *mtran* double mutants. However, no obvious effect of loss of mTRANs could be detected on cytosolic translation, as assessed by ribosome-loading of nuclear-encoded *UBIQUITIN-CONJUGATING ENZYME 21* (*UBC21*). Together, our findings provide compelling evidence that mTRAN proteins are key components of plant mitoribosomes required for translation initiation.

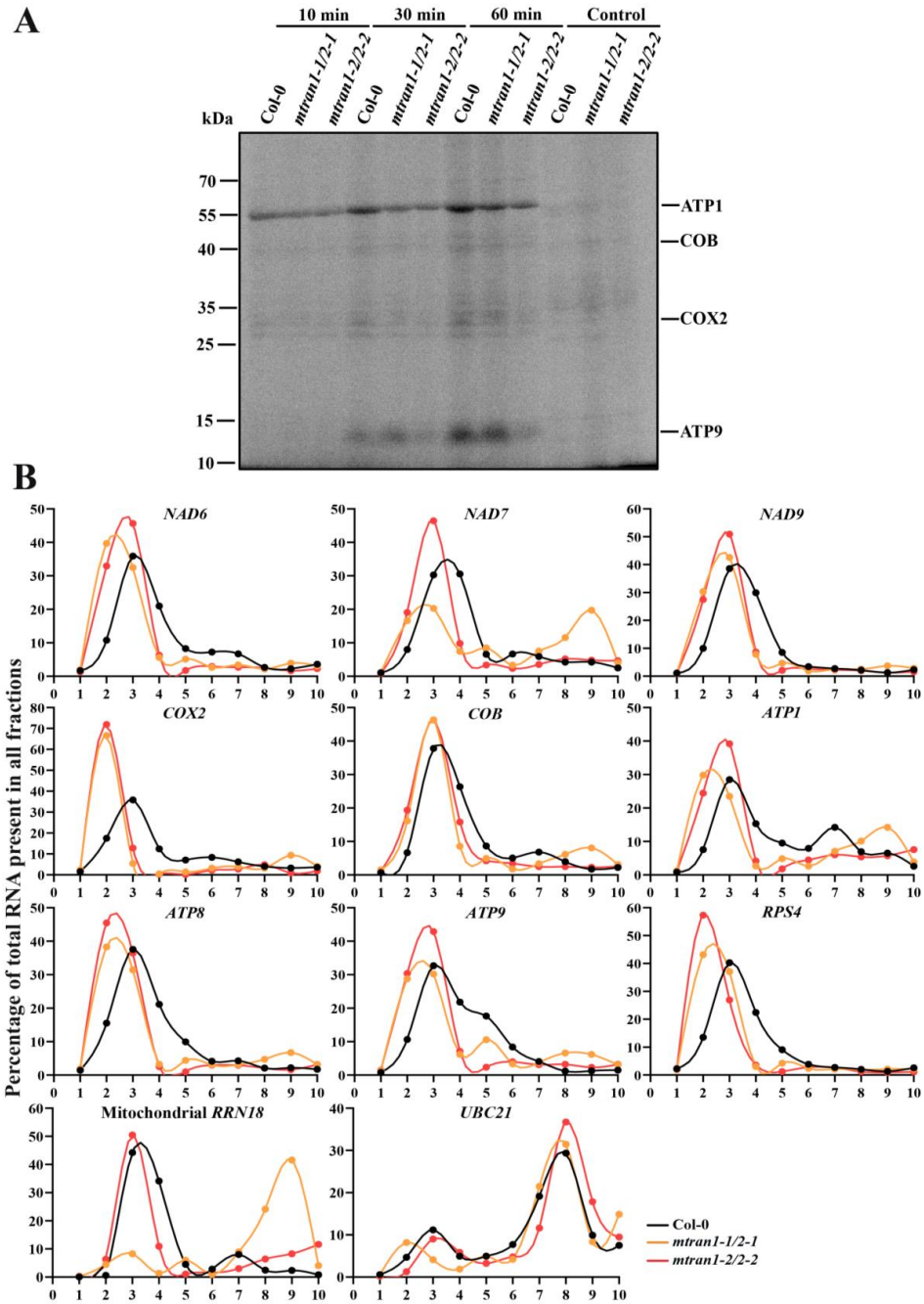

Figure 6. mTRAN1 and mTRAN2 are required for efficient translation initiation in mitochondria. A. Autoradiogram of *in organello* protein synthesis for 10, 30 and 60 min using purified mitochondria from Col-0, *mtran1-1/2-1* and *mtran1-2/2-2*. Sodium acetate was used as substrate to assess bacterial contamination in the controls (60 min). The molecular weight (kDa) and names of identified mitochondrially-encoded proteins are indicated. **B.** Polysome

profiling for mitochondrially-encoded transcripts: OXPHOS subunits, mitoribosomal subunit *RPS4* and mitochondrial rRNA *RRN18*, and nuclear-encoded transcript *UBC21*. Percentage of total mRNA in all fractions was measured by qRT-PCR.

Structural modelling suggests that mTRAN proteins have PPR protein like-structures

As we showed that mTRAN proteins are part of the mtSSU (Table S2) and required for translation initiation (Fig. 6), we looked at the predicted protein structures to anticipate if the proteins could bind mitochondrial mRNAs to help the mtSSU initiate translation. Structures of mTRAN proteins without the predicted mitochondrial targeting sequences (MTS) (Fukasawa et al., 2015) were modelled using AlphaFold (Jumper et al., 2021), RoseTTAFold (Baek et al., 2021) and iTASSER structure prediction programs (Yang and Zhang, 2015) (Fig. S8). The modelled partial mTRAN1 structure extracted from the cryo-EM structure of the mitoribosome from *Brassica oleracea var. botrytis* (cauliflower) (Waltz et al., 2020) is also presented for comparison (Fig. S8). Overall, the protein structures shown by prediction tools and Waltz et al. (2020) suggest that mTRAN1 and mTRAN2 have tetratricopeptide-repeat (TPR)/PPR protein like-structures. PPR proteins are known as RNA-binding proteins involved in RNA processing, splicing, stability, editing, and translation (Delannoy et al., 2007; Schmitz-Linneweber and Small, 2008). The three programs predicted that mTRAN1 and mTRAN2 contain 8-12 PPR-like repeats. The cryo-EM structure of the plant mitoribosome by Waltz et al. (2020) proposed that mTRAN1 is formed by 6 PPR-like repeats, based on the number of PPR repeats predicted by the TPR-pred software (Karpenahalli et al., 2007).

We then attempted to find potential mTRAN-RNA target sites using aPPRove (Harrison et al., 2016) and the PPRCODE prediction web server (Yan et al., 2019), but none of them were able to find any potential RNA-binding sites for mTRAN1 and mTRAN2, suggesting that mTRANs may belong to a PPR-like protein class that does not obey the rules of the PPR code and may bind RNA in a different manner.

mTRAN1 directly binds to putative mitoribosome binding sites in the 5'UTRs of mitochondrial mRNAs

As potential RNA binding sites could not be predicted for mTRANs using the PPR code, we searched for conserved potential mitoribosome binding sites in the 5'UTRs of mitochondrial mRNAs. Next, we performed motif analysis with the Multiple Expectation-maximization for Motif Enrichment (MEME) online motif search tool and identified a potential CUUUxU-like

mitoribosome binding site in the 5'UTRs of 26 mitochondrial mRNAs (Fig. 7A and S9, Table S8B and S8C). Waltz et al. (2020) suggested that the plant mitoribosome might recognize an AxAAA-related motif, which is located 19 bases upstream of the start codons in 17 mitochondrial mRNA 5'UTRs. The MEME motif search tool was unable to identify the AxAAA-related motif, but we found a similar AAGAAx-like motif in 30 UTRs when including the intercistronic UTRs (Fig. 7A and S9, Table S8C). Furthermore, we could manually find an overlapping AxAAAG-like motif in the 5'UTRs of 17 mitochondrial mRNAs (Fig. 7A and S9, Table S8B and S8C). In summary, we could identify at least one CUUUxU or AAGAAx/AxAAAG motif in all 30 mitochondrial mRNA's 5'UTRs (Fig. S9).

As mTRAN1 is the main isoform in Arabidopsis mitochondria, we performed RNA electrophoretic mobility shift assays (REMSAs) to test whether mTRAN1 can bind to the CUUUxU or the AAGAAx/AxAAAG motifs identified in the 5'UTRs of mitochondrial mRNAs (Fig. 7C). mTRAN1 lacking its MTS predicted by MitoFates (Fukasawa et al., 2015) was expressed in *E. coli* as a fusion protein with the 6xHistidine (His) and the SMALL UBIQUITIN-RELATED MODIFIER 3 (SUMO3) tags in its N-terminus to increase the solubility of the recombinant protein. The 6xHis-SUMO3 double tag was used as negative control. Both 6xHis-SUMO3-mTRAN1 and 6xHis-SUMO3 were successfully purified from *E. coli* extracts in soluble forms (Fig. S10). Synthesized Cy5-labelled RNA probes, containing one or multiple of the predicted mitoribosome binding motifs in the 5'UTRs of *NAD9*, *NAD7*, *COX2* and *RPL5/COB*, were obtained (Fig. 7A and 7B). Mutated probes were also synthesized to verify the specificity of mTRAN1 binding (Table S9). Our REMSAs showed that mTRAN1 could bind to the wild type *NAD9*, *NAD7*, *COX2*, *RPL/COB5* and *ATP1* probes specifically (Fig. 7C). Although some unspecific shifts were observed for *NAD7* and *ATP1*, it was clear that only mTRAN1 could bind enough wild type probe to cause a visible decrease in free probe. In all cases, specific mutation of the CUUUxU/AAGAAx/AxAAAG motif (see Table S9) inhibited binding of mTRAN1. In contrast, no sequence-specific bindings were observed between SUMO3 and the wild type probes that showed a comparably-sized shift as for mTRAN1. Together, our findings indicate that mTRAN1 binds to both CUUUxU and AAGAAx/AxAAAG motifs, which we suggest to act as mitoribosome binding sites in the 5'UTRs of plant mitochondrial mRNAs, to initiate translation.

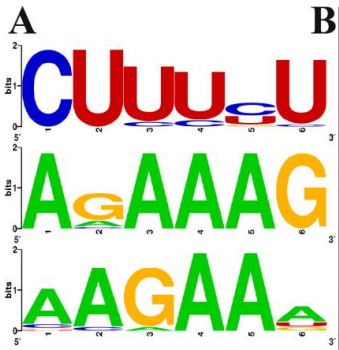

B

Gene	Motif	Wild type sequence (5'-3')
NAD9	AGAAAG CUUUCU	CGGAACUACAAGAAAGCUUUCUUUAU
NAD7	AAAAAG	UGUGUAAAAAAAAAAGCUGGUGGGGC
COX2	CUUUUU	AUUCCCAUCUCUUUUUUCUUGGUUGG
COB/RPL5	AGAAAG	GAGGATGGGGAGAAAGCGGGCCGAGA
ATP1	CUUUUU	UAAAUUAUUCCUUUUUUUUUUCUAAA

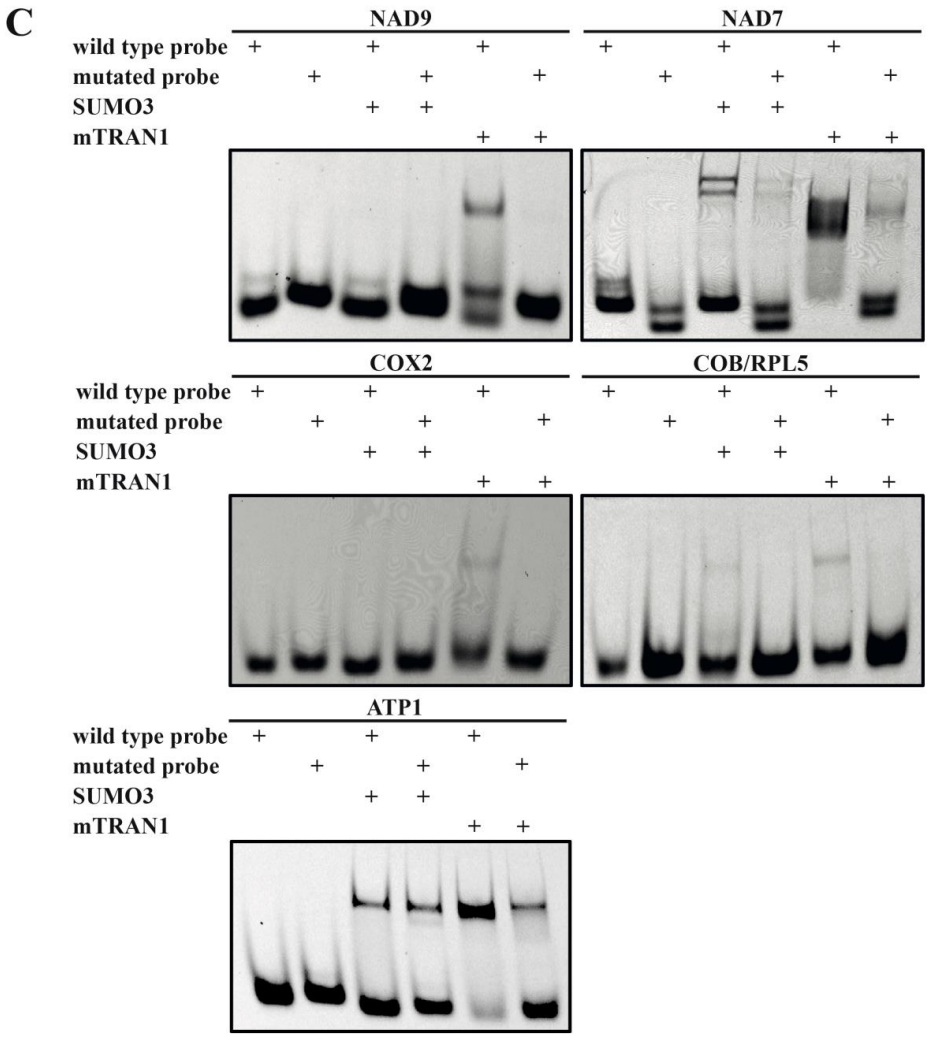

Figure 7. mTRAN1 can directly bind potential mitoribosome binding sites. A. The motif analysis of the 5'UTRs of mitochondrial mRNAs by Multiple Expectation-maximization for Motif Enrichment (MEME) online motif search tool identified potential mitoribosome binding

site CUUUxU and AAGAAx. The other potential mitoribosome binding site AxAAAG was identified by a manual search. The motifs were illustrated by the WebLogo (https://weblogo.berkeley.edu/logo.cgi). **B.** The 5'UTRs of four selected mitochondrial mRNAs (*NAD9*, *NAD7*, *COX2*, *COB*/*RPL5*) contain potential mitoribosome binding sites (underlined) identified by the motif analysis. Binding of recombinantly purified mTRAN1 to the fluorescently-labelled RNA probes was tested by RNA electrophoretic mobility shift assays (REMSAs). The binding sites were changed in the mutated probes (see Table S9). **C.** REMSAs confirmed the binding of mTRAN1 to the four 5'UTRs of mitochondrial mRNAs. His-SUMO3 was used as the negative control. mTRAN1 had strong specific bindings with *NAD9*, *NAD7* and *COX2* that could not be observed in SUMO3 and when the binding sites were mutated.

mTRAN proteins are universal mtSSU translation initiation factors

The motif analysis suggested that mTRANs may recognize motifs in the 5'UTRs of all mitochondrial mRNAs. To assess whether the translation of mitochondrial mRNAs is indeed affected in the *mtran* mutants, we performed ribosome profiling analysis (Ribo-seq), in which short RNAse-protected mRNA fragments covered by the translating ribosomes (called ribosome footprints) were isolated and subsequently sequenced. To compare the relative density of ribosome footprints on each mitochondrial mRNA between the *mtran* mutants and the wild type, the calculated densities were normalized to both mRNA length and abundance determined by qRT-PCR (Table S10). As observed in our polysome fractionation analysis, all mitochondrial mRNAs in the *mtran* mutants showed much lower ribosome loading levels compared to the wild type (Fig. 8A). It should be noted that a single, possibly artefactual, footprint observed in *ccmFN1* masked the reduction in footprints across the rest of the *ccmFN1* mRNA in both *mtran* double mutants compared to Col-0. In general, *mtran1-2/2-2* have lower ribosome densities compared to the *mtran1-1/2-1* mutant, especially on mRNAs encoding OXPHOS proteins (~0.5x on average). Visualisation of mitoribosome footprints of several representative mitochondrial mRNAs, including *NAD9* and *NAD7* (complex I), *COX2* (complex IV), and *ATP1* and *ATP9* (complex V), clearly showed that the translation activity was remarkably low in *mtran1-2/2-2* and moderately low in *mtran1-1/2-1* as compared to in Col-0 (Fig. 8B). This shows that not only a subset, but virtually all mitochondrial mRNAs depend on mTRAN proteins for translation initiation, indicating that mTRAN proteins are universal mtSSU subunits involved in translation initiation.

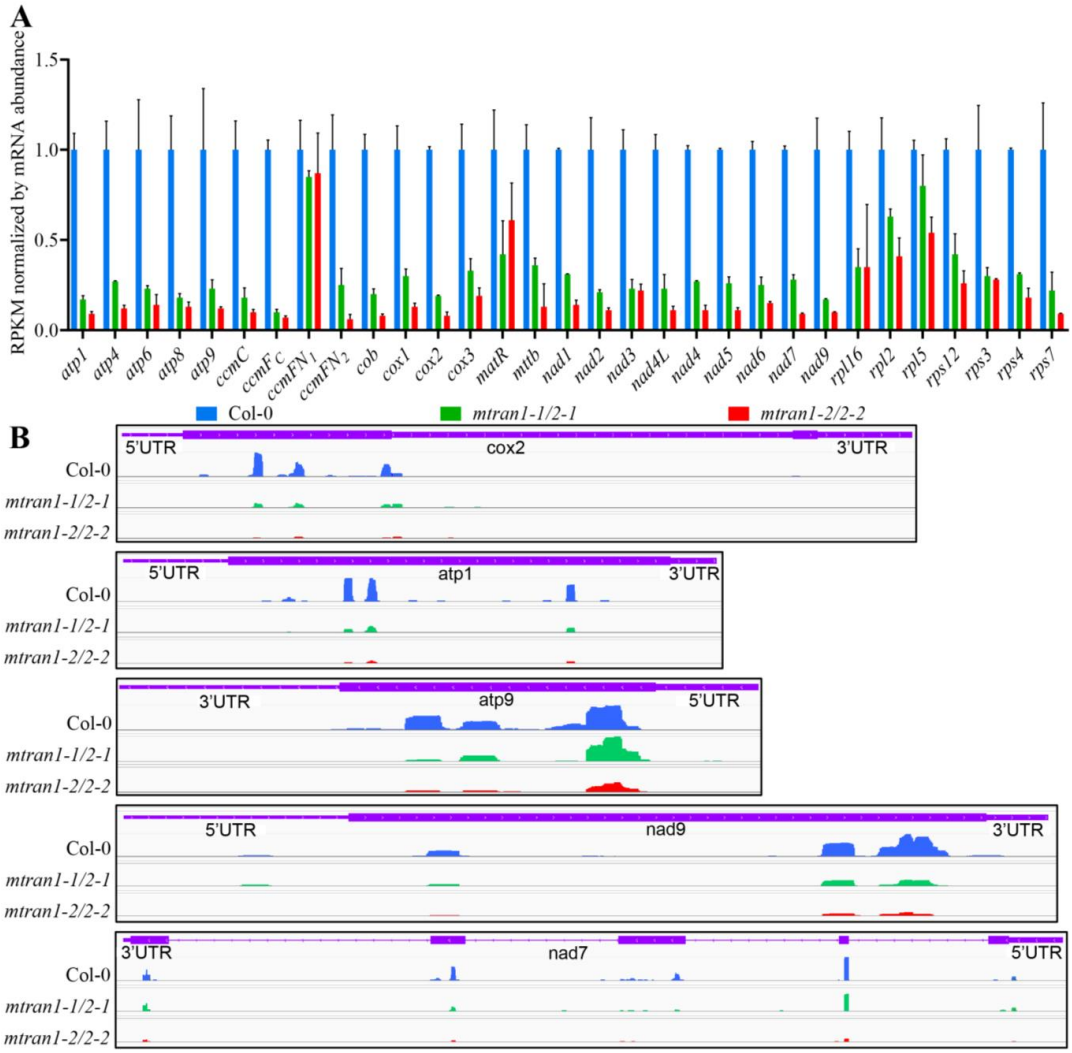

Figure 8. mTRAN proteins are universal mtSSU translation initiation factors. **A.** Loss of mTRANs decreases mitochondrial ribosome footprints. Reads per kilobase million (RPKM) normalized by mRNA abundance of the *mtran* double mutants were normalized to Col-0. Means ± SE (n=2). **B.** Density of mitochondrial ribosome footprints on mitochondrially-encoded *COX2*, *ATP1*, *ATP9*, *NAD9* and *NAD7* was obtained by Integrative Genomics Viewers (IGV) software using auto-scale.

DISCUSSION

For many years, mTRAN1 (AT4G15640) and mTRAN2 (AT3G21465) have been annotated based on poor characterization. Our phylogenetic analysis revealed that mTRAN1 and mTRAN2 are land plant-specific proteins and likely exist as single-copy genes in most plant-

species. Based on the more pronounced growth defects in the *mtran1* single mutants than in the *mtran2* single mutants, lack of consistent detection of mTRAN2 in proteomic studies, and the finding that mTRAN1 has a larger number of protein copies than mTRAN2 per mitochondrion (Fuchs et al., 2020), it appears that mTRAN1 is the major mTRAN isoform in Arabidopsis. When *mTRAN1* is however knocked out, *mTRAN2* can apparently take over the bulk of the shared functions. When knocking out both isoforms, a range of phenotypes was observed from embryo-lethality (*mtran1-3/2-3*), very severe growth defects (*mtran1-2/2-2*), to moderate growth defects *(mtran1-1/2-1*). With mTRAN1 likely to be the major isoform, the milder phenotype of *mtran1-1/2-1* plants can be explained by the presence of the T-DNA in the 10th intron of *mTRAN1*, likely resulting in a partially active protein. This was confirmed by our MS/MS analysis, in which mTRAN1 was detected only in *mtran1-1/2-1* but not in *mtran1-2/2-2*. Why *mtran1-2/2-2* is (just) viable and *mtran1-3/2-3* is not, is however not as clear. We thus propose that *mTRANs* are essential genes in plants.

mTRAN proteins have been annotated as ACs in TAIR. Nevertheless, we were unable to trace the sources for this annotation. Gehring (2010) suggested that mTRAN2 contains a putative AC core motif, but it does not possess significant similarity to experimentally identified ACs. The lack of complementation by mTRANs in a bacterial cAMP synthase complementation assay and normal cAMP content in the *mtran1 mtran2* double mutants, despite severe growth deficiencies, indicates that they are unlikely to be ACs.

Knocking out *mTRAN1* and *mTRAN2* reduced abundance of complex I, III, IV and V subunits and their activity. As all complexes that contain mitochondrially-encoded subunits were strongly deficient, mTRANs must have a very fundamental function in the biogenesis of the OXPHOS system in plants. In comparison, mutants in another fundamental mitochondrial functions such as mitochondrial/chloroplast RNA polymerase *rpotmp* are only affected in abundance of complex I and IV. This very severe deficiency in the cytochrome *c* oxidase respiratory pathway is further supported by the apparent reliance of *mtran* double mutants on the alternative oxidase pathway. Together, this suggests that impaired ATP production by the OXPHOS system is the likely cause of their growth retardation phenotype. This may be conveyed at a systemic level by negatively affecting growth hormone signalling, as observed by a general downregulation of auxin-responsive genes in the RNA-seq data (Table S4). Such an antagonistic relation between mitochondrial retrograde/UPR^{mt} signalling and auxin has been suggested previously (Ivanova et al., 2014), and is underlined by the upregulation of mitochondrial retrograde regulation (MRR) markers at the transcript and protein level. Similar

to two previous studies, in which mitochondrial respiration was significantly impaired, we observed a consistent downregulation of chloroplast-encoded transcripts (Adamowicz-Skrzypkowska et al., 2020; Zubo et al., 2014). In some cases where mitochondrial function is sufficiently impaired, an as yet unknown (possibly retrograde) signalling pathway apparently can reduce chloroplast transcription.

mTRAN1 and mTRAN2 interacted with 17 mtSSU ribosomal proteins. During the course of our study, two proteomic studies were published that purified Arabidopsis mitoribosomes by independent biochemical enrichments and co-IPs (Rugen et al., 2019; Waltz et al., 2019). Complementary to our findings, both of these studies identified mTRAN1/2 as components of the mtSSU. Besides ribosomal proteins, our co-IP also identified 5 plant-specific rPPR proteins identified as core elements of mtSSU (Rugen et al., 2019; Waltz et al., 2019). We also discovered proteins interacting with mTRAN proteins that were identified only in our analysis, including mitochondrially-encoded NAD7/NAD9, which were both less abundant in the *mtran* double mutants. We therefore suspect that we captured nascent NAD7/NAD9 peptides that were actively being translated by the mitoribosome. By analyzing the mitochondrial transcriptomes, we could however not see clear evidence for a reduced mRNA editing/splicing capacity in the *mtran* double mutants.

In organello protein synthesis assay showed that mitochondrially-translated proteins, including ATP1, COB, COX2 and ATP9, had a slower rate of translation in the *mtran* double knockout mutants than in the wild type. This confirms our hypothesis that mTRAN1 and mTRAN2 are key mtSSU components required for efficient translation in mitochondria. Polysome fractionation of a wide range of mitochondrial mRNAs showed a clear shift towards the lighter fraction in *mtran* double mutants compared to the wild type. All mRNAs were much more abundant in the lightest – mitoribosome-free – mRNA-containing fraction (fraction 2) in the *mtran* double mutants than in Col-0, where generally less than 10-20% mRNA was found. This indicates that a large proportion of the mitochondrial mRNA's are not bound by the mitoribosomes, demonstrating inefficient translation initiation. Of note, the shifts were also observed in case of *NAD6* and *RPS4* mRNAs, though NAD6 showed no changes and RPS4 was more abundant at protein level in the *mtran* double mutants. Also, the Ribo-seq analysis showed reduced ribosome coverage of *NAD6* and ribosomal protein-encoding mRNAs in the *mtran* double mutants. This suggests that NAD6 could be more stable as a protein, possibly even if not incorporated into the final complex I. The increased steady-state protein abundance of ribosomal subunits RPS4 and RPL16, as well as mitochondrial translation factor LETM1

and many other nuclear-encoded ribosomal proteins, suggest the cell is trying to compensate for reduced mitochondrial translation and energy status by increasing the production or decreasing the turnover of mitoribosomal components. This impaired mitochondrial translation likely also results in the upregulation of transcription of virtually all mitochondrial genes in *mtran1-2/2-2* as observed by RNA-seq. The particularly high induction of mitochondrial tRNA transcripts and higher abundance of tRNA ligases/synthases further suggest a perceived defect in mitochondrial translation. Interestingly, the ribosome fractionation showed that for a very small fraction of mRNAs (generally less than 10%), there was extremely high-ribosome loading in the *mtran* mutants, especially in *mtran1-1/2-1* (Fig. 6B), as observed in fractions 8-9. We propose that this small fraction of mRNAs could still be bound by the *mtran* mutant mitoribosomes, perhaps due to different secondary/tertiary structure of the 5'UTR. As a result, these rare 'bindable' mRNA's may then be heavily translated by multiple mitoribosomes, partially compensating for the lack of initiation on the vast majority of mRNAs. This compensation particularly in the *mtran1-1/2-1* mutant (in which the mTRAN1 protein can still be partially detected) likely explains the much higher vigor of the *mtran1-1/1-2* mutants compared to *mtran1-2/2-2* plants.

Our findings raise the question of how mTRAN proteins, being essential plant-specific mtSSU subunits, could play such a fundamental role in mitochondrial translation initiation. The polysome fractionation results suggest that the problem lies in the very first steps, where the mitoribosome detects and binds the mRNA. Plant mitochondrial mRNAs lack a Shine-Dalgarno sequence, nor do plant mitochondrial rRNAs have anti-Shine Dalgarno sequences (Hazle and Bonen, 2007). Our data suggest that mTRANs are the recognition factors, which would mean that in plant mitochondria a protein-mRNA interaction mediates ribosome binding, rather than an rRNA-mRNA interaction. A recent study of the cryo-EM structure of plant mitoribosomes by Waltz et al. (2020) proposed that mTRAN1 (named as ms83 and rPPR10 by the authors) is a PPR protein, which are known as RNA-binding proteins. However, mTRAN proteins are far from being 'classical' PPR proteins. First of all, the largest searchable PPR database, which is based on 44562 PPR protein sequences from over 1000 transcriptomes (https://ppr.plantenergy.uwa.edu.au/), does not identify mTRANs as PPR proteins. Furthermore, while the prediction tool TPRpred predicts several other ribosomal rPPRs as PPR proteins with 100% confidence, it only gives a confidence score of 4-14% for mTRAN1 and mTRAN2. Additionally, the structure of *mTRAN* genes with 10 introns and 11 exons is highly aberrant from the gene structure of classical PPR proteins (Figure 2A), which very rarely have

more than 1 intron (Lurin et al., 2004). However, protein structure prediction tools, including AlphaFold, RoseTTAFold and iTASSER, showed that mTRAN proteins are likely to have PPR protein like-structures. Unfortunately, potential binding for mTRANs could not be predicted by aPPRove (Harrison et al., 2016) and the PPRCODE prediction web server (Yan et al. (2019). This further suggests that mTRAN proteins probably bind RNA in a different manner than 'classical' PPR proteins. Based on available protein structure predictions, 6-10 repeated motifs could be found in the mTRAN protein structure, which would suggest they could interact with a mRNA motif of around 6-10 bases, matching our identified CUUUxU/AAGAAx/AxAAAG motifs. Though the cryo-EM structure cannot precisely determine the structure of mTRANs, modelling suggested mTRANs sit in a cleft where the incoming mRNA may be positioned (Fig 9). In agreement, several mtSSU proteins that were modelled to locate most closely to mTRAN1 in this cleft were identified by our co-IP, including mS23, mS47, uS8m, uS11m, uS15m, bS6m and uS5m. Waltz et al. (2020) hypothesized that mTRAN1 is part of the plant-specific cleft that might recognize an AxAAA-related motif of mitochondrial mRNA 5′ UTRs, thus acting as a Shine-Dalgarno (SD)–anti-SD-like recognition system. In addition, their motif analysis suggested that the 5'UTRs of only 17 mitochondrial mRNAs contained an only loosely-conserved AxAAA consensus. However, our study showed that the problem of translation initiation not only occurred with *NAD9*, *COX2* and *ATP9*, but also happened with all other mitochondrially-encoded genes, of which many do not contain such an AxAAA 5'UTR motif, but rather a CUUUxU or AAGAAx motif.

Indeed, the ribosome footprinting showed that the density of mitoribosome loading levels on all mRNAs were much lower in the *mtran* mutants than in the wild type. Thus, mTRAN proteins must be universal mRNA recognition factors embedded into the plant mitoribosomes, rather than mRNA-specific initiation cofactors (Derbikova et al., 2018; Green-Willms et al., 1998). The universally-reduced mitoribosome loading in the *mtran* double mutants is also very different from the ribosome loading in *rps10* mutants (Kwasniak-Owczarek et al., 2019), which is defective in a mtSSU subunit thought to be involved in elongation (Hermann-Le Denmat et al., 1994). In the *rps10* mutants, variable increased or decreased ribosome loading is observed on mRNAs encoding OXPHOS components, but higher ribosome loading was found for translation- and cytochrome *c* maturation-related mRNAs. This striking difference further supports the notion that mTRANs are involved in translation initiation, and not in elongation. Interestingly, ribosome footprints of mitochondrially-encoded ribosomal proteins were lower in the *mtran* mutants than in the wild type, though the global mitochondrial MS/MS and

immunoblot analyses showed that these proteins were more abundant. This suggests that even though loss of *mTRANs* reduces the universal translation initiation capacity, mitochondrially-encoded ribosomal proteins are more stable after being synthesized to compensate for a decrease in translational activity.

The Arabidopsis mitochondrial mRNAs have relatively long 5'UTRs (ranging from 45 to 645 or more bases), which is different from mammals but relatively similar to yeast (Derbikova et al., 2018). The analysis of ribosome footprints using chloramphenicol to artificially "freeze" the translating mitoribosomes on mRNAs could not allow us to consistently "catch" the translation initiation stage, in which the interaction between the mtSSU and mRNAs is relatively fast and unstable (Planchard et al., 2018). Our independent motif analysis showed that the 5'UTRs of mitochondrial mRNAs contain two potential mitoribosome binding sites CUUUxU and AAGAAx/AxAAAG. We showed that mTRAN1, the main isoform of mTRANs in Arabidopsis, could directly bind to both mitoribosome binding sites. Together, this suggests that mTRANs prefer A/U-rich regions in the 5'UTRs of mitochondrial transcripts for protein-RNA binding to help mtSSU bind mRNAs to initiate translation. The sites do not appear to be at a particular distance from the start codon (Fig. S9), so we hypothesize that either the 2/3D structure of the 5'UTRs may bring the ribosome binding sites physically closer to the start codon, or plant mitoribosomes can efficiently scan long 5'UTRs to find the correct AUG, perhaps with the help of other mRNAs-specific co-factors (Haili et al., 2016). In conclusion, this study establishes that mTRAN proteins are not adenylyl cyclases as previously suggested. Instead, we have now shown that mTRANs are essential components of the plant mtSSU that are required for mitoribosome-RNA binding to initiate translation. These findings indicate that translational initiation by mitochondrial ribosomes occurs in a fundamentally different way in plants as compared to in fungi and animal systems.

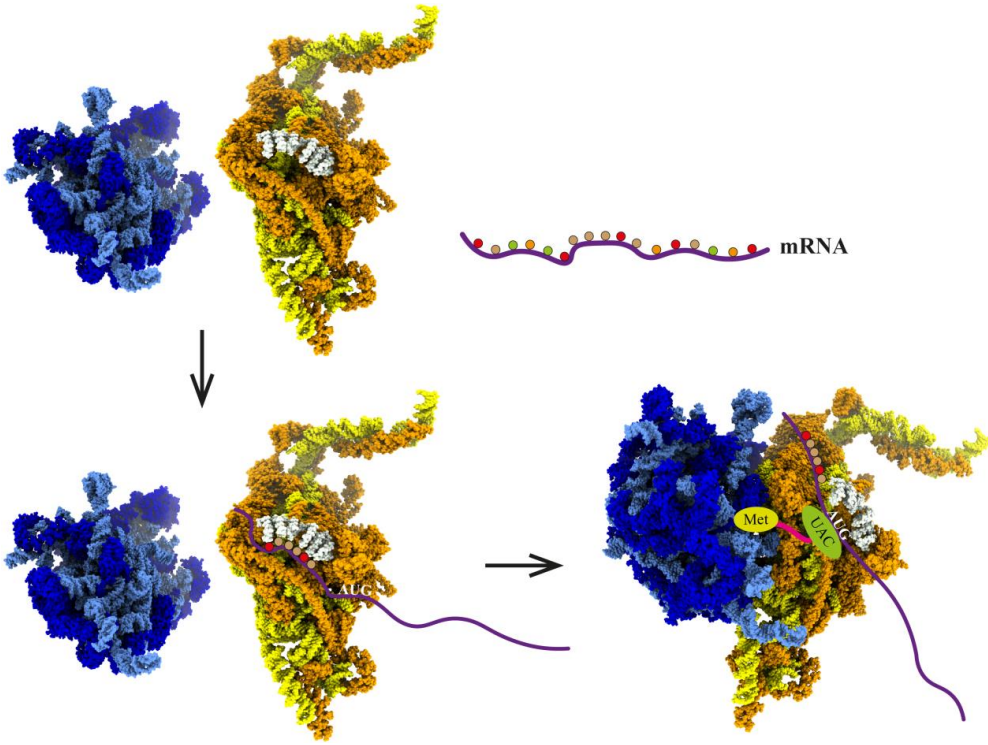

Figure 9. mTRAN1 can bind A/U-rich regions in the 5'UTRs of mitochondrial mRNAs to mediate translation initiation. Before translation occurs, the mtSSU (proteins: orange, rRNA: yellow) and mtLSU (proteins: dark blue, rRNA: light blue) are separated. To initiate translation, mTRAN1 (white) potentially binds a CUUUxU/AAGAAx/AxAAAG motif in the 5'UTRs of the mRNA and may recruit the Methione-tRNA. The mtSSU may scan down the mRNA to find the start codon (AUG), potentially with the help of other co-factors. Once the codon:anticodon interaction occurs, the mtLSU interacts with the mtSSU and the initiation completes. The cryo-EM structure of higher plant mitoribosomes is based on the structure described by Waltz et al. (2020).

MATERIALS AND METHODS

A complete "material and methods" section is provided in the Supplementary Information.

ACKNOWLEDGEMENTS

We thank Dr. Ola Gustafsson for technical assistance to confocal microscopy analysis. We thank Prof. Klas Flärdh for his advice on the cAMP complementation assay. We thank Dr. Malgorzata Kwasniak-Owczarek and Prof. Hanna Janska for their advice on *in organello* protein synthesis and polysome profiling assays. We thank the POPS platform with support of Saclay Plant Sciences-SPS (ANR-17-EUR-0007) for the RNA-seq analysis. We thank Ewa Krupinska and Dr. Wolfgang Knecht for their advice on recombinant protein expression. We thank Dr. Peter Kindgren for his advice on REMSAs. We thank Prof. Ian Max Møller for his critical comments on the manuscript. This project was supported by the Swedish Research Council (Vetenskapsrådet 2017-03854; 2021-04358), Crafoord Foundation (20170862; 20190868), Carl Trygger Foundation (CTS 17 487), Kungl. Fysiografiska Sällskapet i Lund and Jörgen Lindström's Foundation and by grants to H. M. from the French National Research Agency No. ANR-20-CE11-0021. The IJPB benefits from the support of Saclay Plant Sciences-SPS (ANR-17-EUR- 0007).

AUTHOR CONTRIBUTION

O.V.A., H.C.T., E.D., H.M. and A.G.R. conceived and planned the project. H.C.T., V.S., S.L., K.B., K.K., A.L-A., B.C, K.H., C.W. and F.L. performed experiments. H.C.T., H.M., E.D., C.W. and O.V.A. analyzed data, and. H.C.T. and O.V.A wrote the manuscript with input from all co-authors.

REFERENCES

Adamowicz-Skrzypkowska, A., Kwasniak-Owczarek, M., Van Aken, O., Kazmierczak, U., and Janska, H. (2020). Joint inhibition of mitochondrial complex IV and alternative oxidase by genetic or chemical means represses chloroplast transcription in Arabidopsis. Philosophical transactions of the Royal Society of London Series B, Biological sciences *375*, 20190409.

Al-Younis, I., Wong, A., and Gehring, C. (2015). The Arabidopsis thaliana K(+)-uptake permease 7 (AtKUP7) contains a functional cytosolic adenylate cyclase catalytic centre. FEBS letters *589*, 3848-3852.

Baek, M., DiMaio, F., Anishchenko, I., Dauparas, J., Ovchinnikov, S., Lee, G.R., Wang, J., Cong, Q., Kinch, L.N., Schaeffer, R.D*., et al.* (2021). Accurate prediction of protein structures and interactions using a three-track neural network. Science *373*, 871-876.

Boyes, D.C., Zayed, A.M., Ascenzi, R., McCaskill, A.J., Hoffman, N.E., Davis, K.R., and Gorlach, J. (2001). Growth stage-based phenotypic analysis of Arabidopsis: a model for high throughput functional genomics in plants. The Plant cell *13*, 1499-1510.

Centeno-Gonzalez, N.K., Martinez-Cabrera, H.I., Porras-Muzquiz, H., and Estrada-Ruiz, E. (2021). Late Campanian fossil of a legume fruit supports Mexico as a center of Fabaceae radiation. Commun Biol *4*, 41.

Delannoy, E., Stanley, W.A., Bond, C.S., and Small, I.D. (2007). Pentatricopeptide repeat (PPR) proteins as sequence-specificity factors in post-transcriptional processes in organelles. Biochem Soc Trans *35*, 1643-1647.

Derbikova, K.S., Levitsky, S.A., Chicherin, I.V., Vinogradova, E.N., and Kamenski, P.A. (2018). Activation of Yeast Mitochondrial Translation: Who Is in Charge? Biochemistry (Mosc) *83*, 87-97.

Fuchs, P., Rugen, N., Carrie, C., Elsasser, M., Finkemeier, I., Giese, J., Hildebrandt, T.M., Kuhn, K., Maurino, V.G., Ruberti, C*., et al.* (2020). Single organelle function and organization as estimated from Arabidopsis mitochondrial proteomics. Plant J *101*, 420-441.

Fukasawa, Y., Tsuji, J., Fu, S.C., Tomii, K., Horton, P., and Imai, K. (2015). MitoFates: improved prediction of mitochondrial targeting sequences and their cleavage sites. Molecular & cellular proteomics : MCP *14*, 1113-1126.

Gehring, C. (2010). Adenyl cyclases and cAMP in plant signaling - past and present. Cell Commun Signal *8*, 15.

Greber, B.J., and Ban, N. (2016). Structure and Function of the Mitochondrial Ribosome. Annu Rev Biochem *85*, 103-132.

Green-Willms, N.S., Fox, T.D., and Costanzo, M.C. (1998). Functional interactions between yeast mitochondrial ribosomes and mRNA 5' untranslated leaders. Mol Cell Biol *18*, 1826-1834.

Haili, N., Planchard, N., Arnal, N., Quadrado, M., Vrielynck, N., Dahan, J., des Francs-Small, C.C., and Mireau, H. (2016). The MTL1 Pentatricopeptide Repeat Protein Is Required for Both Translation and Splicing of the Mitochondrial NADH DEHYDROGENASE SUBUNIT7 mRNA in Arabidopsis. Plant physiology *170*, 354-366.

Harrison, T., Ruiz, J., Sloan, D.B., Ben-Hur, A., and Boucher, C. (2016). aPPRove: An HMM-Based Method for Accurate Prediction of RNA-Pentatricopeptide Repeat Protein Binding Events. PloS one *11*, e0160645.

Hazle, T., and Bonen, L. (2007). Comparative analysis of sequences preceding protein-coding mitochondrial genes in flowering plants. Molecular biology and evolution *24*, 1101-1112.

Hermann-Le Denmat, S., Sipiczki, M., and Thuriaux, P. (1994). Suppression of yeast RNA polymerase III mutations by the URP2 gene encoding a protein homologous to the mammalian ribosomal protein S20. Journal of molecular biology *240*, 1-7.

Hooper, C.M., Castleden, I.R., Tanz, S.K., Aryamanesh, N., and Millar, A.H. (2017). SUBA4: the interactive data analysis centre for Arabidopsis subcellular protein locations. Nucleic acids research *45*, D1064-D1074.

Ivanova, A., Law, S.R., Narsai, R., Duncan, O., Lee, J.H., Zhang, B., Van Aken, O., Radomiljac, J.D., van der Merwe, M., Yi, K*., et al.* (2014). A Functional Antagonistic Relationship between Auxin and

Mitochondrial Retrograde Signaling Regulates Alternative Oxidase1a Expression in Arabidopsis. Plant physiology *165*, 1233-1254.

Jumper, J., Evans, R., Pritzel, A., Green, T., Figurnov, M., Ronneberger, O., Tunyasuvunakool, K., Bates, R., Zidek, A., Potapenko, A.*, et al.* (2021). Highly accurate protein structure prediction with AlphaFold. Nature *596*, 583-589.

Kacprzak, S.M., Dahlqvist, A., and Van Aken, O. (2020). The transcription factor ANAC017 is a key regulator of mitochondrial proteotoxic stress responses in plants. Philosophical transactions of the Royal Society of London Series B, Biological sciences *375*, 20190411.

Karimova, G., Pidoux, J., Ullmann, A., and Ladant, D. (1998). A bacterial two-hybrid system based on a reconstituted signal transduction pathway. Proceedings of the National Academy of Sciences of the United States of America *95*, 5752-5756.

Karpenahalli, M.R., Lupas, A.N., and Soding, J. (2007). TPRpred: a tool for prediction of TPR-, PPR- and SEL1-like repeats from protein sequences. BMC bioinformatics *8*, 2.

Kuhn, K., Yin, G., Duncan, O., Law, S.R., Kubiszewski-Jakubiak, S., Kaur, P., Meyer, E., Wang, Y., Small, C.C., Giraud, E.*, et al.* (2015). Decreasing electron flux through the cytochrome and/or alternative respiratory pathways triggers common and distinct cellular responses dependent on growth conditions. Plant physiology *167*, 228-250.

Kummer, E., Leibundgut, M., Rackham, O., Lee, R.G., Boehringer, D., Filipovska, A., and Ban, N. (2018). Unique features of mammalian mitochondrial translation initiation revealed by cryo-EM. Nature *560*, 263-267.

Kwasniak-Owczarek, M., Kazmierczak, U., Tomal, A., Mackiewicz, P., and Janska, H. (2019). Deficiency of mitoribosomal S10 protein affects translation and splicing in Arabidopsis mitochondria. Nucleic acids research *47*, 11790-11806.

Kwasniak-Owczarek, M., Tomal, A., and Janska, H. (2022). Assessment of Protein Synthesis in Mitochondria Isolated from Rosette Leaves and Liquid Culture Seedlings of Arabidopsis. Methods in molecular biology *2363*, 183-197.

Logan, D.C., and Leaver, C.J. (2000). Mitochondria-targeted GFP highlights the heterogeneity of mitochondrial shape, size and movement within living plant cells. J Exp Bot *51*, 865-871.

Lurin, C., Andres, C., Aubourg, S., Bellaoui, M., Bitton, F., Bruyere, C., Caboche, M., Debast, C., Gualberto, J., Hoffmann, B.*, et al.* (2004). Genome-wide analysis of Arabidopsis pentatricopeptide repeat proteins reveals their essential role in organelle biogenesis. The Plant cell *16*, 2089-2103.

Mai, N., Chrzanowska-Lightowlers, Z.M., and Lightowlers, R.N. (2017). The process of mammalian mitochondrial protein synthesis. Cell Tissue Res *367*, 5-20.

Manna, S. (2015). An overview of pentatricopeptide repeat proteins and their applications. Biochimie *113*, 93-99.

Moller, I.M., Rasmusson, A.G., and Van Aken, O. (2021). Plant mitochondria - past, present and future. Plant J.

Montoya, J., Ojala, D., and Attardi, G. (1981). Distinctive features of the 5'-terminal sequences of the human mitochondrial mRNAs. Nature *290*, 465-470.

Moutinho, A., Hussey, P.J., Trewavas, A.J., and Malho, R. (2001). cAMP acts as a second messenger in pollen tube growth and reorientation. Proceedings of the National Academy of Sciences of the United States of America *98*, 10481-10486.

Mower, J.P. (2020). Variation in protein gene and intron content among land plant mitogenomes. Mitochondrion *53*, 203-213.

Noll, M., Hapke, B., Schreier, M.H., and Noll, H. (1973). Structural dynamics of bacterial ribosomes. I. Characterization of vacant couples and their relation to complexed ribosomes. Journal of molecular biology *75*, 281-294.

Planchard, N., Bertin, P., Quadrado, M., Dargel-Graffin, C., Hatin, I., Namy, O., and Mireau, H. (2018). The translational landscape of Arabidopsis mitochondria. Nucleic acids research *46*, 6218-6228.

Rao, R.S., Salvato, F., Thal, B., Eubel, H., Thelen, J.J., and Moller, I.M. (2017). The proteome of higher plant mitochondria. Mitochondrion *33*, 22-37.

Rugen, N., Straube, H., Franken, L.E., Braun, H.P., and Eubel, H. (2019). Complexome Profiling Reveals Association of PPR Proteins with Ribosomes in the Mitochondria of Plants. Molecular & cellular proteomics : MCP *18*, 1345-1362.

Schmidt, O., Pfanner, N., and Meisinger, C. (2010). Mitochondrial protein import: from proteomics to functional mechanisms. Nature reviews Molecular cell biology *11*, 655-667.

Schmitz-Linneweber, C., and Small, I. (2008). Pentatricopeptide repeat proteins: a socket set for organelle gene expression. Trends Plant Sci *13*, 663-670.

Senkler, J., Senkler, M., Eubel, H., Hildebrandt, T., Lengwenus, C., Schertl, P., Schwarzlander, M., Wagner, S., Wittig, I., and Braun, H.P. (2017). The mitochondrial complexome of Arabidopsis thaliana. Plant J *89*, 1079-1092.

Small, I.D., and Peeters, N. (2000). The PPR motif - a TPR-related motif prevalent in plant organellar proteins. Trends in biochemical sciences *25*, 46-47.

Van Aken, O., Ford, E., Lister, R., Huang, S., and Millar, A.H. (2016). Retrograde signalling caused by heritable mitochondrial dysfunction is partially mediated by ANAC017 and improves plant performance. Plant J *88*, 542-558.

Van Aken, O., Pecenkova, T., van de Cotte, B., De Rycke, R., Eeckhout, D., Fromm, H., De Jaeger, G., Witters, E., Beemster, G.T., Inze, D.*, et al.* (2007). Mitochondrial type-I prohibitins of Arabidopsis thaliana are required for supporting proficient meristem development. Plant J *52*, 850-864.

Waltz, F., Nguyen, T.T., Arrive, M., Bochler, A., Chicher, J., Hammann, P., Kuhn, L., Quadrado, M., Mireau, H., Hashem, Y.*, et al.* (2019). Small is big in Arabidopsis mitochondrial ribosome. Nat Plants *5*, 106-117.

Waltz, F., Soufari, H., Bochler, A., Giege, P., and Hashem, Y. (2020). Cryo-EM structure of the RNA-rich plant mitochondrial ribosome. Nat Plants *6*, 377-383.

Yan, J., Yao, Y., Hong, S., Yang, Y., Shen, C., Zhang, Q., Zhang, D., Zou, T., and Yin, P. (2019). Delineation of pentatricopeptide repeat codes for target RNA prediction. Nucleic acids research *47*, 3728-3738.

Yang, J., and Zhang, Y. (2015). I-TASSER server: new development for protein structure and function predictions. Nucleic acids research *43*, W174-181.

Zubo, Y.O., Potapova, T.V., Tarasenko, V.I., Borner, T., and Konstantinov, Y.M. (2014). The rate of transcription in Arabidopsis chloroplasts depends on activity of alternative electron transfer pathway in mitochondria. Dokl Biochem Biophys *455*, 76-79.

SUPPLEMENTARY FIGURES

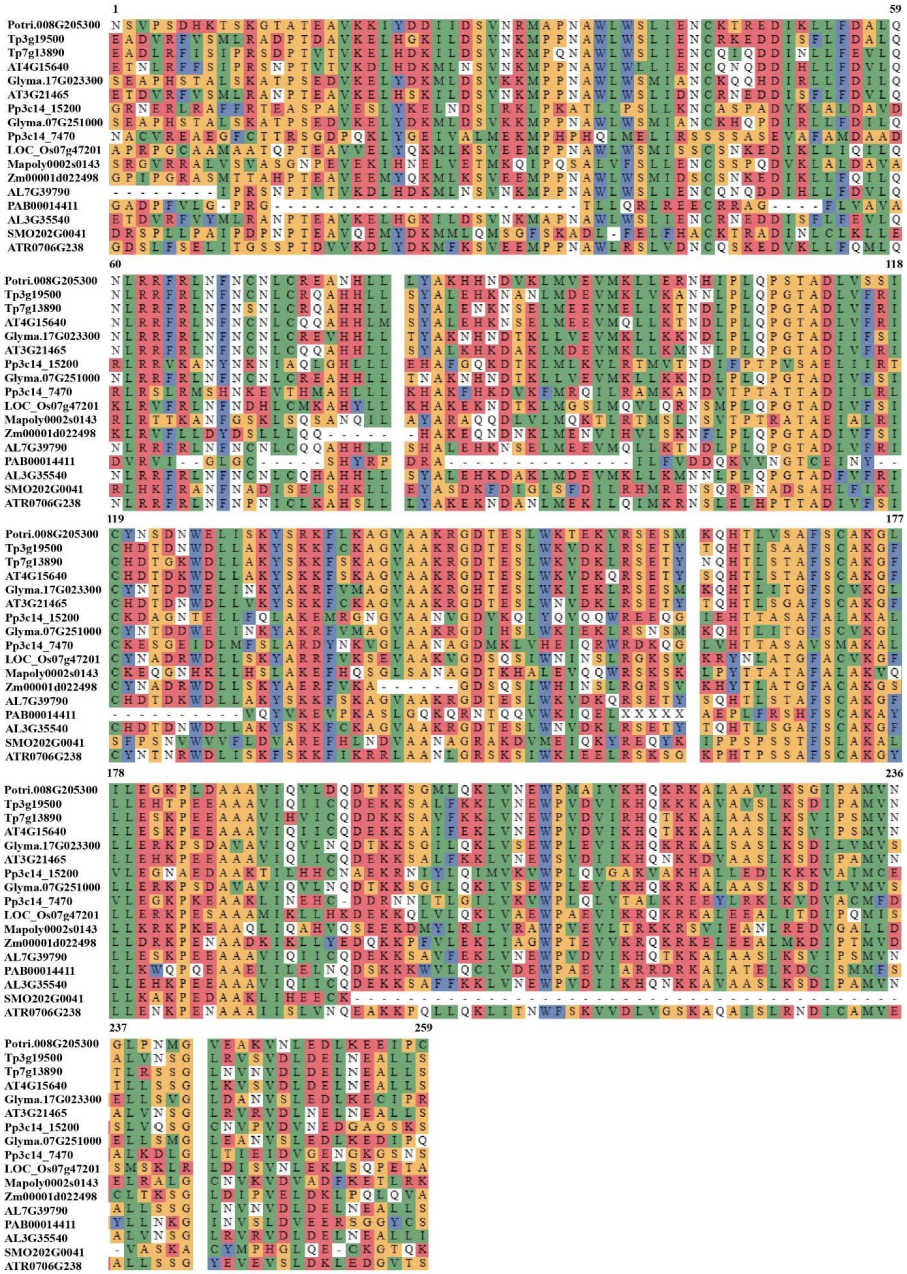

Figure S1. Alignment of the conserved parts of mTRAN proteins from land plant species. All proteins sequences were collected from PLAZA 4.5 (Van Bel et al., 2018). Multiple sequence alignment (MSA) was generated using the algorithm MUSCLE followed by MSA trimming within the PLAZA platform.

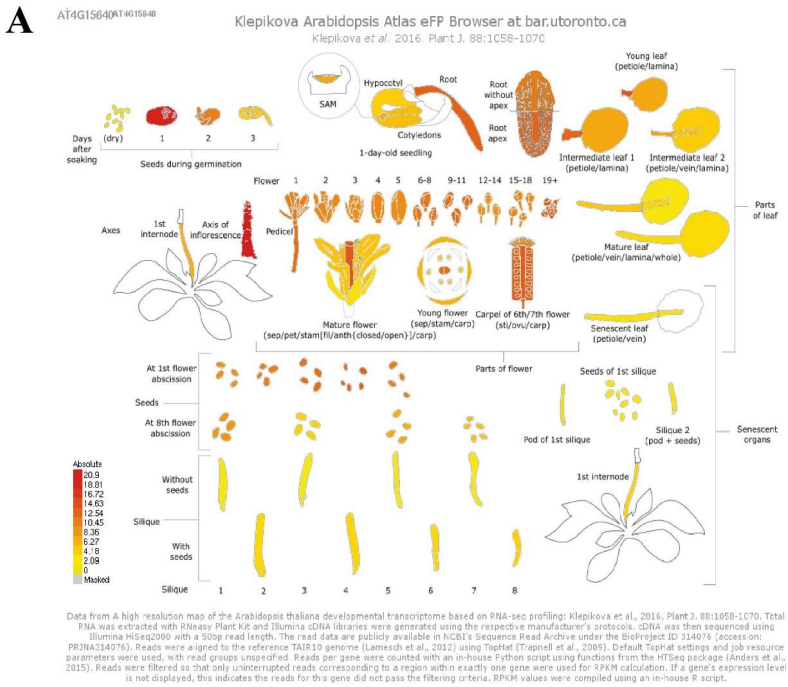

Figure S2. Expression patterns of *mTRAN1* and *mTRAN2* in different tissues of *Arabidopsis thaliana*. The Arabidopsis Genome Identifiers (AGI) of mTRAN1 and mTRAN2 were queried in Arabidopsis eFP Browser (http://bar.utoronto.ca/efp/cgi-bin/efpWeb.cgi) using Data Source "Klepikova Atlas".

A

***mtran1-3* (heterozygous) x *mtran2-3* (homozygous)**

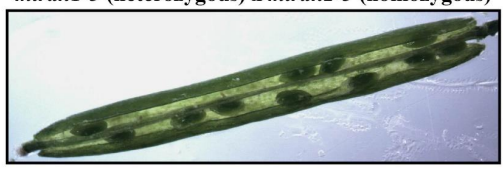

***mtran1-3* (wild type) x *mtran2-3* (homozygous)**

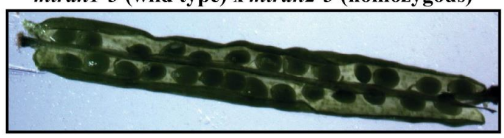

B

Genotype	Number of screened siliques	Number of screened seeds	Number of normal seeds	Number of empty spaces
mtran1-3 (heterozygous) x *mtran2-3* (homozygous)	25	467	287 (61.5%)	180 (38.5%)
mtran1-3 (wild type) x *mtran2-3* (homozygous)	10	280	249 (88.9%)	31 (11.1%)
Col-0	10	327	310 (94.8%)	17 (5.2%)

C

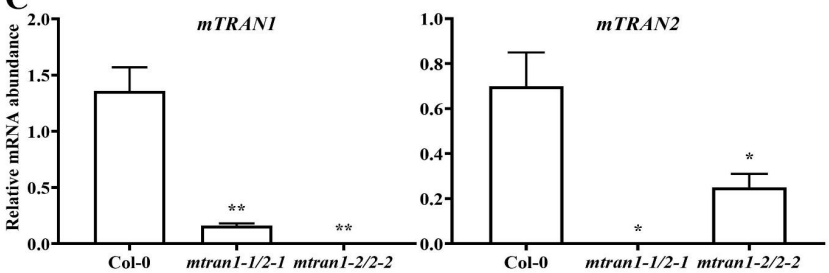

D

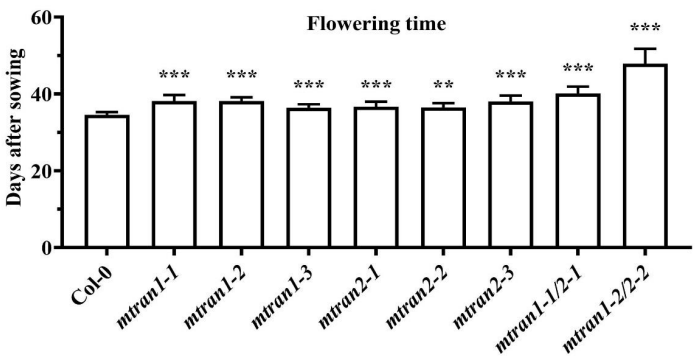

Figure S3. Phenotypic analysis of the double knockout *mtran* mutants. A. *mtran1-3/2-3* is embryo lethal. Pictures of dissected siliques of *mtran1-3* (heterozygous) x *mtran2-3* (homozygous) and *mtran1-3* (wildtype) x *mtran2-3* (homozygous) are shown. **B.** Number of seeds and empty space of dissected siliques of *mtran1-3* (heterozygous) x *mtran2-3* (homozygous), *mtran1-3* (wildtype) x *mtran2-3* (homozygous) and Col-0 (the wildtype) was analyzed. **C.** The loss of function of *mTRAN1* and *mTRAN2* transcripts in *mtran1-1/2-1* and *mtran1-2/2-2*. Seedlings at developmental stage 1.04 (Boyes et al., 2001) were collected in pools and relative mRNA abundance were measured by qRT-PCR (n = 3) and normalized to Col-0 samples (±SE). **D.** Determination of flowering time of plants grown in soil. Data are given as 9 plants/genotype. Statistically significance was based on Student's *t* test (*=P<0.05, **=P<0.01, ***=P<0.001).

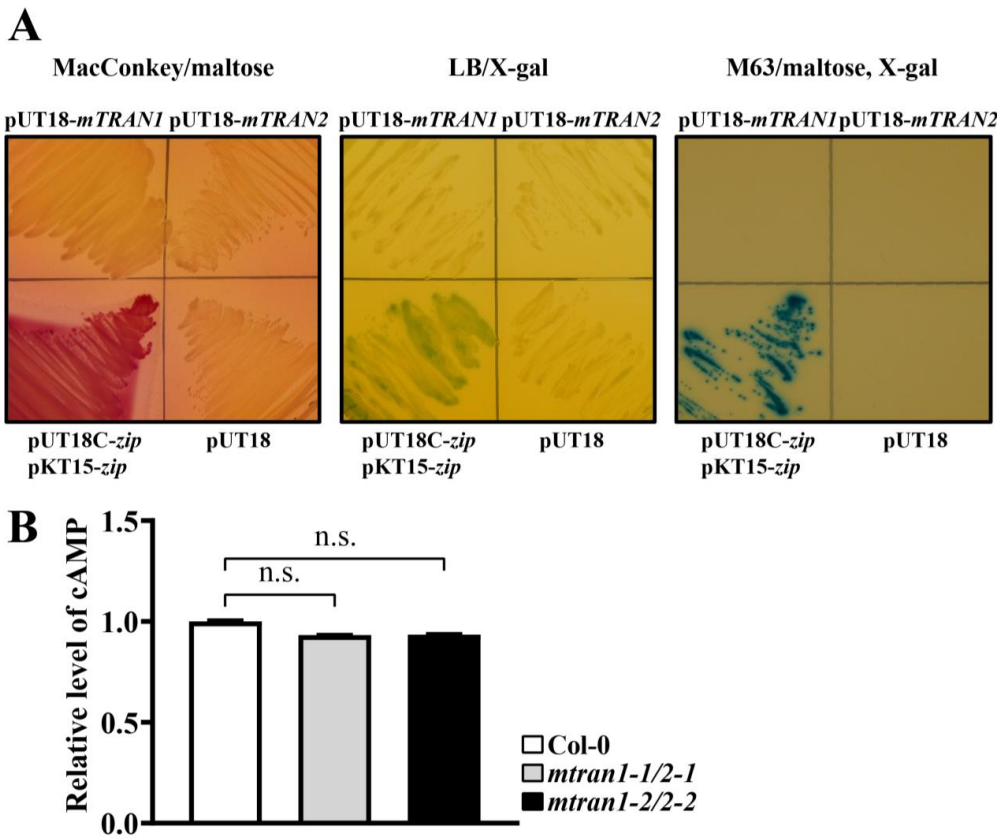

Figure S4. mTRAN1 and mTRAN2 do not have adenylyl cyclase activity. A. The bacterial cAMP synthase complementation assay was based on the Bacterial Adenylate Cyclase Two-Hybrid System. For positive control, pUT18C-*zip* and pKT15-*zip* were co-transformed into *BTH101*. For negative control, the empty vector pUT18 was transformed into *BTH101*. Transformed cells were plated on MacConkey/maltose (left panel), LB/X-gal (middle panel) and M63/maltose, X-gal media (right panel). **B.** cAMP content measurement *in planta*. The endogenous cAMP content of the *mtran* double mutants was normalized to Col-0. Statistical significance was based on Student's *t* test (n=3) (±SE). n.s=non-significant. FW=fresh weight.

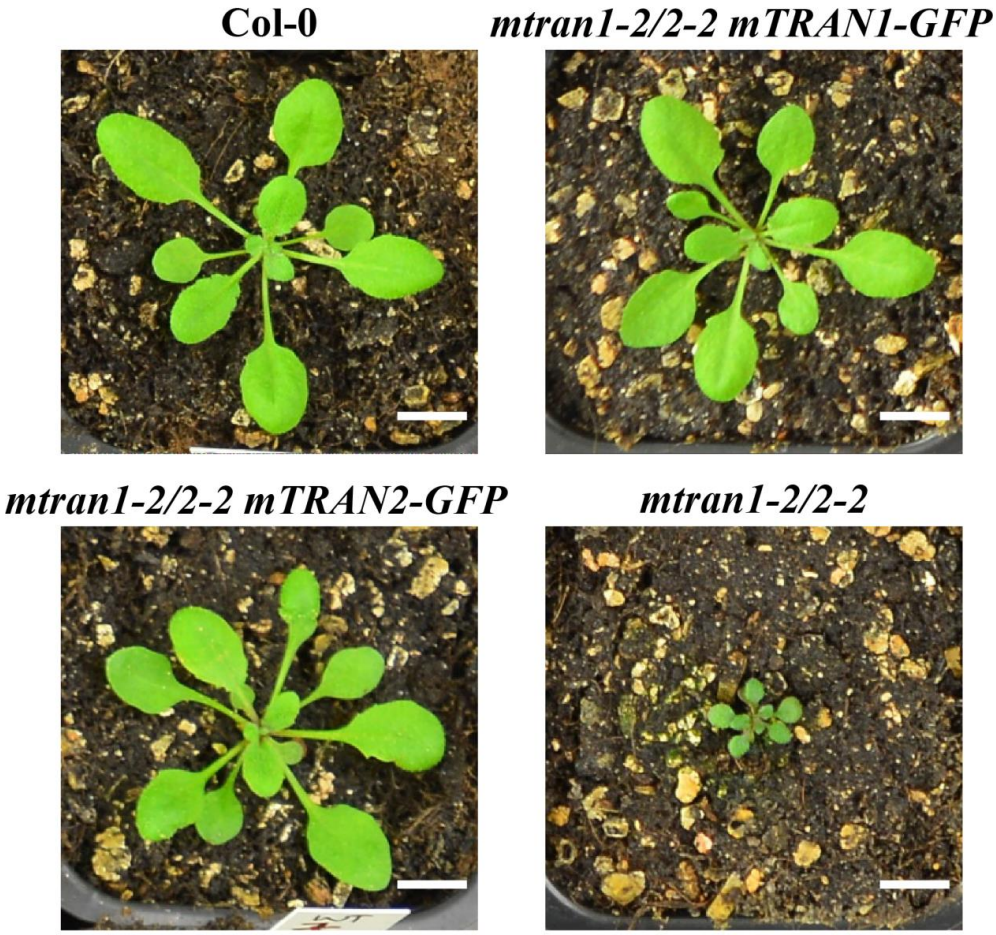

Figure S5. Phenotypes of *mtran1-2/2-2 mTRAN1/2-GFP* complementation lines. The picture of representative plants was taken on the 25th day of growth. Scale bar: 1 cm.

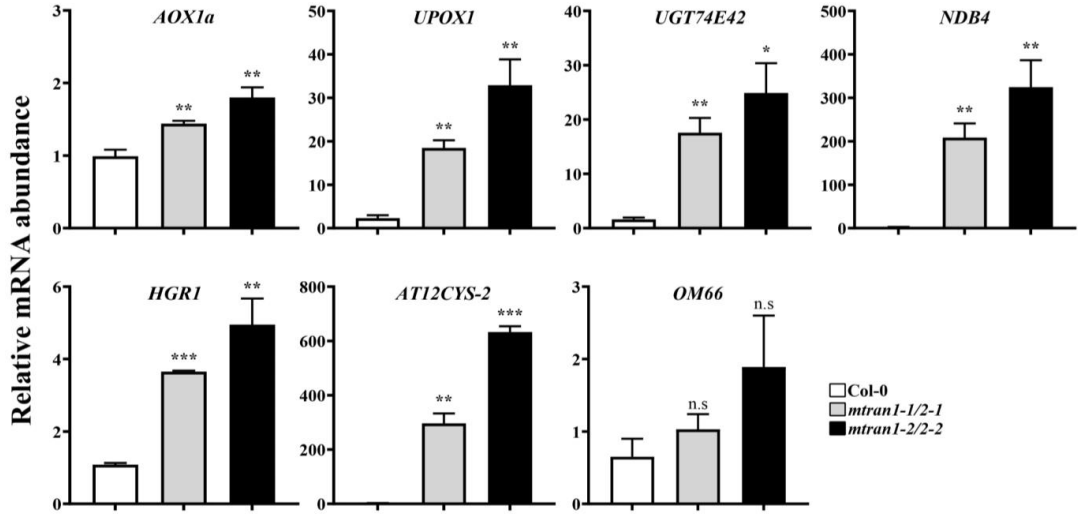

Figure S6. Loss of *mTRAN1* and *mTRAN2* results in upregulation of mitochondrial retrograde/unfolded protein response (UPR^{mt}) signalling markers. Relative mRNA abundance of *mtran1-1/2-1* and *mtran1-2/2-2* were measured by qRT-PCR (n=3) and normalized to Col-0 (±SE). Statistical significance was based on Student's *t* test (*=P<0.05, **=P<0.01, ***=P<0.001). n.s=non-significant.

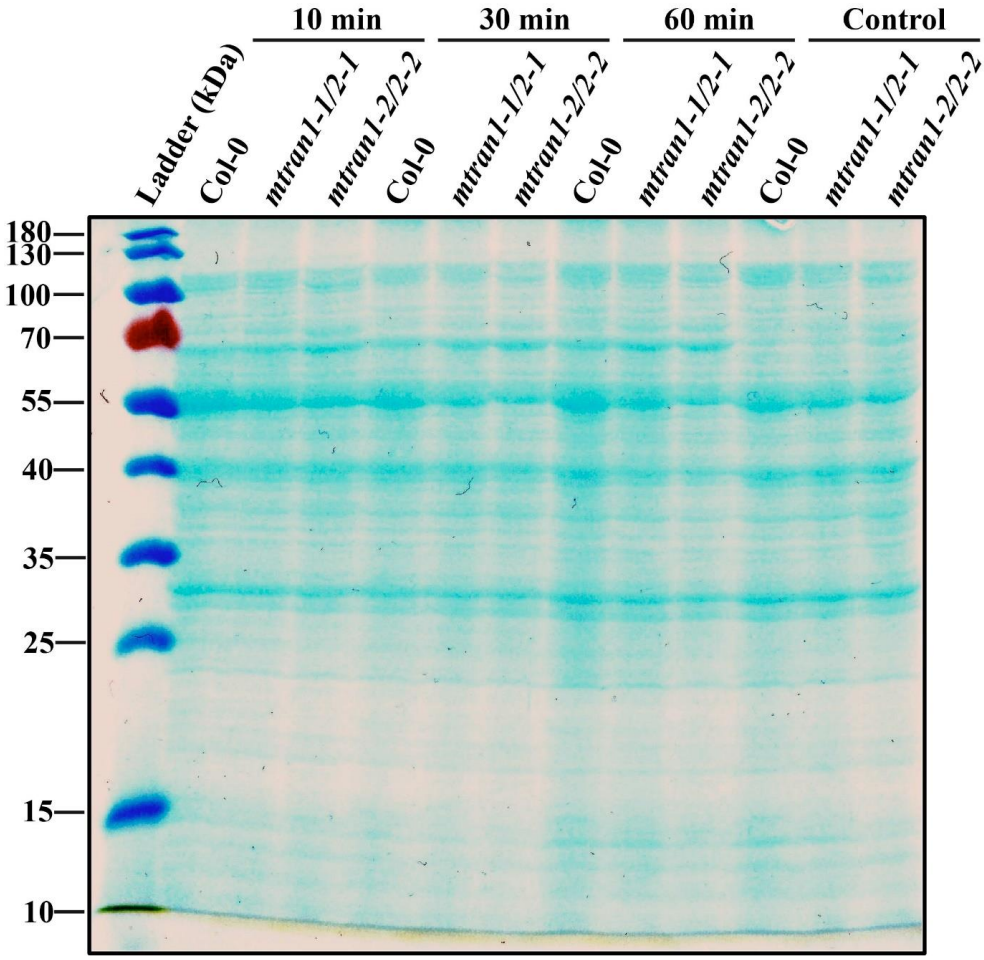

Figure S7. Coomassie Brilliant Blue staining of mitochondrial proteins resolved on SDS-PAGE after *in organello* protein synthesis assays. The assays were conducted for 10, 30 and 60 min using purified mitochondria from Col-0, *mtran1-1/2-1* and *mtran1-2/2-2*. In the control reactions (60 min), sodium acetate was used as substrate to assess bacterial contamination. The molecular weight (kDa) is shown on the left side of the gel.

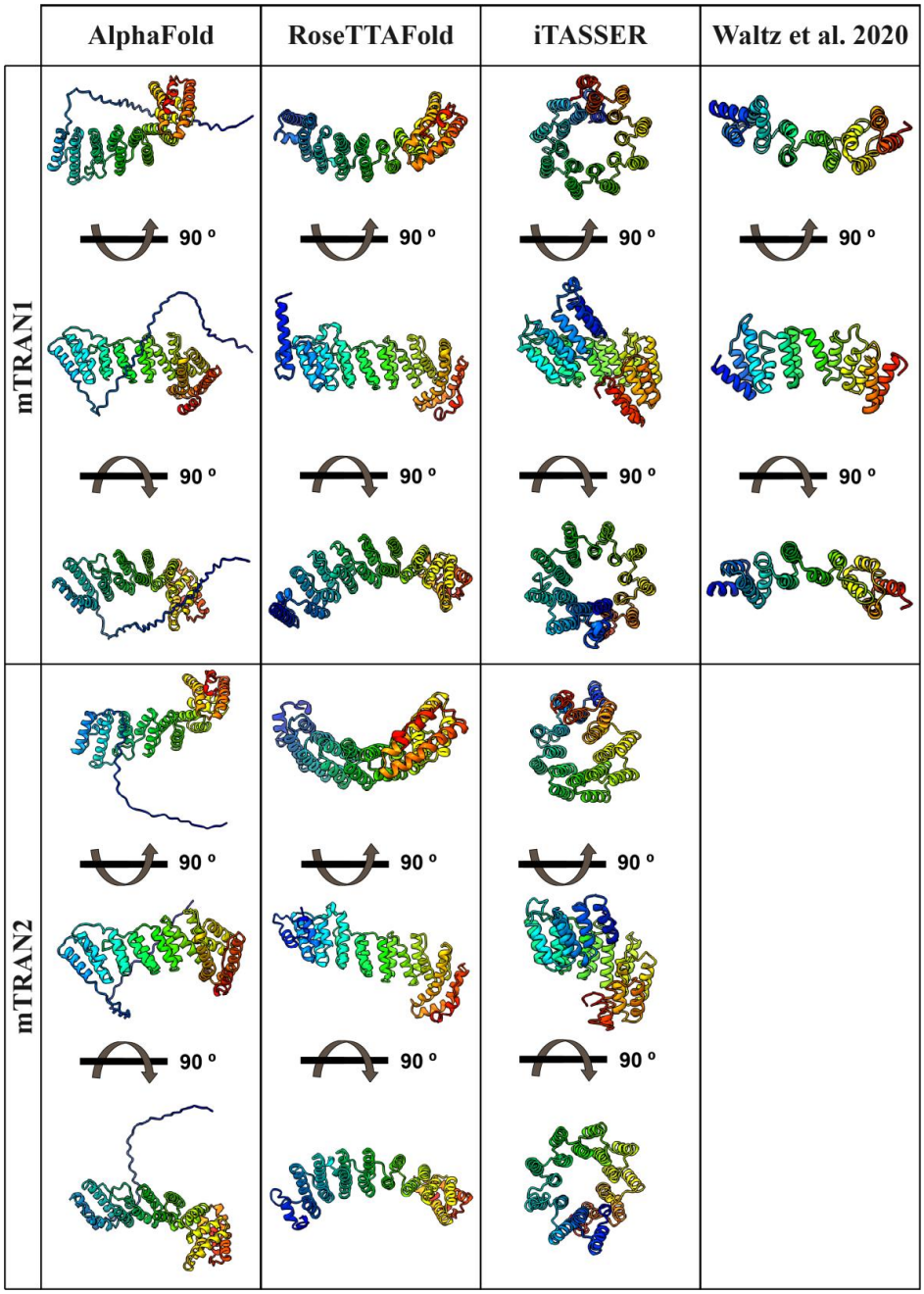

Figure S8. Predicted protein structures suggest that mTRAN1 and mTRAN2 have PPR protein like-structures. Protein structures of mTRAN1 and mTRAN2 without mitochondrial targeting sequences predicted by MitoFates (Fukasawa et al., 2015) were modelled by AlphaFold (Jumper et al., 2021), RoseTTAFold (Baek et al., 2021) and iTASSER (Yang and Zhang, 2015). The predicted structure of mTRAN1 from Waltz et al. (2020) is also presented to be compared with their other predicted structures.

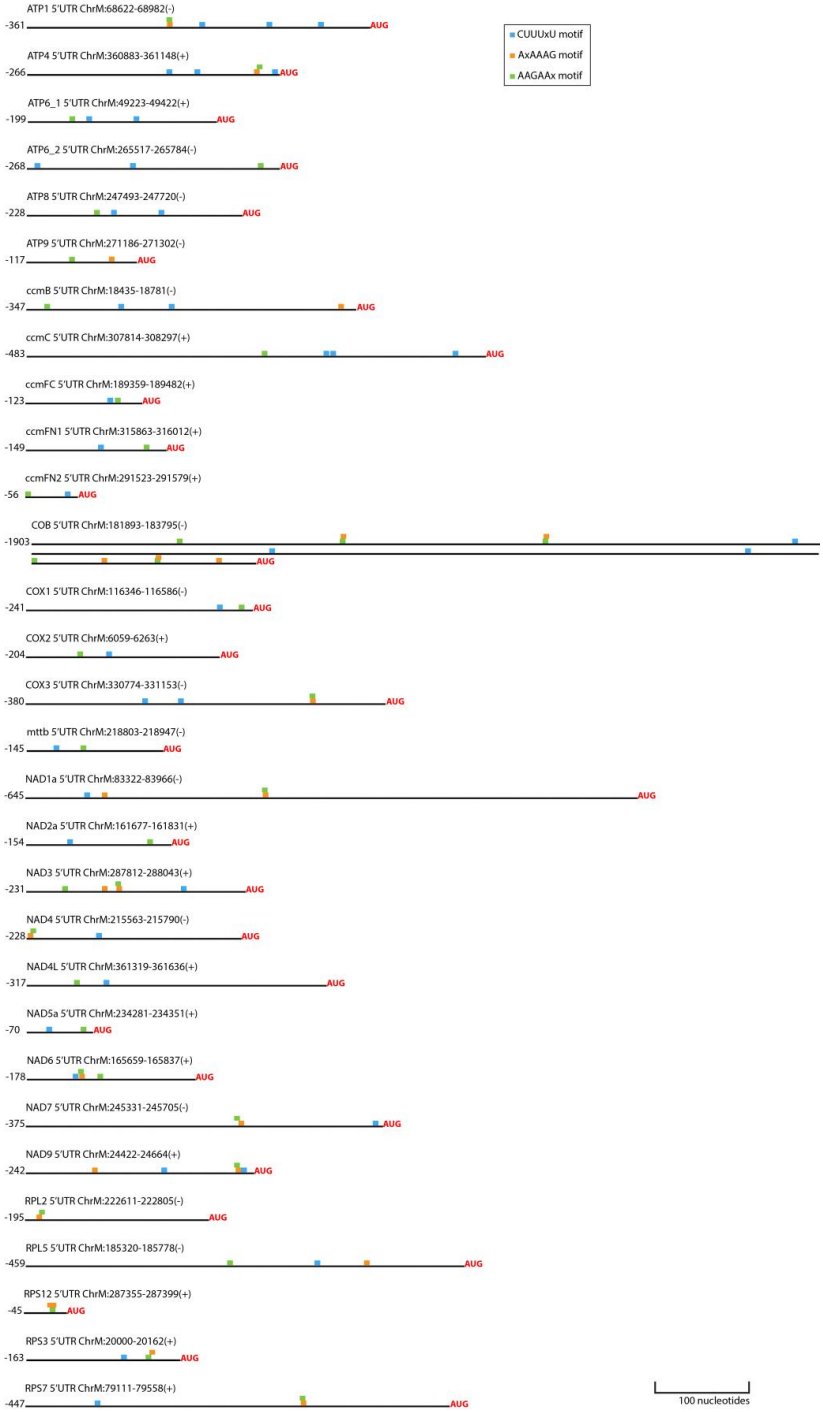

Figure S9. The position of mitoribosome binding sites in the 5'UTRs of mitochondrial transcripts. Blue box = CUUUxU. Orange box = AxAAAG. Green box = AAGAAx. Scale bar = 100 nucleotides. AUG = start codon.

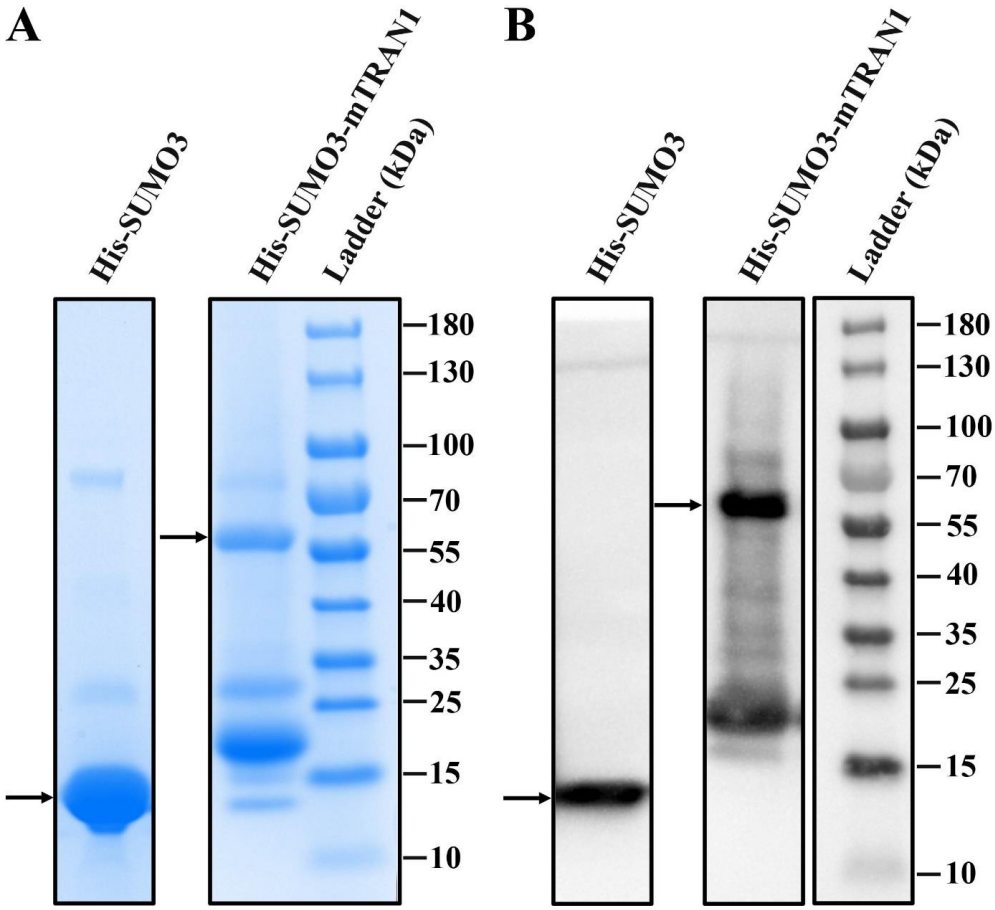

Figure S10. Purified His-SUMO3 and His-SUMO3-mTRAN1 from *E. coli*. The purified proteins were resolved on SDS-PAGE followed by Coomassie Brilliant Blue (CBB) staining (**A**) and western blot using an antibody against the 6xHis tag (**B**). Arrows indicate the purified proteins. The molecular weight (kDa) is indicated.

SUPPLEMENTARY TABLES

Table S1. Mitochondrial proteomic study of the *mtran* double mutants.

Table S2. Proteins identified as interacting with mTRAN1 and mTRAN2 *in planta.* A. A summary list of proteins co-immunoprecipitated with mTRAN1-GFP and mTRAN2-GFP. **B.** All proteins identified as interacting with mitoGFP *in planta*. **C.** All proteins identified as interacting with mTRAN1 and mTRAN2 *in planta*.

Table S3. RNA-seq analysis of *mtran1-2/2-2*.

Table S4. Gene ontology analysis of DEGs found in RNA-seq analysis of *mtran1-2/2-2*.

Table S5. Microarray and RNA-seq datasets used for meta-analysis. A. List of DEGs of *mtran1-2/2-2* versus other mitochondrial perturbations in Arabidopsis. **B.** Comparison of common pairwise DEGs calculated via the Sørensen-Dice similarity coefficient.

Table S6. Organellar transcriptome analysis of *mtran1-2/2-2*. A. Mitochondrial transcriptome of *mtran1-2/2-2*. **B.** Chloroplastic transcriptome of *mtran1-2/2-2*. **C.** Mitochondrial transcriptome of *mtran1-2/2*-2 versus *rpotmp* versus *atphb3*.

Table S7. Splicing and editing analysis of mitochondrial transcripts of *mtran1-2/2*-2.

Table S8. Motif analysis of the 5'UTRs of mitochondrial mRNAs. **A.** The 5'UTR sequences of mitochondrial mRNAs. **B.** Motif analysis of the mitochondrial mRNA's 5'UTRs without putative inter-cistronic 5'UTRs using MEME search tool and manual search. **C.** Motif analysis of the mitochondrial mRNA's 5'UTRs with putative inter-cistronic 5'UTRs using MEME search tool and manual search.

Table S9. **Synthesized Cy5-labelled RNA probes used for REMSAs.**

Table S10. Analysis of mitochondrial ribosome footprints of the *mtran* double mutants.

Table S11. All primers used in this study.

SUPPLEMENTARY INFORMATION

BACTH cAMP complementation method

The Bacterial Adenylate Cyclase Two-Hybrid (BACTH) system (Karimova et al., 1998) is usually used for characterization of protein-protein interaction *in vivo*. However, this system can also be used for reporting AC activity as the *E. coli* strain that lacks endogenous AC activity, for example, the *BTH101* strain, can be complemented with a functional AC expression construct, leading to cAMP production. Consequently, cAMP binds to the catabolite activator protein (CAP), forming the cAMP/CAP complex, which is a positive regulator of genes of the *lac* and *mal* operons involved in lactose and maltose catabolism. Therefore, AC-complemented bacteria are able to ferment lactose or maltose, which can be observed when plated on either indicator or selective media. The catalytic domain of AC (CyaA) from *Bordetella pertussis* contains two complementary fragments, T25 and T18, that do not have AC activity if they do not interact with each other. For the positive control, the plasmids pKT25-zip and pUT18C-zip were co-transformed into *BTH101* (*E. coli cya*). Consequently, the positive control plated on either indicator or selective media will show Cya^+ phenotype (*E. coli* Cya^+). On the MacConkey/maltose medium, *E. coli* Cya^+ could ferment maltose, thus the colonies appear bright red due to the acidification resulting from fermentation(Karimova et al., 1998) (Fig. S4A, left panel). On the LB/X-gal medium, *E. coli* Cya^+ produced cAMP that activated the *lacZ* gene encoding β-galactosidase (Karimova et al., 1998), which in turn hydrolyzed X-gal to form 5-bromo-4-chloro-indoxyl that spontaneously dimerized to produce an insoluble blue pigment. As a result, the colonies formed by *E. coli* Cya^+ appear blue in color (Fig. S4A, middle panel). On the M63 medium, *E. coli* Cya^+ could catabolize maltose as the unique carbon source. X-Gal was added for better observation of growth of colonies (Fig. 4A, right panel). For the negative control, the empty vector pUT18 was transformed into *E. coli cya*, which formed colorless colonies on MacConkey/maltose and LB/X-gal media and could not grow on the M63 medium (Fig. S4A).

MATERIALS AND METHODS

Phylogenetic analysis

All proteins sequences were collected from PLAZA 4.5 (Van Bel et al., 2018). Multiple sequence alignment (MSA) was generated using the algorithm MUSCLE followed by MSA trimming within the PLAZA platform. The edited MSA was used to construct a rooted phylogenetic tree using ClustalX with a bootstrap of 1000 replicates. Node numbers indicate bootstrap values.

Generation of stable transgenic lines carrying *mTRAN1/2-GFP* and complementation lines *mtran1-2/2-2 mTRAN1/2-GFP*

The full-length coding sequences of *mTRAN1* and *mTRAN2* were amplified by PCR from Arabidopsis Col-0 cDNA. The sequences were cloned into the pDONR221 Gateway vector, then cloned into the 35S binary vector pB7FWG2 (Karimi et al., 2002). Stable transgenic and complementation lines were generated by transforming the constructs into Arabidopsis Col-0 and *mtran1-2/2-2* by floral dipping, respectively. Homozygous transgenic plants were obtained by selecting seeds on half-strength MS agar plates containing 5 mg/mL Basta (Glufosinate Ammonium).

Subcellular localization

Homozygous plants carrying *35S::mTRAN1-GFP* and *35S::mTRAN2-GFP* were grown on MS agar plates for 7 days. Root tissues of seedlings were harvested just prior to the experiment and incubated with 500 nM MitoTracker^{TM} Red CMXRos (ThermoScientific) for 30 min. mTRAN1/2-GFP and MitoTracker-labelled mitochondria were visualized by a confocal laser scanning microscope (Leica SP8 DLS) using excitation wavelengths of 488 nm (mTRAN1/2-GFP) and 552 nm (MitoTracker-labelled mitochondria) and emission wavelength of 580 nm for both targets. Subsequent images were captured and processed by LAS X Life Science Microscope Software (Leica).

T-DNA insertion mutants

T-DNA insertion lines for *mtran1* (SALK_044671, GABI_915G12 and WiscDsLox485-488E21) and *mtran2* (SALK_054298, SALK_096907 and SALK_099373) were obtained from the European Arabidopsis Stock Centre. T-DNA insertion homozygous lines were genotyped by standard PCR using the left and right gene-specific primer (LP and RP) and the left border

primer of the T-DNA insertion (LB) (Table S11). The genomic position of T-DNA insertion was confirmed by sequencing. The double knockout mutants *mtran1-1/2-1* and *mtran1-2/2-2* were obtained by crossing the single mutants for *mtran1* and *mtran2* as following: SALK_044671 (*mtran1-1*) x SALK_054298 (*mtran2-1*), GABI_915G12 (*mtran1-2*) x SALK_096907 (*mtran2-2*). Homozygous double mutants were genotyped by PCR.

Plant growth conditions and phenotyping

All plants were grown under long day condition (16h light/8h dark, approximately 120 µmol photons m^{-2} s^{-1}). Seeds were surface sterilized by liquid sterilization method as described in Tran and Van Aken (2022). Sterilized seeds were sown on MS agar plates (half-strength MS medium, 0.05% (w/v) MES, 1% (w/v) sucrose, 0.1% (v/v) Gamborg B5 vitamins, 0.8% (w/v) phytoagar, pH 5.7) followed by stratification at 4ºC in the dark for 3 days prior to transferring to the growth chamber. Plate-based phenotypic analysis was performed as described in Boyes et al. (2001). Root length measurement was performed in ImageJ from seedlings grown on vertically placed MS agar plates on day 5, 7 and 9. Seeds sown on soil were also stratified at 4ºC in the dark for 3 days prior to transferring to the growth chamber. Measurement of rosette leaf area was performed in ImageJ on day 15, 18, 21, 24, 27 and 30. Data for growth phenotypic analysis was obtained from at least 60 plants/genotype for plate-based phenotypic analysis, 15 plants/genotype for root length measurement, 9 plants/genotype for measurement of rosette leaf area and determination of flowering time.

For mitochondrial purification, sterilized seeds were grown in liquid half-strength MS medium (same ingredients as MS agar medium but without phytoagar) with shaking gently at 100 rpm in long day light condition. Col-0 and *mtran1-1/2-1* were grown for 14 days. As *mtran1-2/2-2* showed a significant growth delay, it was grown for 21 days in total. Therefore, plant material from all genotypes was collected at the same time and all mitochondrial isolations were done on the same day for the sake of giving more consistent results. For *in organello* protein synthesis, mitochondria were purified from plants grown in liquid half-strength MS medium supplemented with 50 µg/ml cefotaxime to reduce the risk of bacterial contamination.

Bacterial cAMP synthase complementation assay and measurement of cAMP content *in planta*

Bacterial cAMP synthase complementation assay was based on the method of BACTH System kit (Euromedex, France). Full length coding sequences of *mTRAN1* and *mTRAN2* were PCR-amplified from Arabidopsis Col-0 cDNA and then cloned into the vector pUT18. The plasmids

were then transformed into the *E. coli* strain *BTH101* and plated on either indicator or selective media to reveal the resulting Cya^+ phenotype as described in the kit protocol. For the positive control, the plasmids pKT25-*zip* and pUT18C-*zip* were co-transformed into *BTH101*. For the negative control, the plasmid pUT18 was transformed into *BTH101*.

For measurement of cAMP content *in planta*, 11-day-old Col-0 and *mtran1-1/2-1* and 18-day-old *mtran1-2/2-2* seedlings grown on MS agar plates were harvested and ground in liquid nitrogen. Measurement of cAMP content *in planta* was performed as described in Gao et al. (2012). Briefly, 0.4 mL of PBS was added to 0.2 g of ground frozen tissues. After centrifugation at 16100 *g* at 4ºC for 15 min, the supernatant was collected and used to measure cAMP concentration using a cAMP-Glo™ assay kit (Promega) and a plate-reading luminometer (CLARIOstar^{Plus}, BMG Labtech) following the kit instructions.

Mitochondrial and chloroplastic purification

Mitochondria were purified from 14-day-old plants (Col-0, *mtran1-1/2-1* and homozygous transgenic plants carrying *mTRAN1-GFP* and *mTRAN2-GFP*) and 21-day-old plants (*mtran1-2/2-2*) grown in liquid half-strength MS medium as described in Tran and Van Aken (2022). For *mTRAN1/2-GFP* plants, the supernatant after the second high-speed centrifugation was collected as the cytosolic fraction. Chloroplasts were isolated from 14-day-old homozygous transgenic plants carrying *mTRAN1-GFP* and *mTRAN2-GFP* grown in liquid half-strength MS medium as described in Flores-Perez and Jarvis (2017). The concentration of mitochondrial and chloroplastic proteins was determined by Bradford assays (Biorad). Isolated mitochondria were used directly for further experimentation requiring intact mitochondria (*in organello* protein synthesis and measurement of mitochondrial respiration) or stored at -80°C for later use (BN-PAGE and immunoblotting). Isolated chloroplasts were stored at -80°C for later immunoblot analysis.

Analysis of mitochondrial complexes

BN-PAGE using 5% (w/v) digitonin for membrane solubilization was carried out with 500 µg mitochondrial protein per lane as described in Schertl and Braun (2015). Activity measurement of the respiratory complexes I, III, IV and V in BN-PAGE was performed as described previously (Cuillerier and Burelle, 2019; Schertl and Braun, 2015; Smet et al., 2011).

Measurement of mitochondrial respiration

Respiratory measurement of freshly isolated mitochondria was performed using a Clark-type oxygen electrode as described in Lyu et al. (2018).

Analysis of mitochondrial protein abundance by tandem mass spectrometry

Isolated mitochondrial pellets were dissolved in 50 µl of 2% SDS in 100 mM TRIS buffer, pH 7.5 for 30 minutes at room temperature with vortexing at 500 RPM. After centrifugation for 3 min at 13000 RPM, the supernatant was used for reduction and alkylation of proteins using DDT and iodoacetamide. Proteins were loaded to S-Trap columns (ProtiFi, Huntington, NY) and digested with trypsin using the manufacturer instructions with 3 hours digestion. Peptides were eluted, dried in a Speedvac, and stored at -20°C before being desalted on C18 columns (The Nest Group, Ipswich, MA) according to the manufacturer instructions and dried before resuspension in 0.1% formic acid, quantification using Nanodrop and storage at -20°C.

Approximately 400 ng peptides per sample were loaded to Evotips and injected on an Evosep One LC system (Evosep, Odense, Denmark) connected online with a Q-Exactive HF-X Mass Spectrometer (Thermo Fisher Scientific, Germany). Peptides were separated on an EV1109 8 cm column (Evosep) using the 60 SPD method. MS data were acquired in profile mode using data independent acquisition (DIA) with settings essentially as described by Bekker-Jensen et al. (2020) with one full MS scan 350-1400 m/z followed by 49 windows DIA with an isolation widths of 13.7 m/z and evenly distributed window centers from 471.5 to 1129.1 m/z. For full MS scans AGC target was 3e6, resolution 120000 and maximum injection time 25 ms. For DIA scans AGC target was 3e6, target resolution 15000, maximum injection time 22 ms and normalized collision energy 27.

Raw data files were converted to mzML using Proteowizard version 3.0.21098 (Chambers et al., 2012) with vendor peakpicking enabled. The mzML files were processed in DIA-NN version 1.8 in library free mode against the UniProt *Arabidopsis thaliana* proteome UP000006548 downloaded on 10th February 2022. In DIA-NN enzymatic cleavage was set after KR with maximum one missed cleavage and cystein carbamidomethylation was set as fixed modification and N-terminal methionine excision as variable modification. Two pass search (match between runs) was enabled with automated mass accuracy estimation and other settings were set to default.

The protein groups matrix file from DIA-NN was used for data analysis. Normalization of quantitative values with Cyclic Loess normalization (Gentleman et al., 2005; Smyth, 2005) and

differential abundance analysis using LIMMA (Ritchie et al., 2015) were performed in NormalyzerDE version 1.14.0 (Willforss et al., 2019).

Co-immunoprecipitation followed by tandem mass spectrometry

Homozygous transgenic plants carrying *mTRAN1-GFP* and *mTRAN2-GFP* generated as described above were grown on half-strength MS agar plates for 11 days. Seedlings were harvested and ground in liquid nitrogen. 3 g of powdered plant material was used per replicate. Co-immunoprecipitation was performed as described in Wendrich et al. (2017). The pH of the protein samples was adjusted to 7.8 before being reduced by DTT to a final concentration 5 mM. The protein samples were incubated in 37°C for 30 min, followed by alkylation by adding iodoacetamide to a final concentration 12 mM and incubation in the dark for 20 min. The samples were digested by addition of sequencing-grade modified trypsin (Promega, Madison, WI, USA) to a final concentration 2 ng/µl and incubation overnight at 37 °C. Formic acid was added to the digested samples and the supernatant containing the peptides was collected by centrifugation at 15000 *g* for 10 min. For tandem mass spectrometry, the peptides were cleaned up on C18 reversed phase micro columns and subjected to reversed phase nano-LC source (Proxeon Biosystems) coupled to an LTQ-Orbitrap Velos Pro mass spectrometer equipped with a nano Easy spray ion source (ThermoScientific). Identification of proteins were carried out with the Mascot Daemon software (version 2.4) and searched against the Arabidopsis database TAIR. To be considered as a true protein identification, all individual ion scores must have a higher score than the score given when using a significant threshold of $p<0.005$.

***In organello* protein synthesis**

In organello protein synthesis was performed as described in Kwasniak-Owczarek et al. (2022). Briefly, 300 µg of freshly isolated mitochondria was resuspended in the translation mix containing 5 mM KH_2PO_4, pH 7.0, 2 mM GTP, 0.4 M mannitol, 60 mM KCl, 2 mM DTT, 50 mM HEPES, 10 mM $MgCl_2$, 10 mM malic acid, 1 mM pyruvate, 4 mM ADP, 0.1% (w/v) BSA, 25 mM unlabelled 19–amino acid solution (Promega), and 30 µCi [^{35}S]Met (>1000 Ci/mmol, Hartmann Analytic). For the control, 25 mM Na-acetate was used instead of malic acid and pyruvate. To inhibit potential contamination of chloroplast and cytoplasmic ribosomes, erythromycin and cycloheximide were added to all reactions to a final concentration of 200 µM and 100 µM, respectively. Reactions were carried out in 100 µl for 10, 30 and 60 min at room temperature on an orbital shaker and stopped by adding 350 mL mitochondria wash

buffer (without BSA) containing 10 mM unlabelled L-methionine and puromycin (50 µg/mL). Radiolabelled proteins were separated by SDS-PAGE and detected by autoradiography.

Immunoblotting of mitochondrial and chloroplastic proteins

Isolated chloroplastic proteins (10 µg) and isolated mitochondrial proteins (10 µg and 20 µg) were separated by SDS-PAGE and transferred to a PVDF membrane using the Trans-Blot Turbo Mini PVDF Transfer Pack (Biorad) and the Trans-Blot Turbo Transfer System (Biorad). Blots were probed with the primary antibodies against the subunits of OXPHOS: NAD6 (PHY1079S), NAD7 (PHY1077S), NAD9 (PHY0516S), COX2 (PHY1413S), ATP1 (PHY2146S), ATP4 (PHY1129S) and ATP8 (PHY1130S) from PhytoAB (U.S.A); RISP from Carrie et al. (2010); ATPβ and PGRL1 from Agrisera (Sweden); and GFP from Thermo Fisher Scientific (U.S.A). Blots were also probed with the primary antibodies against mitoribosomal proteins RPS4, RPS10 and RPL16 (Agrisera) that were kindly provided by Prof. Hanna Janska (University of Wroclaw, Poland); mitochondrial translation factor LETM1 (Zhang et al., 2012); mitochondrial retrograde signalling markers UPOX and AOX (De Clercq et al., 2013); IMM proteins OM66 and TIM17, and OMM proteins TOM40 and VDAC from Prof. James Whelan (La Trobe University, Australia). Anti-rabbit antibodies conjugated with horseradish peroxidase (HRP) were used as secondary antibodies, except for AOX and VDAC, an anti-mouse antibody-HRP was used. Chemiluminescence was detected by using Clarity Western ECL Substrate (Biorad) and the ChemiDoc XRS+ System (Biorad).

qRT-PCR

Total RNA was extracted from 11-day-old Col-0 and *mtran1-1/2-1* seedlings and 18-day-old *mtran1-2/2-2* seedlings grown on MS agar plates using the Spectrum™ Plant Total RNA Kit (Sigma Aldrich). cDNA synthesis and qRT-PCR was performed as described in Broda and Van Aken (2018) using the iScript™ cDNA Synthesis Kit (Biorad) and CFX384 Real-time PCR Detection System (Biorad) using SYBR green detection assays, respectively. The nuclear gene *UBIQUITIN-CONJUGATING ENZYME 21* (*UBC21*) was used for data normalization. Transcripts were measured in technical duplicate from three independently biological replicates.

RNA-seq analysis

11-day-old Col-0 and 18-day-old *mtran1-2/2-2* seedlings grown on MS agar plates were harvested at developmental growth stage 1.04 (Boyes et al., 2001). Each sample was composed

of 4-5 seedlings (approximately 50 mg fresh weight). Three biological replicates of Col-0 and *mtran1-1/2-1* were analyzed. Total RNA was extracted using the Spectrum™ Plant Total RNA Kit (Sigma Aldrich) according to the supplier's instructions and was further purified using the RNA Clean & Concentrator Kits (Zymo Research®, California, U.S.A.). RNA-seq libraries were constructed by the POPS platform (IPS2) using the TruSeq Stranded Total RNA kit with Ribozero Plant (Illumina®, California, U.S.A.) according to the supplier's instructions. The libraries were sequenced in single-end (SE) mode with 75 bases for each read on a NextSeq500. Adapter sequences and bases with a Q-Score below 20 were trimmed out from reads using Trimmomatic (v0.36, Bolger et al. (2014)) and reads shorter than 30 bases after trimming were discarded. After trimming, between 57 and 84 million of SE reads per sample were obtained. The bioinformatics and statistical analysis were carried out using pipelineOGE available at https://forgemia.inra.fr/GNet/pipelineoge (Baudry et al., 2022).

Data Availability

The RNA-Seq project was deposited (Gene Expression Omnibus (Edgar et al., 2002)): http://www.ncbi.nlm.nih.gov/geo/; accession no. GSE186586. All steps of the experiment, from growth conditions to bioinformatic analyses, were detailed in CATdb (Gagnot et al., 2008): http://tools.ips2.u-psud.fr.fr/CATdb/ according to the MINSEQE 'minimum information about a high-throughput sequencing experiment'.

Meta-analysis of transcriptome datasets

A full list of the transcriptome datasets of *mtran1-2/2-2* and 22 additional Arabidopsis mitochondrial mutants and chemical treatments affecting mitochondrial function can be found in Table S5. Transcripts were considered to be significantly differentially expressed if ppde.p > 0.95 or $P_{adj} < 0.05$ (after False Discovery Rate correction) with two-fold change. The similarities among all datasets were evaluated by comparison of common pairwise DEGs calculated via the Sørensen-Dice similarity coefficient (DSC) with formula $DSC(a,b) = 2n_{ab}/(n_a + n_b)$. Therefore, the DSC between two datasets ranges from 0 to 1. The complete matrix of DSC values for *mtran1-2/2-2* and 22 additional datasets was hierarchically clustered in TIGR Multi-experiment Viewer 4.9.0 using Euclidean Distance and represented as a heat map.

Purification of polysomal RNA

Polysomal RNA from 11-day-old Col-0 and *mtran1-1/2-1* seedlings and 18-day-old *mtran1-2/2-2* seedlings grown on MS agar plates was purified as described in Barkan (1993) with

modifications. 1 mL of polysome extraction buffer (0.2 M Tris-HCl, pH 9.0, 0.2 M KCl, 35 mM $MgCl_2$, 25 mM EGTA, 0.2 M sucrose, 1% v/v Triton X-100, 2% v/v Polyoxyethylene-10-tridecyl ether, 0.5 mg/ml heparin, 100 mM 2-betamercaptoethanol, 100 µg/ml chloramphenicol and 25 µg/ml cycloheximide) was added to 0.2 g of ground frozen tissues and the sample was vortexed until thawed. Debris from extraction was removed by centrifugation at 4°C and max speed for 1 min and filtered through a QIAshredder column (Qiagen). The sample was incubated on ice for 10 min to solubilize membranes and centrifuged at 4°C and max speed for 5 min. Sodium deoxycholate was added to the supernatant to a final concentration of 0.5% w/v. The sample was incubated on ice for 5 min to complete microsomal membrane solubilization and centrifuged at 4°C and max speed for 15 min to pellet insoluble material. The supernatant (450 µl) was layered onto 4 ml sucrose gradients (55:40:30:15% w/v sucrose in 40 mM Tris-HCl, pH 8.0, 20 mM KCl, 10 mM $MgCl_2$, 100 µg/ml chloramphenicol, 0.5 mg/mL heparin and 25 µg/ml cycloheximide) and fractionated by ultracentrifugation (SW50.1 rotor, 4°C, 45000 rpm, 65 min). After that, 10 fractions (~445 µl each) were collected from the top of the gradient and subjected to total RNA isolation using phenol/chloroform/isoamyl (25:24:1) (Sigma Aldrich). Isolated RNA from all fractions were treated with 2.5 M LiCl to remove the heparin as described previously (del Prete et al., 2007). The same volume of RNA from each fraction was used for cDNA synthesis and qRT-PCR as described above.

Ribo-Seq library preparation and sequencing

Mitoribosome footprints were prepared from Arabidopsis flower buds as previously described (Planchard et al., 2018). Ribosome footprints were depleted from ribosomal RNAs after first strand cDNA synthesis using custom biotinylated oligonucleotides matching major rRNA contaminants found in previous experiments (Planchard et al., 2018). Ribo-Seq libraries were prepared using the TruSeq Small RNA library preparation kit (Illumina). Next generation sequencing was performed on a NovaSeq6000 instrument (Illumina) using a SP-100 flowcell and a single end 75 nt pass. Mitochondrial mRNA abundances were determined by RT-qPCR using the same set of primers described in Planchard et al. (2018).

Bioinformatic analyses

Ribo-Seq sequencing data were processed and mapped as previously described in Planchard et al. (2018). Ribo-Seq RPKMs were calculated based on reads mapping to mitochondrial and nuclear coding sequences following a procedure detailed in Chotewutmontri and Barkan (2018)

and translation efficiencies were calculated as ratios of ribosome footprint RPKMs to mRNA abundances determined by RT-qPCR.

Predicted protein structure of mTRAN1 and mTRAN2

Protein sequences of mTRAN1 and mTRAN2 lacking their MTS predicted by MitoFates (http://mitf.cbrc.jp/MitoFates/cgi-bin/top.cgi) (Fukasawa et al., 2015) were used for protein structure prediction tools AlphaFold (ColabFold: AlphaFold2 using MMseqs2 https://colab.research.google.com/github/sokrypton/ColabFold/blob/main/AlphaFold2.ipyn) (Jumper et al., 2021), RoseTTAFold (https://robetta.bakerlab.org/) (Baek et al., 2021) and iTASSER (https://zhanggroup.org/I-TASSER/) (Yang and Zhang, 2015). The PPR codes of mTRAN1 and mTRAN2 were searched in aPPRove (Harrison et al., 2016) and PPR Code Prediction Web Server http://yinlab.hzau.edu.cn/pprcode/ (Yan et al., 2019).

Motif analysis of the 5'UTRs of mitochondrial mRNAs

The sequences of the 5'UTRs of mitochondrial transcripts were based on the recently re-annotated *Arabidopsis thaliana* ecotype Col-0 mitochondrial genome (NC_037304) (Sloan et al., 2018). Briefly, coordinates corresponding to the 5'UTRs were used to retrieve the corresponding sequences using BEDTools (command "getfasta") (Quinlan and Hall, 2010). If the transcript contained several alternative overlapping 5'UTRs, the longest 5'UTR was selected. The 5'UTRs of fully spliced transcripts, which are upstream of the first exons, were selected in case of trans-spliced transcripts *NAD1*, *NAD2* and *NAD5*. Because the mitochondrial genome contains polygenic transcriptional units, some distinct genes share the same 5'UTRs, for example, *NAD4L* and *ATP4*, *RPL5* and *COB*, *NAD3* and *RPS12*. There is also some suggestion that the second gene in polycistronic mRNAs may have its own 5'UTR and ribosome binding site in between the two genes, but these are not defined. Therefore, we analysed the collection of mitochondrial 5'UTRs both with and without these putative inter-cistronic 5'UTRs. The motif analysis of mitochondrial mRNA's 5'UTRs was performed using Multiple Expectation-maximization for Motif Enrichment (MEME) online motif search tool and identified a potential mitoribosome binding site CUUUxU and AAGAAx. The MEME motif search tool was unable to identify the AxAAA-related motif, but a AxAAA-like motif, AxAAAG, was manually searched in the 5'UTRs of mitochondrial mRNAs.

Recombinant protein purification and REMSAs

pET-26b(+)-*His-SUMO3-mTRAN1* plasmid with codon optimization was obtained from GeneScript (U.S.A). pET-26b(+)-*His-SUMO3* plasmid was generated from pET-26b(+)-*His-*

SUMO3-mTRAN1 plasmid by PCR using Phusion Site-Directed Mutagenesis Kit (ThermoScientific). The plasmids were expressed in *E. coli* Tuner DE3 by IPTG induction to a final concentration of 1 mM at OD_{600} = 0.6-0.8 at 18ºC for 20 hours. Protein purification was performed using GE Healthcare HisTrap FF columns according to the manufacturer's instructions. Purified protein concentrations were determined by Bradford assays (Biorad). 5'Cy5 labelled probes were obtained from Sigma Aldrich. REMSAs were performed as described previously (Kindgren et al., 2015; Schallenberg-Rudinger et al., 2013) with modifications. Briefly, reactions consisting of 10 µl 2x binding buffer (2.5x THE, 40 µg/ml BSA, 5 mM DTT, 0.5 mg/ml Heparin, 200 mM NaCl), 5 µl purified protein and 10 µl probes were incubated at 25ºC for 15 min and loaded onto a pre-run 5% native gel in 1x THE (34 mM Tris, 66 mM HEPES, 0.1 mM EDTA pH=8) that was run at 4ºC. The gels were imaged with a Typhoon 9500 (GE Healthcare).

Accession numbers

The sequences of genes analyzed in this article can be found in TAIR under the following accession numbers: *AT4G15640* (*mTRAN1*), *AT3G21465* (*mTRAN2*), *AT3G22370* (*AOX1a*), *AT2G21640* (*UPOX1*), *AT1G05680* (*UGT74E2*), *AT2G20800* (*NDB4*), *AT5G09570* (*AT12CYS-2*), *AT2G41730* (*HRG1*), *AT3G50930* (*OM66*), *ATMG00270* (*NAD6*), *ATMG00510* (*NAD7*), *ATMG00070* (*NAD9*), *ATMG00220* (*COB*), *ATMG00160* (*COX2*), *ATMG01190* (*ATP1*), *ATMG00480* (*ATP8*), *ATMG01080* (*ATP9*), *ATMG00290* (*RPS4*), *ATMG01390* (*RRN18*) and *AT5G25760* (*UBC21*).

SUPPLEMENTARY REFERENCES

Baek, M., DiMaio, F., Anishchenko, I., Dauparas, J., Ovchinnikov, S., Lee, G.R., Wang, J., Cong, Q., Kinch, L.N., Schaeffer, R.D*., et al.* (2021). Accurate prediction of protein structures and interactions using a three-track neural network. Science *373*, 871-876.

Barkan, A. (1993). Nuclear Mutants of Maize with Defects in Chloroplast Polysome Assembly Have Altered Chloroplast RNA Metabolism. The Plant cell *5*, 389-402.

Baudry, K., Delannoy, E., and Colas des Francs-Small, C. (2022). Analysis of the Plant Mitochondrial Transcriptome. Methods in molecular biology *2363*, 235-262.

Bekker-Jensen, D.B., Bernhardt, O.M., Hogrebe, A., Martinez-Val, A., Verbeke, L., Gandhi, T., Kelstrup, C.D., Reiter, L., and Olsen, J.V. (2020). Rapid and site-specific deep phosphoproteome profiling by data-independent acquisition without the need for spectral libraries. Nature communications *11*, 787.

Bolger, A.M., Lohse, M., and Usadel, B. (2014). Trimmomatic: a flexible trimmer for Illumina sequence data. Bioinformatics *30*, 2114-2120.

Boyes, D.C., Zayed, A.M., Ascenzi, R., McCaskill, A.J., Hoffman, N.E., Davis, K.R., and Gorlach, J. (2001). Growth stage-based phenotypic analysis of Arabidopsis: a model for high throughput functional genomics in plants. The Plant cell *13*, 1499-1510.

Broda, M., and Van Aken, O. (2018). Studying Retrograde Signaling in Plants. Methods in molecular biology *1743*, 73-85.

Carrie, C., Giraud, E., Duncan, O., Xu, L., Wang, Y., Huang, S., Clifton, R., Murcha, M., Filipovska, A., Rackham, O.*, et al.* (2010). Conserved and novel functions for Arabidopsis thaliana MIA40 in assembly of proteins in mitochondria and peroxisomes. The Journal of biological chemistry *285*, 36138-36148.

Chambers, M.C., Maclean, B., Burke, R., Amodei, D., Ruderman, D.L., Neumann, S., Gatto, L., Fischer, B., Pratt, B., Egertson, J.*, et al.* (2012). A cross-platform toolkit for mass spectrometry and proteomics. Nature biotechnology *30*, 918-920.

Chotewutmontri, P., and Barkan, A. (2018). Multilevel effects of light on ribosome dynamics in chloroplasts program genome-wide and psbA-specific changes in translation. PLoS genetics *14*, e1007555.

Cuillerier, A., and Burelle, Y. (2019). Hybrid Clear/Blue Native Electrophoresis for the Separation and Analysis of Mitochondrial Respiratory Chain Supercomplexes. J Vis Exp.

De Clercq, I., Vermeirssen, V., Van Aken, O., Vandepoele, K., Murcha, M.W., Law, S.R., Inze, A., Ng, S., Ivanova, A., Rombaut, D.*, et al.* (2013). The membrane-bound NAC transcription factor ANAC013 functions in mitochondrial retrograde regulation of the oxidative stress response in Arabidopsis. The Plant cell *25*, 3472-3490.

del Prete, M.J., Vernal, R., Dolznig, H., Mullner, E.W., and Garcia-Sanz, J.A. (2007). Isolation of polysome-bound mRNA from solid tissues amenable for RT-PCR and profiling experiments. RNA *13*, 414-421.

Edgar, R., Domrachev, M., and Lash, A.E. (2002). Gene Expression Omnibus: NCBI gene expression and hybridization array data repository. Nucleic acids research *30*, 207-210.

Flores-Perez, U., and Jarvis, P. (2017). Isolation and Suborganellar Fractionation of Arabidopsis Chloroplasts. Methods in molecular biology *1511*, 45-60.

Fukasawa, Y., Tsuji, J., Fu, S.C., Tomii, K., Horton, P., and Imai, K. (2015). MitoFates: improved prediction of mitochondrial targeting sequences and their cleavage sites. Molecular & cellular proteomics : MCP *14*, 1113-1126.

Gagnot, S., Tamby, J.P., Martin-Magniette, M.L., Bitton, F., Taconnat, L., Balzergue, S., Aubourg, S., Renou, J.P., Lecharny, A., and Brunaud, V. (2008). CATdb: a public access to Arabidopsis transcriptome data from the URGV-CATMA platform. Nucleic acids research *36*, D986-990.

Gao, F., Han, X., Wu, J., Zheng, S., Shang, Z., Sun, D., Zhou, R., and Li, B. (2012). A heat-activated calcium-permeable channel--Arabidopsis cyclic nucleotide-gated ion channel 6--is involved in heat shock responses. Plant J *70*, 1056-1069.

Gentleman, R., Carey, V.J., Huber, W., Irizarry, R.A., and Dudoit, S. (2005). Bioinformatics and computational biology solutions using R and Bioconductor, Vol 1 (Springer).

Harrison, T., Ruiz, J., Sloan, D.B., Ben-Hur, A., and Boucher, C. (2016). aPPRove: An HMM-Based Method for Accurate Prediction of RNA-Pentatricopeptide Repeat Protein Binding Events. PloS one *11*, e0160645.

Jumper, J., Evans, R., Pritzel, A., Green, T., Figurnov, M., Ronneberger, O., Tunyasuvunakool, K., Bates, R., Zidek, A., Potapenko, A.*, et al.* (2021). Highly accurate protein structure prediction with AlphaFold. Nature *596*, 583-589.

Karimi, M., Inze, D., and Depicker, A. (2002). GATEWAY vectors for Agrobacterium-mediated plant transformation. Trends Plant Sci *7*, 193-195.

Karimova, G., Pidoux, J., Ullmann, A., and Ladant, D. (1998). A bacterial two-hybrid system based on a reconstituted signal transduction pathway. Proceedings of the National Academy of Sciences of the United States of America *95*, 5752-5756.

Kindgren, P., Yap, A., Bond, C.S., and Small, I. (2015). Predictable alteration of sequence recognition by RNA editing factors from Arabidopsis. The Plant cell *27*, 403-416.

Kwasniak-Owczarek, M., Tomal, A., and Janska, H. (2022). Assessment of Protein Synthesis in Mitochondria Isolated from Rosette Leaves and Liquid Culture Seedlings of Arabidopsis. Methods in molecular biology *2363*, 183-197.

Lyu, W., Selinski, J., Li, L., Day, D.A., Murcha, M.W., Whelan, J., and Wang, Y. (2018). Isolation and Respiratory Measurements of Mitochondria from Arabidopsis thaliana. J Vis Exp.

Planchard, N., Bertin, P., Quadrado, M., Dargel-Graffin, C., Hatin, I., Namy, O., and Mireau, H. (2018). The translational landscape of Arabidopsis mitochondria. Nucleic acids research *46*, 6218-6228.

Quinlan, A.R., and Hall, I.M. (2010). BEDTools: a flexible suite of utilities for comparing genomic features. Bioinformatics *26*, 841-842.

Ritchie, M.E., Phipson, B., Wu, D., Hu, Y., Law, C.W., Shi, W., and Smyth, G.K. (2015). limma powers differential expression analyses for RNA-sequencing and microarray studies. Nucleic acids research *43*, e47.

Schallenberg-Rudinger, M., Kindgren, P., Zehrmann, A., Small, I., and Knoop, V. (2013). A DYW-protein knockout in Physcomitrella affects two closely spaced mitochondrial editing sites and causes a severe developmental phenotype. Plant J *76*, 420-432.

Schertl, P., and Braun, H.P. (2015). Activity measurements of mitochondrial enzymes in native gels. Methods in molecular biology *1305*, 131-138.

Sloan, D.B., Wu, Z., and Sharbrough, J. (2018). Correction of Persistent Errors in Arabidopsis Reference Mitochondrial Genomes. The Plant cell *30*, 525-527.

Smet, J., De Paepe, B., Seneca, S., Lissens, W., Kotarsky, H., De Meirleir, L., Fellman, V., and Van Coster, R. (2011). Complex III staining in blue native polyacrylamide gels. J Inherit Metab Dis *34*, 741-747.

Smyth, G.K. (2005). limma: Linear Models for Microarray Data. In Bioinformatics and Computational Biology Solutions Using R and Bioconductor, R. Gentleman, V.J. Carey, W. Huber, R.A. Irizarry, and S. Dudoit, eds. (New York, NY: Springer New York), pp. 397-420.

Tran, H.C., and Van Aken, O. (2022). Purification of Leaf Mitochondria from Arabidopsis thaliana Using Percoll Density Gradients. Methods in molecular biology *2363*, 1-12.

Van Bel, M., Diels, T., Vancaester, E., Kreft, L., Botzki, A., Van de Peer, Y., Coppens, F., and Vandepoele, K. (2018). PLAZA 4.0: an integrative resource for functional, evolutionary and comparative plant genomics. Nucleic acids research *46*, D1190-D1196.

Waltz, F., Soufari, H., Bochler, A., Giege, P., and Hashem, Y. (2020). Cryo-EM structure of the RNA-rich plant mitochondrial ribosome. Nat Plants *6*, 377-383.

Wendrich, J.R., Boeren, S., Moller, B.K., Weijers, D., and De Rybel, B. (2017). In Vivo Identification of Plant Protein Complexes Using IP-MS/MS. Methods in molecular biology *1497*, 147-158.

Willforss, J., Chawade, A., and Levander, F. (2019). NormalyzerDE: Online Tool for Improved Normalization of Omics Expression Data and High-Sensitivity Differential Expression Analysis. Journal of proteome research *18*, 732-740.

Yan, J., Yao, Y., Hong, S., Yang, Y., Shen, C., Zhang, Q., Zhang, D., Zou, T., and Yin, P. (2019). Delineation of pentatricopeptide repeat codes for target RNA prediction. Nucleic acids research *47*, 3728-3738.

Yang, J., and Zhang, Y. (2015). I-TASSER server: new development for protein structure and function predictions. Nucleic acids research *43*, W174-181.

Zhang, B., Carrie, C., Ivanova, A., Narsai, R., Murcha, M.W., Duncan, O., Wang, Y., Law, S.R., Albrecht, V., Pogson, B.*, et al.* (2012). LETM proteins play a role in the accumulation of mitochondrially encoded proteins in Arabidopsis thaliana and AtLETM2 displays parent of origin effects. The Journal of biological chemistry *287*, 41757-41773.

Printed by Media-Tryck, Lund 2023 NORDIC SWAN ECOLABEL 3041 0903

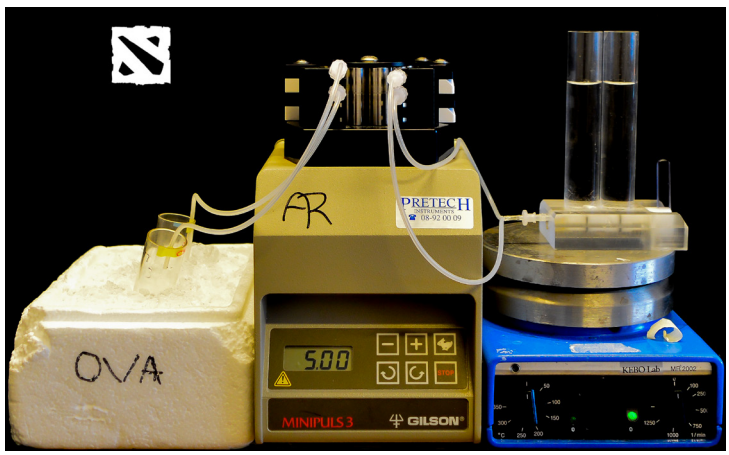

Department of Biology
Faculty of Science
Lund University
ISBN 978-91-8039-599-1